Discovery of an extracellular stress sensory protein in *Beauveria bassiana* and identification of photolyase encoding *phr-1* sequences in five entomopathogenic fungi

A Thesis
Submitted to the College of
Graduate Studies and Research
in Partial Fulfillment of the Requirements
for the Degree of Doctor of Philosophy in Applied Microbiology
in the Department of Food and Bioproduct Sciences
University of Saskatchewan
Saskatoon
By
Kelly R. Aasen

PERMISSION TO USE

In presenting this thesis in partial fulfillment of the requirements for a Postgraduate degree from the University of Saskatchewan, I agree that the Libraries of this University may make it freely available for inspection. I further agree that permission for copying of this thesis in any manner, in whole or in part, for scholarly purposes may be granted by the professor or professors who supervised my thesis work or, in their absence, by the Head of the Department or the Dean of the College in which my thesis work was done. It is understood that any copying or publication or use of this thesis or parts thereof for financial gain shall not be allowed without my written permission. It is also understood that due recognition shall be given to me and to the University of Saskatchewan in any scholarly use which may be made of any material in my thesis.

Requests for permission to copy or to make other use of material in this thesis in whole or part should be addressed to:

Head of the Department of Food and Bioproduct Sciences

University of Saskatchewan

Saskatoon, Saskatchewan, S7N 5A8

Canada

GENERAL ABSTRACT

Entomopathogenic fungi (EPF) are being developed as an alternative to chemical insecticides and several, including *Beauveria bassiana* are currently important tools in integrated pest management. However, their ability to bring about effective control of pest insects can be compromised by environmental stresses and conditions, including short-wave ultraviolet radiation (UVR) and high temperatures. The work described in this thesis: 1) identified a region of a candidate photolyase gene (*phr-1*) in five different genera of EPF, which encoded a portion of a putative cyclobutane pyrimidine dimer photolyase (CPD-PHR; named after the type of DNA damage they repair and the encoding gene, respectively), 2) established that in *B. bassiana*, tolerance to UVR or heat can be induced in conidiospores (CS) or blastospores (BS), respectively, by cell-free filtrate (CFF) suspected to contain an extracellular sensory component like factor (ELF), 3) identified key steps required for tolerance induction and 4) characterized a gene candidate to encode ELF (*elf*) and its encoded product using a combination of molecular biological and microbiological techniques, which provided evidence to suggest that the candidate gene encodes a functional ELF and propose some cellular components which may be involved in its potential interaction with the cell.

Note that ELF is named after the extracellular sensory component (ESC) from *Escherichia coli*, but not due to known or suspected similarities in their sequence, structure or specific function, but rather because of their predicted ability, once activated by heat (in this particular case), to increase environmental tolerance in treated cells. Furthermore, this response was termed ELF/ESC induced tolerance (EIT), which is similar to the definition used by the late Dr. Rowbury and his colleagues. Currently, EIT is characterized only by an increase in

environmental tolerance, measured as viability, following treatment with activated ESC or ELF. However, if more specific functions or roles for ESC, ELF or EIT were discovered than these definitions would require revision to accommodate such findings.

In addition to the determinants of infection controlled by the fungus and host, including their molecular biology, physiology and biochemistry, the environment where they subsist is of great importance. Environmental conditions, including available moisture, wind, temperature, solar UVR and type of insect pest, all influence the ability of EPF to establish pathogenesis. High heat stress and UVR are of most importance when EPF are applied to crops during daylight hours since prolonged solar exposure can cause inactivation of fungal spores leading to decreased insect mortality. Both of these stresses and their impacts on fungi were studied during this thesis research.

Sunlight is the main source of UVR in nature and its short to medium wavelengths (< 315 nm) were of most importance in this study. These wavelengths can damage DNA through the creation of cyclobutane pyrimidine dimers (CPDs) which can be lethal to cells due to their ability to halt DNA replication and gene expression. This type of damage is most efficiently repaired by CPD-PHR dependent photoreactivation, which can repair ~ 90% of CPDs but is dependent on the availability of light at 380-410 nm. The *phr-1* gene has been shown to encode CPD-PHR in other fungi and was studied here in five genera of EPF. A region of a putative *phr-1* that had sequence conservation with known *phr-1* from other filamentous fungi was found in EPF from the genera *Beauveria*, *Isaria*, *Lecanicillium, Metarhizium* and *Tolypocladium*. This region encoded several conserved characteristics known to be functionally important for the of CPD-PHR in DNA repair. Furthermore, homology modeling was used to predict the structure/ function of the products encoded by this region of putative *phr-1* and provided evidence that they

contained structural homology with those that had CPD-PHR repair activity (E.C. 4.1.99.3). In addition, homology modeling was able to differentiate the products encoded by the putative *phr-1*s in the studied EPF and a model CPD-PHR from the two other protein types belonging to the photolyase (PHR)/cryptochrome (CRY) family that are also found in fungi. The predicted molecular phylogeny of the putative CPD-PHRs was consistent with the established phylogenetic relationships of these fungi, with the exception of *Lecanicillium*. These results are the first for a putative *phr-1* in EPF from the genera *Isaria*, *Lecanicillium* and *Tolypocladium*.

Another phenomenon was also studied in this thesis. It had been shown in bacterial and yeast cultures that extracellular factors (for example ESCs and ELFs) are present and appear to be involved in cellular sensing of environmental stress conditions, such as high temperature and can induce tolerance to various environmental stresses, including heat and UVR. However, this phenomenon has not been studied in any filamentous fungi. This investigation was conducted to determine if CS or BS from *B. bassiana* were responsive to preheated CFF and possessed a phenomenon which resembles EIT to heat and/or UVR, which is characterized by an increase in the survival rates of challenged cells. The results showed that tolerances of CS and BS to UVR (under non-photoreactivating conditions) or heat (55 °C), respectively, were increased following treatment with preheated CFF. Several novel bioassays were also developed to screen for and characterize ELF candidate (EC) proteins produced by *B. bassiana*. These included a poly-acrylamide-based, *in situ* bioassay and a whole cell, pull-down assay that were employed to identify several ECs and one such candidate, EC1 (~ 28 kDa), potentially interacted with BS. Furthermore, bioassays with purified EC1 and EC2 showed that only the glycosylated EC1 possessed the ability to increase heat tolerance in BS and appeared to be an ELF based on this result, which was consistent with the current understanding of the effects of EIT.

Analysis of EC1 and EC2 by electrospray ionization with tandem mass spectrometry (ESI-MS/MS) revealed that they were the same protein and differed by EC1 being glycosylated. An expressed sequence tag (EST) encoding peptide sequences, representing six of the eleven parent ions found in EC1/EC2 by ESI-MS/MS, was identified in the public data base of ESTs from *B. bassiana*. As a result, this EST was considered to be a candidate to partially encode for ELF in *B. bassiana* and was used to design oligonucleotide primers to amplify the remaining coding regions of the gene using polymerase chain reaction (PCR) based methods. This led to the identification of a potential 741 bp open reading frame (ORF) that encoded a total of eight out of a possible eleven parent ions derived from EC1 and EC2. *In silico* analysis revealed that the ORF encoded a protein with other features that were also consistent with those observed in the likely ELF, such as its nascent derived size (25.9 kDa), candidate glycosylation sites and predicted secretion signal peptide. The candidate *elf* was inserted into an expression cassette and introduced into the methylotrophic yeast *Pichia pastoris* where expression of *elf* could be controlled by the presence of methanol. This strategy was successful in yielding a cell line able to produce transgenic-ELF (TG-ELF) that was able to confer elevated tolerance to heat in BS to a level that was similar to ELF produced by *B. bassiana*. This provided additional evidence that *elf* encoded a functional ELF.

The molecular function(s) of ELF currently remain unknown, as no sequence homologues of ELF with defined functions have been established. Furthermore, structural models could not confidently predict functions for the likely ELF studied here. Nonetheless, it was apparent that the ELF involved in establishing heat tolerance in BS was a small secreted cysteine rich protein (SSCP) because of its size [< 300 amino acid residues (aa)], abundance of cysteine (5.2%) and is secreted, which are characteristics consistent with other SSCPs. The ELF also

contains three, 63 aa internal repeats, which have been thought to be involved in rapid protein evolution in other organisms. Furthermore, correlative clues were found that suggested the apparent interaction between ELF and BS is of low affinity, which is consistent with other agonist-receptor interactions that are involved in signal transduction.

In summary, photoreactivation and EIT, though representing separate responses can occur simultaneously and require coordination from *B. bassiana* in response to environmental stress and contribute to its general stress tolerance mechanisms. This thesis established that the EPF studied contained a candidate *phr-1* region that encodes a portion of a putative CPD-PHR, which has features that are consistent with their involvement in photoreactivation. In addition, a novel phenomenon for environmental stress tolerance induction was established in *B. bassiana*. Furthermore, the gene (*elf*) and its encoded protein product (ELF) (which is involved in establishing EIT to heat in BS) are both described for the first time.

ACKNOWLEDGMENTS

I dedicate this thesis to my parents, Jeanette and Richard Aasen and my wife, Tracey Aasen.

In addition to the essentials of life, my parents provided me with unrelenting support in whatever I have ever done, starting at an early age. They allowed me to discover nature, be it in the back yard or at the lake and cultivated my curiosity of it. Without them I would have surely taken a different path, but for this I am thankful to you both. Also, thank you to the rest of my family both immediate and extended; your support was always felt.

Tracey, you are truly my other half. Thank you for supporting me throughout my studies. I enjoy your curiosity and this attribute in you has helped maintain mine, which is critical for my own self and as a scientist.

I would like to acknowledge the members of my advisory committee Drs. Korber (Chair), Tyler (past Chair), Vujanovic (past Chair), Qiu, Rozwadowski and Van Kessel. I thank them for their direction, critique and discussions they have provided to help my research and own development as a scientist. Thank you to the department secretaries. You all have made the office a friendly place to be. Thank you to Dr. Schmutz for allowing me access to her lab and thank you to her lab team for their technical assistance. I am grateful for the Horner, D. Hantelman, Parr, Zielke, Harvey, Molson and devolved Scholarships and NSERC for supporting my education and this research. Also, thank you to StressMarq and the U of S for their travel support.

Thank you to all the members of the GGK lab that I have had the pleasure of working with over the years. A special thanks to Dinka Besic, Bill Reid, Dr. Sohail Qazi and Dr. Zafer Dallal Bashi for their friendship, conversations, scientific insight and motivation. Also, thanks to David McKinnon for his friendship, our conversations and his humor, which was always welcome. Also, thank you to the rest of my friends both at the University and outside for your support and kindness. I wish you all the best in the future.

Last, but definitely not least, my deepest thanks and gratitude go to my supervisor, Dr. George Khachatourians. What can I say about a man who has been called a Sherpa or a Guru? George, you are the most decent, grounded and honourable person that I have ever had the pleasure of meeting. Thank you for the years of friendship, mentorship and guidance. Your impact has been powerful; both in my academic life by helping me develop as a student and a scientist and in my personal life by aiding my growth as a person. I have many fond memories of you and your interactions with your students, especially during our lab meetings which were always very educational and enjoyable. As one of your last students I would like to thank you for everything you have done for us and wish you all the happiness.

TABLE OF CONTENTS

LIST OF FIGURES

LIST OF TABLES

LIST OF ABBREVIATIONS

(6-4)-PHR	(6-4)pyrimidine-pyrimidone photolyase
(6-4)PP	(6-4)pyrimidine-pyrimidone
aa	Amino acid residue
ARSEF	Agricultural Research Service Entomopathogenic Fungi
AS	Ammonium sulphate
ATCC	American Type Culture Collection
BLAST	Basic local alignment search tool
BS	Blastospore(s)
BSA	Bovine serum albumin
CFF	Cell-free filtrate
CFU	Colony forming unit
CN-PAGE	Clear native polyacrylamide gel electrophoresis
CPD	Cyclobutane pyrimidine dimer
CPD-PHR	Cyclobutane pyrimidine dimer photolyase
CRY	Cryptochrome
CS	Conidiospore(s)
Cz64	*Cercospora zeae-maydis* (6-4)-PHR
d	Day(s)
DASH-CRY	*Drosophila*, *Arabidopsis*, *Synechocystis* and *Homo-CRY*
EC	Extracellular sensory component-like factor candidate
EIT	Extracellular sensory component/extracellular sensory component-like factor induced tolerance
ELF	Extracellular sensory component-like factor
elf	Extracellular sensory component-like factor gene
EPF	Entomopathogenic fungi
ESC	Extracellular sensory component
ESI-MS/MS	Electrospray ionization with tandem mass spectrometry
ESR	Environmental stress response
EST	Expressed sequence tag

FAD	Flavin adenine dinucleotide
GO	Gene ontology
h	Hour(s)
HSP	Heat shock protein
HSR	Heat shock response
MAPK	Mitogen-activated protein kinase
M_r	Relative molecular mass
MTHF	5,10-methenyltetrahydrofolate
NER	Nucleotide excision repair
nt	Nucleotide residue
OD	Optical density
ORF	Open reading frame
PBS	Phosphate buffered saline
PCR	Polymerase chain reaction
PHR	Photolyase; used refer to PHRs in general
phr-1	Gene that encodes CPD-PHR
PTM	Post-translational modification
RACE	Rapid amplification of cDNA ends
R_f	Retention factor
RPM	Revolutions per minute
s	Second(s)
SAPK	Stress activated protein kinase
SDS-PAGE	Sodium dodecyl sulphate polyacrylamide gel electrophoresis
SEM	Standard error of the mean
SSCP	Small secreted cysteine rich protein
SsDC	*Sclerotinia sclerotiorum* DASH-CRY
TaPH	*Trichoderma atroviride* CPD-PHR
TG-ELF	Transgenic-ELF
u	Units of activity
UV	Ultraviolet

UV-A	Ultraviolet-A; 315-400 nm
UV-B	Ultraviolet-B; 280-315 nm
UV-C	Ultraviolet-C; 200-280 nm
UVR	Ultraviolet radiation
VM	Vogel's medium
WT	Wild type
YPG	Yeast extract peptone glucose medium
YPGA	Yeast extract peptone glucose medium with agar

1.0 GENERAL INTRODUCTION

Entomopathogenic fungi possess the ability to infect and kill insects. This group of fungi has been studied since the 1800s with an emphasis on managing diseases that were problematic to the silk worm industry in France. Agnostino Bassi showed that the muscardine disease which affected silk worms (*Bombyx mori*) and others was caused by *B. bassiana* (Audouin, 1838). These findings contributed to Pasteur (1874) and LeConte (1873) suggesting that EPF could be used in the management of insect pests. The great Russian scientist, Elie Metchnikoff, who is better known for his contributions in vertebrate pathology and won the Nobel Prize in 1908 for the discovery of phagocytosis and other contributions in immunity, also discovered that the green muscardine disease that affected various insects was caused by *Metarhizium anisopliae* (Reviewed in Lord, 2005; Khachatourians, 2009). Like his contemporaries, he too saw the potential of this fungus as a control agent and even suggested that it could be manipulated to improve its virulence. Following Metchnikoff's findings *M. anisopliae* was mass produced by Krassilstschik (1888) and used on the sugar beet curculio (*Cleonus punctiventris*) with limited success. In the U.S., also in the late 19th century, Francis H. Snow established a program at the University of Kansas to produce *B. bassiana* CS and distribute them to farmers for control of the chinch bug (*Blissus leucopterus*). Farmers provided favourable reports initially, but enthusiasm diminished and the program was terminated by the early 20th century (Lord, 2005). One of the conclusions from Snow's strategy was that effective control of the insect pest was not possible, since the fungus could not establish itself in the field, likely because the environmental conditions were not favourable for the fungus to do so (Billings and Glenn, 1911).

In the 1940's, with the discovery and widespread use of chemical insecticides, the potential of EPF, and other biologicals, was overshadowed. These chemicals created an inappropriate comparative model for a majority of the microbial insecticides, which has been referred to as the chemical insecticide paradigm (Waage, 1998). As a result, the use of EPF has been based on an unfair comparison to chemical insecticides, rather than in the context of their ecology, as part of an integrated pest management system (Waage, 1998).

With the advent of molecular biology in the middle of the 20th century and the establishment of its central dogma (Crick, 1970) and the development of transgenic technologies, a new set of tools was made available for the study and improvement of EPF and other biological controls. Most recently, many of the studies in EPF have focused on improving their field efficacy, for example by manipulating the functionality (Fan *et al.*, 2007) or expression (St Leger *et al.*, 1996) of catabolic enzymes involved in pathogenesis, or by introducing heterologous genes, such as scorpion neurotoxin (Wang and St Leger, 2007), scorpine with salivary gland and midgut peptide 1 (Fang *et al.*, 2011) or an archaeal CPD-PHR to promote DNA repair and increase ultraviolet radiation UVR tolerance (Fang and St Leger, 2012). Furthermore, as the number of identified promoters, genes and gene products increases, so does the biologist's transgenic arsenal to improve the effectiveness of EPF, for instance through augmentation of their ability to tolerate environmental stresses. In this regard, genome sequencing of EPF has benefited from the development of next generation sequencing technologies (Reviewed in Martín *et al.*, 2013), including those based on pyrosequencing (Ronaghi *et al.*, 1996) and oligonucleotide ligation and detection (Brenner *et al.*, 2000) and recently the genomes of *Cordyceps militaris* (Zheng *et al.*, 2011), *Metarhizium acridum*, *M. anisopliae* (Gao *et al.*, 2011) and *B. bassiana* (Xiao *et al.*, 2012) have been sequenced. This genomic information coupled with an improved

understanding of the ecology as well as the developmental and molecular biology of EPF, will provide insight into improving their use as biological insecticides.

Implementation of EPF in biological control of insect pests has become more accepted by the public as a potential alternative to synthetic chemical insecticides (Lord, 2005) and a similar trend is true for biopesticides in general. As a result, the worldwide market for these products, collectively termed biological pesticides, has increased by roughly 20% annually (the time frame was not provided) and is estimated to be worth $500-800 million U.S. as of 2009 (de Guzman, 2009). Two main reasons for the increase in market share of biopesticides are concerns of the environmental safety of chemical pesticides and potential for continued development of resistance to them by insects (Khachatourians, 2009; Hajek and Delalibera, 2010). In contrast, there is a decreased chance for the development and selection of resistance to EPF since pathogenesis is multigenic due to the complex nature of the interaction between the organisms (Khachatourians and Qazi, 2008; Khachatourians, 2009).

In addition to the determinants of disease controlled by the fungus and host, such as their molecular biology, physiology and biochemistry, the environment where the EPF and insect subsist is of great impact (Feng *et al.*, 1994; Khachatourians *et al.*, 2002; Khachatourians and Qazi, 2008). The dependence of these fungi on a narrow range of environmental conditions has limited their widespread adoption as insecticides (Fargues, 2003). Environmental conditions, such as available moisture, wind, temperature, solar UVR and type of insect pest, all influence the ability of EPF to establish pathogenesis. High heat stress and UVR are of the most importance when EPF are applied during daylight hours since prolonged solar exposure can cause inactivation of fungal spores leading to decreased insect mortality (Vestergaard *et al.*, 1995; Inglis *et al.*, 1997). This thesis focused on the effects of, and responses to UVR, and

supra-optimal temperatures in several EPF belonging to the order Hypocreales within the Families Clavicipitaceae and Cordycipitaceae. These families includes the best studied and most economically important species of EPF (Reviewed in Khachatourians, 2009).

Insecticidal inoculants containing EPF from the genera *Beauveria*, *Lecanicillium* or *Metarhizium* most often utilize CS as the infectious fungal propagule (Roberts and St Leger, 2004; Khachatourians, 2009). Relative to other fungal cell types, CS are better suited to application due to their resistance to desiccation and other environmental conditions or insults. Even so, sub-lethal doses of UVR can delay both CS germination and insect infection, resulting in a reduction of the effective virulence of the EPF (Ignoffo *et al.*, 1977). As a result, the ability of an EPF, applied as a pesticide, to survive and recover from insults caused by high temperature and/or UVR will directly impact its ability to be an effective control agent. With respect to this, characterization and evaluation of EPF metabolism and physiology, as well as the genetic regulation of these components under stress conditions, is critical in the acquisition of a comprehensive understanding of these complex processes. While it is neither possible nor practical to eliminate the effects of detrimental field conditions, a comprehensive understanding of the effects of environmental stress on fungal pathogenesis can help guide applied research and development. Furthermore, application of this understanding may lead to improvements of the ability of *B. bassiana* and other EPF to function as biological insecticides, such as increasing their ability to mitigate against insults that may be induced by environmental conditions.

Aspects of stress responses to UVR and heat in EPF have been addressed in other theses conducted at the University of Saskatchewan, particularly the ability to repair UVR induced DNA damage, with an emphasis on nucleotide excision repair (NER) (Chelico, 2004), as well as heat stress tolerance and the proteomic response to heat stress (Xavier, 1998). In this thesis, the

ability of several EPF to respond to and mitigate the effects of UVR and high temperature were of primary interest, specifically: (i) photorepair of UVR challenged EPF and the *in silico* characterization of putative CPD-PHRs via their candidate encoding gene, *phr-1*; and (ii) a novel heat stress response that is controlled by an extracellular protein. The gene and protein naming conventions established in *Neurospora crassa* will be used throughout this thesis as described by Kinsey (1998).

Although much is known about photoreactivation in fungi, there is a lack of understanding of the molecular biology that controls this process in EPF (Chelico *et al.*, 2005; Chelico *et al.*, 2006). Central to this is the lack of data regarding the sequence of both *phr-1* and its gene product. To date, the sequences of only four putative *phr-1* from EPF have been deposited within public data bases, derived from genomic sequencing of *M. acridum* CQMa 102 [GI: 322696650; (Gao *et al.*, 2011)], *M. anisopliae* Agricultural Research Service Entomopathogenic Fungi (ARSEF) 23 [GI:322707580; (Gao *et al.*, 2011)], *C. militaris* CM01 [GI:346325901; (Zheng *et al.*, 2011) and *B. bassiana* ARSEF 2860 [ADAH01000118.1; 26568-27071; (Xiao *et al.*, 2012)].

Due to the importance of photoreactivation in the survival of EPF in the field, this thesis was initiated to determine if fungi belonging to the genera *Beauveria*, *Isaria*, *Lecanicillium*, *Metarhizium* and *Tolypocladium* possessed a gene that likely encodes a functional CPD-PHR. Photoreactive capabilities were confirmed in ultraviolet-C (UV-C) challenged CS and conserved regions of a candidate *phr-1* from the EPF were amplified, cloned and sequenced. *In silico* techniques were used to (i) study the conservation of functionally important features, (ii) model the structure of these putative CPD-PHR regions to assist in function prediction and (iii) analyse

the phylogenetic relationship between the putative CPD-PHR from EPF and other filamentous fungi.

In contrast to photoreactivation, very little is known about the molecular component(s) or mechanism(s) that are involved in the extracellularly mediated response to heat stress in EPF or any other organisms. The first evidence of a similar phenomenon was reported some 15 years ago in *E. coli* (Hussain *et al.*, 1998) and later in *Campylobacter jejuni* (Murphy *et al.*, 2003) and *Saccharomyces cerevisiae* (Vovou *et al.*, 2004). In *E. coli*, this phenomenon appears to be controlled by secreted, diffusible proteins termed ESCs (Rowbury and Goodson, 1999a), which are activated external of the cell by a variety of chemical and physical stresses (Rowbury and Goodson, 1999b) and can induce an elevated tolerance to various environmental stresses in sensitive *E. coli*. This system is reported to permit *E. coli* to sense a variety of stresses through the ESCs and thought to allow its cells to pre-emptively respond to and better survive the impending environmental insult. Some physiological characterization has been performed on the ESC system, with a vast majority of it in *E. coli*. However, very little is known about ESC itself and there is a need for the discovery of this putative molecule and its characterization. Therefore, the discovery of ELF and the related EIT in *B. bassiana* was pursued. This phenomenon was studied through the use of several innovative whole cell bioassays using a combination of microbiology and molecular biology based techniques, permitting the identification and characterization of an ELF and its encoding gene for the first time in any organism.

The results of this thesis provide insight into the physiological roles and molecular features of putative CPD-PHRs from five EPF and ELF in *B. bassiana* through the use of various micro- and molecular biology based approaches. The intention is that these findings will help augment the design and use of EPF based insecticides.

The thesis research was based on the following hypothesis and objectives:

1.1 Hypothesis

There were two hypotheses under consideration of this thesis. First, if photoreactivating conditions increased survival in UV-C challenged EPF, such as those belonging to the genera *Beauveria, Isaria, Lecanicillium, Metarhizium* and *Tolypocladium,* then they will possess a candidate *phr-1*, encoding a putative CPD-PHR with features that are functionally important for its role in DNA repair. Second, if the tolerance of *B. bassiana* to heat or UVR stress is increased by preheated CFF that was prepared from their cultures, then this response is mediated by secreted proteins (i.e. ELF) that are responsive to or activated by heat.

1.2 Aims and objectives

This thesis focused on the following objectives:

a) To establish photoreactivation in UVR challenged CS from several EPF to implicate the presence of CPD-PHR and its corresponding gene, *phr-1*.

b) To ascertain the sequence of a conserved region within the candidate *phr-1* from several EPF that is known to encode the α-helical domain of CPD-PHR in other organisms.

c) To deduce the amino acid sequences of the gene products encoded by the candidate *phr-1*, which will provide insight into their phylogeny and information on some of the key molecular features required for CPD-PHRs to perform DNA repair.

d) To determine if *in silico* analysis of the putative CPD-PHRs can differentiate them from other related PHR/CRY proteins also found in filamentous fungi.

e) To determine if *B. bassiana* possessed a phenomenon that resembles EIT to heat or UVR stress and establish some of the functional parameters required for its study.

f) To establish which cell types produced by *B. bassiana* are responsive to ELF.

g) To ascertain if other EPF are responsive to the ELF encoded in *B. bassiana*.

h) To determine the molecular composition, general structure and other macromolecular features of ELF.

i) To obtain the DNA sequence of *elf*.

j) To determine if ELF is a genetically encoded trait and if it is functional when expressed heterologously.

1.3 Organization of thesis

The organization of this thesis was according to "manuscript-style" option of the College of Graduate Studies and Research.

2.0 LITERATURE REVIEW

Heat stress and UVR are associated with solar radiation and are important factors restricting EPF under sun-exposed agricultural environments (Roberts and Campbell, 1977; Fargues *et al.*, 1997b). The term 'inactivation' was first used by Ignoffo *et al.* (1977) to describe the effect of UVR on EPF, characterized by a reduced ability to cause insect mortality with increasing doses of UVR prior to insect inoculation. Heat stress has also been found to inactivate EPF and is the result of a decrease in viability and slowed fungal development following exposure to a supra-optimal temperature for the required duration. An important difference between the two stressors is that UVR ceases once the fungus begins to propagate within the hemocoel. In contrast, the harmful effects of heat stress can be of impact throughout the infection process via the ambient temperature and behavioral fever and can also aggravate the detrimental effects of solar radiation (Smits *et al.*, 1996). Furthermore, it has been shown in field experiments that insect behavioral activity and temperature have a greater impact on disease progression than inactivation by ultraviolet-B (UV-B) (Inglis *et al.*, 1997). Nonetheless, both are important and influence the ability of EPF to be an effective insecticide and will be discussed in the following sections of this literature review.

2.1 Studies of UVR tolerance in EPF

Repair of UVR induced DNA damage, and photobiology of nucleic acids and cells are historically well recognized, and the fundamentals of these topics are shown in a comprehensive review by Smith and Hanawalt (1969). Sunlight is the main source of UVR in nature and was the first physical damage inducing agent used to study the effects of UVR on EPF. The harmful

wavelengths of ultraviolet-A (UV-A; 315-400 nm) and, particularly, UV-B (280-315 nm) are of the greatest interest in EPF studies (Moore *et al.*, 1993; Fargues *et al.*, 1997b). While, the shortwave UV-C spectrum (200-280 nm) is considered the most harmful to biological systems, it does not reach the earth's surface due to atmospheric absorption and (Wang, 1976). Due to the ease of use, constancy and ability to use defined spectrums, simulated sunlight and ultraviolet (UV) lamps have been used to study the effects of UVR on EPF and other organisms. With regards to simulated sunlight, special care must be taken to ensure the appropriate spectrum is present. This should include little to no UV-C, some UV-B (peak of 315 nm) and more UV-A (peak of 380 nm), in addition to infrared and visible light (Zimmermann, 1982).

The inactivating effect of UVR was established using *Nomuraea rileyi* CS that were challenged with simulated sunlight that contained a relatively small amount of UV-C (Ignoffo *et al.*, 1976). After irradiation for 4 h, the CS were transferred to a leaf surface where the host insect would be confined for 48 h. Following this, the time to fungal mortality and insect infection was measured and showed that the half-life and percent original activity of the fungus was 2.4 hour (h) and 13.5 h, respectively. In contrast, Gardner *et al*. (1977) found that 10 days (d) of natural sunlight were required to reduce the insecticidal activity of *N. rileyi* to 10.6%. This large difference in time required to bring about a similar decrease in activity suggests crucial differences between these experiments were present. It is possible that differences existed between the environmental conditions of the two experiments, such as temperature and relative humidity which are known to influence EPF viability (Zimmermann, 1982). Also, the conidial concentration during irradiation differed, which can affect the dose received by the CS through physical shielding of the UVR (Chelico, 2004). Furthermore, it appeared that the simulated natural sunlight, employed as the source of UVR by Ignoffo *et al.* (1976) differed from natural

light, which was apparent by the differences in results obtained by Gardner *et al.* (1977) who used the latter source of UVR to challenge the same EPF. These results demonstrate the need for standardization of UVR sources, as well as other important variables so that meaningful comparisons can be made between inquiries (Wang, 1976).

Since the late 1970's a great deal of field and applied research has been performed on a variety of EPF to characterize their UVR tolerance to natural/simulated sunlight or a defined UV spectra by measuring the effects on germination, survival and/or pathogenicity. Measuring the germination rates of challenged CS has been a popular method of assessing UVR tolerance in EPF (Zimmermann, 1982; Smits *et al.*, 1996; Costa *et al.*, 2001; Chelico *et al.*, 2006; Fernandes *et al.*, 2007; Nascimento *et al.*, 2010). This method employs microscopy to view conidial morphology on slide cultures, solid media or in liquid media. A difficulty with using germination is that the assays have not been standardized and as a result the time when germination is measured differs between studies. This, combined with differences in irradiation conditions and the concentration of CS used, makes comparing germination values very difficult. Another important consideration for this method is that germinated CS may not develop into a colony forming unit (CFU) or be able to establish an infection. This is because processes involved in development can be negatively affected by UVR induced damage, and their consequences may not be manifested until long after germination, which is requisite for both CFU development and the establishment of an infection, which are positively correlated (Fargues *et al.*, 1997b; Inglis *et al.*, 1997).

Measuring viability post challenge is another strategy that has been used to assess UVR tolerance in EPF. This has been studied using either culturability (Braga *et al.*, 2001a; Braga *et al.*, 2001b; Braga *et al.*, 2001c) or CFUs (Inglis *et al.*, 1993; Smits *et al.*, 1996; Fargues *et al.*,

1997b; Inglis *et al.*, 1997; Chelico *et al.*, 2006). Culturability is determined similar to germination, but is enumerated after seven days post challenge. Furthermore, this method may be more robust than measuring germination because more than seven days would be sufficient for most viable propagules to germinate and develop and would not be as sensitive to differences in the time of measurement. Measurements based on CFUs are also more robust than those that are germination based, since they are also endpoint assessments of survival, as long as the enumeration is performed before the colonies over grow, causing the values to be underestimated, but late enough so viable propagules have sufficient time to form a CFU; generally two to five days is sufficient depending on the EPF and cell type studied (Chelico *et al.*, 2006).

Pathogenicity can also be used to measure UVR tolerance in EPF, as a function of the inactivation caused by the challenge (Hu *et al.*, 1996; Fargues *et al.*, 1997b; Inglis *et al.*, 1997). The concentration of CS irradiated is of particular importance when insect mortality is measured as to ensure all CS assayed received a consistent dose of UVR and were not shielded, due to an excessive number of CS per volume/area that was irradiated. Hu *et al*. (1996) demonstrated this effect by irradiating conidial suspensions of *B. bassiana* at concentrations of 10^8, 10^7 and 10^6 CS mL^{-1}. They found that only suspensions of 10^6 or 10^7 CS mL^{-1} showed a great reduction in percent mortality following UVR challenge, due to the shielding effect provided by higher concentrations of CS. Therefore, the concentration of the conidial suspension is of importance when designing such UVR experiments so that meaningful conclusions can be drawn from the data generated.

In addition to the general methods used to assess UVR tolerance many more differences exist between studies, including the type of EPF used, host insect, UV irradiance [W m^{-2} $second^{-1}$ (s)], duration of challenge and dose (J m^{-2}). As a result it is very difficult to make comparisons

between studies and necessitates the standardization of methods where applicable. Huang and Feng (2009) developed a method that has potential to help provide consistent UVR tolerance values. Here a modeling method was used to estimate the UVR tolerance as a function of the lethal UV-B dose for twenty *B. bassiana* isolates. This method required germination to be used as the measurement of viability; however it could be adapted to be used with other methods of measurement. The apparatus used to perform the UVR challenge contained an integrated microprocessor that enabled irradiance corrections four times per second. Although this may present a capital cost barrier, the strict control of UVR would certainly provide very accurate doses. This method would be useful to provide useful insight into relative UVR tolerance of EPF and could be combined with high-throughput enumeration tools to screen for UVR tolerant strains.

2.2 Types of DNA damage induced by short wave UVR

Solar UVR is divided into 3 groups which have common photochemical effects: UV-A, UV-B and UV-C wavelengths. Ultraviolet-A induced damage is caused by photo-oxidation of cellular molecules, such as lipids, proteins and DNA. The shorter wave lengths of the UVR spectrum that reach the Earth's surface (> 290 nm) are a part of the UV-B class. Although UV-B can also cause oxidative damage, its most deleterious biological effects are through the generation of DNA lesions caused by direct absorption of UVR photons. A DNA lesion is a type of DNA damage that alters its base structure, chemical composition, or tertiary structure. Lesions however, are not mutations but are mutagenic. They become mutations once the damaged base(s) is erroneously repaired and replicated; thus resulting in a permanent change within an organism's genome. Such DNA lesions can also be generated by UV-C and even

though this spectrum does not reach the Earth's surface, its biological effects have been shown to be the most detrimental (Wang, 1976). The UV-C spectrum is closest to the maximum absorption (254 nm) of DNA and therefore produces the DNA lesion generating photochemical reactions more efficiently that UV-B. Although UV-B can also induce oxidative damage and effect non-DNA molecules, the physical effects of UV-C on DNA are largely similar to those of UV-B (Reviewed in Ravanat *et al.*, 2001) and will be included together when discussing the effects of UVR induced DNA damage.

The pyrimidine bases cytosine and thymine absorb more UVR than purine bases (Wang, 1976). When pyrimidine bases are adjacent on a DNA molecule, dimerization reactions can occur from the energy transferred by the UVR photons. These reactions have been found to form two main types of dimers: CPD and (6-4)pyrimidine-pyrimidones [(6-4)PP], with the former comprising 70-90% of the UVR induced DNA photoproducts (Wang, 1976) (The TT CPD is the most common and is shown in Figure 2.1). The approximate distribution of CPD yield (lesions 10^{-4} bases J^{-1} m^{-2}) in DNA induced by UV-B for each reaction has been found to be 1.0, 0.6, 0.2 and 0.1 for TT, TC, CT and CC dimers, respectively (Ravanat *et al.*, 2001). A four-membered ring is formed between adjacent pyrimidines as a result of the saturation of the C5-C6 double bond. Due to the steric constraints, only *syn* containing isomers can be formed in DNA and oligonucleotides, with the *cis-syn* variety being generated in excess to the *trans-syn* (Ravanat *et al.*, 2001).

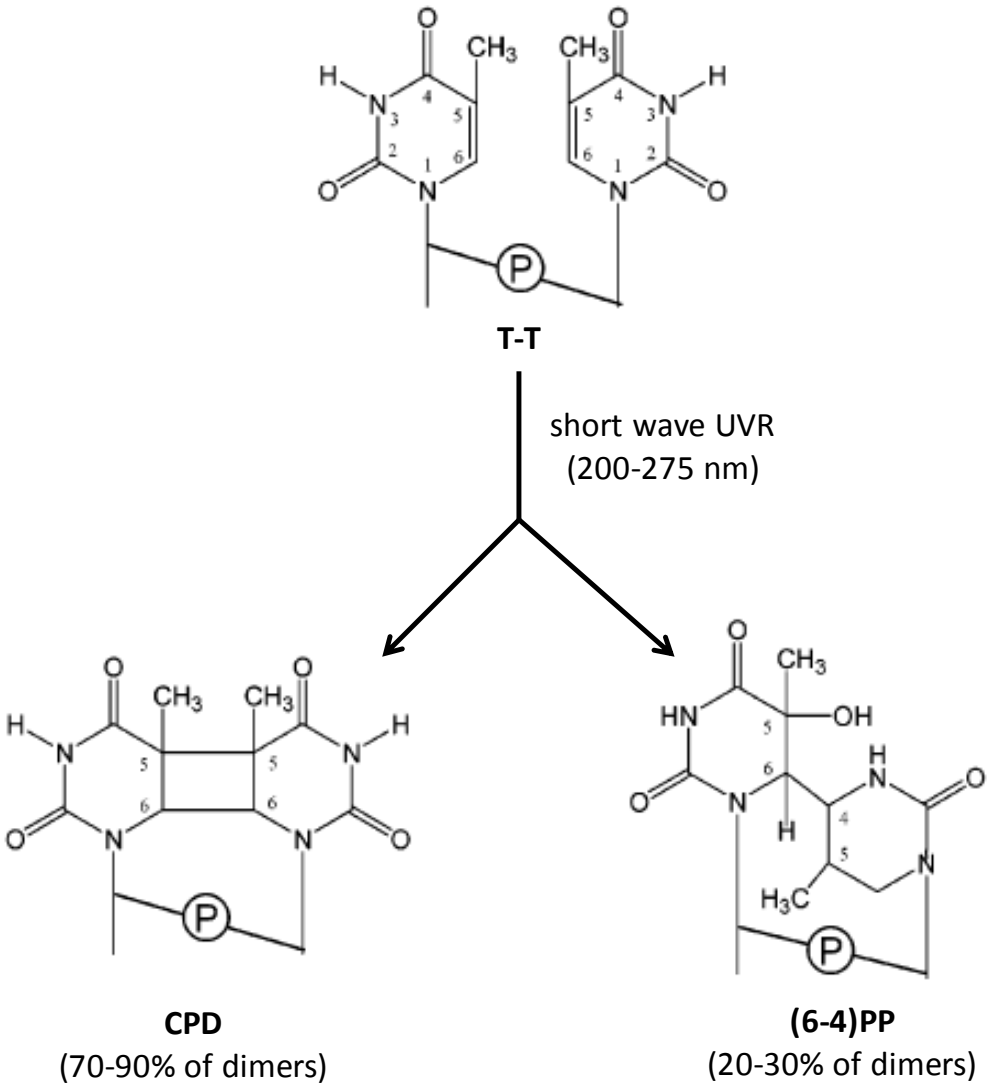

Figure 2.1 Structure of CPD and (6-4)PP DNA photoproducts induced by short wave UVR. Shown in the figure are the two major photoproducts that can form between adjacent pyrimidines, here shown at T-T sites, with the exception that (6-4)PPs are not formed between C-T. Also shown is the approximate proportion of each photoproduct formed in DNA following short wave UVR (Adapted from Sancar, 2003).

The second, less common DNA dimer induced by UVR is (6-4)PP is also shown in Figure 2.1. The (6-4)PP is formed from a cycloaddition involving the C5-C6 bond of the 5'-end pyrimidine and the C4 carbonyl group of the 3′-end thymine. This results in the formation of an unstable oxetane intermediate which is spontaneously rearranged to the (6-4)PP. This dimer, accounts for 20-30% of the total dimers induced by UV-C (Kim *et al.*, 1994) but only 10% under simulated sunlight (Yoon *et al.*, 2000). Under conditions of very high UV doses, it is possible for (6-4)PP to reach up to 40% of total photoproducts since these dimers are not reversible by UVR, unlike CPDs (Rahn and Hosszu, 1969). It is also possible for a Dewar valence isomer to be formed as an isomer of (6-4)PP, but is only through UV-B irradiation. The formation of the Dewar valence isomer, like the (6-4)PP, is preferred at T-C (LeClerc *et al.*, 1991).

With respect to UV-A induced DNA damage, its effects are much less than UV-B/UV-C because most of the energy is absorbed by other endogenous photosensitizers and DNA damage is caused by subsequent photo-oxidation reactions (Reviewed in Ravanat *et al.*, 2001). Briefly, these DNA damaging reactions have been termed type I (one-electron oxidation or hydrogen abstraction) and type II (singlet oxygen oxidation). Type I reactions can oxidize guanine and thymine to form 8-oxo-guanine or thymine glycols, respectively (Ravanat *et al.*, 2001). Type II reactions produce singlet oxygen ($^1O_2$) in the lower energy state through energy transfer from the excited photosensitizer to molecular oxygen. This $^1O_2$ has been found to react with electron rich molecules but guanine is the only base of DNA that is suited for the reaction type.

2.3 Studies of DNA repair in EPF

It has been observed in addition to reduced viability and pathogenicity, that UVR also delayed germination in EPF (Hunt *et al.*, 1994; Morley-Davies *et al.*, 1995). Hunt *et al*. (1994)

suggested this delay was needed for DNA repair and that reducing this delay would be beneficial for CS in the field.

The DNA repair pathway termed photoreactivation uses energy harvested from blue light wavelengths by CPD-PHR and (6-4)PP-photolyase [(6-4)-PHR] to monomerize CPDs and (6-4)PPs, respectively and improves survival of UVR challenged cells (refer to sections 2.4.2.1 and 2.4.2.2 for further details). The photoreactivation of UVR challenged CS was studied in *Lecanicillium longisporum* and *Aphanocladium album* where visible light (> 400 nm; wavelengths not conducive for photoreactivation), at irradiances of 12 or 150 W m^{-2} was used to promote photoreactivation (Braga *et al.*, 2002). This study showed that 12 W m^{-2} had no effect on the culturability of CS following UVR challenge in either fungi and 150 W m^{-2} of visible light reduced culturability by 20-40% depending on the UVR dose. This was an unexpected result since visible light has not been reported to be detrimental to fungal growth. Furthermore, a *Trichoderma* sp. was used as a positive control for photoreactivation and only showed an increase in culturability of 5-10% following photoreactivation. In contrast, Berrocal-Tito *et al*. (2007) reported an increase in survival of > 100-fold (following photoreactivation) in *phr-1*$^{-}$ *E. coli* complemented with *phr-1* from *Trichoderma atroviride* compared to those that were not. A significant difference in methodology is apparent in the study conducted by Braga *et al*. (2002) compared to Berrocal-Tito *et al*. (2007). This is because Braga and his colleagues used a filter to exclude visible light < 400 nm; however these are the optimal photoreactivating wavelengths for flavin containing CPD-PHRs (Sancar, 2003) and explains the lack reported photoreactivation phenotype. Also, the concentration of the CS suspension was not mentioned.

A comprehensive study was performed by Chelico *et al*. (2006) to determine the putative NER and photoreactivation capabilities of several EPF using UV-C radiation to induce the

formation of CPDs and (6-4)PPs in EPF DNA. Additional information on NER can be found in section 2.4.1 and for photoreactivation in sections 2.4.2.1 and 2.4.2.2. The pathway used by the fungi to repair most of the DNA damage was controlled by the presence or absence of unfiltered white light during post-UVR incubation to promote photoreactivation or NER, respectively. In addition, the concentration of CS was selected so that shielding would not influence their survival. The survival of irradiated CS was increased in all EPF by incubation in the presence of white light, compared to those incubated without. For example, after a dose of 240 J m^{-2}, survival increased by approximately 12 to 10,000-fold depending on the EPF. Furthermore, the survival curve of all EPF began with a 'shoulder', even under non-photoreactivating conditions. These 'shoulders' indicated that no killing occurred at the lower UVR doses and was followed by an exponential reduction in survival following higher doses. Such a 'shoulder' may indicate either insufficiency of the inactivating dose [based on the target theory (Kiefer, 1971)] or that the involved repair mechanisms were not overwhelmed by the presence of dimers. Therefore, it would be expected that the shoulder would be extended under photoreactivating conditions compared to repair in the dark (i.e. NER) because photorepair of DNA is more efficient than NER (Wang, 1976). This effect was observed by Chelico *et al*. (2006) who found that a dose of 36 J m^{-2}, compared to 60-120 J m^{-2}, was needed to measurably reduce survival in CS incubated without or with light, respectively. This study was the first to demonstrate that the photoreactivation phenomenon occurred in EPF.

The first report of DNA repair in EPF was presented by Chelico *et al*. (2005). This study was performed with *B. bassiana* CS and reported survival and quantified CPD formation induced by UV-C irradiation by exploiting the activity of T4 endonuclease V which nicks double-stranded DNA where a CPD is present. The formation of CPDs was inversely correlated with

survival and CPDs accumulated as a function of UVR dose in CS treated with or without light. However, those receiving photoreactivating light showed a maximum of ~ 15 CPDs 10 kb^{-1} of DNA, while those incubated in the dark had approximately twice the CPDs, with ~ 27 10 kb^{-1} of DNA at a dose of 500 J m^{-2} and survival rates of 0.0004% and ~ 0%, respectively.

The formation of CPDs induced by UV-B irradiation (> 290 nm) was also quantified in *M. acridum* by Nascimento *et al.* (2010). This study used the T4 endonuclease V method to quantify CPDs and found that their formation was proportional to UV-B dose and the quantity of CPDs was inversely related to germination. Following the highest UV-B dose (5.4 KJ m^{-2}), 83% and 99% of the CS germinated within 12 and 48 h, respectively, and this dose induced the formation of 0.255 CPDs 10 kb^{-1} of DNA. The UV-B irradiance used (1 W m^{-2}), although environmentally relevant (approximate to the UV-B irradiance during a sunny summer afternoon in Hangzhou, China), required 90 min of irradiance to be achieved, likely causing the number of CPDs induced to be underestimated compared to if a higher rate of irradiance was used. The use of higher irradiances would improve the accuracy of estimating the number of CPDs induced in the fungus since CPD repair is time dependent and would occur throughout the duration of the UVR challenge. This effect would be more obvious at even lower irradiances, where the rate of CPD formation would be equal to or less than the rate of removal. In this case, even very high doses may fail to produce a detectable number of CPDs. Although, it is not possible to directly compare the irradiance used in the studies by Nascimento *et al.* (2010) and Chelico *et al*. (2006) since they used UV-B and UV-C, respectively, it is clear that UV-C is more efficient in inducing CPD formation in DNA. For example, 0.240 KJ m^{-2} of UV-C was able to induce 5-12 CPDs 10 kb^{-1} of DNA in *B. bassiana*, while 5.4 KJ m^{-2} of UV-B induced only 0.255 CPDs 10 kb^{-1} of DNA.

The germination rates of and the number if CPDs in *M. acridum* following 5.4 KJ m^{-2} of UV-B was consistent with a dose that was low enough to be within the shoulder portion of the survival curve (Chelico *et al.*, 2005). However, Nascimento *et al.* (2010) did not mention if photoreactivating light was present during or after the UV challenge, therefore it is not possible to comment on light-dependent DNA repair in this study. It is of importance that this parameter be controlled and stated, especially in studies involving DNA repair following ecologically relevant UV intensities, as visible light and UVR are mutually inclusive in nature.

Much is known about DNA repair in fungi, with a great deal of work performed using the model yeast and filamentous fungus *S. cerevisiae* and *N. crassa*, respectively, but there is a major lack of understanding of the molecular biological principles that control these processes in EPF. Central to this is the lack of data regarding gene and protein sequences of the molecular machinery that are involved in DNA repair. Although homologues of many of the components known to be involved in DNA repair, such as the (6-4)-PHR, CPD-PHR and several required for NER, were present in the genomes of *M. acridum*, *M. anisopliae* (Gao *et al.*, 2011), *C. militaris* (Zheng *et al.*, 2011) and *B. bassiana* (Xiao *et al.*, 2012), the functional characterization of an EPF DNA repair system was not published until 2008.

Chelico and Khachatourians (2008) provided characterization of putative NER deficient mutants in *B. bassiana*. These mutants, generated by UVR, were UVR sensitive and likely deficient in NER, as shown by the loss of a shoulder in their UVR survival curves following incubation in the dark combined with a greater accumulation of CPDs in them compared to the wild type (WT). These putative NER mutants retained functional photoreactivation pathways. Photorepair was also studied by Fang and St. Leger (2012) through the genetic disruption of CPD-PHR and (6-4)-PHR in *Metarhizium robertsii* (this strain was formerly known as *M.*

anisopliae). This confirmed that the corresponding genes encoded the predicted repair activities involved in the removal of CPDs and (6-4)PPs. In addition, it was found that CPDs accumulated in the CS of *M. robertsii* when exposed to sunlight (cloudless day, 0.6 mW [nm m^{-2}]$^{-1}$ at 295 nm) from 11 pm onward and plateaued between 4 pm and 6 pm. In contrast, the formation of (6-4)PPs by solar-radiation did not outstrip the ability of *M. robertsii* to remove them. The CPD repair in both *M. robertsii* and *B. bassiana* was augmented by expressing a more efficient archaeal CPD-PHR from *Halobacterium salinarum*, which increased photorepair by > 30 (Fang and St Leger, 2012). Furthermore, solar-irradiated WT spores took 14 d to kill 58% of mosquitoes (*Anopheles gambiae*), whereas CS expressing the transgenic CPD-PHR took 11 d to kill 100%. This work demonstrated that transgenic improvement is a useful strategy to improve the UV tolerance of EPF.

2.4 The CPD and (6-4)PP repair systems

An inherent characteristic of the storage of genetic information in DNA is that the molecule is not chemically inert. Therefore, it is susceptible to insults from a variety of chemical and physical agents, which can corrupt the information and compromise its ability to be read as the same as before the insult. This can result in the loss or change in the corresponding biological function encoded by the DNA. As a result, an extensive array of DNA repair mechanisms has evolved. Interestingly, the need for such mechanisms was not apparent to Francis Crick, upon discovering the structure of DNA (Crick, 1974).

This section will focus on repair mechanisms possessed by fungi enabling them to repair the main types of UV-C/UV-B induced DNA damage, i.e. CPDs and (6-4)PPs. Therefore, photoreactivation and NER will be the primary interest since they account for the vast majority

of repair of CPDs and (6-4)PPs (Friedberg *et al.*, 2006). A variety of other DNA repair pathways, such as base excision repair, recombinational repair and mitochondrial repair, are also utilized by fungi but repair other types of DNA damage (Reviewed in Goldman *et al.*, 2002; Goldman and Kafer, 2004; Inoue, 2011). For example, base excision repair can remove damaged bases that have undergone methylation, oxidation or deamination. Excision is achieved through glycolysis of the N-glycosyl bonds between the damaged base and deoxyribose phosphate backbone (Friedberg *et al.*, 2006). This is followed by the creation of a free 5' deoxyribose phosphate end by apurinic/apyrimidinic endonuclease to create an appropriate substrate for DNA polymerase to fill-in the excised base with subsequent covalent joining of the DNA strand by DNA ligase.

Pathways to tolerate DNA damage have also been documented and include postreplication repair, translesion DNA synthesis, damage checkpoints and histone modification (Friedberg *et al.*, 2006). These pathways, unlike photoreactivation and NER, do not repair lesions; instead they provide the cell with mechanisms to tolerate them. For example, when damaged DNA is recognized by the replicative machinery during DNA synthesis the process is stalled so that repair can occur. Translesion DNA synthesis can overcome this arrest through two specialized 'sloppy copier' DNA polymerases (POLη and POLι) which bind to the stalled complex (Reviewed in Friedberg, 2003). This generates a conformational change in the complex to place POLη in close proximity with the lesion, allowing it to synthesize DNA through the lesion-containing template strand in spite of the damage. The replicative bypass is then completed by POLι, which introduces several more nucleotide residues (nts) and replication resumes as normal after this.

2.4.1 Nucleotide excision repair

Nucleotide excision repair is the most flexible DNA repair pathway. In addition to UVR induced damage, including CPDs and (6-4)PPs, NER is also capable of repairing bulky base adducts induced by chemical mutagens or other damage that cause DNA helix distortion (Friedberg *et al.*, 2006). The most complete models of NER have been obtained from studies in *S. cerevisiae* and humans (Friedberg *et al.*, 2006). These studies have revealed that NER is coupled to transcription and involves the assemblage of a large multiprotein complex called the repairosome. An overview of NER in *S. cerevisiae* is shown in Figure 2.2. Once the DNA damage is detected by the DNA-binding protein, RAD-14 (radiation sensitive 14), the repairosome is sequentially recruited to the site and assembled. Helicase activity, possessed by RAD-3 (5' to 3' activity) and RAD-25 (3' to 5' activity) associated with transcription initiation factor II H, unwinds the DNA, approximately 30 bp surrounding the lesions, to form a denaturation bubble. The damage containing strand is then cut by the RAD-1/RAD-10 complex and RAD-2 endonucleases several bases to the 5' and 3' side of the lesion, respectively. The corresponding gap in the DNA strand is then filled-in by the replicative DNA polymerases (Polε or Polδ) which use the strand complementary to the gap as a template. The repair is completed by covalent attachment of the newly synthesized strand to the existing DNA strand by DNA ligase.

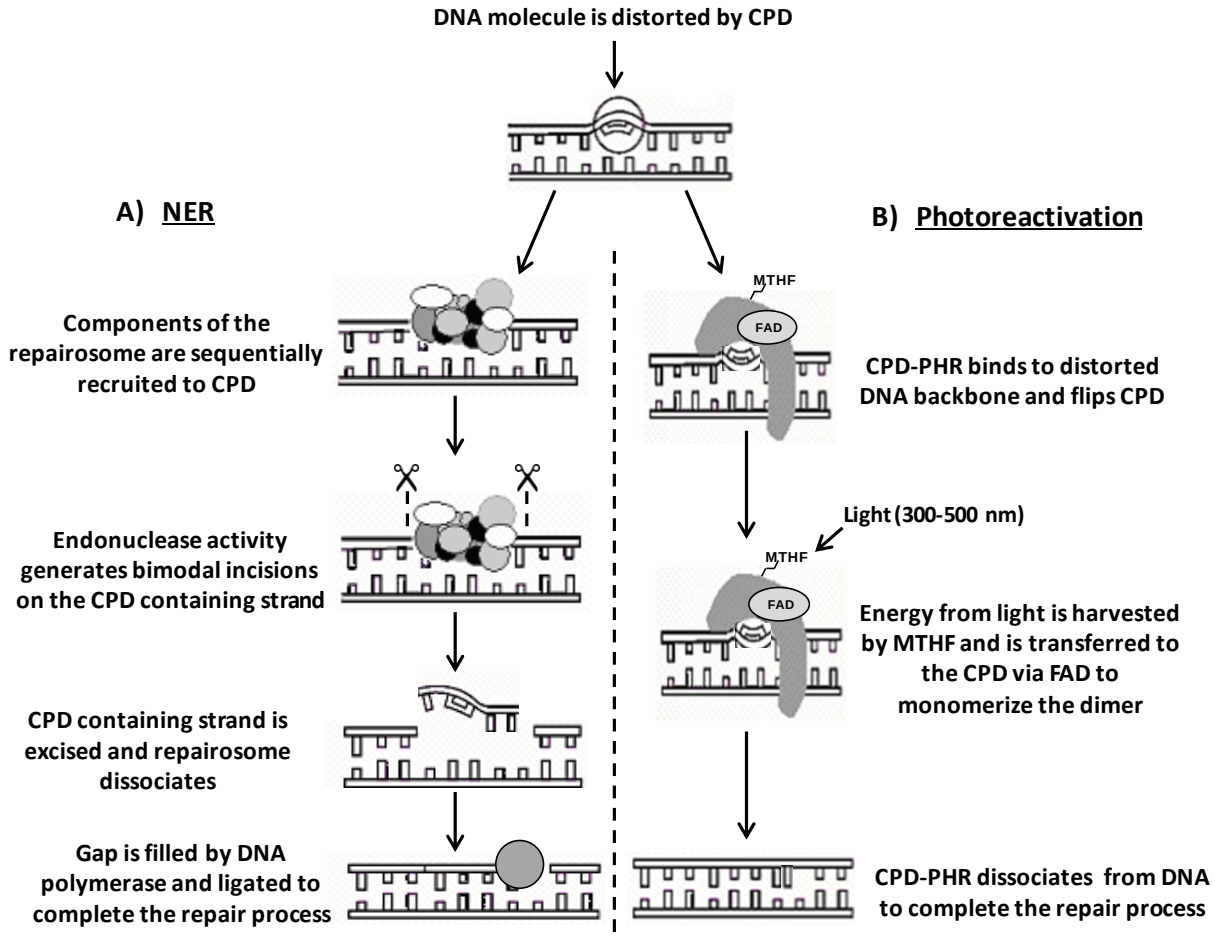

Figure 2.2 Overview of CPD repair process by NER and photoreactivation. The processes of A) NER by the repairosome and B) photoreactivation by CPD-PHR are shown. For additional detail see sections 2.4.1 or 2.4.2.1 for NER or photoreactivation, respectively (Adapted from Chelico, 2004).

Photoreactivation and NER appear to complement each other, as the presence of the repairosome improves photorepair of the section of the strand of DNA that was not actively transcribed, through the ability of the repairosome to alter local chromatin structure and to improve the access of CPD-PHR to dimers (Reviewed in Sancar, 2000). Furthermore, in the absence of light, CPD-PHR stimulates NER on the non-transcribed strand. In *E. coli*, this is thought to be through CPD-PHRs ability to flip the CPD out of the helix and further distort the DNA structure, which is a strong determinant for the interaction between the repairosome and DNA damage (Sancar *et al.*, 1984).

There is a subset of the NER pathway called global genomic repair that functions in inactive DNA (not being actively transcribed) irrespective of it being a part of the heterochromatin or on the non-transcribed strand of an active region (Friedberg *et al.*, 2006). Only the DNA damage recognition step differs and is controlled by the RAD-7/RAD-16 complex, rather than RAD-14. Here, the RAD-16 functions as a helicase and RAD-7 promotes the accessibility of the NER complex to non-transcribed double or single stranded DNA which can be blocked by histones or RNA polymerase, respectively. Once the damage is recognized, the NER pathway is identical to that which occurs in actively transcribed DNA. It is worth noting that *S. cerevisiae* with non-functional RAD-7 or RAD-16 is only slightly UV sensitive since RAD-7/RAD-16 are only responsible for the removal of 20 to 30% of CPDs repaired by NER (Verhage *et al.*, 1994).

The role of NER and its involvement in the DNA damage response has not been as well characterized in filamentous fungi. The reason for the dichotomy in the understanding of NER between *S. cerevisiae* and filamentous fungi is the presence of redundant NER pathways in the latter. The presence of these pathways has increased the difficulty in generating mutants with UV sensitive phenotypes. However, this hurdle has been overcome as NER in *Aspergillus nidulans* (Goldman *et al.*, 2002; Goldman and Kafer, 2004) and *N. crassa* (Inoue, 2011) has been extensively studied. Furthermore, many of the homologues of the NER complex in *S. cerevisiae* can be found in these and other filamentous fungi including EPF through the available fungal DNA sequence databases, suggesting that the components of the repairosome are largely conserved in fungi. In addition, putative NER mutants have been generated and characterized in *B. bassiana* (Chelico and Khachatourians, 2008) and the presence of a *rad-1* homologue in three *Beauveria* spp., *Isaria farinosa, M. anisopliae* and *Tolypocladium inflatum* has been confirmed experimentally by Southern hybridization (Chelico, 2004).

As mentioned above, the redundant repair pathways have made generating UV sensitive mutants very difficult. This required that the activities of both MUS-38 (a homologue of RAD-1) and MUS-18 be abolished in *N. crassa* in order for a UV sensitive phenotype to shown (Hatakeyama *et al.*, 1998). Interestingly, MUS-18, was discovered to be involved in a novel pathway capable of the excision of both CPD and (6-4)PP (Yajima *et al.*, 1995) and was later characterized in the fission yeast *Schizosaccharomyces pombe* (Reviewed in McCready *et al.*, 2000). Sequences encoding homologues of MUS-18 are present in the genomes of the EPF *B. bassiana* (Xiao *et al.*, 2012), *C. militaris* (Zheng *et al.*, 2011), *M. acridum* and *M. anisopliae* (Gao *et al.*, 2011), as determined by a basic local alignment search tool (BLAST) using the corresponding amino acid sequences from *N. crassa* as inputs. However, studies have not been

conducted in EPF that focus on this pathway and represent an area that requires attention so that UVR repair in EPF can be better understood.

An interesting new area of research is the regulation of NER pathways through ubiquitination (Reviewed in Li *et al.*, 2011). Although much of the research has been conducted in mammalian systems, it is likely that these regulatory pathways are also involved with NER in lower eukaryotes. For instance, EPF contain sequences that encode candidate homologues of the E1 ubiquitin-activating enzyme, E2 ubiquitin-conjugating enzyme and E3 ubiquitin-protein ligases, as determined by a query using the BLASTp tool with the corresponding sequences from *S. cerevisiae* as inputs. This ubiquitin-mediated regulation is achieved through both proteasomal degradation-dependent and -independent mechanisms (Ramadan and Meerang, 2011). For instance, during global genomic repair the UV damaged DNA-binding protein forms an E3 ligase complex to initiate chromatin remodeling by poly-ubiquitination of the histone to help accommodate the assembly of the NER complex. The E3 ligase then polyubiquitinates XPC (xeroderma pigmentosum group) and improves DNA-binding efficiency of the XPC-HR23B (a RAD-23 homologue) complex, which is involved in damage recognition. A subunit of the UV damaged DNA-binding protein 2 is then polyubiquitinated and degraded through the proteasomal pathway, facilitating the dissociation of the damaged DNA-binding protein-E3 ligase complex from the site of UV induced DNA damage.

2.4.2 Structure and functional biology of photoreactivating enzymes and other related proteins

Biological responses to light have long been an area of interest in scientific research. Several light dependent responses, such as those involved in growth, regulation of the circadian

clock and photoreactivation, have been found to be controlled by a group of apoenzymes classified into three main groups (Reviewed in Sancar, 2003; Partch and Sancar, 2005). Two of these, the CPD-PHRs and (6-4)-PHRs, specifically repair CPDs and (6-4)PPs, respectively, while CRYs are involved in light dependent growth responses and regulation of the circadian clock in plants and animals, respectively. Both PHRs and CRYs are 50-70 kDa proteins that contain two cofactors, one is always flavin adenine dinucleotide (FAD) and the presence and type of the second is dependent on the type of PHR/CRY, but is usually 5,10-methenyltetra-hydrofolate (MTHF) or 8-hydroxy-5-deazaflavin, in rarer cases. The (6-4)-PHRs are considered a single class and can be found in many eukaryotes, such as insects (Todo *et al.*, 1993) and some fungi (Bluhm and Dunkle, 2008).

The CPD-PHR and CRY groups have been further categorized into classes. For CPD-PHR these are simply named class I, II and III, which are generally found in bacteria and microbial eukaryotes, archaea and metazoan eukaryotes, and bacteria, respectively (Reviewed in Sancar, 2003; Müller and Carell, 2009). These were grouped due to the sequence similarity of CPD-PHRs in the same class (Figure 2.3). The CRY classes are named for the type of organism in which they are typically found: plant-CRY, insect-CRY, vertebrate-CRY and the DASH-CRY (Brudler *et al.*, 2003), which have been identified in *Synechocystis* and named for their homo-logy with CRYs from *Drosophila*, *Arabidopsis* and *Homo* (Reviewed in Sancar, 2003; Partch and Sancar, 2005). The DASH-CRYs are thought to have evolved divergently, while plant-CRYs and the other two CRYs are thought to be more closely related to class III CPD-PHR and (6-4)-PHR, respectively (Oztürk *et al.*, 2008).

Figure 2.3 Unrooted phylogenetic tree showing relationships between PHR and CRY proteins from fungi and other organisms. Highlighted clades indicate phylogenetically distinct groups of PHR/CRY. Asterix (*) and plus (+) symbols designate examples of CPD-PHR from EPF and classes of PHR/CRY found in fungi, respectively. Homology searches and alignments for phylogenetic analysis were performed as described in section 3.3.6 and the sequences used are listed in Table 3.2. Branch support values were provided for important points of divergence and the scale conveys branch lengths to the number of substitutions per site. The taxon labels include the organism the input sequence was derived from and its accession number. This analysis was performed using the service provided by Dereeper *et al*. (2008). The maximum likelihood method in the PhyML program (v3.0 aLRT) was used to reconstruct the phylogenetic tree. Support for internal branching was evaluated using the bootstrap method with 200 replicates (Guindon and Gascuel, 2003). The substitution models were selected assuming an estimated proportion of invariant sites equal to 0.026 and the gamma shape parameter was estimated to be 1.062.

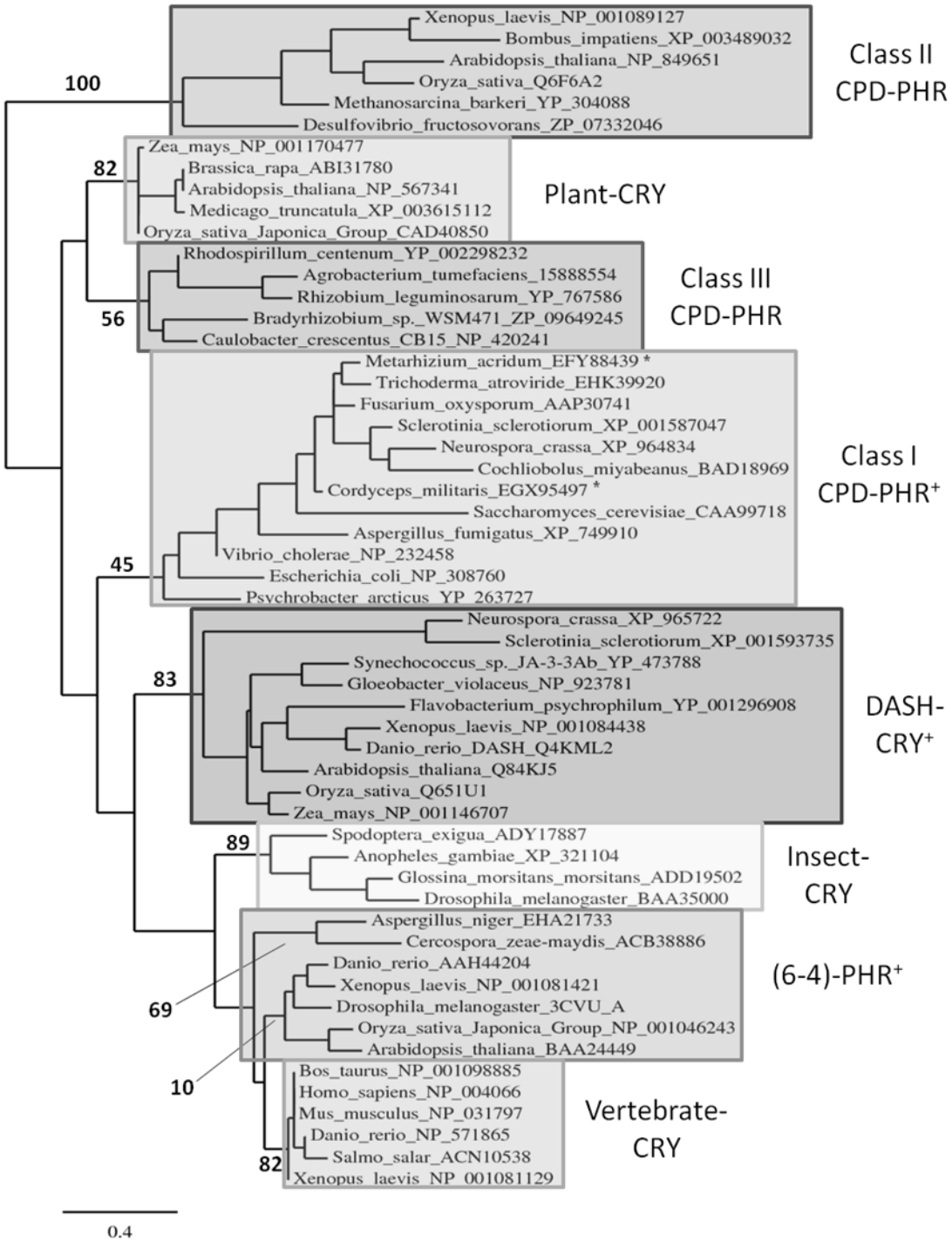
Xenopus_laevis_NP_001089127
Bombus_impatiens_XP_003489032
Arabidopsis_thaliana_NP_849651
Oryza_sativa_Q6F6A2
Methanosarcina_barkeri_YP_304088
Desulfovibrio_fructosovorans_ZP_07332046
Class II CPD-PHR
100
Zea_mays_NP_001170477
Brassica_rapa_ABI31780
Arabidopsis_thaliana_NP_567341
Medicago_truncatula_XP_003615112
Oryza_sativa_Japonica_Group_CAD40850
Plant-CRY
82
Rhodospirillum_centenum_YP_002298232
Agrobacterium_tumefaciens_15888554
Rhizobium_leguminosarum_YP_767586
Bradyrhizobium_sp._WSM471_ZP_09649245
Caulobacter_crescentus_CB15_NP_420241
Class III CPD-PHR
56
Metarhizium_acridum_EFY88439 *
Trichoderma_atroviride_EHK39920
Fusarium_oxysporum_AAP30741
Sclerotinia_sclerotiorum_XP_001587047
Neurospora_crassa_XP_964834
Cochliobolus_miyabeanus_BAD18969
Cordyceps_militaris_EGX95497 *
Saccharomyces_cerevisiae_CAA99718
Aspergillus_fumigatus_XP_749910
Vibrio_cholerae_NP_232458
Escherichia_coli_NP_308760
Psychrobacter_arcticus_YP_263727
Class I CPD-PHR+
45
Neurospora_crassa_XP_965722
Sclerotinia_sclerotiorum_XP_001593735
Synechococcus_sp._JA-3-3Ab_YP_473788
Gloeobacter_violaceus_NP_923781
Flavobacterium_psychrophilum_YP_001296908
Xenopus_laevis_NP_001084438
Danio_rerio_DASH_Q4KML2
Arabidopsis_thaliana_Q84KJ5
Oryza_sativa_Q651U1
Zea_mays_NP_001146707
DASH-CRY+
83
Spodoptera_exigua_ADY17887
Anopheles_gambiae_XP_321104
Glossina_morsitans_morsitans_ADD19502
Drosophila_melanogaster_BAA35000
Insect-CRY
89
Aspergillus_niger_EHA21733
Cercospora_zeae-maydis_ACB38886
Danio_rerio_AAH44204
Xenopus_laevis_NP_001081421
Drosophila_melanogaster_3CVU_A
Oryza_sativa_Japonica_Group_NP_001046243
Arabidopsis_thaliana_BAA24449
(6-4)-PHR+
69
Bos_taurus_NP_001098885
Homo_sapiens_NP_004066
Mus_musculus_NP_031797
Danio_rerio_NP_571865
Salmo_salar_ACN10538
Xenopus_laevis_NP_001081129
Vertebrate-CRY
10
82
0.4

All CRYs share 25-40% sequence similarity with PHRs, with the most sequence similarity being found in the N-terminal region of CRY, termed the PHR homology region, which contains the α-helical domain . However, the diverse functionality of CRY proteins is partially achieved through variation in the C-terminal region (Miyamoto and Sancar, 1998). Many CRYs, especially those from plants also have a C-terminal extension of 50-250 aa that has no sequence similarity to CPD-PHRs (Ahmad and Cashmore, 1993). Interestingly, overexpression of this extension in *Arabidopsis* induced a phenotype similar to continuous blue light exposure, even under red light, suggesting this region was involved in self-regulating the CRY-dependent light response (Yang *et al.*, 2000). Similarly, fungal CPD-PHRs have an N-terminal tail of approximately 140 aa, which, in addition to possessing putative signals for nuclear and mitochondrial translocation, may also be involved in their auto-regulation through a suspected interaction with homologues of the white-collar protein, a class of photoreceptors (Berrocal-Tito *et al.*, 2007).

Although only moderately related by sequence (25-40%), the PHR and CRY proteins are very close structural homologues and their Cα backbones are nearly superimposable (Reviewed in Sancar, 2003; Müller and Carell, 2009). This is evident through the solved structures of several PHRs (Park *et al.*, 1995; Tamada *et al.*, 1997) and the PHR homology region of CRYs (Brudler *et al.*, 2003). Solved PHR structures contain two domains connected by a long loop; an N-terminal α/β-domain and a C-terminal α-helical domain. The α-helical domain contains the catalytic FAD and the second chromophore is located between the two domains, near the surface of the protein. Close to the middle of the α-helical domain is a hole of approximately 10 Å which is thought to allow solvent and oxygen to access the FAD and is of the correct size and

polarity to allow CPD entry, so that FAD is within van der Waals contact distance (Park *et al.*, 1995).

Photoreactivation is a DNA repair mechanism that reverses damage through the transfer of electrons acquired from light (300-500 nm) energy absorbed by bound cofactors. In contrast with the versatile NER, both CPD-PHR and (6-4)-PHR specifically repair CPDs and (6-4)PPs, respectively, while CRYs have been found to be involved in the regulation of the circadian rhythm (Reviewed in Sancar, 2003; Müller and Carell, 2009). It has been found that some cross functionality between these groups exists. For instance, the CPD-PHR from the marsupial *Potorous tridactylus*, which possesses repair activity, was shown to also affect the circadian clock in mice (Chaves *et al.*, 2011). This was achieved by expressing the CPD-PHR in *cry-1*/*cry-2* double knockout mutants which restored the molecular oscillator in the liver, implying this CPD-PHR can function as a CRY protein, in addition to a DNA repair enzyme. The processes of, CPD-PHR and (6-4)-PHR will be reviewed below.

2.4.2.1 The CPD-PHRs

Classical photoreactivation, controlled by CPD-PHR, was the first DNA repair mechanism to be discovered (Rupert *et al.*, 1958) and will be the definition for photoreactivation used here on, unless otherwise stated. These enzymes are monomeric proteins consisting of 450-550 aa and possess two covalently bound chromophores. Fungi have class I CPD-PHR, which are also found in some bacteria and archaea, while class II and III are generally found in higher eukaryotes (Kim *et al.*, 1996a; Hirouchi *et al.*, 2003) and some bacteria (Oztürk *et al.*, 2008), respectively. Depending on the organism, transcription of *phr-1* can be induced by blue light

(Berrocal-Tito *et al.*, 2007), visible light (Alejandre-Durán *et al.*, 2003), UV light and also a variety of chemical mutagens (Sancar *et al.*, 1995).

Repair of CPDs by CPD-PHR is more efficient than NER and when light is present up to 90% of CPDs can be corrected through this mechanism (Wang, 1976). Photoreactivation is accomplished using energy harvested by the reduced FAD cofactor from near-UV photons (300-500 nm), allowing specific binding and repair of CPDs by CPD-PHR (Sancar *et al.*, 1987a). Notably, this repair is achieved with complete fidelity to the original DNA sequence. Class I CPD-PHRs also possess a second chromophore in addition to FAD (Jorns *et al.*, 1987; Sancar *et al.*, 1987b). The second chromophore of CPD-PHRs may be either MTHF or an oxidized 8-hydroxy-5-deazaflavin derivative and is used to distinguish the type of CPD-PHR, i.e. folate or flavin containing types. The second chromophore is not required for repair; however, its presence can increase the reaction rate of the enzyme by 10 to 100-fold when light is limiting due to its higher extinction coefficient and maximum absorption at a longer wavelength compared to the reduced active form of FAD (Payne and Sancar, 1990). The maximum absorptions of folate and flavin containing types of CPD-PHRs differ, being 380-410 nm and 435-445 nm, respectively (Reviewed in Sancar, 2003).

The mechanism of class I CPD-PHR mediated repair will be addressed here (Figure 2.2B). A CPD-PHR can bind to damaged DNA, independent of light, and through a base flipping mechanism the CPD is placed into the active site cavity of the enzyme. The photon absorbed by the secondary chromophore, either MTHF or 8-hydroxy-5-deazaflavin, can then be transferred to the CPD, through FAD, to monomerize the dimer. An electron then is donated back to the semi-reduced flavin radical to regenerate the reduced form of the FAD molecule.

The enzyme can then dissociate from the repaired site and the process can be repeated as long as FAD remains associated (Sancar, 2003).

Interestingly, neither the presence nor the absence of the secondary chromophore affects the ability of CPD-PHR to interact with its substrate (Hamm-Alvarez *et al.*, 1989; Malhotra *et al.*, 1992). Rather, key structural features are important to the affinity and specificity of the enzyme including: (i) the positively charged groove that runs across the surface of the helical domain, (ii) a 'hole' in the centre of the groove with correct dimension that accommodates the dimer and (iii) the FAD that is at the bottom of the hole (Sancar, 2003). In addition, CPD-PHR can also bind other types of DNA damage, although less stably than with CPDs. The DNA-binding of CPD-PHR is structure-specific, rather than sequence-specific (Sancar, 2003). This implies that its specificity is a result of the backbone structure of the DNA duplex at the binding site and the chemical structure of the lesion, so that binding can occur and the lesion can fit the hole. This is in contrast with sequence specific DNA-binding proteins whose interactions are controlled mainly by hydrogen bonding in the major and minor groove of the duplex. In general, the binding affinity of structure specific DNA-binding proteins is sequence independent (Sancar, 2003).

With regards to the active site of CPD-PHR, it appears that the hole itself is required for FAD to be within close enough proximity to allow direct electron donation to the CPD. It has been determined through site-directed mutagenesis (Li *et al.*, 1991) and time-resolved electron paramagnetic resonance experiments (Kim *et al.*, 1993) that Trp306 is essential for electron transfer to FAD, a requirement for monomerization of CPD. However, the crystal structure of CPD-PHR from *E. coli* (Park *et al.*, 1995) revealed that Trp306 was located near the surface of the protein and could not be directly involved in the electron transfer to FAD. Upon inspection

of the crystal structure two potential pathways for electron transfer became evident (Reviewed in Sancar, 2003; Brettel and Byrdin, 2010). One pathway was sequentially through Trp306, Trp358 and Trp382 to FAD involving three electron hops. The second was through α-helix 15, between residues 358-366. It was confirmed that an electron transfer occurred from Trp382 to the flavin within the appropriate time frame (Aubert *et al.*, 2000). However, mutations that affected the tryptophan triad were not found to affect the enzymes repair activity photorepair (Li *et al.*, 1991; Kavakli and Sancar, 2004). A recent study by Liu *et al*. (2012) has provided evidence for electron transfer by the tunneling pathway through α-helix 15. This report has shown that both the forward and back donation of an electron to initiate repair and cofactor restoration, respectively, occurs through the electron tunneling pathway.

2.4.2.2 The (6-4)-PHRs

Before 1993, it was thought that repair of (6-4)PPs was dependent on NER. Todo *et al*. (1993) discovered a (6-4)-PHR from *D. melanogaster* that was able to repair (6-4)PPs, which can be lethal if even one was left unrepaired. The mode of action of (6-4)-PHR is similar to CPD-PHR, namely through the use of a base flipping mechanism and electron transfer from FAD to monomerize the dimer (Reviewed in Sancar, 2003). In addition to insects, this group of PHR has also been characterized in plants (Nakajima *et al.*, 1998), fungi (Bluhm and Dunkle, 2008) and other animals, such as *Xenopus laevis* (Kim *et al.*, 1996b), but not bacteria. Although this system was not found to be associated with photoreactivation in *B. bassiana* (Chelico, 2004), its presence was confirmed in *M. anisopliae* (Fang and St Leger, 2012).

2.4.2.3 The CRYs

Most of the understanding of CRY function is derived from genetic studies (Sancar, 2003). This is because of the difficulties in obtaining recombinant CRY proteins due to the loss and/or oxidation of the bound cofactors required for their function. Both folate and FAD are cofactors of the CRYs from plants and animals. Placental mammals do not possess PHR activity (Li *et al.*, 1993), therefore the discovery of CRYs, as a PHR homologue, amongst human ESTs was unexpected (Adams *et al.*, 1995). These were later found to be involved in circadian clock-setting using both light-dependent and light-independent mechanisms (Reviewed in Partch and Sancar, 2005).

The first CRY was discovered in *Arabidopsis thaliana* and was found to be encoded by *hy-4* (hypocotyl elongation response) (Ahmad and Cashmore, 1993) and will be used here to provide a brief overview of CRY function. Plants with mutations in this gene lost responsive-ness to blue-light and were found to have restricted morphological features, such as stem elongation and stimulation of leaf expansion, indicating that a component of the blue-light signalling pathway had been disrupted. Furthermore, HY-4 shared sequence similarity with CPD-PHR from *E. coli* (Ahmad and Cashmore, 1993) and also co-purified with flavin (Lin *et al.*, 1995), but did not have repair activity (Malhotra *et al.*, 1995). It appeared that CRYs influenced photomorphogenic changes in *A. thaliana* through modulation of gene expression (Ma *et al.*, 2001). This has been demonstrated through analysis of *cry1*/*cry2* mutants which lost the ability to regulate many genes in response to blue light.

2.4.2.4 The DASH-CRYs

The PHR/CRY family was expanded with the discovery of DASH-CRY in the cyano-bacterium *Synechocystis* (Hitomi *et al.*, 2000; Ng and Pakrasi, 2001) and later in other organisms including the filamentous fungi *Sclerotinia sclerotiorum* (Veluchamy and Rollins, 2008) and *Fusarium fujikuroi* (Castrillo *et al.*, 2013). The DASH-CRYs were originally classified as CRYs because they did not contribute to photoreactivation *in vivo* (Hitomi *et al.*, 2000; Worthington *et al.*, 2003). However, it has been shown that CRY-3 from *A. thaliana* has the ability to repair CPDs in single stranded DNA (Selby and Sancar, 2006). This difference in functionality is supported by the phylogenetics of these proteins whereby the DASH-CRYs appear to be more closely related to CPD-PHRs than (6-4)-PHRs and share specificity to CPDs as do CPD-PHRs (Figure 2.3). Nonetheless, DASH-CRYs appear to be involved in conventional CRY-like functions; however, there is a lack of understanding of the physiological function of these proteins, although some clues exist. For instance, DASH-CRY mutants in *S. sclerotiorum* were developmentally normal, other than a decrease in sclerotial mass and an increase in the number of pigmented hyphal projections on apothecial stipes under UV-A (Veluchamy and Rollins, 2008). This suggested DASH-CRY does not play an obvious role in light responses in fungi and that redundant pathways may exist, potentially masking the resulting phenotype in DASH-CRY mutants (Kleine *et al.*, 2003). However, in *F. fujikuroi* CRY-DASH mutants morphological and pigmentation differences were observed, in addition to variations in secondary metabolism (Castrillo *et al.*, 2013).

2.5 Studies of heat tolerance in EPF

The EPF are generally mesophiles, possessing optimal growth temperatures of 25-30 °C (Roberts and Campbell, 1977). For example, *B. bassiana* can grow when exposed to temperatures between 8 to 35 °C with a maximum thermal threshold of 37 °C (Fargues *et al.*, 1997a). Therefore, it is a requirement in integrated pest management programs to use an EPF that can grow and develop in the temperature range found in the ecosystem it is to be used. This concept has been used to select EPF for the control of insects, such as curculionids at temperatures below 15 °C (Doberski, 1981) and noctuids at temperatures above 25 °C (Ignoffo *et al.*, 1976). There continues to be interest on the impacts of heat and other stress on EPF and much research has been focused on characterizing the heat tolerance of this group of fungi under a variety of conditions. Temperatures above those conducive for growth are considered supraoptimal and may be a source of high heat stress that can cause inactivation in a time dependent manner. Fernandes *et al.* (2008) characterized the heat tolerance of CS in a variety *Beauveria* spp.. They found that after 1 h at 45 °C, > 60% of the germinated in > 70% of the strains tested, with the range of germination being 0% to 100%. However, the impacts of heat stress can be modified by the conditions present during the challenge.

The effects of heat can be altered by relative humidity and the nature of the medium (liquid, semi-liquid, dry) the propagules are challenged in, all which influence the thermal death point. It is well known from sterilization techniques that heat treatment is much more efficient at reducing viability when water, either free liquid or vapor, is present. This prompted the study by Zimmermann (1982) of the heat tolerance of *M. anisopliae* using CS and germination measurements, by challenging them for 30 min under various temperatures and relative humidity. As expected, results of this test showed that the median lethal time of *M. anisopliae* CS was

inversely correlated with relative humidity. It was found that the median lethal temperature was 42 °C in a liquid suspension and 50.5 °C, 57.5 °C and 68.8 °C at 100%, 76% and 33% relative humidity, respectively. The consideration of relative humidity is very important when studying heat tolerances in any biological system. In nature, relative humidity can fluctuate due to precipitation, the substrate and others factors. In addition, once an EPF has infected an insect, the fungal biomass that propagates within the hemocoel is in a contained, liquid environment, which does not allow for evaporative cooling. This is especially important when compounded with a phenomenon, termed behavioral fever, which some insects exhibit.

Although the highest summer temperatures of most of the world's arable land rarely reach 45 °C or greater, heat stress remains an important consideration since it can also aggravate the detrimental effects of solar UVR (Smits *et al.*, 1996). Insects are cold blooded; however it is well known that several types of insects, including grasshoppers (Carruthers *et al.*, 1992), locusts (Elliot *et al.*, 2002) and flies (Kalsbeek and Mullens, 2001) thermoregulate by basking in the sun or seeking shade. Furthermore, infected insects, such as grasshoppers will seek higher temperatures or bask in the sun to increase their internal body temperature by 5 to 15 °C above the surrounding air temperature (Carruthers *et al.*, 1992) and subject themselves to a behavioral fever (Reviewed in Roy *et al.*, 2006).

The mechanisms by which behavioral fever contributes to an insect overcoming infections are not well understood, however two hypotheses have been pursued. The first suggests that the elevated body temperature reached via the fever is likely deleterious to the pathogen (Arthurs and Thomas, 2001). This is supported by the temperature range required for growth by the mesophilic EPF, such as *B. bassiana* and *Metarhizium* spp. (Fargues *et al.*, 1997a; Ouedraogo *et al.*, 1997) and the negative correlation between the insect's internal temperature

being above the EPF's maximum growth temperature and mycosis induced insect mortality (Inglis *et al.*, 1996; Ouedraogo *et al.*, 1997; Arthurs and Thomas, 2001). The second hypothesis is that the insect immune response may be augmented by thermoregulation (Ouedraogo *et al.*, 2003). Ouedraogo *et al*. (2003) investigated the effects of thermoregulation on hemocyte kinetics. It was found that thermoregulation helped to suppress fungal growth, possibly by the maintenance of hemocyte population levels which were higher and correlated with increased phagocytosis of BS in thermoregulating locusts (*Locusta migratoria*), in addition to the direct deleterious effects of elevated temperatures on the fungus. There is a clear cumulative effect between the elevated internal body temperature and the insect's immune response at fever temperatures that are sub-lethal to the fungus. For example, *B. bassiana* cannot establish mycosis within a grasshopper whose body temperature is at 35 ºC, which is below the maximum growth temperature of the fungus (~ 37 ºC) (Carruthers *et al.*, 1992). Therefore, supra-optimal, but sub-lethal temperatures, when combined with the responses to fungal infection by the insect, may be sufficient to prevent fungal growth and mycosis.

The ability of the insect to achieve a behavioral fever requires that the EPF respond and adapt to the elevated temperatures, which is achieved partially through the induction of heat shock proteins (HSPs) or other responses to increase their tolerance to heat stress (Xavier and Khachatourians, 1996). Another biological strategy is to utilize mechanisms that interfere with or inhibit the fever. This has been shown to occur in locusts infected with *M. robertsii* but not *M. acridum*, where fever was relatively short-lived in the former (Hunt and Charnley, 2011). Central to this phenomenon was the production of destruxin A by *M. robertsii*, but not *M. acridum*. However, fever was inhibited in locusts infected with the fever-causing *M. acridum* by injecting destruxin A (Hunt and Charnley, 2011). In addition to the ability to reduce the

behavioral fever, *M. acridum* has been shown to tolerate higher temperatures than other related fungi, a characteristic that is important when considering its thermal ecology.

A study was performed by Fernandes *et al.* (2010) to characterize the heat tolerances of three species of *Metarhizium*: *M. acridum, M. anisopliae* and *M. flavoviride.* They found that the heat tolerance of *M. acridum* CS was higher than the other two. After an 8 h challenge at 45 °C, the relative germination of the *M. acridum* strains was 70-100% while it was nearly 0% for the others. Similar trends were found by Rangel *et al*. (2005). Furthermore, *M. acridum* CS germinated at 40 °C, albeit at a decreased rate, while the other *Metarhizium* spp. did not (Rangel *et al.*, 2010). Additional studies of *M. acridum* are required to provide a better understanding of the underlying mechanisms that enable it to tolerate heat better than other related species. A clue was provided by the fact that its maximum growth temperature is not higher than other EPF. This suggests the tolerance is likely due to differential accumulation of protective compounds, such as trehalose or more effective repair mechanisms, rather than *M. acridum* possessing an inherent ability to function at elevated temperatures via structure/function differences of key molecular components. In addition to isolate selection, other strategies exist for the improvement of heat tolerance, such as the nutrition and culturing conditions.

Ying and Feng (2006) found that *B. bassiana* cultured on Sabouraud medium with 4% (w v^{-1}) glucose and 50 μg mL^{-1} Mn^{2+} produced CS that were the most heat tolerant, compared to those produced on other media formulations. Interestingly, this tolerance decreased when Fe^{3+} or Cu^{2+} were used as the metal additive and could not be explained by the authors. However, it was later reported by Xie *et al*. (2010) in *B. bassiana* that SOD-2 activity was elevated, suppressed and inhibited by Mn^{2+}, Cu^{2+} and Fe^{3+}, respectively. This observation may help explain the effects of these metals on heat tolerance, since SOD-2 can protect against oxidative damage

that can occur during heat stress. Rangel *et al*. (2008) were interested in the tolerance of *M. anisopliae* CS to heat and UV-B and how they would be effected by the presence of nutritional (carbon source starvation), heat or osmotic stress during CS production. They found that CS produced from cultures grown on minimal media were more stress tolerant than those from rich medium. Conidiospores produced on minimal medium had relative germination rates of ~ 98 and 90% following UV-B or heat challenge, respectively, while 50% germinated following either stress in the group cultured on rich medium. In addition, exposing the cultures to a sub-lethal heat shock after inoculation which is known to induce the heat shock response (HSR), generally produced CS with higher tolerance to heat and UVR. Moreover, an osmotic shock with 1.0 M of NaCl or 0.4 M of KCl produced a similar increase in UVR or heat tolerance, respectively. Rangel *et al.* (2011) also demonstrated that *M. robertsii* CS produced on a rich medium (potato dextrose agar plus yeast extract) under continuous visible light were able to tolerate heat and UV-B challenges better than those grown in the dark. Furthermore, these survival rates were similar to CS grown on a minimal medium in the dark. Again using *M. robertsii,* Rangel *et al*. (2012) found another method for improving heat tolerance, this time using the drug/plant hormone salicylic acid. They found that CS produced from cultures grown on rich medium supplemented with 1-4 mM salicylic acid had increased heat stress tolerance, with about 80% relative germination compared to 40% in both the control and those supplemented with 8 mM salicylic acid.

A practical detriment caused by many of the above treatments that increased heat tolerance was a reduction in CS yield. This appeared to be caused by the increased stress during growth and conidiation. For example, carbon starved cultures produced only about 1% of the CS of that produced by the control (Rangel *et al.*, 2008), while the salicylic acid treatment reduced

conidial yield by 50% compared to the control (Rangel *et al.*, 2012). The exception was treatment with visible light, which did not reduce CS yield, but would it be expected to since fungi often demonstrate phototropism and conidiate in response to light (Galland and Lipson, 1987). Although the above culturing treatments increased environmental stress tolerance, many are not currently amenable to large-scale production of EPF CS due to the reduction in yield which is paramount. Furthermore, the impacts on the fungal insecticidal activity of the resulting CS need to be established before these protocols will be adopted. It is probable that these problems may be at least partially overcome through the blending of several culturing techniques to find an appropriate compromise between CS yield, stress tolerance, insecticidal activity and other important characteristics required by the EPF to be an effective and practical control agent.

The heat tolerance of BS has also been studied in EPF. Xavier (1998) characterized the heat tolerances of BS produced from representative species of *Beauveria*, *Isaria*, *Lecanicillium*, *Metarhizium* and *Tolypocladium*. To assess heat tolerance BS were incubated in liquid medium at 55 °C for 30 min before being plated. The heat challenge reduced CFU counts to ~ 0.01% of that produced by the unchallenged controls, except for *M. anisopliae* and *T. inflatum* which were 0.05% and 0.003%, respectively (Xavier, 1998). This study also demonstrated that heat shock induced subsequent thermotolerance in each of these fungi, as apparent by a 10-100x increase in survival rates. The optimal pre-incubation (i.e. heat shock) to induce the HSR was found to be 45 °C for 1h and the viability of the treated BS was > 91% for all except one strain of *Beauveria brongniartii* which was 84.6%. Comparatively, the heat tolerance in *B. bassiana* was increased by a larger degree in BS through a heat shock (≥ 10-fold) than in CS produced on a minimal medium (2-fold) (Rangel *et al.*, 2008). This notable increase in thermotolerance may be due to the upregulation of many HSPs involved in the establishment of tolerance (Xavier, 1998). One

such HSP was determined to be a functional homologue of HSF-1 (heat shock factor 1) in several EPF (Xavier *et al.*, 1999). Further studies of HSPs are needed to improve the understanding of the underlying mechanisms involved in the induction of heat tolerance in EPF. Clearly, methods which allow the predictable control of heat tolerance in EPF would be an asset in the field, even though heat shock may not be appropriate for preparing field inoculum due to practical limitations, such as the heating requirement.

Heat tolerant varieties of *M. anisopliae* have also been developed using continuous culturing under increasingly higher temperatures to select for heat tolerant strains (de Crecy *et al.*, 2009). This was performed over four months with 22 cycles of growth and dilution and yielded two heat tolerant varieties with improved growth at 36.5 °C compared to the WT. Interestingly, the entomopathogenicity of these varieties, as measured by percent mortality of a susceptible host insect, was comparable to the WT at 28 °C but was decreased at 36 °C. This study was able to demonstrate in principle, that selection of a complex phenotype, such as heat tolerance is possible with this method. However, pleiotropic effects should be expected with such a strategy due to the possibility of multiple genetic changes over the course of the selection.

2.6 Deleterious effects of heat stress and their associated repair or tolerance systems in EPF

Responding to environmental insults is a common need amongst all life and is of particular importance for fungi and other immobile organisms. Nearly every biomolecule is susceptible to the diverse effects of temperatures and those that are supra-optimal for growth can induce various detrimental biocidal effects in cells. These include oxidation, desiccation and osmotic changes, in addition to the influences on the thermodynamics in general (Attfield, 1997).

As a result, the cellular response to supra-optimal heat is broad and shares features with responses to other environmental stresses which cause similar detrimental effects. The commonality between stress responses has prompted them to be collectively termed the environmental stress response (ESR) with the HSR representing a subset of the collective (Gasch *et al.*, 2000). The HSR in *S. cerevisiae* is the best characterized amongst fungi and > 100 genes are responsive to supra-optimal heat, in addition to other stresses (Gasch *et al.*, 2000). Proteases and molecular chaperones represent two classes of HSPs that have been studied but many more exist and their functions span a wide range, such as the maintenance of membrane homeostasis and genetic regulation. Here, the general detrimental effects of heat stress and the tolerance mechanisms used by fungi will be reviewed, with examples from EPF provided where possible.

One of the best studied products of the HSR are HSPs. The major HSPs were defined based on their abundance following heat shock (exposure of a sub-lethal but supra-optimal temperature), which increased HSP production and generally repressed the remainder of the proteome (Subjeck *et al.*, 1982). Through the use of a similar criterion, Xavier and Khachatourians (1996) found that the expression of 38-71 polypeptides was enhanced in the EPF *B. brongniartii*, depending on the strain, following a heat shock of 42 °C for 1 h and were deemed to be HSPs. The characterization of several HSPs in *B. bassiana*, *T. inflatum*, *M. anisopliae*, *I. farinosa* and *L. longisporum* has revealed that they may function as transcription factors, as is the case in other fungi (Xavier *et al.*, 1999). These factors bound to a DNA oligomer containing the perfect-type (Hashikawa *et al.*, 2006) heat shock element sequence from fungi and this binding activity was further increased at temperatures that are supra-optimal to these fungi. These factors have been studied extensively in yeast and play an important role in regulating the expression of other genes that are responsive to heat stress (Morano *et al.*, 2012).

Many HSPs are molecular chaperones involved in protein folding under both optimal and supra-optimal temperature conditions, but their functions have been found to be most critical during elevated temperatures. This is due to their ability to counteract the increased protein misfolding caused by higher temperatures that occurs both during and after protein synthesis. Many chaperones are upregulated or produced solely during the HSR or ESR (in response to other stresses) and collectively can be defined as the chaperome (Reviewed in Morano *et al.*, 2012). By convention, HSPs have been named according to their molecular mass. The best studied of these is the HSP-70 chaperone, which has been shown to protect polypeptides emerging from ribosomes, assist in protein targeting/translocation, refold damaged proteins and plays a part in their recycling. Barelli *et al*. (2011) reported that *hsp-70* was upregulated at 37 °C in *M. robertsii*. Another chaperone, HSP-90, has been detected in the proteome of *M. acridum* expressed in both CS and mycelia (Barros *et al.*, 2010). More specific HSP research is required to fully understand their impact on establishment of thermotolerance in EPF.

Heat stress can also degrade the structural integrity of the cell and lead to the loss of internal solutes, ionic and pH imbalances and thus disrupting many cellular processes, which can cause cell death (Reviewed in Attfield, 1997). To alleviate this, fungi such as *Aspergillus niger* can alter the lipid profile of their cell membrane to modulate its fluidity in response to heat by increasing the proportion of saturated fatty acids (Morozova *et al.*, 2001). In addition, the accumulation of hydrophobins in CS has been correlated with thermotolerance in *B. bassiana* and *Paecilomyces fumosoroseus* (Ying and Feng, 2004). Hydrophobins have also been found to provide CS with their hydrophobic properties (Jeffs *et al.*, 1999). One such hydrophobin, CP-15, through the use of RNA-mediated silencing has been implicated in tolerance to heat and oxidative, but not osmotic or UV stress (Ying and Feng, 2011). Silencing of *cp-15* also resulted in

the reduction of *cp-15* expression and total hydrophobin containing protein extracts to 10% and 83% of WT levels, respectively. In another study, cell wall and membrane stability were found to be negatively affected in *B. bassiana* GPI-anchored β-1,3-glucanosyltransferase mutants, which decreased both heat tolerance and pathogenicity (Shizhu *et al.*, 2011). These enzymes are involved in cross-linking carbohydrate chains involved in cell wall synthesis and are required for its structural integrity, especially at higher temperatures. Clearly, cellular stability is important at all times; however, this need is elevated at supra-optimal temperatures where heat stress can compromise it, as shown in the above examples.

Heat can also cause desiccation, which can lead to a loss of osmotic equilibrium and cellular turgor pressure. As a result, fungi (Managbanag and Torzilli, 2002) and a wide range of other organisms accumulate high levels of trehalose and mannitol in response to heat. Trehalose, a glucose disaccharide, is well known to protect proteins and lipids, acting as chemical chaperone of sorts which enables them to remain in biologically active conformations during desiccation and also prevent aggregation of denatured proteins (Reviewed in Singer and Lindquist, 1998b; Crowe, 2007). However, the abnormal persistence of high levels of trehalose can interfere with chaperone mediated protein refolding and mutants unable to degrade trehalose have been found to be thermosensitive (Singer and Lindquist, 1998a). Therefore, degradation of trehalose during recovery is essential for maintaining cellular function. The sugar alcohol mannitol has also been implicated in heat tolerance through its role as both an osmolarity (Chaturvedi *et al.*, 1997) and oxidation protectant (Trail and Xu, 2002).

In *M. anisopliae*, heat tolerance has been correlated with trehalose and mannitol levels in CS and these levels could be altered through the composition of the medium the CS were produced on (Rangel *et al.*, 2008). This study demonstrated that CS harvested from a minimal

medium, without glucose, accumulated more trehalose and mannitol (15 and 38 mg g^{-1} CS, respectively), compared to CS harvested when glucose was present (5 and 10 mg g^{-1} CS, respectively). The accumulation of both mannitol and trehalose may not be universal responses to heat in all fungi. In *B. bassiana*, only trehalose was found to accumulate following a 6 h exposure at 35 °C, rising from 4.2 to 88.3 mg g^{-1} biomass, with a correlation to heat tolerance (Liu *et al.*, 2009). However, mannitol has been shown to influence the heat tolerance of this fungus through the study of mannitol metabolism mutants (Wang *et al.*, 2012b). This was done by creating Δ*mpd* (mannitol dehydrogenase knock-out) and Δ*mtd* (mannitol dehydrogenase knock-out) mutants in *B. bassiana*, with genes required for mannitol synthesis or degradation inactivated, respectively. Mannitol was decreased in both mutants, but in Δ*mpd* it was decreased by approximately 2 to 4-fold more than in Δ*mtd*, while trehalose contents were increased by ~ 50% in both, compared to the WT. Both mutants had reduced heat tolerance compared to the WT. The heat tolerance of the Δ*mpd* strain, as measured by the rate of germination at 45°C, was approximately half that of Δ*mtd* and was explained by the relative reduction in mannitol accumulation in the former compared to the latter. Interestingly, heat tolerance decreased in both mutants compared to the WT even though trehalose levels were increased. This was thought to be a result of the specific role of each of these compounds since trehalose could not complement for a loss in mannitol levels. It is curious that *B. bassiana* does not accumulate mannitol above basal levels in response to heat, yet this molecule appears to play a role in heat tolerance.

Damaging reactive oxygen species arise both as a consequence of normal aerobic metabolism and from environmental insults, including high temperatures, causing cell damage by oxidizing biomolecules such as lipids, protein and DNA. This oxidative damage can negatively impact cellular function leading to delayed growth or cell death (Reviewed in

Moradas-Ferreira *et al.*, 1996). As a result, fungi and other organisms have developed oxidative damage defense enzymes, such as superoxide dismutase and catalase which, respectively, convert superoxide to hydrogen peroxide and hydrogen peroxide to water and molecular oxygen. However, studies in *B. bassiana* have shown that superoxide dismutase mutants did not have significantly different tolerances to heat than WT (Xie *et al.*, 2010). These findings differed from those generated from superoxide dismutase mutants in *Cryptococcus neoformans*, which were found to have reduced heat tolerance (Giles *et al.*, 2005). In contrast to superoxide dismutase, *B. bassiana* mutants with disrupted *catA* (catalase-A), which is spore-specific, had significantly reduced CS heat tolerances (Wang *et al.*, 2013). However, heat tolerance was not affected in mutants that had catalase genes disrupted that encoded products normally targeted to the peroxisome, the cytoplasm or for secretion. The increase in conidial heat tolerance was consistent with the expression of *catA*, which was at its greatest level in germinating CS and its transcript was not detectable after this stage of development. This report demonstrated spore-specific catalase plays a role in the mitigation of oxidative effects produced by heat stress in the CS of *B. bassiana*.

2.7 Heat stress sensing

2.7.1 Intracellular sensing of heat and signal transduction

Fungi respond to large variety of environmental stimuli, including temperature to maintain homeostasis. Sensing of the stimulus and relay of the message is prerequisite for subsequent responses to occur. In fungi, many genes responsive to heat stress are controlled by the transcription factors HSF-1 and MSN-2/4 (multicopy suppressor of sucrose non-fermenting), which are the transcriptional regulators of the HSR and ESR, respectively (Reviewed in Morano

et al., 2012). Functional homologues of HSF-1 have been revealed in several EPF by Xavier *et al*. (1999). These were able to bind to the heat shock element containing the characteristic nGAAn triple inverted repeat, consistent with the findings in other fungi (Sorger and Pelham, 1987). While the functionally redundant, MSN-2 and MSN-4 are involved in regulating genes containing their recognition site, called the stress response element, such as *catA* (Wieser *et al.*, 1991). The cellular response to various environmental stimuli, including temperature requires many components involved in sensing, transduction and integration external signals. This process is known as signal transduction and allows cells to amplify a signal received through the detection of a stimulus to produce many internal signals to generate large cellular changes. The pathways used by filamentous fungi involved in the transduction of environmental signals appear to be integrated with others stress response and signal transduction pathways compared to those in *S. cerevisiae,* which seem to operate in a more independent manner (Bahn *et al.*, 2007). Furthermore, these pathways and the subsequent acquisition of stress tolerances have been shown to be negatively affected in *B. bassiana* with an inactivated Golgi attached calcium pump, which may be involved in the post-translational processing of components involved in signaling networks (Wang *et al.*, 2013). Below is a brief summary of the most current findings in EPF pertaining to environmental signal transduction. Barranco-Florido *et al.* (2013) have also addressed this topic in a recent review.

2.7.1.1 Mitogen-activated protein kinases (MAPKs)

The signal transduction mechanisms which regulate the ESR in fungi are primarily controlled by pathways involving MAPKs and well characterized examples of these exist in fungi, such as the HOG-1 (high osmolarity glycerol 1) pathway in *S. cerevisiae* which is most

responsive to osmotic stress (reviewed in Bahn *et al.*, 2007). Some MAPKs, like HOG-1 and its homologues have also been termed stress activated protein kinases (SAPKs) which connotes their involvement in the regulation of the ESR; however, their involvement in the heat response are less understood. Signal transduction via these pathways is thought to be initiated by sensing of a stimulus which inhibits autophosphorylation of a phosphotransfer protein by histidine kinase and prevents the phosphotransfer protein from binding with the response regulator. This allows the regulator to interact with MAPK kinase kinase and activate the SAPK cascade. This pathway is completed with the nuclear importation of phosphorylated MAPK and the activation of various transcription factors, such as MSN-2/4 through their hyperphosphorylation, needed to induce an assortment of genes required for the ESR (Garreau *et al.*, 2000). The role of SAPKs in the regulation of the ESR appears to differ amongst fungi.

In a *B. bassiana* mutant with disrupted *hog-1*, decreased tolerances to hyperosmotic and oxidative stress were observed while temperature tolerance (tested at 32 °C) was not reduced to the same degree (Zhang *et al.*, 2009). These phenotypes differed from that of *hog-1* mutants in *S. cerevisiae* which were less responsive to osmotic stress (Brewster *et al.*, 1993), but was similar to those in *S. pombe* (Degols *et al.*, 1996) and *Candida albicans* (Smith *et al.*, 2004) since their SAPK cascades responded to a variety of stresses including heat. Interestingly, the HOG-1 homologue in *A. nidulans* was activated by osmotic and oxidative stress but null mutants were not sensitive to osmotic stress, suggesting there are likely alternate pathways involved in response to this stress (Kawasaki *et al.*, 2002). However, these mutants did produce CS that were sensitive to oxidative and heat stress in addition to other phenotypes that differed from the WT. Compared to yeast, the SAPK systems are less well understood in filamentous fungi. In general, their responses resemble that of *S. pombe* in that they appeared to be more integrated

with other stress response pathways, being able to respond to various stresses, compared to *S. cerevisiae* which possess more segregated SAPK pathways (Reviewed in Bahn *et al.*, 2007).

Genetic disruption and characterization of the corresponding knock-out mutants has also been used to characterize other non-SAPKs in *B. bassiana*, such as the SLT-2 (suppression at low temperature 2) (Luo *et al.*, 2012) and YERK-1 (yeast extra cellular regulated kinase 1) types (Zhang *et al.*, 2010). These studies demonstrated SLT-2 played a role in thermotolerance, likely attributable to the altered trehalose accumulation and compromised cell wall structure observed in the mutant, while the YERK1 homologue appeared to be required for the formation of functional appresoria needed to penetrate the insect cuticle, but did not influence heat tolerance

2.7.1.2 Histidine kinases

The reason for yeast SAPKs responding to a narrower range of stresses may be due to the number of sensor kinases these fungi encode, which appear to be required for them to respond to the various stimuli. The yeast *S. cerevisiae, S. pombe* and *C. albicans* possess one, three and three histidine kinases, respectively, while filamentous fungi have a larger variety, such as *N. crassa* which has nine or more histidine kinases (Catlett *et al.*, 2003). Interestingly, the downstream constituents of the two component system, such as phosphotransfer proteins and response regulators are common amongst fungi, suggesting that many of the histidine kinases are redundant or that extensive cross talk occurs between signaling pathways (Catlett *et al.*, 2003).

In *M. robertsii*, *mhk-1* (*M. robertsii* group III histidine kinase 1), encoding a homologue of the histidine kinase involved in the HOG-1 pathway, has been studied through its genetic disruption and complementation (Zhou *et al.*, 2012). The *mhk-1* mutant displayed increased hyphal tolerances to H_2O_2 and hyperosmolarity, increased CS thermotolerance, decreased CS

resistance to UV-B and menadione (a chemical that causes the formation of reactive oxygen species), and reduced virulence to yellow mealworm (*Tenebrio molitor*) larvae. The role of this type of histidine kinase in stress responses varies amongst fungi, especially in filamentous types, but the tolerances to heat, oxidation and osmolarity are generally increased when the downstream SAPK pathways are activated (Reviewed in Bahn *et al.*, 2007). Disruption of *mhk-1* was also observed to increase the transcripts of nine genes, including three catalase genes, but decreased others, including three superoxide dismutases, suggesting that catalase and superoxide dismutase play different roles in response to oxidative stress produced from divergent sources (Zhou *et al.*, 2012). Furthermore, the HOG-1 homologue in *mhk-1* mutants was found to have reduced levels of phosphorylation in response to H_2O_2 or heat stress, but increased levels when exposed to osmotic stress or menadione. From this observation, it is plausible that HOG-1 may be activated in response to a variety of stresses in *M. robertsii*. This could occur through signal integration between MHK-1 and a different histidine kinase(s) or other signaling pathways involved in sensing stimuli that MHK-1 cannot detect. This level of regulation has been suggested to occur in other filamentous fungi which possess an extensive number of histidine kinases; thus integrated signaling pathways would likely be required for these organisms to regulate their stress response in this manner (Catlett *et al.*, 2003).

2.7.1.3 Protein kinase A and G protein-signaling regulators

Regulation of the ESR is also controlled by other kinases that are not MAPKs. As mentioned above, upon detection of heat stress the ESR transcription factors MSN-2/4 are activated through hyperphosphorylation by SAPK within the nucleus. This modification can be prevented and reversed in response to cyclic adenosine monophosphate, but likely not through

protein kinase A. This is because protein kinase A is known to negatively regulate MSN-2 and MSN-4, through phosphorylation in response to cyclic adenosine monophosphate (Gorner *et al.*, 1998), therefore other kinases may be involved (Garreau *et al.*, 2000). Genetic disruption of protein kinase A in *M. anisopliae* was reported by Fang *et al*. (2009), although its influence on heat tolerance was not. However, the protein kinase A mutant was shown to be more sensitive to some oxidative stress and the upregulation of approximately one third of genes expressed during growth on insect cuticle were attributed to protein kinase A.

Protein kinase A is controlled by upstream G protein coupled receptors and regulators which act to transduce environmental signals though balancing the rates of GDP/GTP exchange (reviewed in Hollinger and Hepler, 2002). When in the active conformation, the Gα subunits of the receptor complex can bind with their regulator which stimulates GTP hydrolysis and halts the signaling pathway. The signaling regulators of these pathways have been characterized in the EPF *M. anisopliae* (Fang *et al.*, 2007) and *B. bassiana* (Fang *et al.*, 2008) through analysis of disruption mutants. The *rgs-1* (regulator of G protein signaling 1) mutants were generated from both EPF and had reduced CS production, consistent with findings in other fungi, such as *A. nidulans* (Hicks *et al.*, 1997); however, only in *B. bassiana* did disruption of *rgs-1* reduce thermotolerance in CS (Fang *et al.*, 2008). More research is needed in this area to better understand the role of G protein-signaling in heat response of EPF, since preliminary studies have revealed fundamental differences.

2.7.1.4 Models for intracellular heat stress sensing

The responses to osmotic and other environmental stresses are well characterized in various yeast and filamentous fungi but less is known about the sensing of heat stress. Initial

theories suggested HSPs acted as cellular thermometers (Craig and Gross, 1991) or total protein misfolding was an indicator of heat stress (Trotter *et al.*, 2002). However, these theories, lacked sufficient supporting evidence and biological relevance since the temperatures used in the studies to produce a HSR would not cause bulk protein aggregation (Nathan *et al.*, 1997). Current evidence supports a model whereby misfolding of newly synthesized polypeptides could be sensed through an increased load on chaperones such as, HSP-70 and HSP-90 (Reviewed in Morano *et al.*, 2012). In support of this, it has been shown that select HSPs, such as HSP-90 can repress HSF-1 activation (Duina *et al.*, 1998) and HSP-70 can be localized into the nucleus for it to interact with HSF-1 upon ethanol challenge (Quan *et al.*, 2004). Furthermore, given the large amount of protein synthesis occurring in growing cells, it is possible that a heat shock could influence the folding of enough newly synthesized polypeptides to compete with HSF-1 for HSP-70/90, thus allowing HSF-1 to be activated since the HSPs would be unavailable to cause repression in this scenario (Morano *et al.*, 2012). However, there appears to be no evidence of these chaperones migrating into the nucleus upon the presence of heat stress, therefore more evidence is required to better support this thought.

2.7.1.5 Direct intracellular heat sensing

Although the precise nature of the signal which cues the HSR remains elusive (Morano *et al.*, 2012) there are many examples of various biomolecules acting as thermosensors whose structure/function are directly altered in response to heat stress (Reviewed in Klinkert and Narberhaus, 2009). For example, the HSP-26 chaperone in *S. cerevisiae* has been shown to reversibly shift from an inactive to an active conformation in response to 36 °C, allowing its activity to be autonomously regulated (Franzmann *et al.*, 2008). Regulators of the HOG-1

homologue in *S. pombe* have also been found to respond to heat (Nguyen and Shiozaki, 1999). These regulatory protein tyrosine phosphatases, PYP-1 and PYP-2, have been found to become insoluble following a heat shock at 48 °C, possibly due to a conformational change, modification or physical interaction with other proteins (Nguyen and Shiozaki, 1999). The inhibition of these enzymes promotes phosphorylation (activation) of the SAPK pathway and induction of the ESR, as described in section 2.7.1.1. Interestingly, the activity of *S. pombe*'s MAPK kinase was not largely affected by heat shock as in other fungi. Thus *S. pombe* has been suspected to lack a heat sensor upstream of this MAPK kinase, supporting the role of PYP-1 and PYP-2 in the regulation of the SAPK cascade in response to heat (Nguyen and Shiozaki, 1999). Such a mechanism for regulation would likely provide a quick response to heat stress but may not provide the means to regulate the upstream components of the SAPK cascade which can be controlled by regulators such as histidine kinases. Similarly, there have been reports of MAPK kinase kinase independent regulation of SAPKs through unknown mechanisms in response to a variety of stresses in both budding (Cheetham *et al.*, 2011) and fission yeast (Zhou *et al.*, 2010). Therefore, the signal transduction required to respond to heat and other appears to be quite complex and our understanding of them is convoluted by an apparent lack of a specific mechanism for heat sensing.

2.7.2 Extracellular heat sensing

As discussed above in section 2.7.1, sensing of heat and other environmental stresses has been described conventionally in the context of their intracellular detection through damaged /altered bio-molecules or autoregulation of their function. In 1998, a major discovery in this area was reported by Hussain *et al*. (1998) who found that *E. coli* was able to respond to environmental stress though a phenomenon that appeared to utilize secreted molecules named

ESCs. This group of molecules was also found to be responsive to heat stress (Rowbury and Goodson, 1999b) in addition to a variety of other physical and chemical stimuli, including as UVR, alkali and acid (Reviewed in Rowbury, 2001b). Similar findings have been reported by Nikolaev (1997a; 1997b) who characterized a heat tolerance response in *E. coli* controlled by a potentially different group of secreted molecules, termed the extracellular adaption factors.

2.7.2.1 Biological function(s) of and responses that involve ESCs

Differences between the ESCs and extracellular adaption factors are apparent. Firstly, extracellular adaption factors are produced during stress conditions while ESCs are produced during both unstressed and stressed conditions. Secondly, ESCs are generally proteins > 10 kDa (Rowbury and Goodson, 2001), whereas extracellular adaption factors are non-proteinaceous molecules that are < 10 kDa (Nikolaev, 1997a). The ESCs are the best studied example of extracellular stress sensing and will be used to illustrate how such a phenomenon has been suspected to function in *E. coli*.

The ESC proteins are synthesized *de novo* and secreted by the cells during unstressed conditions (Rowbury and Goodson, 2001). In addition, ESCs can be activated, independent of cells, by heat in a temperature dependent manor with 55 °C being optimal for the promotion of EIT to some types (Rowbury, 2005). The mechanism of ESCs apparent activation has yet to be revealed; however, in the case of heat stress sensing, a conformational change may be required (Rowbury and Goodson, 2001). Once activated, ESCs diffuse (or may move by a flow, depending on the environment) and interact with sensitive cells likely through cell surface receptors or by direct uptake to eventually induce tolerance to heat and other stresses (Rowbury and Goodson, 2001; Rowbury, 2001a; Rowbury, 2001b). This response, here termed EIT, is similar to the definition used by the late Dr. Rowbury and his colleagues (2005; 2006) and is

currently characterized only by an increase of survival in environmental stress challenged cells (measured as viability) following treatment with activated ESCs or ELFs. However, if more specific functions or roles for ESC, ELF or EIT were discovered than their definitions would require revision to accommodate such findings.

The ESCs are suspected to exist as several types and can be activated by and induce tolerances to a variety of conditions (Rowbury, 2005). For example, heat stress (~ 45-55 °C) has been found to activate ESCs, enabling them to induce tolerances in *E. coli* to acid (pH 3.0) and alkali (pH 11.0) conditions as well as UVR and heat (49 °C) (Rowbury, 2003a). The thermotolerance inducing ESC(s) also appear be activated by mild acid and alkali, UVR and Cu^{2+}, in addition to heat (Rowbury, 2002). Once active, ESCs exhibit pheromonal properties since they can diffuse to unstressed cells (Rowbury and Goodson, 2001) and are thought to provide early warning of the potentially incoming stress to the cells so they may initiate the appropriate stress response (Rowbury, 2001a; Rowbury, 2001b).

A criticism of Rowbury's work is that none of these molecules were studied in a purified form, thus his studies were conducted with CFF containing cocktail of ESCs and other biomolecules produced by an *E. coli* culture (in addition to the constituents of the growth medium), complicating the results and making it nearly impossible to elucidate the following: a) how many ESC types exist, b) how stress conditions activate them and c) once activated, which ESC(s) induce a particular stress response. However, it has been shown in all cases that ESCs are able to induce EIT in cells other than those that produced them, suggesting these molecules are involved in cell-cell communication (Reviewed in Rowbury, 2005).

Phenomena resembling those controlled by ESCs or extracellular adaption factors in *E. coli* have also been demonstrated in other organisms, such as the Gram negative bacteria *C.*

jejuni (Murphy *et al.*, 2003) and *Pseudomonas fluorescens* (Nikolaev *et al.*, 2000), and the Gram positive *Bacillus subtilis* (Nikolaev and Voronina, 1999) and *Luteococcus japonicus* (Vorob'eva *et al.*, 2003), and in the eukaryote *S. cerevisiae* (Vovou *et al.*, 2004). It should be noted that these molecules are thought to be proteins in *C. jejuni* and *L. japonicus*, in addition to *E. coli*, and are non-proteinaceous molecules of < 10 kDa in the others, with the exception of those from *S. cerevisiae* which did not have their composition determined. An important difference in the methodologies used to study this phenomenon in *E. coli* and *S. cerevisiae* was the latter used CFF that was recovered from cultures that were exposed to heat stress, while in the *E. coli* studies it was recovered from an unchallenged culture. Therefore, Vovou *et al*. (2004) could not determine if the causative molecules were also produced by unstressed *S. cerevisiae* cells. It was however established that ESCs produced by *E. coli* could be activated both in the presence and absence of cells. Therefore, it is not possible to infer if a true mechanistic difference exists between the functioning of these molecules in *E. coli* and *S. cerevisiae* (Rowbury, 2005).

It was found in yeast that tolerance to heat was reduced by cycloheximide, suggesting *de novo* protein synthesis was involved in the establishment of heat tolerance induced by CFF from pre-conditioned cultures (Vovou *et al.*, 2004). Interestingly, survival of yeast pre-conditioned by a 37 °C heat shock and challenged in fresh medium was comparable to that of non-heat shocked cells challenged in CFF prepared from heat challenged cultures. This similarity of the survival rates produced by the above two treatments suggested the responses cued by the treatments may not provide different levels of heat tolerance. It is unclear if the physiological responses induced by pre-conditioning cells with a heat shock differ from that of EIT or other similarly behaving phenomena. However, it does appear that these two mechanisms at the very least may represent different modes of heat tolerance induction.

2.7.2.2 Stress sensing by ESCs

It is not known how many types of ESC are produced by *E. coli*. Nonetheless, it has been proposed that several exist and that individual types can be activated by a variety of stress conditions, both physical and chemical (Reviewed in Rowbury, 2005). Although it is yet to be determined, the means of ESC activation is possibly through a conformational change(s) and will be considered below (Rowbury and Goodson, 2001). In addition, a logical requirement for cells to respond appropriately to stress through ESC sensing would be for the conformation of the activated ESC to be specific to the stress condition that caused it. Since the conformation of biomolecules is always dependent on their environment (Morano *et al.*, 1998), it is theoretically possible for a single ESC type to be converted to a unique activated form, corresponding to a particular environmental stimulus. However, in nature, multiple stresses are often encountered simultaneously, which complicates the proposed ability of a single ESC type to be activated by a variety stress conditions (Rowbury, 2005), since each stress could impose structural restrictions on the ESC molecules.

For the sake of considering Rowbury's proposition that a single ESC type can be activated by multiple environmental stress conditions and induce tolerances to a variety of environmental challenges, let us contemplate that activated ESCs interact with cells through specific surface receptors (or other cellular target) (Rowbury and Goodson, 2001). In addition, it would be likely that ESCs possess a specific binding site for each unique receptor they interact with, since ligand-receptor interactions are generally specific (Lambert, 2004). In the case of ESCs, each binding site is more likely to interact with its receptor when the ESC is in an active conformation, which has been suggested to occur following their exposure to particular environmental stress conditions (Rowbury and Goodson, 2001). Although unproven, it is possible that

the speculated interaction between ESC and receptor/target is required to transduce the signal carried by active ESC to produce EIT to a particular stress. However, for a single ESC type to be activated by and induce tolerance to several stress conditions, it may require the ability to yield a variety of active conformations that are specific to each environmental stress condition that activated it. In this was each conformation may result in the positioning of a specific binding site(s) to interact with its unique receptor target(s) that is involved in EIT to the particular stress condition(s). However, a particular active conformation may not persist if an ESC molecule is sensitive to activation by multiple stresses. This is because each subsequent or simultaneous conformational change that is imposed on an already activated ESC molecule could alter its global topography, which may restrict the ability of the formerly correctly positioned binding site to remain in such a position where it is able to interact.

As a result, the structural fluidity of ESCs may limit their ability to achieve an active conformation that is able to cause EIT to a variety of stress conditions. Therefore, when the principle of Ockham's razor is applied, it may be more likely that ESCs exist as individual types that are activated by a particular stress, rather than multiple. This is because in order for the cell to respond with the appropriate EIT, the conformation of the activated ESC needs to be specific to the stress. By secreting several types of ESCs that are activated by only a particular stimulus, the organism is able monitor the conditions that surround it and may be able to respond to several different environmental stresses simultaneously. However, other cellular mechanisms could also be involved in the transduction of the signal carried by active ESC and may be able to integrate other environmental signals to regulate the cellular response. Clearly, more research is needed in this area to elucidate how EIT occurs and the role of ESC activation.

In addition to stress type, the intensity of stress can also be measured since higher temperatures were able to activate ESCs more quickly and were more effective at inducing tolerances and thus may function as extracellular thermometers (Rowbury, 2005). It has been shown that some ESCs are responsive to different ranges of a particular environmental stress and their ability to be activated depends on the culture conditions they were synthesized under. For example, ESCs synthesized at pH 7.0 were activated by pH 5.0 but not at more alkaline conditions, while ESCs synthesized at pH 9.0 were not as responsive to this pH (Rowbury and Goodson, 1999a). However, thermal sensing ESCs have not been demonstrated to function in this way; nonetheless Rowbury (2005) has speculated that they may. At least for some pH responsive ESCs, it is possible that that multiple forms exist or their sensitivities can be modified. In addition to being sensitive to a variety of environmental stress conditions, ESCs remained stable following exposure to high temperatures. The components produced by *E. coli* (Rowbury and Goodson, 1999a), *S. cerevisiae* (Vovou *et al.*, 2004) and *C. jejuni* (Murphy *et al.*, 2003) remained responsive to activation following an incubation of 75 °C for 15 min, 100 °C for 5 min and 100 °C for 10 min, respectively, and could increase heat tolerance in cells. In contrast, when CFF prepared from *E. coli* was incubated at 100 °C for 15 min, its ability to increase heat tolerance was reduced to a level comparable to cells treated with fresh medium.

2.7.2.3 The heat response model and ESCs

The proposition of an extracellular heat sensing mechanism is not at odds with the existing models which are built on the findings that heat is sensed intracellularly. At the very least, ESCs and similarly functioning molecules may serve a redundant role in cellular sensing of stress. It has also been shown that removal of ESCs and similarly behaving molecules appeared

to not alter normal growth and development of the cell when depleted by proteolysis or other treatments. This feature has also been exploited to provide confidence in their existence and functionality (Murphy *et al.*, 2003; Rowbury, 2005). Although the responses induced by ESCs are unknown, the level of heat tolerance induced by an EIT like phenomenon, as measured by survival is comparable to that produced by a conventional heat shock treatment in *S. cerevisiae* (Vovou *et al.*, 2004), suggesting these responses may share common features or at least produce similar levels of tolerance. The use of deletion or conditional mutants to disrupt the various HSPs involved in the HSR would be useful to elucidate if similarities between EIT and the HSR existed.

2.7.2.4 The potential for an EIT type response in EPF

An ESC-like phenomenon has yet to be discovered in any filamentous fungi. This group of organisms is quite adaptable and is able to survive and grow in a variety of environmental conditions and thus must be able to sense and respond to them to maintain homeostasis. It has been shown that filamentous fungi possess an extensive variety of histidine kinases which have been suspected to be involved in the response to a variety of stimuli, including environmental stress (Catlett *et al.*, 2003). However, the mode of activation of many of these histidine kinases is unknown and only a few were predicted by Catlett *et al.* (2003) to contain a transmembrane domain, which is often involved in extracellular sensing. Although the lack of this domain does not eliminate the possibility for the sensing of signal with the cell, it has been suspected that some of these histidine kinase could receive extracellular signals through receptor proteins that interact with the environment through interactions with a ligand (Catlett *et al.*, 2003). Such a mechanism for sensing and signaling has been found to be involved in the regulation of

chemotaxis by the chemotaxis histidine kinase in *E. coli* (Reviewed in Levit *et al.*, 1998). However, the exact signal which elicits the physiological response to heat, through intracellular sensing, has yet to be determined (Morano *et al.*, 2012).

Interestingly other distance interactions, such as quorum sensing in Gram positive bacteria also employ transmembrane histidine kinases to detect the oligopeptide quorum factors (Reviewed in Schauder and Bassler, 2001). Conversely, quorum factors produced by most Gram negatives (homoserine lactones) diffuse freely across the cellular membrane where they can interact with their internal target, LUXR. It is possible that the proteinaceous examples of ELFs may share similarities with oligopeptide quorum factors with regards to their mode of cellular detection, i.e. perhaps through an interaction with a cell surface target.

Studies that focus on the identification of ELFs and the characterization of the related responses in EPF and other filamentous fungi are needed. Note that ELF is named after the ESC from *E. coli*, not due to known or suspected similarities in their sequence, structure or specific function. Instead they are termed 'like' because of their predicted ability that once activated (by heat in this thesis) they may increase survival in treated cells when challenged with environmental stress, as do ESCs. This tolerance is termed EIT. However, few specifics are known regarding EIT and currently is only characterized by its ability to increase tolerance in cells, measured by viability. The discovery of ELFs and their related responses in EPF and other filamentous fungi may provide a better understanding of their environmental stress sensing and tolerance induction. Such as discovery would also contribute to an expansion of the understanding of EPF ecology and may hasten their successful implementation as microbial insecticides.

2.7.2.5 Difficulties in studying ESCs and extracellular adaption factors

The above examples represent the limited extent of understanding of ESCs, extracellular adaption factors, other similarly behaving molecules and their associated responses. These studies have focused primarily on characterizing the molecules and their related stress responses using whole-cell bioassays to detect perturbations in cellular tolerance to a variety of environmental stresses. These and other phenomena have been collectively termed distance interactions and historically have encountered opposition largely because the responses they elicit are often extremely variable (Reviewed in Nikolaev, 2000). However, the issue of variability should not be unexpected when assaying for the presence of an unknown molecule, which requires an undetermined interaction with sensitive cells to produce increased stress tolerance through an unknown mechanism. Clearly, the lack of understanding of these molecules and the responses they elicit would limit the methodologies available to researchers interested in their study. As a result, the field of extracellular stress sensing has escaped the attention of modern molecular biology and its discovery was owed to the use of traditional microbiological methods, paired with idea based experimentation (El-Sharoud and Rowbury, 2006). The discovery of a gene or gene product involved in an ESC-like response would represent an important discovery. Such a finding has eluded researchers and its discovery, like the phenomenon itself, would require the integration of both traditional methods and idea based experimentation, but would also require modern molecular biology.

3.0 PHOTOLYASE GENE STUDIES IN FIVE GENERA OF EPF

3.1 Abstract

In nature, EPF encounter UVR by way of solar radiation that induces DNA damage, such as CPDs, which can be lethal to the cell. This type of damage is most efficiently repaired by CPD-PHR dependent photoreactivation, which can repair ~ 90% of CPDs when light at 380-410 nm is present. In this study, photoreactivation and *phr-1* candidates from five genera of EPF were examined. This was performed with PCR based methods to amplify a conserved region of putative *phr-1*, which encodes a portion of the α-helical domain in CPD-PHR in other organisms. Analysis of the *phr-1* candidates in several fungi revealed that it encoded many conserved, functionally important characteristics for class I CPD-PHRs, such as binding sites for MTHF, FAD and CPD, and amino acids implicated in electron transfer by a tunneling pathway. Furthermore, homology modeling was used to predict the structure/function of the portion of putative CPD-PHR encoded by the *phr-1* candidates and provided evidence that they contained structural homology with proteins that have CPD-PHR repair activity (E.C. 4.1.99.3). This method could differentiate the putative CPD-PHRs and a model CPD-PHR from known (6-4)-PHR and DASH-CRY sequences which are the only other PHR/CRYs found in filamentous fungi. Phylogenetic models suggested that the putative CPD-PHRs from EPF cosegregated into clades containing CPD-PHR from other fungi that belonged to the Order Hypocreales. These results are the first reports of candidate *phr-1* that encode a putative CPD-PHR, in EPF from the genera *Isaria*, *Lecanicillium* and *Tolypocladium*.

3.2 Introduction

Implementation of EPF as biological control agents for pest insects is becoming more accepted by the public as a potential alternative to synthetic chemical insecticides. In addition to the determinants of insect disease controlled by the fungus and host, including their molecular biology, physiology and biochemistry, the environment where they subsists is of great impact (Feng *et al.*, 1994; Khachatourians *et al.*, 2002; Khachatourians and Qazi, 2008). Environmental conditions, such as relative humidity, temperature and solar UVR all influence the ability of EPF to establish pathogenesis (Fargues, 2003). Insecticidal inoculants containing EPF from the genera *Beauveria*, *Lecanicillium* or *Metarhizium* most often utilize CS (Roberts and St Leger, 2004; Khachatourians, 2009). Relative to other fungal cell types, CS are better suited to this application due to their resistance to desiccation and other environmental conditions or insults. Even so, UVR can cause a reduction in the effectiveness of EPF in causing insect control (Ignoffo *et al.*, 1977). As a result, the response to UVR stress by EPF has been an area of interest to researchers.

It has been established that the short (UV-C) to medium (UV-B) wave lengths of UVR are the most harmful to EPF, because of the DNA damage they induce (Fargues, 2003). Both wavelengths can cause CPDs and (6-4)PPs, and when cells are exposed to UV-C, these dimmers can account for 70% (Wang, 1976) and 20-30% (Kim *et al.*, 1994) of the induced DNA photoproducts, respectively. The formation of CPDs and their repair *in vivo* has been observed in the EPF *B. bassiana* (Chelico *et al.*, 2005), *M. acridum* and *M. robertsii* (Nascimento *et al.*, 2010). Chelico *et al.* (2005) found that CPDs were repaired by both NER and by classical photoreactivation in *B. bassiana*, mostly likely mediated by CPD-PHR. Repair of CPDs by CPD-PHR is more efficient than NER and when light is present up to 90% of the CPDs can be

repaired through this mechanism (Wang, 1976). Nonetheless, NER is not dispensable and is essential for cell survival since it can also repair other types of DNA damage, such as (6-4)PPs. Photoreactivation of CPDs by CPD-PHR is accomplished using energy from light (380-410 nm) that is harvested by its cofactors to monomerize the CPDs (Reviewed in Sancar, 2003). Furthermore, this repair is achieved with complete fidelity to the original DNA sequence.

Fungi only possess class I CPD-PHRs which can also be found in bacteria and archaea. Class I CPD-PHR, distinguished by their divergent phylogeny (refer to Figure 2.3) compared to class II, III and the other CRYs, are known to be monomeric proteins consisting of 450-550 aa and possessing two covalently bound chromophores. One is always FAD which is required for DNA-binding and repair (Jorns *et al.*, 1987; Sancar *et al.*, 1987a). The second chromophore is dependent on the type of CPD-PHR and may be either MTHF or 8-hydroxy-5-deazaflavin. Although the second chromophore is not required for repair, it can increase the reaction rate by 10 to 100-fold when light is limiting due to its higher extinction coefficient and an absorption maximum at longer wavelength compared to the reduced active form of flavin (Payne and Sancar, 1990).

The PHR/CRY family was expanded with the discovery of repair functionality of (6-4)-PHR and a type of CRY called DASH-CRY (Brudler *et al.*, 2003). The (6-4)-PHRs specifically repair (6-4)PPs and have been found in many metazoan eukaryotes (Todo *et al.*, 1993) and some fungi (Bluhm and Dunkle, 2008). However, (6-4)PP repair was not found to be associated with photoreactivation in *B. bassiana* (Chelico, 2004) but was detected in *M. anisopliae* (Fang and St Leger, 2012). The DASH-CRYs have also been found in fungi but not found to be involved in DNA repair (Veluchamy and Rollins, 2008). The taxonomic relatedness of the entire PHR/CRY family is evident by the sequence similarity they share with each other within the, α-helical

domain which contains a FAD-binding region and other functionally important features (Ahmad and Cashmore, 1993; Hsu *et al.*, 1996). The diverse functionality of CRY proteins is achieved in part through variation in their C-terminal region. In this regard, classical CRY proteins lack DNA repair activity but instead function as blue light receptors and can be involved in synchronizing the circadian clock (Miyamoto and Sancar, 1998).

Although much is known about photoreactivation in fungi, there is a lack of understanding of the molecular biology that controls this process in EPF. Central to this is the lack of information regarding the sequence of both *phr-1* and the CPD-PHR it encodes. To date, only one CPD-PHR from an EPF has been functionally characterized and was found in *M. robertsii* (Fang and St Leger, 2012). Analysis of the genomes of *M. acridum* CQMa 102 (Gao *et al.*, 2011), *C. militaris* CM01 (Zheng *et al.*, 2011) and *B. bassiana* ARSEF 2860 (Xiao *et al.*, 2012) revealed that each encoded a putative CPD-PHR. The UVR stress tolerances of six EPF have been characterized under conditions conducive for photoreactivation and NER (Chelico *et al.*, 2006). This work demonstrated that fungi from the genera *Beauveria, Isaria, Lecanicillium, Metarhizium and Tolypocladium* could survive UV-C challenge better if photoreactivating light was present. Thus, it was hypothesized this group of fungi, as is the case of other organisms, likely possess *phr-1* encoding a functional class I CPD-PHR since this type of PHR has been found to control the light-dependent removal of CPDs in other fungi (Alejandre-Durán *et al.*, 2003; Berrocal-Tito *et al.*, 2007; Fang and St Leger, 2012).

In this section, photoreactivation was confirmed in UV-C challenged CS from EPF belonging to the genera *Beauveria, Isaria, Lecanicillium, Metarhizium and Tolypocladium.* Conserved regions of *phr-1* candidates from these EPF were amplified, cloned and sequenced. *In silico* techniques were used to: (i) determine the conservation of functionally important

residues, (ii) differentiate the putative CPD-PHRs from (6-4)-PHR and DASH-CRY types through function prediction based on homology modeling and (iii) analyse the phylogenetic relationship between the putative CPD-PHR from EPF and other filamentous fungi.

3.3 Materials and methods

3.3.1 Preparation of cultures

Fungal isolates used for this study included *B. bassiana* GK2016 (laboratory isolate) and those obtained from either American Type Culture Collection (ATCC) or ARSEF: *B. bassiana* ARSEF 3113; *I. farinosa* ATCC 1360; *L. longisporum* ATCC 46578; *M. anisopliae* ARSEF 2038; and *T. inflatum* ATCC 18981 (Table 3.1). Both anamorph and teleomorph names are mentioned in Table 3.1 to make the reading by a general audience more accessible to mycologists and taxonomists. Fungal conidial stocks at 10^7 mL^{-1} stored at –30 °C in 10% (v v^{-1}) glycerol were thawed and 100 µL was used to inoculate plates containing the growth medium containing yeast extract 0.2% (w v^{-1}), peptone 1% (w v^{-1}), glucose 2% (w v^{-1}), (YPG) with 1.5% agar (w v^{-1}) (YPGA) using the spread plate technique. Fungi were incubated in the dark for 10 d at 27 °C for all but *L. longisporum* and *T. inflatum* which were incubated at 24 °C.

Table 3.1 List of EPF used is this thesis section.

Anamorph	**Teleomorph**	**Strain**
Beauveria bassiana	*Cordyceps bassiana*	GK2016
Beauveria bassiana	*Cordyceps bassiana*	ARSEF 3113
Tolypocladium inflatum	*Elaphocordyceps subsessilis*	ATCC 18981
Metarhizium anisopliae	*Metacordyceps taii*	ARSEF 2038
Isaria farinosa	*Cordyceps memorabilis*	ATCC 1360
Lecanicillium longisporum	*Cordyceps confragosa*	ATCC 46578

Conidiospores were harvested from plates by adding 5-8 mL of aqueous sterile 0.02% (v v^{-1}) Tween 80 and physical agitation with a bent glass rod. This suspension was passed through a Pasteur pipette containing glass wool to remove mycelia and agar particles. The filtrate was collected in a sterile glass tube and retained ~ 80% CS and ≤ 0.1% of the mycelia found in the original culture scrapings. This suspension was rinsed twice by centrifugation at 6000 x*g* (IEC MicroMax, USA) for 1 min and resuspension in 1 mL of sterile distilled water to remove residual growth medium. The resulting CS suspension was used to create either CS stocks (stored at -30 °C) for inoculations or CS suspensions used in UVR challenge assays, which contained 10^8 CS mL^{-1} in 10% (v v^{-1}) glycerol or 10^9 CS mL^{-1} in sterile distilled water, respectively.

Liquid fungal cultures were prepared by inoculating YPG or Vogel's medium [VM; 0.5% (w v^{-1}) KH_2PO_4, 0.25% (w v^{-1}) 3Na citrate · $2H_2O$, 0.20% (w v^{-1}) NH_4NO_3, 0.02% (w v^{-1}) $MgSO_4 \cdot 7H_20$, 0.01% (w v^{-1}) $CaCl_2 \cdot 2H_2O$, 0.0009% (w v^{-1}) $ZnSO_4 \cdot 7H_2O$, 0.0001% (w v^{-1}) $FeSO_4 \cdot 7H_2O$, 0.00004% (w v^{-1}) $CuSO_4 \cdot 5H_2O$, 0.000014% (w v^{-1}) $MnSO_4 \cdot H_2O$, 0.000011% (w v^{-1}) $Na_2B_4O_7 \cdot 10H_20$, 0.000005% (w v^{-1}) $(NH_4)_6Mo_7O_{24} \cdot 4H_2O$ in 2% (w v^{-1}) glucose] in an Erlenmeyer flask filled to 20% capacity with 10^6 CS mL^{-1}. Cultures were incubated in the dark, at 27 °C for 68-72 h in a Gyrotory Water Bath Shaker Model G76 (New Brunswick Scientific, Edison, NJ, USA) at 150 revolutions per min (RPM). Fungal biomass was harvested by passing the liquid cultures through a pre-weighed, 4.25 cm diameter, Whatman #2 filter paper under vacuum and rinsed once with phosphate buffered saline [PBS; 0.2 M phosphate buffer, 0.9% (w v^{-1}) NaCl, pH 6.5]. The filter containing the fungal biomass was weighed to determine the fresh (wet) weight of the filtered fungi.

Escherichia coli DH5α (Invitrogen, Carlsbad, USA) was grown in Lysogeny broth agar (10 g L^{-1} bacto tryptone, 5 g L^{-1} yeast extract, 10 g L^{-1} NaCl, 15 g L^{-1} agar, pH 7.5), containing ampicillin (100 µg mL^{-1}) when necessary to select for transformants. The media was inoculated from frozen stocks of *E. coli* stored in 50% (v v^{-1}) Lysogeny broth and 50% (v v^{-1}) glycerol at -30 °C. A sterile loop was used to scrap along the top of the frozen stock and was streaked for colony isolation along a Lysogeny broth agar containing Petri dish and incubated over night at 37 °C. A single colony was transferred using a sterile inoculation needle into 10 mL of Lysogeny broth in a 50 mL flask. Cultures were incubated overnight at 37 °C in a water bath with rotation at 220 RPM.

3.3.2 Photoreactivation bioassay

The UV irradiation of CS was performed as described by Chelico *et al*. (2006) with modifications. Freshly prepared suspensions containing 10^7 CS mL^{-1} in 20 mL of 50 mM PBS, pH 6.5 supplemented with 0.02% (v v^{-1}) Tween-80 to prevent cell clumping were transferred into glass Petri dishes (surface area = 64 cm^2). The suspensions were exposed to UV-C radiation (UVP Mineralight R52G, UVP Inc., Upland, CA, USA) between 200-280 nm, with λ_{max} = 254 nm and irradiance of 0.4 W m^{-2}, as measured by a Blak-Ray® Ultraviolet Intensity Meter, model J225 (UVP, San Gabriel, USA). Irradiation was performed at 23 °C in the absence of light wavelengths needed for photoreactivation (366-435 nm) (Giese *et al.*, 1953) and the suspension was continuously agitated using a magnetic stirrer and bar. During the UV-C challenge, 1 mL samples were taken at intervals that provided the CS with a UV-C dose of 0, 60 or 120 J m^{-2}, which required 0, 2.5 or 5 min, respectively. These samples were diluted in 50 mM PBS with 0.02% (v v^{-1}) Tween-80 to produce ten-fold, serial dilutions and spotted in quadruplicate onto

two YPGA plates as 25 µL aliquots containing an estimated $2.5x10^1 – 2.5x10^5$ CS, depending on the dilution. These plates where then incubated as in 3.3.1 under conditions to either hinder or promote photoreactivation, which was controlled by the absence or the presence of full spectrum light supplied by two fluorescent 34 W lights (Sylvania F40T12/CW/SS, Denver, USA) that were 50 cm directly above the plates, respectively. After 18 h, the light source was removed and the fungi were incubated in the dark for a total of five days. The colony development of the fungi was observed daily from two to five days after UV challenge and CFU were enumerated and used to calculate percent survival, relative to those produced by the unchallenged CS.

3.3.3 Nucleic acid isolation and analysis

Genomic DNA from fungi was prepared as follows. Fresh fungal biomass was collected by vacuum filtration through a 2.5 cm diameter, 0.45 µm pore size, nitrocellulose membrane from liquid cultures grown under specified conditions (see section 3.3.1). It was then frozen with liquid nitrogen and ground with mortar and pestle to disrupt the fungal cells, which was assessed microscopically. This ground fungal material was then used to extract genomic DNA with the DNeasy Plant Mini Kit (Qiagen, Valencia, USA) following the manufacturer's directions. All DNA was quantified spectrophotometrically.

Fungal biomass was prepared for RNA extraction by cultivation in liquid media for three days in the absence of light and exposed to a 34 W full spectrum fluorescent light (Sylvania F40T12/CW/SS, Denver, USA) for 30 min at a distance of 50 cm to induce *phr-1* expression, as per Alejandre-Durán *et al.* (2003). The fungi were harvested by vacuum filtration using a 2.5 cm diameter, 0.45 µm pore size, frozen with liquid nitrogen, ground by mortar and pestle and RNA was extracted with Trizol (Invitrogen, Carlsbad, USA) as per the manufacturer's directions. The

RNA yield and quality was determined by formaldehyde agarose gel electrophoresis as per Sambrook and Russell (2001).

Plasmid DNA was extracted from *E. coli* DH5α (Invitrogen, Carlsbad, USA) using the GeneJET Plasmid Miniprep Kit (Fermentas, EU) following the manufacturer's directions.

3.3.4 Agarose gel electrophoresis

Extracted DNA and PCR products were solubilized in 6X loading buffer [0.25% (w v^{-1}) bromophenol blue, 0.25% (w v^{-1}) xylene cyanol, 40% (w v^{-1}) sucrose] and separated using electrophoresis through 1-1.5% (w v^{-1}) agarose gels containing 0.5 µg mL^{-1} ethidium bromide in 40 mM Tris-HCL, 20mM acetic acid, 10 mM ethylenediaminetetraacetic acid, pH 8.0, using the protocol described by Sambrook and Russel (2001).

Extracted RNA was solubilized in NorthernMax® formaldehyde load dye (Invitrogen) and separated using electrophoresis through a 1% (w v^{-1}) denaturing agarose gel containing 0.5 µg mL^{-1} ethidium bromide in 4.2 g L^{-1} 3-(N-morpholino)propanesulfonic acid, 4.2 g L^{-1} sodium acetate, 1.9% (v v^{-1}) formaldehyde and 10 mM ethylenediaminetetraacetic acid using the protocol described by Sambrook and Russel (2001).

Separated DNA and RNA in the gels were visualized by a short-wave/long-wave UV-B trans-illuminator (UVP, Upland, USA) and photographed using a digital camera. Digital images were processed using Adobe Photoshop version 6 (San Jose, CA, USA).

3.3.5 Amplification of *phr-1* candidates with PCR and rapid amplification of cDNA ends (RACE)

An alignment of class I CPD-PHR was performed with sequences from *Fusarium oxysporum*, *T. atroviride*, *N. crassa*, *Aspergillus fumigatus* and *Cochliobolus miyabeanus* (Table

3.2). The putative *phr-1* sequences from *C. militaris*, *M. anisopliae*, *M. acridum* and *B. bassiana* were not included in the alignment because they were not publicly available at the time. Degenerate primers were designed from conserved regions of *phr-1* that encoded amino acids predicted to be within or near the α-helical domain of CPD-PHR (Park *et al.*, 1995). These primers were named PhrF1, PhrF2, PhrR1 and PhrR2 and all had degeneracies of 64-fold, except PhrR2 had 48 (Table 3.3). Custom oligonucleotides were synthesized and purified by Alpha DNA (Montreal, Canada). All PCRs were performed using a Techne Genius Thermocycler (Staffordshire, UK). Reactions using genomic DNA (1 μg per reaction) as template contained DreamTaq PCR Master Mix (Fermentas, EU), 0.1% (v v^{-1}) Triton X-100 to improve primer annealing (Bachmann *et al.*, 1990) and 0.5 mM of the designated forward and reverse primers. The temperature cycles of the PCR used were: 300 s at 94 °C x1; 60 s at 94 °C, 60 s at 51 °C, 60 s at 72 °C x40; and 15 min at 72 °C x1. All temperature cycles were followed by a 4 °C incubation. The amplicons were resolved on a 1% (w v^{-1}) agarose gel and the bands containing DNA, predicted to be amplified from *phr-1* based on the product's size, were removed from the gel with a sterile scalpel. These products were recovered using the GeneJET gel extraction kit (Fermentas, EU) and sequenced [by National Research Council Plant Biotechnology Institute, (Saskatoon, Canada)] using the same primers they were amplified with.

Table 3.2 List of PHR and CRY sequences used in this study.

Organism			GenBank accession number							
Kingdom	Genus species	Strain	CPD-PHR class			(6-4)-PHR	CRY type			
			I	II	III		DASH	Plant	Insect	Vertebrate
Fungi	*Arthroderma gypseum*	CBS 118893	XP_003172732							
	Aspergillus clavatus	NRRL 1	XP_001269979							
	Aspergillus flavus	NRRL3357	XP_002382347							
	Aspergillus fumigatus	Af293	XP_749910[b]							
	Aspergillus nidulans	FGSC A4	XP_657991							
	Aspergillus niger	CBS 513.88	XP_001402217							
	Aspergillus niger	ATCC 1015				EHA21733				
	Aspergillus oryzae	RIB40	BAE61131							
	Beauveria bassiana[a]	GK2016	JX134052							
	Beauveria bassiana[a]	GK2016	JX134058							
	Beauveria bassiana[a]	ARSEF 3113	JX134053							
	Botryotinia fuckeliana	NA	CCD34389							
	Candida tenuis	ATCC 10573	EGV62004							
	Cercospora zeae-maydis	NA				ACB38886[d]				
	Clavispora lusitaniae	ATCC 42720	XP_002614457							
	Cochliobolus miyabeanus	NA	BAD18969[b]							
	Cordyceps militaris[a]	CM01	EGX95497[b]							
	Debaryomyces hansenii	CBS767	XP_456362							
	Fusarium oxysporum	NA	AAP30741[b]							
	Gibberella zeae	PH-1	XP_380973							
	Glarea lozoyensis	ATCC 74030	EHL02245							
	Isaria farinosa[a]	ATCC 1360	JX134056							
	Lecanicillium longisporum[a]	ATCC 46578	JX134057							
	Lecanicillium longisporum[a]	ATCC 46578	JX134060							
	Leptosphaeria maculans	JN3	CBX91336							
	Metarhizium acridum[a]	CQMa 102	EFY88439[b]							
	Metarhizium anisopliae[a]	ARSEF 23	EFY99158							
	Metarhizium anisopliae[a]	ARSEF 2038	JX134055							
	Metarhizium anisopliae[a]	ARSEF 2038	JX134059							
	Microsporum canis	CBS 113480	XP_002843638							
	Nectria haematococca	mpVI 77-13-4	XP_003053859							
	Neosartorya fischeri	NRRL 181	XP_003172732							
	Neurospora crassa	NA	XP_964834[b c]				XP_965722			
	Neurospora tetrasperma	FGSC 2508	EGO53807							
	Penicillium chrysogenum	Wisconsin 54-1255	XP_002566149							
	Phaeosphaeria nodorum	SN15	XP_001791207							
	Pichia farinosa	CBS 7064	XP_002843638							
	Pichia guilliermondii	ATCC 6260	XP_001482066							
	Pyrenophora teres	f. teres 0-1	XP_003297506							
	Saccharomyces cerevisiae	IMI 206040	EGA76693[b]							
	Sclerotinia sclerotiorum	1980 UF-70	XP_001587047[b]				XP_001593735[d]			
	Sordaria macrospora	k-hell	XP_003347602							
	Talaromyces stipitatus	ATCC 10500	XP_002480865							
	Tolypocladium inflatum[a]	ATCC 18981	JX134054							
	Trichoderma atroviride	IMI 206040	EHK39920[bd]							
	Trichoderma reesei	QM6a	EGR48366							
	Trichoderma virens	Gv29-8	EHK19098							
	Trichophyton equinum	CBS 127.97	EGE08070							
	Trichophyton rubrum	CBS 118892	XP_003237491							
	Verticillium albo-atrum	VaMs.102	XP_002999933							

Table 3.2 Continued.

Organism			GenBank accession number							
Kingdom	Genus species	Strain	CPD-PHR class			(6-4)-PHR	CRY type			
			I	II	III		DASH	Plant	Insect	Vertebrate
Bacteria	*Agrobacterium tumefaciens*	str. C58			NP_354235					
	Bradyrhizobium WSM471	NA			ZP_09649245					
	Caulobacter crescentus	CB15			NP_420241[c]					
	Desulfovibrio fructosovorans	JJ		ZP_07332046[c]						
	Escherichia coli	Sakai	NP_308760[b c]							
	Flavobacterium psychrophilum	JIP02/86					YP_001296908			
	Gloeobacter violaceus	PCC 7421					NP_923781			
	Psychrobacter arcticus	273-4	YP_263727[b]							
	Rhizobium leguminosarum	bv. viciae 3841			YP_767586					
	Rhodospirillum centenum	SW			YP_002298232					
	Synechococcus JA-3-3Ab	NA					YP_473788			
	Vibrio cholerae	N16961	NP_232458[b]							
Archaea	*Methanosarcina barkeri*	str. Fusaro		YP_304088						
Plantae	*Arabidopsis thaliana*	NA		NP_849651		BAA24449	Q84KJ5[c]	NP_567341[c]		
	Brassica rapa	NA						ABI31780		
	Medicago truncatula	NA						XP_003615112		
	Oryza sativa	Japonica Group		Q6F6A2		NP_001046243	Q651U1	CAD40850		
	Zea mays	NA					NP_001146707	NP_001170477		
Animalia	*Anopheles gambiae*	str. PEST							XP_321104[c]	
	Bombus impatiens	NA		XP_003489032						
	Drosophila melanogaster	NA				3CVU_A[c]			BAA35000	
	Glossina morsitans	morsitans							ADD19502	
	Spodoptera exigua	NA							ADY17887	
	Bos taurus	NA								NP_001098885
	Danio rerio	NA				AAH44204	Q4KML2			NP_571865
	Homo sapiens	NA								NP_004066[c]
	Mus musculus	NA								NP_031797
	Salmo salar	NA								ACN10538
	Xenopus laevis	NA		NP_001089127[c]		NP_001081421	NP_001084438			NP_001081129

(a) Indicates EPF with putative CPD-PHR sequences from this study and others.
(b) Class I CPD-PHR sequences that were included in the analysis with the other PHR/CRY sequences.
(c) Known PHR/CRY sequences used for homology searching to find related sequences.
(d) Fungal sequences used as controls for structure/function predictions with iTASSER and CombFunc servers.

Table 3.3 Sequences of oligonucleotide primers used in this study for degenerate PCR, RACE and confirmation of *phr-1* products.

Primer	Sequence (5' → 3') [a]	Organism	Use
PhrF1	GCIGTITAYASNCGNTGGT	All EPF tested	Degenerate PCR
PhrF2	IGGYTGIGGRTCNACNCC		Degenerate PCR
PhrR1	GTIGCITGGMGRGANTTYTA		Degenerate PCR
PhrR2	ICCCCAICCNCCRTKRTT		Degenerate PCR
GK-F1.1	TGGCGGGGAGGGAATTCTATCGCCA	*B. bassiana GK2016*	3' RACE
GK-F1.2	CGCCACGTATTGGTCAGATGGCCAC		3' RACE
GK-F2.2	TGCGACAGCTGAATCACATGGGC		3' RACE and *phr1* confirmation[b]
GK-R1.1	TCGCCCATGCGCCAGTCAAGG		5' RACE and *phr1* confirmation[b]
GK-R2.1	CCCAGTTTTGCCCTCACACCAGGCG		5' RACE and 5' nested RACE
AR-F1.1	GCCCCGTATTAGTCAGAAGGGCCCA	*B. bassiana ARSEF 3113*	3' RACE
AR-F2.1	GCCTGGTGTGAGGGCAAAACCGG		3' RACE and 3' nested RACE
AR-R1.1	CGCCCATGCGCCCGTCTATGAGTA		5' RACE
AR-R2.1	CGGTTTTGCCCTCACACCAGGCG		5' RACE and 5' nested RACE
If-F1.1	GAACTTGCGTGCGGACCGCGA	*I. farinosa*	3' RACE
If-F2.1	CCCCGTATGGTGGTCGCGTC		3' RACE and 3' nested RACE
If-R1.1	AGACGCGACCACCATACGGGGC		5' RACE
If-R2.1	CGCTGTATTCGCCAACGCGC		5' RACE and 5' nested RACE
Ll-F1.1	GCTTCCCGATCGTTGACGCCGC	*L. longisporum*	3' RACE
Ll-F1.2	ATGCGCCAGCTTCGCCACTCG		3' RACE
Ll-F2.1	GCATAACCGCACGCGCATGG		3' nested RACE and *phr1* confirmation[b]
Ll-R1.1	GGTTGGAGGCGAAGTCTCCGT		5' RACE and *phr1* confirmation[b]
Ll-R1.2	GAAACGACCATGCGCGTGCGG		5' RACE and 5' nested RACE
Ll-R2.2	GCGAAGCTGGCGCATTGCGG		5' nested RACE
Ma-F1.1	GGTGCGATGGCAAGACTGGCT	*M. anisopliae*	3' RACE
Ma-F2.1	GCGCCAGCTGAACCACTCGGGAT		3' RACE and *phr1* confirmation[b]
Ma-R1.1	AGACCGCTTACCCTTGCGCCAAT		5' RACE and *phr1* confirmation[b]
Ma-R2.1	CCCGAGTGGTTCAGCTGGCG		5' RACE and 5' nested RACE
Ti-F1.1	GAGGGCCGCACTGGCTTCCCT	*T. inflatum*	3' RACE and *phr1* confirmation[b]
Ti-F2.1	GGCGCAAGGGCGAGCGGTAC		3' RACE and 3' nested RACE
Ti-R1.1	AGAGCCCCAGCCCCCGTGGT		5' RACE
Ti-R2.1	CGCTCGCCCTTGCGCCAGTCT		5' RACE and 5' nested RACE
Ti-R2.2	GGCGACGATCATTCGGCAGCGG		5' nested RACE and phr1 confirmation[b]

(a) Degenerate sequences code: R = G or A, K = G or T, S = G or C, M = A or C, Y = T or C, N = any and I = inosine.

(b) The designated primers were used to confirm the 3' RACE products were from putative *phr-1*.

The PCR technique, RACE (Frohman *et al.*, 1988) was employed to obtain the remaining 5' and 3' regions of putative *phr-1* that flanked the regions isolated from fungal DNA. The RNA from each fungus was used to create a cDNA containing 5' or 3' adapters using the FirstChoice® RLM-RACE Kit (Invitrogen, Carlsbad, USA). Products were amplified in 25 µL PCRs with Platinum® Taq High Fidelity DNA polymerase (Invitrogen, Carlsbad, USA) as per the manufacturer's directions with the exception of using 1 µL of reverse transcription reaction with 0.4 mM of the appropriate *phr-1* primer and 0.6 mM of the outer 5' or 3' RACE primer supplied by the manufacturer. The *phr-1* primers for RACE and product confirmation were designed using the putative *phr-1* sequences obtained from the EPF (Table 3.3). Touchdown PCR (Don *et al.*, 1991) was used to amplify the putative *phr-1* sequences with the following temperature cycles: 120 s at 94 °C x1; 30 s at 94 °C, 100 s at 68 °C x5; 30 s at 94 °C, 30 s at 65 °C, 100 s at 68 °C x5; 30 s at 94 °C, 30 s at 63 °C, 100 s at 68 °C x5; 30 s at 94 °C, 30 s at 61 °C, 100 s at 68 °C x25; and 10 min at 68 °C. The presence of PCR products were determined by electrophoresis through a 1.5% (w v^{-1}) agarose gel.

The above RACE reactions were used as templates for nested PCRs utilizing RACE and *phr-1* specific primers to, respectively, anneal to internal priming sites on the 5'and 3' nested RACE adapters and putative *phr-1* sequences. These 25 µL reactions were catalysed by one unit of activity (u) of recombinant Taq DNA Polymerase (Invitrogen, Carlsbad, USA) as per the manufacturer's directions with the exception of using 2 µL of the initial RACE reaction as template and 0.3 mM and 0.6 mM of the appropriate *phr-1* and inner RACE primer, respectively. Touchdown PCR was used for these nested reaction with the following temperature cycles: 120 s at 94 °C x1; 30 s at 94 °C, 30 s at 70 °C, 120 s at 72 °C x5; 30 s at 94 °C, 30 s at 67 °C, 120 s at 72 °C x5: 30 s at 94 °C, 30 s at 64 °C, 120 s at 72 °C x5; 30 s at 94 °C, 30 s at 61 °C, 120 s at 72

°C x25; and 15 min at 72 °C x1. The presence of PCR products was determined by electrophoresis through a 1.5% (w v^{-1}) agarose gel.

All RACE products of expected size were recovered by gel purification as above. These products were tested for nested *phr-1* sequences by PCR using the same protocol as the nested RACE reaction, except 0.3 mM of the primers designated for *phr-1* confirmation were included. Candidate *phr-1* products were inserted into pCR® 4-TOPO (Invitrogen, Carlsbad, USA) and used to transform chemically competent *E. coli* DH5α (Invitrogen, Carlsbad, USA) as per the manufacturer's directions. Transformants were selected using ampicillin (100 µg mL^{-1}) and X-gal (50 µg mL^{-1}) to screen the colonies for plasmid and insert presence, respectively. Colony PCR (Sambrook and Russell, 2001) was used to confirm that the transformants contained the putative *phr-1* insert. Plasmids were extracted and the inserts were sequenced [by National Research Council Plant Biotechnology Institute (Saskatoon, Canada)] using M13 forward (-20) and M13 reverse priming sites.

3.3.6 Sequence analysis

Nucleotide and amino acid alignments were performed using ClustalW with the default settings [http://www.ebi.ac.uk/Tools/ clustalw2/index.html; (Larkin *et al.*, 2007)]. Amino acid sequences were deduced using EMBOSS Transeq [http://www.ebi.ac.uk/emboss/transeq/ index.html; (Rice *et al.*, 2000)].

The amino acid sequences deduced from the putative *phr-1* regions were analyzed using the PROSITE database. The Expert Protein Analysis System proteomics server was used to scan input sequences for known protein domains, families and functional sites present in the PROSITE database using the default settings (de Castro *et al.*, 2006).

Homology searches and alignments for phylogenetic analysis were performed using the phylogeny.fr service [www.phylogeny.fr; (Dereeper *et al.*, 2008)]. Sequence homologues of PHRs and CRYs were found using the 'Blast Explorer' function (Dereeper *et al.*, 2010) with the indicated sequence inputs to query for homologues of each PHR/CRY type (Table 3.2). All queries were performed with an E-value cut-off of 10^{-5} and returned approximately 2900 hits for each, except for the class II CPD-PHRs from *X. laevis* and *Desulfovibrio fructosovorans* which had 345 and 622 hits, respectively. A subset of identified homologues was selected to provide a comprehensive representation of PHR and CRY sequences to be used for phylogenetic analysis. Phylogenetic analysis of only class I CPD-PHRs from fungi was also performed and included the putative CPD-PHR sequences found in this study.

All sequences were aligned with MUSCLE (v3.7) using default settings and a maximum of 16 iterations (Edgar, 2004). Curation was performed with Gblocks using the default settings, to remove ambiguous regions that contained gaps or were poorly aligned (Castresana, 2000). This was performed so that (a) the minimum length of a block after cleaning was ≥ 10 aa, (b) all gap positions were removed for the final alignment, (c) no segments with contiguous non-conserved positions were bigger than eight amino acids (i.e. were rejected) and (d) the minimum number of sequences for a flank position was 85% as per Castresana (2000). The maximum likelihood method in the PhyML program (v3.0 aLRT) was used to reconstruct the phylogenetic tree with the default settings. The substitution models were selected assuming an estimated proportion of invariant sites for each model (Castresana, 2000). To account for rate hetero-geneity across sites, four gamma-distributed rate categories were used and the gamma shape parameter was estimated directly from the data. Support for internal branching was evaluated

using the bootstrap method with 200 replicates (Guindon and Gascuel, 2003). Phylogenetic trees were illustrated with TreeDyn (v198.3) using the default settings (Chevenet *et al.*, 2006).

3.3.7 Protein structure/function prediction

Structure/function prediction was achieved using the iTASSER (Roy *et al.*, 2010) and CombFunc (Wass *et al.*, 2012) servers which use homology modeling to predict structure and/or function from input protein sequences. This was performed as directed by the servers' instructions with the default settings. The test sequences used were the putative CPD-PHRs from the EPF studied here.

The CPD-PHR, (6-4)-PHR and DASH-CRY sequences from *T. atroviride, Cercospora zeae-maydis* and *S. sclerotiorum*, respectively, were used as control inputs for the corresponding PHR and CRY types found in fungi. This was performed to determine the servers' ability to differentiate between these CRY/PHR types and improve confidence in the results of the functions predicted for the putative CPD-PHR sequences.

As required by the servers' limitations in modeling proteins with multiple domains, only the region that contained the α-helical domain was submitted for each sequence. These sequences were found to have homology with templates in the protein data bank with solved structures which allowed the structure/function of each of the putative CPD-PHRs and control sequences to be predicted with very high confidence (reported as C-scores and percent confidence by the iTASSER and CombFunc servers, respectively). This was due to the test sequences having > 50% sequence similarity with known structures, whereas only ~ 20% is required to provide accurate structure modeling (Kelley and Sternberg, 2009). Consensus values for gene ontology (GO) prediction were reported as GO-Score and support vector machine probability for

iTASSER and CombFunc, respectively. Cut-offs of 0.5 were used for GO-Scores and probabilities to ensure the best false-positive and false-negative rates were obtained (Roy *et al.*, 2010; Wass *et al.*, 2012).

3.4 Results and discussion

3.4.1 Photoreactivation of UV-C irradiated CS

Survival of EPF CS challenged with 60 or 120 J m^{-2} of UV-C was higher after treatment with light than without (Figure 3.1A) and is the hallmark of the photoreactivation phenomenon (Rupert *et al.*, 1958). The results of this bioassay showed that EPF strains that received 'white' light treatment survived UV-C in the following ranked order: *L. longisporum* > *B. bassiana* ARSEF 3113 > *B. bassiana* GK2016 > *I. farinosa* > *T. inflatum* > *M. anisopliae*. In addition, the growth and development of the colonies was hastened by approximately one to two days, depending on the strain, following photoreactivation, compared to the CS that were not permitted to perform photoreactivation (no light) (Figure 3.1B).

Figure 3.1 Photoreactivation of UV-C challenged CS from five genera of EPF. The fungus used is indicated between panels A and B. Panel A shows survival of UV-C challenged CS following incubation with (○) or without (●) the presence of full spectrum white light following the indicated dose. This data was obtained from three trials and error bars show standard error of the mean (SEM). Panel B shows representative photographs of 1 cm^2 sections of YPGA containing UV-C irradiated CS taken daily over two to five days, post challenge (indicated to the far right). These show the relative growth and development of CFUs that arose from CS treated with (+) or without (-) photoreactivating light post UV-C challenge. Shown for each fungus and both treatments was the lowest inoculum that produced CFUs following incubation without light. For all CS that received no UV-C (0 J m^{-2}) this inoculum was ~ 25 CS and for those that received 120 J m^{-2} UV-C it was ~ 2.5 x 10^4 CS for *B. bassiana* ARSEF 3113, *L. longisporum* and *M. anisopliae* or 2.5 x 10^5 CS for *B. bassiana* GK 2016, *I. farinosa* and *T. inflatum*.

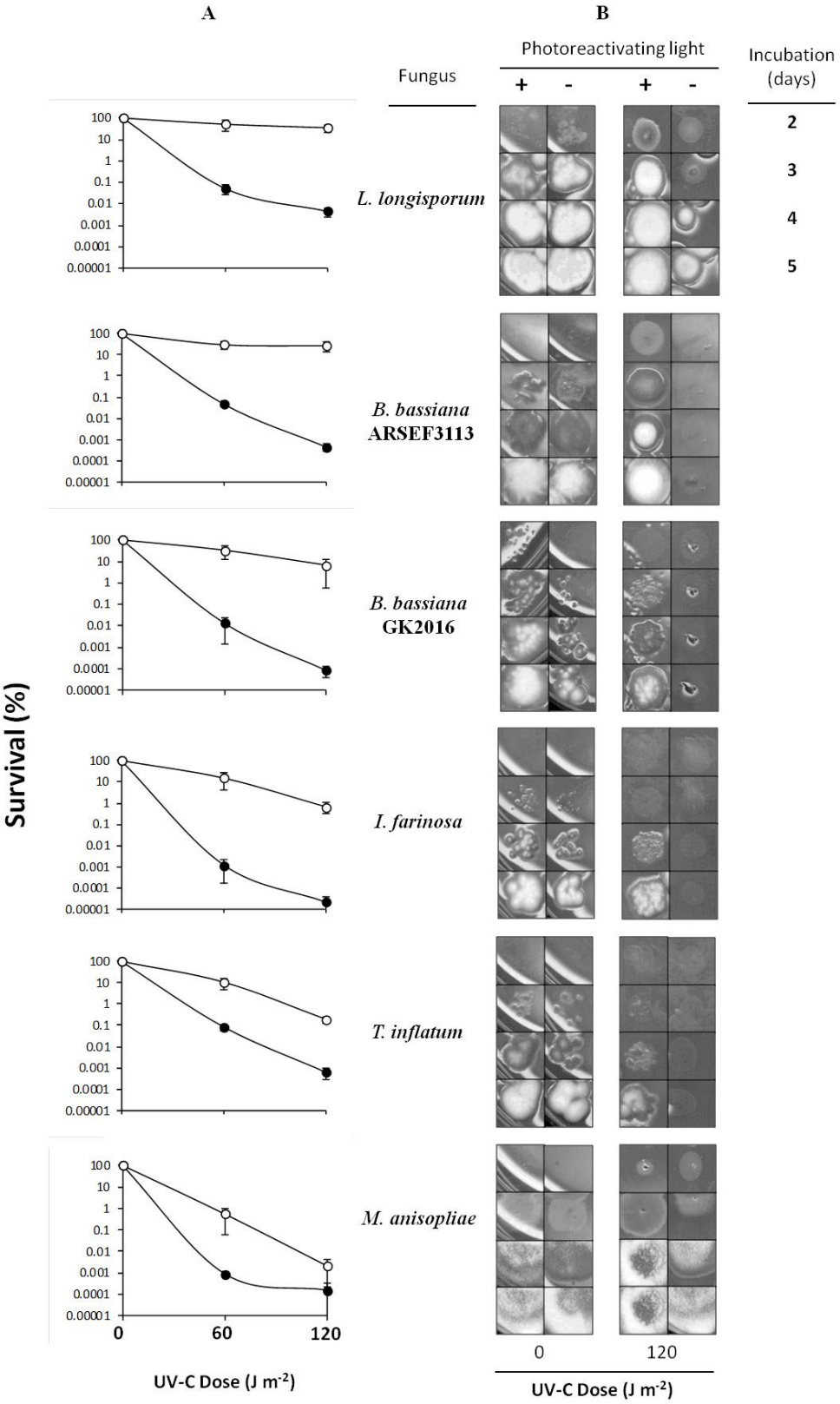
A
B
Fungus
Photoreactivating light
+
-
+
-
Incubation (days)
2
3
4
5
L. longisporum
B. bassiana ARSEF3113
B. bassiana GK2016
I. farinosa
T. inflatum
M. anisopliae
Survival (%)
100
10
1
0.1
0.01
0.001
0.0001
0.00001
0
60
120
UV-C Dose (J m-2)
0
120
UV-C Dose (J m-2)

These reductions in growth, development and viability are likely contributed to by UV-C induced lesions, such as CPDs and (6-4)PPs. These dimers are required to be repaired sufficiently before germination can proceed and can lead to delayed colony development and reduction in viability at higher doses of UVR (Chelico and Khachatourians, 2008; Nascimento *et al.*, 2010). Conidia incubated in the presence of light can better recover from the UV-C insult most likely through repair of dimers by PHRs. Studies in *B. bassiana* have shown that CS not permitted to photoreactivate following UV-C challenge contained approximately double the number of CPDs compared to those that were exposed to white light (Chelico *et al.*, 2005). Furthermore, photoreactivation was sufficient to enable rapid germination of irradiated CS in both wild-type and putative NER mutants in *B. bassiana* (Chelico and Khachatourians, 2008). Although, (6-4)PP repair was not found to be associated with photoreactivation in *B. bassiana* (Chelico, 2004), it has been demonstrated in *M. robertsii* (Fang and St Leger, 2012). Nonetheless, induction of (6-4)PPs by UV-C is known to occur at a third of the rate of CPDs (Kim *et al.*, 1994) and can be repaired by NER which is functional irrespective of light. The ability of the EPF strains to better survive UV-C irradiation following treatment with photoreactivating light provided credence to pursue the presence of a gene that may be potentially involved this phenomenon, *phr-1*, encoding the enzyme CPD-PHR.

3.4.2 Amplification and sequence analysis of putative *phr-1* regions

With the confirmation of photoreactivation in the EPF, it was hypothesized that they may encode a class I, CPD-PHR, which would be consistent to findings in other filamentous fungi (Berrocal-Tito *et al.*, 1999; Alejandre-Durán *et al.*, 2003; Kihara *et al.*, 2004). The CPD-PHR sequences from five filamentous fungi were used to assist in degenerate primer design through

alignment of the deduced amino acid sequences encoded by the model *phr-1*s (Figure 3.2A). Several regions were found to be conserved between these fungi. The DNA sequences encoding four such regions within or close to the α-helical domain of CPD-PHR were used as templates to design degenerate oligonucleotide primers. This domain is known to contain many important residues involved in functions, such as CPD-, FAD- and MTHF-binding (Berrocal-Tito *et al.*, 1999; Kihara *et al.*, 2004). The primers were named PhrF1, PhrF2, PhrR1 and PhrR2 and had 64-fold degeneracy, except PhrR2 which had 48-fold, and all included two inosine bases in the 5' end of the primers to improve amplification of the predicted product (Knoth *et al.*, 1988). The PCRs using the primers PhrF2 and PhrR2 produced a product of ~ 400 bp from the genomic DNA of each of the EPF, while PhrF1 and PhrR1 generated a product of expected size (~ 800 bp) only from *I. farinosa* (Figure 3.2B, Lanes 1-6).

Figure 3.2 Degenerate primer design and amplification of putative *phr-1* sections from six EPF using PCR and RACE. Panel A shows an amino acid alignment of a conserved region in class I CPD-PHRs from the filamentous fungi *T. atroviride* (Ta, CAA08916, 629aa, region 285-584), *F. oxysporum* (Fo, AAP30741, 630aa, region 286-585), *N. crassa* (Nc, CAA41549, 642aa, region 289-588), *A. fumigatus* (Af, XP_749910, 586aa, region 243-541) and *C. miyabeanus* (Cm, BAD18969, 634aa, region 287-586). Highlighted areas represent conserved regions that were used to design the respective primers, which are indicated by arrows that designate their 5' to 3' orientation. The α symbol designates where the α-helical domain begins and extends to the C-terminal end of the protein, as defined by Park *et al.* (1995). Panel B shows results of PCR and RACE to amplify the putative *phr-1* sections in EPF. Primer set PhrF2/R2 was used for PCRs shown in lanes 1-5 and set PhrF1/R1 in lane 6. The RACE products shown in lanes 7-11 were amplified using 3' RACE primers with the *phr-1* specific primers GK-F1.2, GK-F2.2, Ma-F1.1, Ma-F2.1 and Vl-F1.1, respectively. Template DNA for the reactions was as follows: lanes 1, 7 and 8 were *B. bassiana* GK2016; 2 was *B. bassiana* ARSEF 3113; 3 was *T. inflatum*; 4, 9 and 10 were *M. anisopliae; 5* and 11 were *L. longisporum*; and 6 was *I. farinosa.* Lanes labeled as L, indicated the DNA ladder and their masses are shown (bp) to the right of all lanes that were from the same gel.

A

```
Ta  QYAVYTPWYRAWMAHIHENLDLLEIYDRPEKNPGATRRTFKTLFDCPIPDAPKNKQLNDE 344
Fo  QYAVYTPWYRSWVAHIHENLDLLELYEPPEKNPSSARKVFAKLFDVEIPDAPKSKRLDGE 345
Nc  QYAVYSPWFRAWIKHIEENPECLEIYEKPGPNPPGTKEKHENLFACSIPEAPEGKRLRDD 348
Af  QYAVYSPWYRTWVAYLNENPGCLEVSEEPGSNPGDARKYFKELFESEVPAAPEHKQLSEE 302
Cm  QYAVYTPWYRAWIAYLHAHPHLLNERSMPEKNPTGFREKFTKLFDSRVPDLPDCKSLTAE 346
    *****:**:*:*: ::. :   *:  . *  **   :. .  **   :*  *. * *  :
      PhrF1

                        α
Ta  EKKRFHGLWPCGEHEAMSRLEKFCDEAVTSYHDRRNIPGDNGTSCLSVHLASGTISSRTC 404
Fo  EKERLRSLWPCGEHEAKKRLDKFCEEMIGNYQKKRNIPAEAGTSSISVHLASGTISARTC 405
Nc  EKARYHSLWPAGEHEALKRLEKFCDEAIGKYAERRNIPAMQGTSNLSVHFASGTLSARTA 408
Af  EKQHLGHLYPAGEHEALRRLEAFLEEKGRDYAEERNMVSGQTTSILSPYFASGLLSARTA 362
Cm  EKERFHHLWPAGEAAAIDRLERFLTEKVIKYKDTRNFPALNSTGRISAHHAAGTLAARTS 406
    ** :   *:*.**  *  **: *  *   .* . **: .   *. :* : *:* :::**.

Ta  VRTARDRNKTKRLDGGHQGIHVWISEVAWRDFYKHVLVNWPYVCMNKPFKPEYANIEWSY 464
Fo  VRTARDRNKTKKLNGGNEGIQTWISEVAWRDFYKHVLVHWPYVCMNKPFKPEYSNISWSY 465
Nc  IRTARDRNNTKKLNGGNEGIQRWISEVAWRDFYKHVLVHWPYVCMNKPFKPTYSNIEWSY 468
Af  IEHAR-RANKGSLQHGDPGLVRWIGEVAWREFYRHVLVHWPFICMNKCFKPEFTNLEWEY 421
Cm  VRMARDINSVKKLDGGKEGIKGWIGEVAWRDFYRHVLVHWPYVCMNKPFKYEYTNIEWEY 466
    :. **   .   *: *. *:  **.*****:**:****:**::**** **  ::*:.*.*
                                  PhrF2

Ta  NMDHFEAWCEGRTGFPIVDAAMRQLNHMGYMHNRCRMIVASFLSKDLLIDWRMGEKYFME 524
Fo  DNEHFAAWCEGRTGFPIVDAAMRQLNHLGYMHNRCRMIVACFLAKDLLLDWRKGERYFME 525
Nc  NVDHFHAWTQGRTGFPIIDAAMRQVLSTGYMHNRLRMIVASFLAKDLLVDWRMGERYFME 528
Af  EEDRFTAWREGKTGFPIVDAAMRQAKQDKWMHNRTRMIVASFLSKDLLLDWRRGERYFME 481
Cm  NDAHFEAWTQGRTGYPIVDAAMRCLKHTGYMHNRLRMITASFLAKHLLLDWRLGEQYFIT 526
    :  :* ** :*:**:**:*****      :**** ***.*.**:*.**:*** **:**:

Ta  HLVDGDFASNNGGWGFSASVGVDPQPYFRVFNPLLQSEKFDPNGEYIRKWIPELKALSDK 584
Fo  HLVDGDFASNNGGWGFSASVGVDPQPYFRIFNPLLQSEKFDPDGDYIRKWVPELKDLDRK 585
Nc  HLIDGDFASNNGGWGFAASVGVDPQPYFRVFNPLLQSEKFDPDGDYIRKWVEELRDLPEL 588
Af  TLIDGDFASNHGGWGFGSSTGVDPQPYFRIFNPLLQSERFDPDGEYIRKWVPELRDIQGA 541
Cm  HLIDGDFASNNGGWGFSASTGVDPQPYFRIFNPWTQSEKFDEQGEFIRLWVKELEDVQGA 586
     *:*******:*****.:*.*********:***  ***:** :*::** *: **. :
              PhrR2       PhrR1
```

B

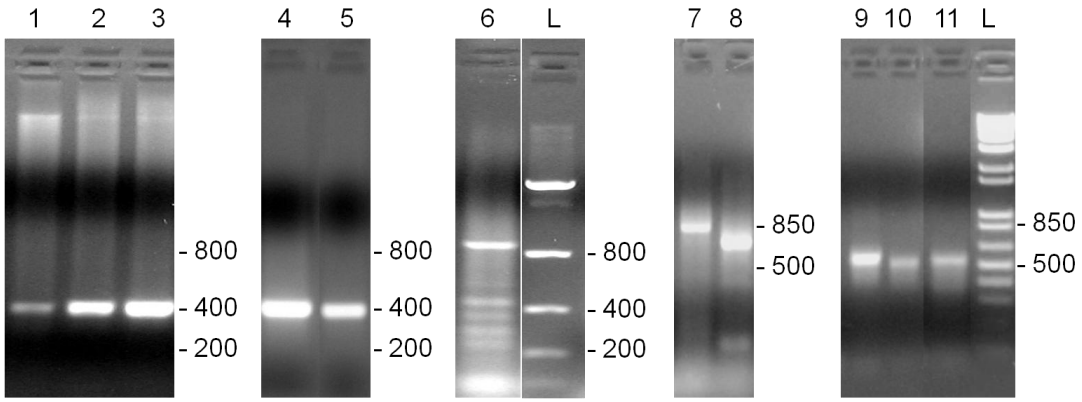

The putative *phr-1* products amplified from EPF DNA were sequenced and assessed as representative of *phr-1* by homology searching with BLASTx queries using the default settings (Altschul *et al.*, 1997). Only one reading frame for each sequence provided a match with CPD-PHRs from non-EPF and produced BLAST scores that ranged from 183-372. The presence of predicted introns was apparent following sequence alignments between the sections of putative *phr-1* from EPF and cDNA from model fungi, since inserts (with several containing stop codons) existed in the former. Further support was provided to the presence of the putative introns since the range of highest scores returned by the BLASTx queries increased to 208-386 (from 183-373) following their removal. Whether the sequences included introns or not, the sections of putative *phr-1* from *B. bassiana* ARSEF 3113 and *T. inflatum* returned the lowest and highest BLAST scores, respectively, and had most sequence similar with *T. atroviride* (83 and 81%, respectively).

The apparent intron-like insertions were 47 to 52 nts and were found at specific conserved locations in the putative *phr-1* sequences (Figure 3.3). There was also less overall sequence conservation within the predicted introns than the surrounding regions, which is consistent with findings in introns of other fungi (Kupfer *et al.*, 2004). In addition, these putative introns were flanked by a 5' GT and 3' AG which are hallmark indicators of the splice site bordering introns in fungi (Kupfer *et al.*, 2004). This is because RNA *cis* elements GU and AG, corresponding to GT and AG, are required by the spliceosome for proper recognition of the splice site during mRNA processing (Maniatis and Tasic, 2002). Furthermore, an internal branch site required for intron removal was identified. These branch sites perfectly matched the DNA consensus sequence of CTA/GAC/T found in *A. nidulans* and *N. crassa* (Kupfer *et al.*, 2004). The sizes of the predicted introns from putative *phr-1s* varied from 47 to 52 nts which were of

similar size compared to *phr-1* introns found in *A. fumigatus* (NC_007194.1; region 500803 to 502611) and *N. crassa* (X58713), which were 48 and 75 nts, respectively. Also, the predicted introns were smaller than the mean size found in other filamentous fungi, being 20 and 70 nts smaller than the mean from *A. nidulans* and *N. crassa*, respectively (Kupfer *et al.*, 2004).

The sequence information from the putative *phr-1s* was used to design nested primers for 3' and 5' RACE to specifically amplify the remaining flanking regions. The RNA from each fungus was extracted and used to create cDNA template for 3' or 5' RACE. Products derived from putative *phr-1* with the initial RACE reactions were expected to produce products of 490-780 bp and 1040-1620 bp for 3' and 5' products, respectively. For both 3' and 5' RACE, the sizes of the products were dependent on the fungi, primer used and size of RACE adapters which were 36 and 44 bp for 3' and 5' RACE, respectively. Regarding polyadenylation, mRNA from *S. cerevisiae* was shown to commonly be A_{55-75} and was taken into account for 3' RACE products (Kushner, 2004). Only 3' RACE reactions resulted in products of expected sizes from *B. bassiana* GK2016 (GK-F1.1, 850 bp; GK-F2.2, 700 bp), *M. anisopliae* (Ma-F1.1, 550 bp; Ma-F2.1, 500 bp) and *L. longisporum* (Ll-F1.1, 550 bp) (Figure 3.2B, Lanes 7-11). Aliquots from the initial RACE reactions that did not produce a product of expected size were used as template for a second RACE reaction to amplify putative *phr-1* products that may be present at low copy number. This was performed with nested inner RACE and gene specific primers that were designed to anneal to the putative *phr-1* product amplified by the first RACE reaction. Only nested 3' RACE with Ll-F2.1 produced an amplicon with the expected size of 500 bp. However, none of the other nested RACE reactions generated products of the expected size, indicating that a putative *phr-1* derived product was not likely present following the first RACE reaction.

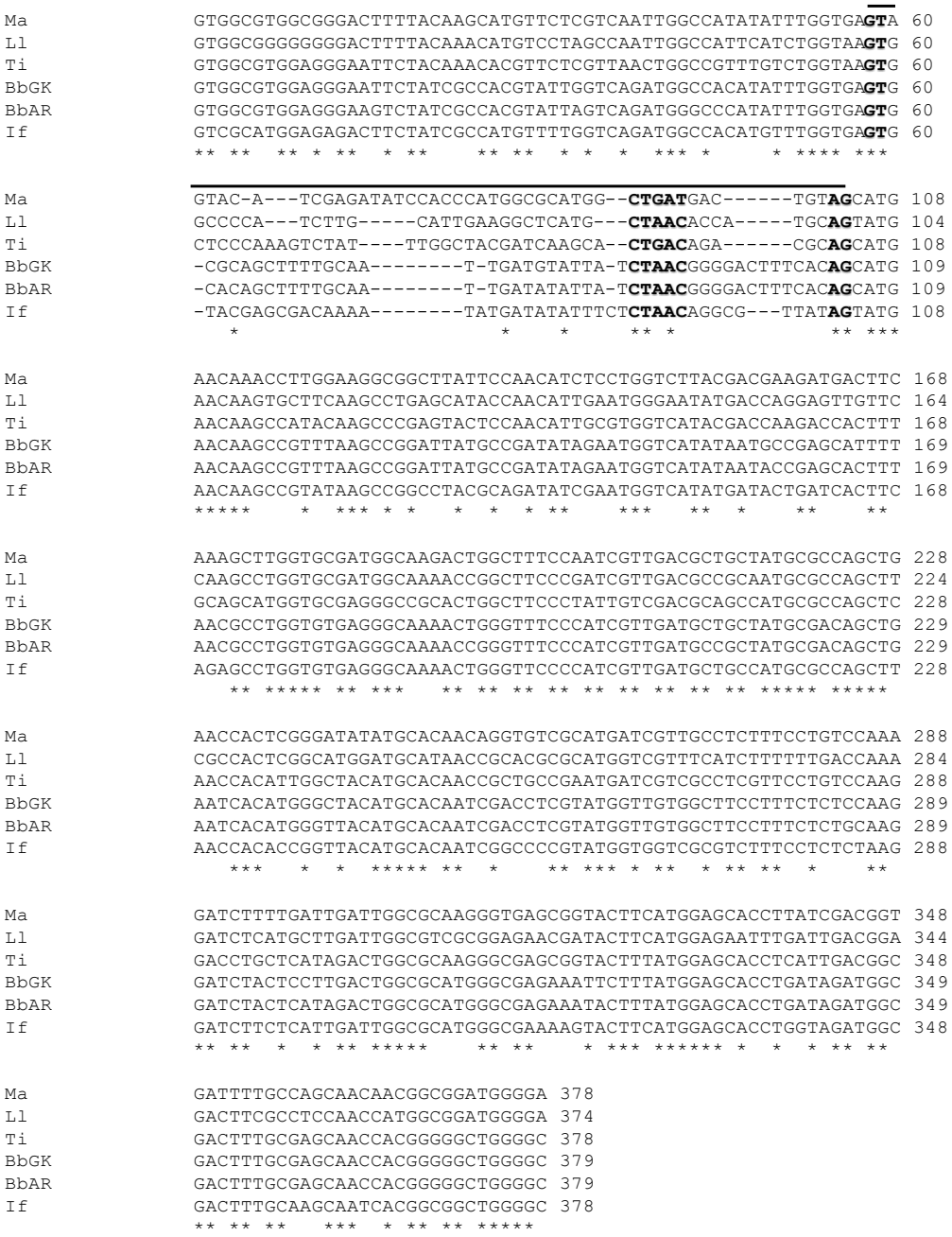

Figure 3.3 Alignment of DNA sequence derived from the putative *phr-1* from several EPF. The above sequences of the putative *phr-1s* were from *M. anisopliae* (Ma), *L. longisporum* (Ll), *T. inflatum* (Ti), *B. bassiana* GK 2016 (BbGK), *B. bassiana* ARSEF 3113 (BbAR) and *I. farinosa* (If). The line indicates the location of the predicted intron. The bolded sequences designate the branch and the flanking GT and AG sequences that are conserved within the 5' and 3' regions of introns in filamentous fungi, respectively. For If, 325 bp located directly 5' of the sequence shown was excluded from the alignment because this region was not present in the sequences generated from the other EPF, due to the size of the products.

The RACE products were confirmed to be putative *phr-1* products by nested PCRs using the primers indicated in Table 3.3. All RACE templates yielded amplicons of expected sizes of ~ 100 bp for both *B. bassiana* GK2016 and *M. anisopliae* and 120 bp for *L. longisporum*. The products were inserted into pCR® 4-TOPO and used to transform *E. coli* and the inserts were sequenced. The putative *phr-1* sequences obtained by 3' RACE from *B. bassiana* GK2016, *M. anisopliae* and *L. longisporum* respectively, revealed an additional 132, 270 and 264 bp, 3' (downstream) of the regions initially obtained from genomic DNA. Alignments between sequences obtained from cDNA and genomic DNA confirmed the presence of the putative intron in the predicted position and matched perfectly with the splice sites bordering the removed intron in the cDNA sequence. The cDNA sequences from *B. bassiana* GK2016, *L. longisporum* and *M. anisopliae* were combined with their respective genomic sequences and analyzed along with the putative *phr-1* sections (introns removed) from the other EPF. The amino acid sequences encoded by these putative *phr-1* sections were deduced by *in silico* translation.

3.4.3 Molecular analysis of regions of putative CPD-PHRs encoded by *phr-1* candidates

The amino acid sequences deduced from sections of putative *phr-1* from *L. longisporum* and *M. anisopliae* were consistent with the location of stop codons in *phr-1* from other filamentous fungi, required to produce a C-terminal α-helical domain of correct size (Figure 3.4A). This domain is known to contain many residues involved in CPD-PHR activity (Reviewed in Sancar, 2003; Müller and Carell, 2009) (Figure 3.4B).

Figure 3.4 Alignment of sections of putative CPD-PHR from EPF with known fungal CPD-PHR proteins and overview of photoreactivation. Panel A shows an alignment of deduced amino acid sequences encoded by the putative *phr-1* from the EPF *B. bassiana* GK 2016 (BbGK), *B. bassiana* ARSEF 3113 (BbAR), I. farinosa (If), L. longisporum (Ll), M. anisopliae (Ma), *T. inflatum* (Ti) and the corresponding region from model class I CPD-PHRs from the filamentous fungi *A. fumigatus* (Af, XP_749910, 586aa, region 281-586), *C. miyabeanus* (Cm, BAD18969, 634aa, region 325-634), *F. oxysporum* (Fo, AAP30741, 630aa, region 324-630), *N. crassa* (Nc, CAA41549, 642aa, region 327-642) and *T. atroviride* (Ta, CAA08916, 629aa, region 324-629). Panel B, shows a diagrammatic overview of photoreactivation. The asterix symbol (*) in the taxon label of panel A indicates a putative CPD-PHR derived from an EPF. The solid line in Panel A denotes the regions from the EPF and Ta that were aligned with (6-4)-PHR and DASH-CRY from *C. zeae-maydis* and *S. sclerotiorum* in Figure 3.5C, respectively. Dashed boxes denote signatures one (S1) and two (S2) for class I CPD-PHR. The start of the α-helical domain (α), binding sites for CPD (+) and the chromophores FAD (●) and MTHF (#) are indicated in Panel A. The solid lined box in panel A designates those residues that were conserved with CPD-PHR from *E. coli*, found to be involved in electron donation to the CPD (Liu *et al.*, 2012). Similar coloured residues indicate those that are most conserved, according to BLOSUM62, light grey = Max, 3.0 and dark grey = Low, 0.5.

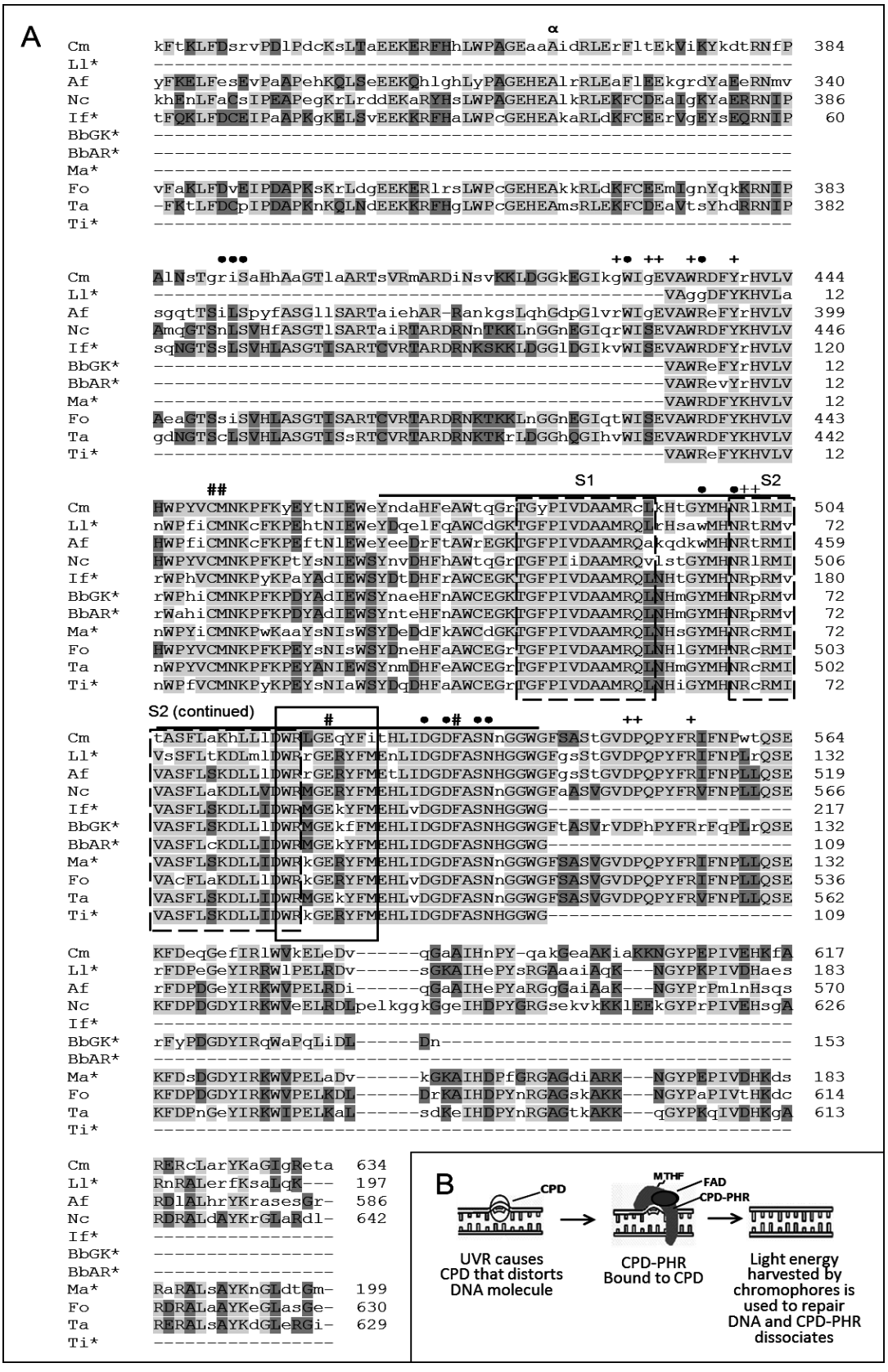
A
α
S1
S2
S2 (continued)
B
CPD
MTHF
FAD
CPD-PHR
UVR causes CPD that distorts DNA molecule
CPD-PHR Bound to CPD
Light energy harvested by chromophores is used to repair DNA and CPD-PHR dissociates

The deduced sequences of the putative CPD-PHR sections were analyzed using the Expert Protein Analysis System proteomics server, which scans input sequences for known protein domains, families and functional sites present in the PROSITE database (de Castro *et al.*, 2006). This analysis predicted that the candidate *phr-1* sequences encode features indicative of class I CPD-PHRs (Figure 3.4A). These included class I signatures one and two which are highly conserved sequence specific indicators for this class of CPD-PHR (Jorns, 1990). Only signature two contained residues (FAD- and CPD-binding) that are known to directly contribute to CPD-PHR activity (Jorns, 1990). With regards to these binding sites, the putative CPD-PHRs (where there was sufficient sequence obtained) contained residues that were conserved amongst CPD-PHR and are thought to be important in MTHF-, FAD- and CPD-binding (Berrocal-Tito *et al.*, 1999; Kihara *et al.*, 2004). Interactions between CPD-PHR and these ligands are essential for CPD repair.

The α-helical domain is conserved amongst all class I CPD-PHRs and also with other PHRs and CRYs, and is thought to be responsible for their differing biological functions, such as DNA repair and light dependent growth responses, respectively (Reviewed in Sancar, 2003; Müller and Carell, 2009) (Figure 3.5A). Although no fungal CPD-PHR had its structure solved, the 267 amino acids in the α-helical domain from *E. coli*'s have been shown to align very well with other class I CPD-PHRs (Park *et al.*, 1995). To date, fungi have been only found to contain class I CPD-PHR, (6-4)-PHR and DASH-CRY types. Class I CPD-PHR and (6-4)-PHRs are thought to have a primarily protective role, repairing CPDs and (6-4)PPs, respectively, caused by UVR, while DASH-CRYs are more involved in circadian clock regulation. These sequences were studied to determine if differences within the α-helical domain existed in key positions that may influence their biological functions. Although similarities are expected, namely FAD-

binding, key molecular differences between PHR/CRY types were identified and used to provide additional confidence in differentiating the putative CPD-PHRs from other PHR/CRYs that have also been found in filamentous fungi.

Differentiation was aided an *in silico* approach, based on conventional sequence analysis and structure/function prediction using homology modeling. One characterized example from a filamentous fungus was selected for each class I CPD-PHR, (6-4)-PHR and DASH-CRY. These were compared with the putative CPD-PHRs from EPF, reported here to serve as controls for the experiment. These model sequences were *T. atroviride* CPD-PHR (TaPH) (Berrocal-Tito *et al.*, 2007) *C. zeae-maydis* (6-4)-PHR (Cz64) (Bluhm and Dunkle, 2008) and *S. sclerotiorum* DASH-CRY (SsDC) (Veluchamy and Rollins, 2008) (Figure 3.5B). To reiterate, one model sequence from each of the three PHR/CRY types found in filamentous fungi (i.e. CPD-PHR, (6-4)-PHR and DASH-CRY were chosen. These control sequences were compared to the sequences encoded by the *phr-1* candidates found in EPF to aid in differentiating the putative CPD-PHRs from other possible PHR/CRY types, which had generally been performed through functional analysis (Sancar, 2000). The conserved region selected for all PHR/CRY sequences was within the α-helical domain and possessed many features required for CPD-PHR function.

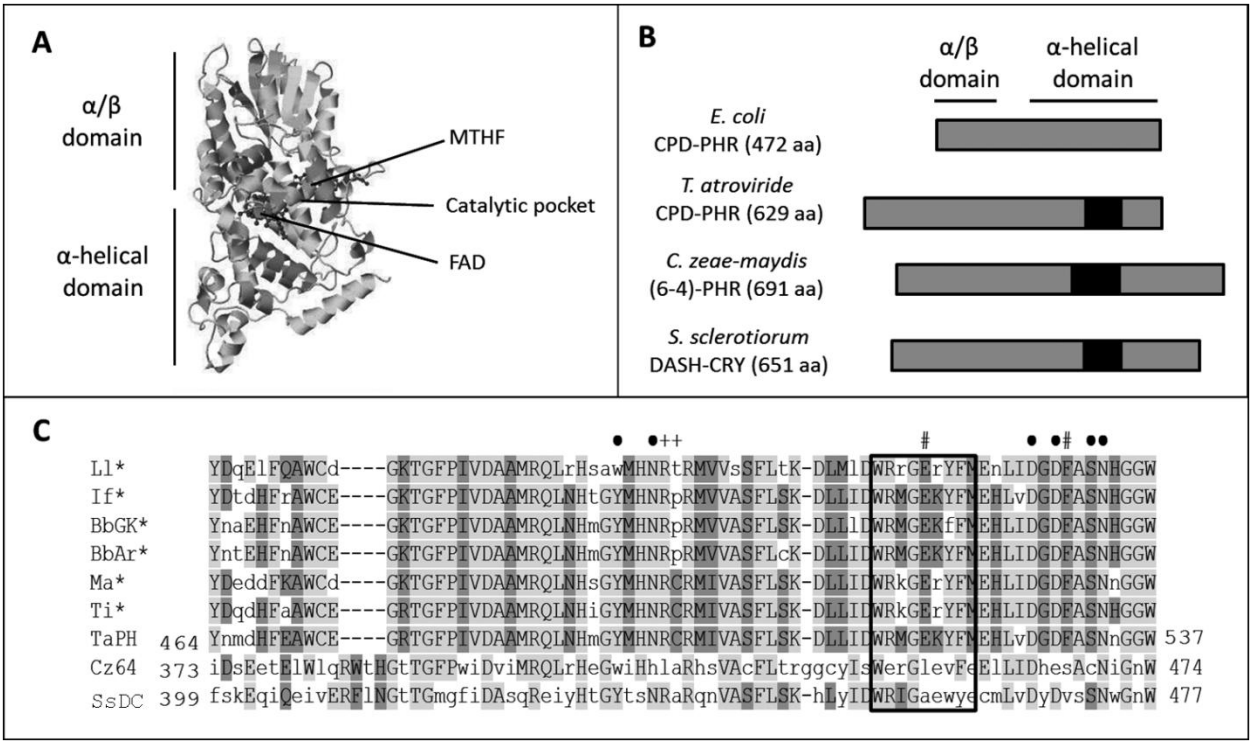

Figure 3.5 Comparison of PHR/CRY sequences found in filamentous fungi. Panel A shows a ribbon diagram representation of the crystal structure of CPD-PHR from *E. coli* [protein data bank code 1DNP, (Park *et al.*, 1995)] adapted from (Sancar, 2003). Panel B shows a schematic comparison of model PHR/CRY types found in filamentous fungi with CPD-PHR from *E. coli*. The PHR/CRYs shown here were selected for comparison with the putative CPD-PHR sequences from EPF, shown in Figures 3.4A. The black sections denote the areas that were analysed in panel C and correspond to aa 464-537, 373-474 and 399-477, in the model sequences from *T. atroviride*, *C. zeae-maydis* and *S. sclerotiorum*, respectively. Panel C shows a curated alignment (including gaps) of the deduced sections of putative CPD-PHRs from the EPF shown in Figure 3.4A with TaPH (CPD-PHR from *T. atroviride*, region 464-537), Cz64 [(6-4)-PHR from *C. zeae-maydis*, Cz64ACB38886, 691aa, region 373-474] and SsDC (DASH-CRY from *S. sclerotiorum*, XP_001593735, 651aa, region 399-477). The taxon labels, sequence labels and designation of sequence conservation are the same as in Figure 3.4A.

An alignment between conserved regions within the α-helical domains of the PHR and CRY proteins revealed that the putative CPD-PHRs from EPF had more sequence conservation with TaPH than Cz64 or SsDC (Figure 3.5C). Of special importance were the residues implicated in CPD-PHR repair activity like FAD-, MTHF- and CPD-binding as well as the residues which aligned with those from *E. coli* (358-366 aa) that have been implicated in electron transfer by the tunneling pathway through α-helix 15 (Liu *et al.*, 2012). A region, corresponding with α-helix 15 in the CPD-PHR from *E. coli* was found in all fungal CPD-PHRs analysed here and had conservation in 6 of the 9 residues (WRMGEKYFM; underlined residues are conserved in the CPD-PHR sequences shown in Figures 3.4A and 3.5C). In contrast, the Cz64 and SsDC only possessed sequence conservation in 3 of the 9 residues, which may compromise their ability to transfer electrons through this pathway.

The binding residues, with four exceptions, were conserved in TaPH and all putative CPD-PHRs from the EPF (Figure 5C). The sequence from *L. longisporum* differed at two positions known to be involved in FAD- and CPD-binding, which were tryptophan and threonine residues, respectively, compared to tyrosine and cysteine residues in TaPH, but was consistent with the CPD-PHR in *A. fumigatus* (Figure 3.5A). The other exceptions were for *I. farinosa* and both *B. bassiana* strains, which contained a proline at the same suspected CPD-binding site location that differed in *L. longisporum*. In addition to these examples, this CPD-binding location appeared to exhibit variation in general, as a total of nine different amino acids were found at this position in various fungal CPD-PHRs, all of which were neutral at pH 7, with five being non-polar and four were polar (not shown). Proline for example, can provide proteins with structural rigidity as a result of its cyclic side chain and is often found as the first residue in an α-helix and also at turns (Berg *et al.*, 2002). The structure of CPD-PHR from any fungi has yet to

be solved. However, the presence of a proline residue is not in contention with previous findings since it was found in the region predicted to be a part of the α-helical domain, which is known to contain many helices (Reviewed in Sancar, 2003). Furthermore, predictions of the structure formed by the putative CPD-PHR sequences placed the proline as well as the observed cysteine and threonine residues at this position, near the start of a helix with the highest confidence that the iTASSER server can provide (Roy *et al.*, 2010).

In comparison, Cz64 was only similar to TaPH in three of the ten functionally important residues, all of which were likely involved in FAD-binding. This was consistent with the function of (6-4)-PHR which do not bind MTHF or CPDs (Glas *et al.*, 2009). Conversely, SsDC was similar to TaPH in 6/6 of FAD-, 1/2 of CPD- and 0/2 MTFH-binding sites. It was expected that MTFH-binding sites would not be conserved, since DASH-CRYs have not been shown to interact with this chromophore. However, the presence of a potential CPD-binding site is interesting. Perhaps SsDC, like the DASH-CRY found in *A. thaliana* may also possess the ability to repair CPDs in single stranded DNA (Selby and Sancar, 2006).

Here it is shown that PHR/CRY sequences can be used in their differentiation and function prediction. The sequence conservation within a functionally important region in other CPD-PHRs suggested that the sequences shown here from EPF very likely encode CPD-PHRs. With the availability of powerful structural modeling tools it is possible to add an additional level of complexity to this analysis and imply functions for these putative CPD-PHR sequences based on their predicted structure.

This was achieved using the iTASSER (Roy *et al.*, 2010) and CombFunc (Wass *et al.*, 2012) servers and both performed well at a recent Critical Assessment of Techniques for Protein Structure Prediction (Kinch *et al.*, 2011). These servers both used homology modeling. In

addition, iTASSER can also employ *ab initio* modeling when structural homologues are not available for a protein of interest; however, this method is less accurate than homology modeling. There are about 16,000,000 unique peptides in the public data banks and only about 86,000 solved protein structures, creating a need to predict structure/function from sequence alone. Homology modeling relies on the observation that the number of protein folds in nature are limited and many distant homologues can adopt remarkably similar structures, even though a degree of sequence dissimilarity exists between them (Baker and Sali, 2001). In this method, known structures/folds of peptides in data banks are compared to similar sequences with unsolved structures. Those deemed a sufficient match are used to expand the protein fold library to improve fold prediction for the sequences of interest. This allows proteins with only limited sequence similarity (~ 20%) with known structures to be modeled accurately (Kelley and Sternberg, 2009).

All putative CPD-PHRs from EPF had > 50% sequence similarity with that from *E. coli*, which has had its structure solved (Park *et al.*, 1995). Furthermore, there are > 14 structures solved that belong to the PHR/CRY group, providing very good templates for the putative CPD-PHR and control sequences, allowing their structures and functions to be modeled and predicted with high confidence, respectively. This analysis confirmed that the putative CPD-PHR and control sequences had structural homology with other known PHR/CRYs. This information was used to predict the corresponding functions from each of the predicted structures using both iTASSER and CombFunc (Figure 3.6).

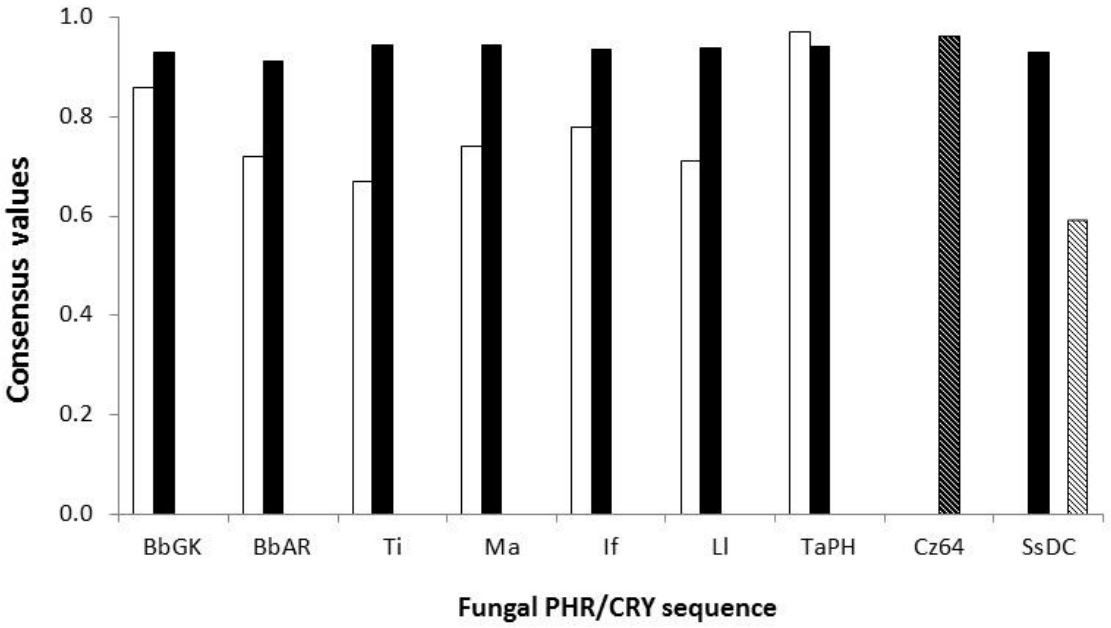

Figure 3.6 Summary of GOs, predicted by homology modeling, for the putative CPD-PHRs and known PHR/CRY types found in filamentous fungi. The PHR/CRY sequences were labeled as in Figure 3.5C. Consensus values for GO predictions are reported as GO-Score and support vector machine probability for results from iTASSER and CombFunc servers, respectively. The CPD-PHR and signal receptor functions predicted by iTASSER are shown as a white bar without and with black lines, while CPD-PHR and (6-4)-PHR functions predicted by CombFunc are shown as a black bar without and with white lines, respectively.

The confidence of the functions predicted for the putative CPD-PHR sequences was considered to be very high. The structures modeled with iTASSER provided C-scores [confidence of predicted structure as per Roy *et al.* (2010), (-5 to 2)] of between 0.58 to1.24 (> -1.5 generally have a correct structure) for the EPF sequences (Roy *et al.*, 2010), while CombFunc reported that 99-100% of the residues were modelled at > 90% confidence. The TaPH and all six putative CPD-PHR sequences were predicted by both iTASSER and CombFunc to have CPD-PHR activity (GO:0003904, E.C. 4.1.99.3). While variation is apparent between the results obtained from both iTASSER and CombFunc, most apparent is the consistency of the consensus values reported by CombFunc, which ranged between 0.912 (*B. bassiana* ARSEF 3113) to 0.946 (*T. inflatum*). In contrast, iTASSER reported consensus values between 0.67 (*T. inflatum*) to 0.97 (*T. atroviride*).

As expected, due to previous findings by Bluhm and Dunkle (2008), Cz64 PHR was predicted to have (6-4)-PHR activity (GO:0003914, E.C. 4.1.99.13). Although this function was predicted by CombFunc only, it had a support vector machine probability of 0.964, the highest obtained in this experiment. Support vector machines are statistical tools used to recognize patterns based on a learning algorithm and are used predict if inputs belong to a particular classification or not (Cortes and Vapnik, 1995). CombFunc used support vector machines to predict and provide a measure of confidence that an input protein sequence had a particular molecular function (Wass *et al.*, 2012).

The results from SsDC were not as obvious due to differences in function prediction between the two servers. It was predicted that SsDC contained CPD-PHR (0.93) and signaling receptor activity (0.59) by CombFunc and iTASSER, respectively. Interestingly, both of these functions have been observed separately in DASH-CRYs (Selby and Sancar, 2006; Veluchamy

and Rollins, 2008) and may be substantiated by some of the features found in the multiple alignments, namely the presence of potential CPD-binding residues. Furthermore, redundant, but biologically relevant functions of the PHR/CRY group, such as FAD- and DNA-binding sites were also predicted in SsDC. Nonetheless, these results indicated that it is possible to differentiate DASH-CRY from other CPD-PHR through prediction of their function, aided by homology modeling. Most obvious was that the pattern of predicted functions for SsDC was different than TaPH and the putative CPD-PHR sequences from EPF, which were predicted to have CPD-PHR activity by both servers (as opposed to only CombFunc for SsDC), but not signaling receptor activity.

Both modeling servers successfully predicted the CPD-PHR control sequence from *T. atroviride* to possess folds/structures strongly associated with CPD-PHR activity. This provided high confidence in the results from the putative CPD-PHRs, which were also predicted to have CPD-PHR activity. These findings were substantiated by the results from the (6-4)-PHR and DASH-CRY controls (Cz64 and SsDC, respectively) that were predicted to possess previously documented functions associated with these types. These results demonstrated that the putative CPD-PHR sequences from the EPF had structural homology with other known CPD-PHRs possessing the ability to repair CPDs. Therefore, they too most likely possess this function. In addition, functional differences were predicted to exist between these and examples of (6-4)-PHR and DASH-CRY from filamentous fungi, which are the only other two types of PHR or CRY known to exist in filamentous fungi. As a result, it was possible to differentiate CPD-PHR from other related proteins through the use of homology modeling.

Additional analysis was performed on the putative CPD-PHRs to better understand the phylogenetic relationships between these and other fungal CPD-PHRs (Figure 3.7). The amino acid sequences selected for this analysis were part of a highly conserved region within the α-helical domain of CPD-PHRs, based on sequence similarity. This region was found in all CPD-PHRs, including the putative sequences from EPF shown in this section, which made it very well suited for the phylogenetic analysis of this protein (Dereeper *et al.*, 2008). In addition to the six putative CPD-PHRs from EPF found in this study, the putative CPD-PHRs from the sequenced EPF *C. militaris* (Zheng *et al.*, 2011) and *M. acridum* (Gao *et al.*, 2011) and a known CPD-PHR from *M. anisopliae* (Gao *et al.*, 2011) were also included along with CPD-PHRs from a cross section of 36 other fungi (Table 3.2). It should be noted that the *M. anisopliae* strain ARSEF 23, has been renamed as *M. robertsii* (Fang and St Leger, 2012) to honor D.W. Roberts, a most distinguished researcher in the field. However, this species will continue to be referred to as *M. anisopliae* here for consistency.

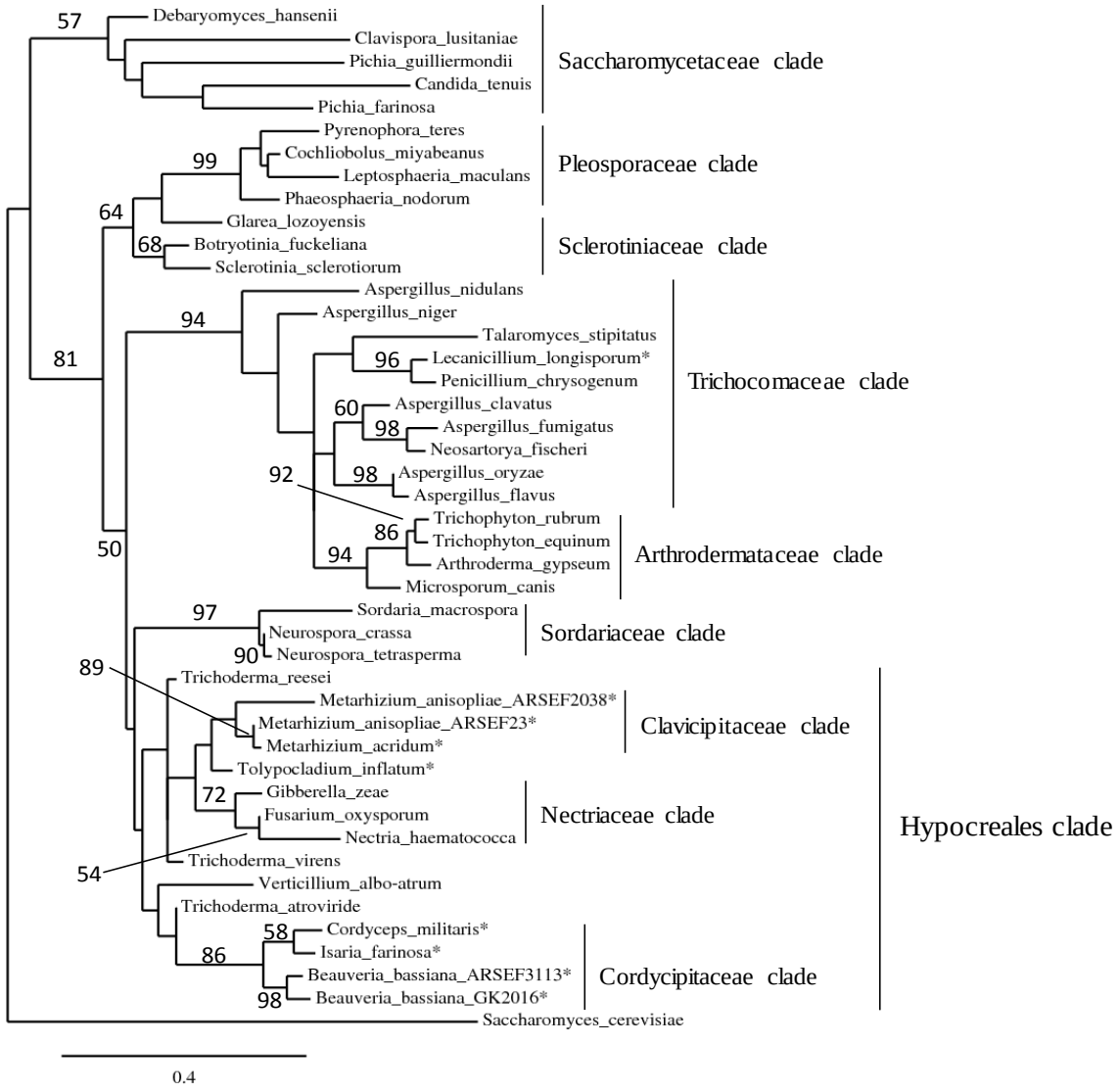

Figure 3.7 Phylogenetic analysis showing predicted relationships between putative and known class I CPD-PHR from EPF and other fungi. Forty five CPD-PHRs were analyzed. The taxon labels indicate the organism from which the input sequences was derived. Clades are named for the family the majority of the fungi the sequences belonged to, with the exception of the Hypocreales clade which is named for its Order. An asterix (*) designated nine putative CPD-PHR sequences from EPF; six from this research and three from others (Gao *et al.*, 2011; Zheng *et al.*, 2011). Branch support values were provided for those > 50%. The scale conveys branch lengths to the number of substitutions per site and *S. cerevisiae* was selected as the outgroup. This analysis was performed using the service provided by Dereeper *et al*. (2008). The maximum likelihood method through the PhyML program (v3.0 aLRT) was used to reconstruct the phylogenetic tree. Support for internal branching was evaluated using the bootstrap method with 200 replicates (Guindon and Gascuel, 2003). The substitution models were selected assuming an estimated proportion of invariant sites equal to 0.195 and the gamma shape parameter was estimated to be 0.869.

The non-EPF CPD-PHRs cosegregated with others that belonged to a common family, which provided confidence for the segregation of the EPF derived sequences. All suspected CPD-PHRs from EPF, except that from *L. longisporum*, cosegregated into the Hypocreales clade. Within the Hypocreales clade, Cordycipitaceae sub-clades contained sequences from two *B. bassiana* strains, *C. militaris* and *I. farinosa*, while Clavicipitaceae sub-clades contained sequences from three *Metarhizium* spp. This grouping was consistent with a more comprehensive phylogenetic study of fungi belonging to Cordycipitaceae and Clavicipitaceae that analyzed multiple loci, such as nuclear ribosomal small and large subunits (Sung *et al.*, 2007).

The putative CPD-PHR from *T. inflatum* appeared to be most related to those which cosegregated into the Clavicipitaceae clade. Interestingly, this fungus was once classified as a Cordycipitaceae but has been found to be more closely related to Clavicipitaceae (Sung *et al.*, 2007). However, phylogenetic reclassification of *T. inflatum* has placed it into a separate family named Ophiocordycipitaceae, which contained other genera of EPF (Gams, 1971); however no CPD-PHR sequences from this family were available for analysis.

The putative CPD-PHR from *L. longisporum* co-segregated with those in the Trichocomaceae clade, although the fungus is considered to be a part of the family Cordycipitaceae, with the Order Hypocreales, like the other EPF here. It is possible that this discrepancy in phylogenetic grouping may be an artifact of the specific sequence analyzed or method used, since Sung *et al.* (2007) used maximum parsimony while maximum likelihood was used here for branch scoring. Maximum likelihood is more complex and has only been used widely since the 1990's due to its computation demands but is especially accurate for establishing phylogenies with molecular sequence (i.e. DNA or protein) data (Guindon and Gascuel, 2003). It should be noted that the genus *Lecanicillium* has been undergoing an extensive reclassification. The genus

Lecanicillium had been proposed in light of molecular phylogenetic studies using the internal transcribed spacers of nuclear ribosomal DNA from fungi previously considered to be a part of the *Verticillium* genus such *L. longisporum*, previously named *Verticillium lecanii* (Zimmermann) (Zare *et al.*, 2000; Gams and Zare, 2001). However, many species within this group have yet to be classified (Gams and Zare, 2001) and work in this area has received additional attention (Kouvelis *et al.*, 2008).

In summary, with the exception of one sequence, all putative CPD-PHRs from EPF cosegregated within the Hypocreales clade, which is consistent with the phylogenetic relationship of EPF established by Sung *et al.* (2007). Furthermore, this pattern of cosegregation provided further evidence that these sequences were likely CPD-PHRs. This is because non-CPD-PHR sequences would not likely cosegregate with CPD-PHR sequences, especially with a pattern that was consistent with their phylogeny.

3.5 Conclusions

In this section it was shown that regions of *phr-1* candidates were found in six EPF with confirmed photoreactivation capabilities that belonged to the genera *Beauveria*, *Isaria*, *Lecanicillium*, *Metarhizium* and *Tolypocladium*. *In silico* translation of these sequences revealed that they encoded a putative CPD-PHR protein with conserved, functionally important residues known to be involved in CPD-, FAD- and MTHF-binding, in addition to those implicated in electron transfer by the tunneling pathway through α-helix 15. Furthermore using sequence analysis and homology modeling, it was established that putative CPD-PHRs could be differentiated from other related PHR/CRYs, which consistently predicted that the EPF sequences had CPD-PHR activity. Lastly, it was shown that the six putative CPD-PHR sequences had a

phylogenetic relationship that was consistent with the established phylogeny of the EPF they were identified in. From this it can be concluded that these EPF likely possess *phr-1*, which encodes a product with many of the hallmark, functional characteristics that are found in CPD-PHRs.

4.0 ESTABLISHING EIT IN *B. BASSIANA*

4.1 Abstract

Several EPF, including *B. bassiana* are important tools in integrated pest management. However, their ability to bring about effective control of pest insects can be compromised by environmental conditions and stresses, such as UVR and high temperatures. The responses to and repair of damage caused by heat and UVR are generally well understood in fungi but research in this field has focused on the intracellular events involved. In *E. coli* it has been shown that factors, named ESCs, are secreted by the bacteria and are involved in sensing stresses, including high temperatures and can induce tolerances to heat and UVR, for example. During growth, these ESCs accumulate in the medium and can be recovered in CFF. This phenomenon has yet to be studied in any filamentous fungi. This study was conducted to determine if a similar phenomenon exists in *B. bassiana* which may be indicative of the presence of ELFs within the CFF. It is shown here that a response that resembles EIT to UV-C (under non-photoreactivating conditions) or heat could be acquired by CS or BS, respectively. However, the conditions required to cause tolerance in CS or BS differed. For example, BS did not require incubation with preheated CFF prior to stress challenge to have tolerance induced, while CS did. In addition, increased tolerance in CS was correlated with several proteins of < 40 kDa that were present in the CFF. Treatment of the CFF with trypsin removed the effect in CS, suggesting that the potential ELF(s) involved is likely proteinaceous. It was not determined here if these proteins were involved in inducing elevated tolerance in BS. This is the first report of

phenomenon resembling EIT occurring in a filamentous fungus. Furthermore, the findings here were prerequisite to screen for putative ELF(s) produced by *B. bassiana* in future studies.

4.2 Introduction

Beauveria bassiana is a commercially important EPF and is employed as an alternative to chemical pesticides to control various pest insects that are important in various industries, such as agriculture and forestry (Khachatourians *et al.*, 2002; Shah and Pell, 2003; Khachatourians, 2009; Hajek and Delalibera, 2010). In the field, *B. bassiana* is challenged with many stressors, not the least of which is heat and solar UVR which can lead to a reduction in fungal viability and effective insect control (Inglis *et al.*, 1997). Like other organisms, EPF possess the ability to respond to deleterious environmental conditions and mitigate some of their harmful impacts. The sensing of these conditions is the initial step in this progression leading to elevated environmental stress tolerance in the cell.

The classical model of stress sensing proposes that stress is generally detected through the damage it causes or some perturbation in cellular physiology (Neidhardt *et al.*, 1990; Reviewed in Morano *et al.*, 2012). For example, some evidence suggests temperature induced misfolding of newly synthesized polypeptides could be sensed through an increased load on chaperones, such as HSP-70 and HSP-90 (Duina *et al.*, 1998; Quan *et al.*, 2004). Still, the precise nature of the signal which cues the HSR has yet to be determined (Morano *et al.*, 2012). It has been established that stress conditions, including elevated temperature can directly influence the activities of specific intracellular components (Reviewed in Klinkert and Narberhaus, 2009). For example, the HSP-26 chaperone in *S. cerevisiae* has been shown to reversibly shift from an inactive to an active conformation in response to 36 °C, allowing its activity to be

autonomously regulated (Franzmann *et al.*, 2008). Although more rapid than other types of regulation, such as those involved in gene expression needed for the HSR, direct enzyme activity regulation generally do not have as large of impact on cellular physiology.

In addition to the above, stress sensing that is mediated by extracellular factors also has a role in the induction of tolerances in several microorganisms to acid, UVR and heat, to name a few. This phenomenon was discovered in *E. coli* (Hussain *et al.*, 1998) and subsequently similar responses have been found in *C. jejuni* (Murphy *et al.*, 2003) and *S. cerevisiae* (Vovou *et al.*, 2004). These responses have been thought to be controlled by extracellular factors, termed ESCs in *E. coli* and appear to be produced and secreted during unstressed conditions. In *E. coli*, ESCs are activated by a number of physical and chemical stressors, such as high temperature, and can cause induction of tolerances to various environmental stress conditions, such as UVR, heat and extreme pH, characterized by an increase in survival of stress challenged cells (Reviewed in Rowbury, 2005). Although, the mechanisms that control activation of ESC/ELF and EIT are unknown, a conformational change and surface receptor interaction have been suggested (Rowbury and Goodson, 2001; Rowbury, 2001a). The limited understanding of ESC biology is exacerbated by the lack of amino acid or DNA sequences corresponding with a candidate protein or its encoding gene for any example of an ESC/ELF.

In contrast to intracellular stress sensing, ESCs in *E. coli* are thought to provide the cell with a means to indirectly detect stress through these secreted proteins, which may potentially allow the cell to prepare for an incoming insult without having been directly exposed to it (Rowbury and Goodson, 1999b; Rowbury, 2001a). Sensing of stress conditions by ESCs is thought to occur through a conformational change of the protein, which activates it and through a subsequent interaction with the cell, the signal carried by active ESC is relayed to the cell.

Furthermore, this phenomenon is also thought to allow non-ESC producing *E. coli* cells to respond to the presence of active ESCs assuming they possessed the components required to for EIT (Rowbury, 2001b). Similar to that in *E. coli*, secreted proteins appear to play a role in establishing stress tolerance in *C. jejuni*. In general the ability of these ESC/ELF molecules to diffuse from one cell to others and influence their stress tolerance has been considered a pheromone-like activity (Rowbury, 2001b), in addition to a distance interaction (Nikolaev, 2000). Distance interactions are defined as the exchange of information between organisms via physical signals, such as extracellular components.

Quorum sensing is one of the best studied examples of a distance interaction and is characterized by the cell-density dependent accumulation of signaling molecules, such as N-acyl homoserine lactones or oligopeptides produced by Gram–negative or Gram–positive bacteria, respectively (Reviewed in Miller and Bassler, 2001). These molecules have been shown to enable cells to modulate gene expression in response to cell-density and are involved in the establishment of sporulation, antibiotic production and biofilm formation to name a few. Quorum responses have also been found to occur in fungi but are generally controlled by aromatic alcohols, such as farnesol, phenylethanol and tryptophol, and are involved in establishing virulence, morphogenesis and biofilm formation in various yeasts (Reviewed in Albuquerque and Casadevall, 2012). It has yet to be determined if these molecules can influence cellular tolerance to environmental stresses.

Although both true quorum factors and ESCs are secreted, they have several differences. For example, quorum factors behave as autoinducers, while ESCs require stress conditions to become activated, which is a required for them to cause EIT (Rowbury and Goodson, 2001). Not surprising due to their functional differences, ESCs and ELFs also differ from the conven-

tional quorum factors in their structural composition. The best documented examples of ESC/ELFs have been found to be proteinaceous molecules of > 10 kDa, achieved through treatment of CFF with trypsin which reduced its ability to increase survival in challenged cells (Rowbury and Goodson, 2001; Murphy *et al.*, 2003; Vorob'eva *et al.*, 2003). In contrast, quorum factors were not found to be proteinaceous, with the exception of the oligopeptides produced by Gram-positive bacteria, which were ~ 1 kDa in *Staphylococcus aureus* (Ji *et al.*, 1995), and were generally homoserine lactones in Gram negatives or aromatic alcohols in fungi.

Due to a lack of evidence for more specific functions ELFs from any organism have yet to be studied in a context other than their ability to increase tolerance to a stress challenge (i.e. EIT) in CFF (containing ESC/ELF) treated cells. This increase in stress tolerance will be the criterion used in this thesis to define EIT. The purpose of this work was to assess the occurrence of and characterize the phenomenon resembling EIT in *B. bassiana* which was a crucial element in verifying the hypothesis that this elevated tolerance is controlled by secreted proteins (ELFs), recovered in CFF and extending this area of research. This was performed by activating the putative ELFs contained in CFF by preheating the filtrate, then assaying for its ability to increase tolerances to UVR and/or heat in treated BS and/or CS over that provided to those treated with preheated fresh medium or other control. This phenomenon has yet to be reported in filamentous fungi and may signify a novel mechanism for the response to stress and tolerance acquisition.

4.3 Materials and methods

4.3.1 Preparation of *B. bassiana* cultures and CS and BS suspensions

Cultures of *B. bassiana* and its CS were prepared as per section 3.3.1. When indicated, culture growth, viability and development was measured as optical density (OD) at 600 nm, CFU

counts through dilution in PBS and plating on YPGA and microscopy at 400x using a hemocytometer as described by Bidochka *et al*. (1987), respectively.

Blastospores were prepared from cultures that were grown in YPG or VM in the dark, at 27 °C for 3 d in a water bath with rotation at 150 RPM and harvested by filtering 5-10 mL of culture through a Pasteur pipette packed with glass wool to remove mycelia. The resulting suspension was rinsed and recovered twice by centrifugation at 6000 x*g* for one minute and resuspended in PBS. The resulting BS suspension was enumerated with the aid of a hemocytometer and viewed at 400x magnification and generally contained $2x10^8$ to $5x10^8$ BS and < 0.1% mycelia.

4.3.2 Preparation and storage of CFF

Liquid cultures prepared as in 4.3.1 were used to prepare CFF. A 7 mL aliquot of culture was filtered through a 2.5 cm diameter, 0.22 µm pore size, polyvinylidene fluoride membrane (Millipore, Durapore® membrane filter, Billerica, MA, USA) and the resulting CFF was collected in a sterile, glass tube. It was found that the ability of CFF to increase tolerance to UVR in CS was lessened when > 8 mL was passed through a single filter, likely due to clogging of the filter, leading to reduced recovery of ELF. The CFF was generally used fresh the same day and kept at ~ 4 °C until required. When necessary for studies that required preparation of CFF from cultures grown for various times, it was stored at -30 °C as 1 mL aliquots in 1.8 mL microfuge tubes and assayed for ELF activity within 1-4 d. The storage of CFF under this condition did not affect its ability to confer tolerance to UVR in CS.

4.3.3 Preheating of CFF and treatment of spores to promote elevated stress tolerance

An overview of the methods used to assay for elevated tolerance to UVR in CS/BS or heat in CS is shown in Figure 4.1 and elevated tolerance to heat in BS in Figure 4.2 and were adapted from those described by Rowbury and Goodson (1999b; 2001; 2003a; 2005).

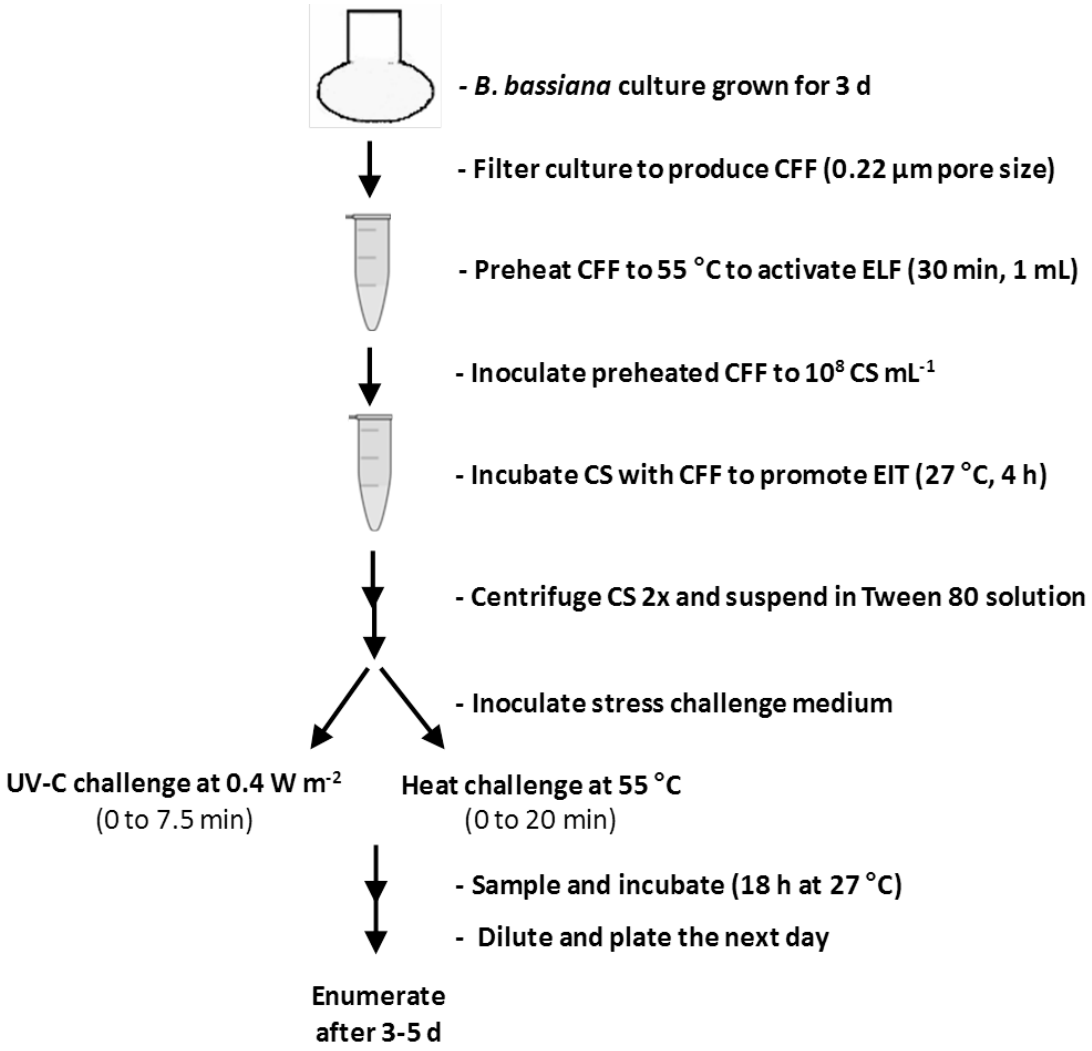

Figure 4.1 Flow chart of the standard and optimized method used to assay for elevated tolerance to UVR (in the absence of photoreactivating light) or heat in CS. A similar method was also used to assay for elevated tolerance to UVR in BS, but differed in that CFF was preheated to 45 °C instead of 55 °C, prior to BS being added.

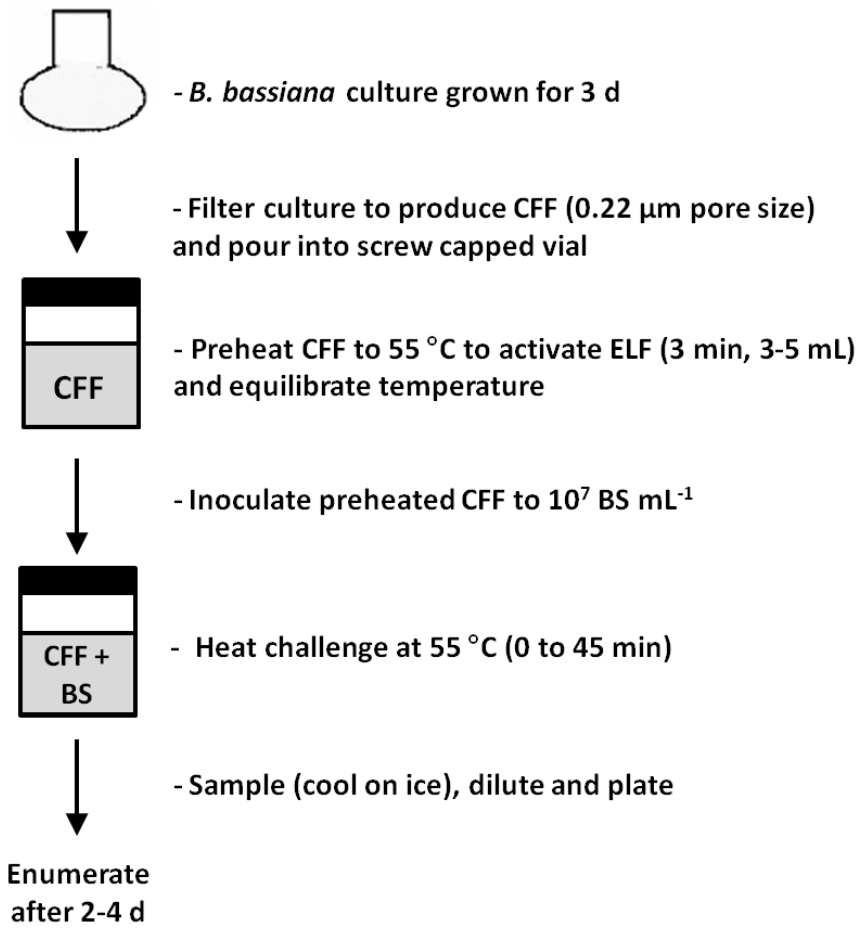

Figure 4.2 Flow chart of the standard and optimized method used to assay for elevated tolerance to heat in BS.

Samples of CFF were warmed to ~ 22 °C by holding in one's hand with occasional shaking, which required approximately 5 min with frozen samples. When indicated, porcine pancreatic trypsin (BDH Biochemical, England) was added to a final concentration of 24 µg mL^{-1} and incubated at 27 °C for 30 min to determine if proteolysis of proteins within the CFF would reduce the tolerance compared to untreated CFF. The proteolytic activity of trypsin is known to be abolished at 55 °C (Villalonga *et al.*, 2005), therefore its activity would not persist following subsequent incubations at 55 °C, as described below.

In preparation for CS focused experiments, CFF was preheated for 30 min at 55 °C (unless otherwise stated) in a water bath to activate ELFs potentially within it. Immediately after preheating the CFF was inoculated with 0.1 mL of 10^9 CS mL^{-1} in sterile distilled water to a final concentration of 10^8 CS mL^{-1} and then incubated for 4 h at 27 °C to induce stress tolerance, which resembles EIT. Following induction, CS were rinsed twice in sterile distilled water, recovered by centrifugation at 6000 x*g* for 2 min and resuspended in 1 mL of 0.02% (v v^{-1}) Tween 80. Washing was performed to remove the residual CFF to help determine if tolerance remained following CFF removal. It was also tested if CFF prepared from liquid used to harvest or rinse CS, could increase tolerance to UVR in CS using the same method to prepare CFF and assay for its ability to produce EIT to UVR in CS. This was done to determine if ELF was secreted by CS during harvest or rinsing. A solution of 0.02% (v v^{-1}) Tween 80 that was used to harvest the CS, or the first sterile distilled water rinse of the same CS were filtered to create CFF. Prior to filtration, these CS suspensions contained ~ 10^9 CS mL^{-1}, which were approximately 10-fold more propagules than was found in a three day liquid culture. Challenge of all CS with UV-C or heat is as described in sections 4.3.4 or 4.3.5, respectively.

In an attempt to induce an elevated tolerance to UVR or heat, BS were treated with the same method used for CS, with the exception that PBS was used instead of 0.02% (v v^{-1}) Tween and CFF was preheated at 45 °C for 30 min, instead of 55 °C, but did not produce an elevated tolerance to either stress. Instead, BS were challenged directly in CFF that was preheated at 55 °C for 3 min in preparation for EIT to heat assays, as described in section 4.3.5, unless otherwise stated.

4.3.4 Assay for EIT to UVR

The UV irradiation of CS or BS was performed as described by Chelico (2004) with modifications. Suspensions containing 2 x 10^6 BS or CS mL^{-1} were prepared in glass Petri dishes (surface area = 64 cm^2) containing 30 mL of 2% (w v^{-1}) glucose and were supplemented with 0.02% (v v^{-1}) Tween 80 when CS were added to prevent their clumping. The suspensions were exposed to UV-C radiation (UVP Mineralight R52G, UVP Inc., Upland, CA, USA) between 200-280 nm, with λ_{max} = 254 nm and an irradiance of 0.4 W m^{-2}, as measured by a Blak-Ray® Ultraviolet Intensity Meter, model J225 (UVP, San Gabriel, USA). Irradiation was performed at 23 °C in the absence of wavelengths needed for photoreactivation (366-435 nm) (Giese *et al.*, 1953) and suspensions were continuously agitated using a magnetic stirrer and bar. During irradiation, 1 mL samples were transferred into glass vials following the appropriate duration to obtain samples that received a maximum dose of 180 J m^{-2} of UV-C which required 7.5 min exposure.

Following UVR challenge the samples where incubated for 18 h at 27 °C under conditions to either promote NER, in the absence of light, or, when stated photoreactivation, in the presence of white light spectrum light supplied by two fluorescent tubes (34 W, Sylvania

F40T12/CW/SS, Denver, USA) that were 50 cm from the samples. After incubation, the CS and BS suspensions were diluted in the same solution they were challenged in to obtain 10 to 100 CFU counts per 0.1 mL when plated on YPGA, which was dependent on the dose the spores received. Aliquots of 100 µL containing BS or CS were drop platted (~ 25 µL drops) onto YPGA in quadruplicate and incubated at 27 °C in the dark and assessed for viability by enumerating CFUs daily for 2-4 and 3-5 d post challenge, respectively. Survival was calculated as the percentage of CFU mL^{-1} that was produced in challenged samples compared to those that were unchallenged. A survival value of 0.1% represents ~ 2 x 10^3 CFU mL because suspensions of 2 x 10^6 BS/CS mL were challenged.

4.3.5 Assay for EIT to heat

To determine if BS or CS could acquire elevated tolerance to lethal temperatures, assays were performed with modifications, as per Xavier (1998) who used 55 °C to challenge BS. Furthermore, 55 °C provided an adequate rate of heat killing to reduce the viable propagules by four to five log values over 45 min which made it practical to employ in the experiments described here. Lower temperatures, such as 45 °C were observed to not significantly reduce the number of viable BS after 1 h incubation (Xavier, 1998).

Prior to the addition of BS or CS, 3-5 mL of heat challenge liquid (CFF, growth medium or PBS), supplemented with 0.02% (v v^{-1}) Tween 80 when CS were added, was preheated for 3 min to allow the temperature to become fully equilibrated to 55 °C, unless stated otherwise. This preheating step was sufficient to promote elevated tolerance to heat in BS challenged in the CFF and was suspected to be achieved through activation of ELF(s) within the CFF and its promotion of EIT. Propagules were then added to the heat challenge medium to achieve a concentration of

10^7 mL^{-1}. Immediately following addition of fungal propagules, the suspensions were mixed for approximately 1 s by a vortex and 1 mL samples were taken and cooled on ice and were used as the unchallenged samples, while other samples were taken throughout the heat challenge as indicated. Samples containing CS or BS were diluted in PBS with or without 0.02% (v v^{-1}) Tween 80, respectively, to achieve suspensions that would yield between 10 and 100 CFUs per 0.1 mL when grown on YPGA. Aliquots of 100 µL containing CS or BS were drop platted onto YPGA in quadruplicate, incubated at 27 °C and assessed for viability by enumerating CFUs daily for 2-4 and 3-5 d post challenge, respectively. Survival was calculated as the percentage of CFU mL^{-1} that was produced in challenged samples compared to those that were unchallenged. A survival value of 0.1% represents ~ 1 x 10^4 CFU mL because suspensions of 1 x 10^7 BS/CS mL were challenged.

4.3.6 Sodium dodecyl sulphate polyacrylamide gel electrophoresis (SDS-PAGE)

Sample preparation for and execution of SDS-PAGE was performed as described by Sambrook and Russell (2001), with modifications. One millilitre samples of CFF were prepared from *B. bassiana* cultured in YPG for 0-4 d. To improve the visualization of protein bands produced by CFF, the protein content of CFF was concentrated with the aid of ammonium sulphate (AS) to facilitate the precipitation of proteins. The protein was concentrated by approximately 30-fold through its resuspension in a smaller volume. To achieve this, 0.53 g of fine ground, ultra-pure AS (MP Biomedical, Solon, Ohio, USA) was added with constant mixing by vortex to saturate the CFF to ~ 80% with AS. These samples were then incubated at 4 °C for 1 h and centrifuged at 10,000 x*g* for 20 min at 4 °C. The resultant pellets, which contained precipitated proteins, were solubilized in 20 µL of sterile distilled water with 10 µL of sample

buffer [6.25% (v v^{-1}) 1 M Tris pH 6.8, 4.65% (w v^{-1}) SDS, 20% (v v^{-1}) glycerol, 10% (v v^{-1}) 2-mercaptoethanol, 0.025% (w v^{-1}) bromophenol blue] and incubated at 80 °C for 1 min in a thermal cycler (Techne Genius Thermocycler, Staffordshire, UK) to denature and solubilize the proteins. Following this, 25 µL of sample or 5 µL of molecular marker was loaded into each well and electrophoresed through a polyacrylamide gel enclosed with a Mini Protean II apparatus (Bio-Rad, USA) at 120 V, generally until the dye front reached the edge of the gel (~ 1 h). The gel was then recovered from the apparatus, rinsed in sterile distilled water for 3 min to remove residual running buffer and stained overnight in blue silver dye [0.12% (w v^{-1}) Coomassie brilliant blue G-250, 10% (v v^{-1}) phosphoric acid, 10% (w v^{-1}) AS and 20% (v v^{-1}) methanol] as described by Candiano *et al*. (2004). The gel was then de-stained in distilled water until the background became clear. Digital images were processed using Adobe Photoshop version 6 (San Jose, CA, USA).

4.3.7 Protein concentration determination

Protein concentrations were estimated by Bradford's (1976) method with the Bio-Rad protein assay (Hercules, USA) and A_{600nm} was determined by microplate reader (Titertek Multiskan, Flow Laboratories, McLean, Va, USA), as directed by the manufacturer. Standard curves were generated using bovine serum albumin (BSA).

4.3.8 Statistical analysis

Statistical analysis was performed with GraphPad Prism 6 (GraphPad, La Jolla, CA). One or two way analysis of variance was performed when $N > 2$ and the separation of the means were analysed by Tukey's multiple comparison test where indicated, to determine which were significantly different using a threshold of $\alpha=0.05$. Experiments were repeated at least twice,

unless stated otherwise and the sample size used to calculate each mean is indicated in the figure, its legend or within the text.

4.4 Results and discussion

4.4.1 Screening for EIT-like responses in *B. bassiana* CS

Growth measured as OD at 600 nm indicated that *B. bassiana* was culturable in both VM and YPG (Figure 4.3). The OD of cultures grown in YPG or VM was similar throughout the duration of the experiment. Following a lag phase, the cultures had a rapid increase in OD until a maximum was reached after 3 d. This was followed by a plateau in OD which indicated stationary phase. In addition, extracellular protein concentration of the culture filtrate was found to continually increase in the medium with time. Protein estimates from CFF produced from *B. bassiana* produced in YPG or VM were approximately 9, 14, 23 or 33 μg mL^{-1} after 1, 2, 3 or 4 d incubation, respectively. The OD increased until 3 d of propagation demonstrating that the fungus was growing and suggesting that a proportion of the extracellular proteins that accumulated up to this time were likely due to primary biosynthesis. Many filamentous fungi are well adapted to be prolific secretors of proteins and is a function of their tip growth (Shaw *et al.*, 2011) and requirement for various extracellular enzymes to convert polymeric organic molecules into forms that can be utilized (Druzhinina *et al.*, 2012). In addition, cell wall 'ghosts', which are indicators of cell lysis were not present in cultures between 0-4 d, upon inspection at 400x magnification.

Analysis of banding patterns (resolved using SDS-PAGE) produced by CFF prepared from *B. bassiana* cultures revealed several protein bands between 10-140 kDa (Figure 4.4). Cultures incubated for between 0-4 d, contained four prominent protein bands between 25 and 40

kDa. After 4 d, three of the four prominent bands became less visible or were not visible at all, following SDS-PAGE analysis. The increase in dye binding of proteins < 10 kDa may indicate the presence of degradation products produced from the larger species in cultures > 3 d. Cultures incubated for < 3 d did not have any obvious protein bands, other than two between 50 and 70 kDa. These bands likely are human keratin which has subunits between 56-70 kDa (Fuchs and Marchuk, 1983) and is a common protein contaminant (Xu *et al.*, 2011), being also found in the ladder containing lane.

Cell-free filtrate that was prepared from *B. bassiana* cultures grown for various durations was assayed for its ability to increase the survival of CS challenged with UV-C using the standard method to assay for EIT to UVR in CS (Figure 4.5A). The requirements for CFF preheating to activate the putative ELF(s) within CFF were not determined here (see section 4.4.2). It was observed that treatment with CFF may have differing effects on the survival of CS (under non-photoreactivating conditions) depending on the dose. None of the CFFs were observed to affect survival following a dose of 90 J m^{-2} of UV-C irradiation. However, when challenged with 120 J m^{-2}, treatment with CFF from a 3 d culture was found to significantly increase CS survival values (4.5-fold) compared to CFF prepared from a 0 d or 4 d culture (Figure 4.5B). This result was consistent with findings in *E. coli* where CFF that was also produced from cultures grown under unstressed conditions was capable of increasing UVR tolerances once preheated (Rowbury, 2005). Furthermore, there was no obvious pattern of tolerance reduction in CS treated with CFF over the course of its storage, as CFF prepared from cultures grown for 0, 1, 2 or 3 d was stored at -30 °C for 4, 3, 2 or 1 d, respectively, while CFF from a 4 d culture was used fresh. This was done so that each trial could be conducted with CS of the same age.

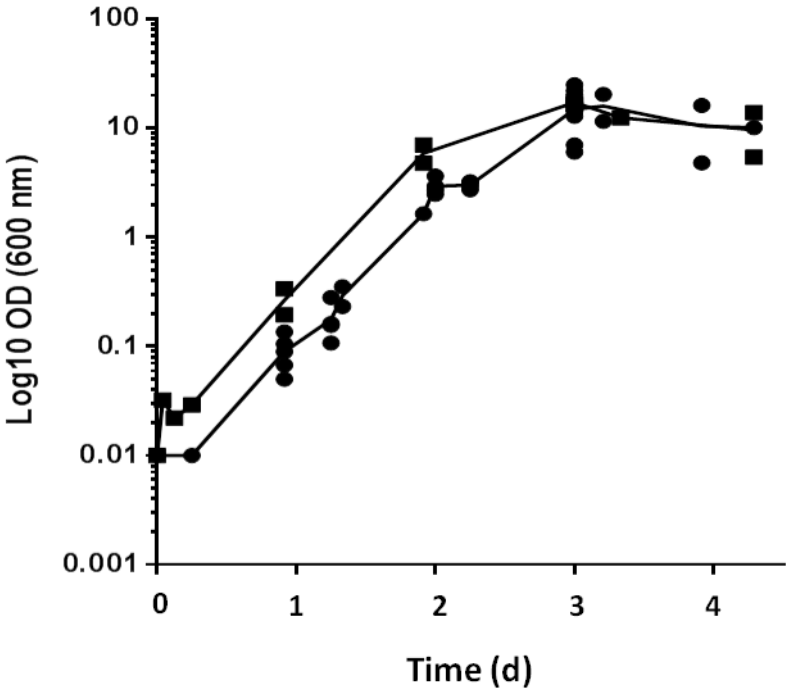

Figure 4.3 Change in OD of *B. bassiana* grown in VM or YPG. Cultures were prepared using the specified methods and conditions (see section 4.3.1). The curves were generated by (GraphPad Prism 6) connecting the means of seven and two trials for VM (●) and YPG (■), respectively.

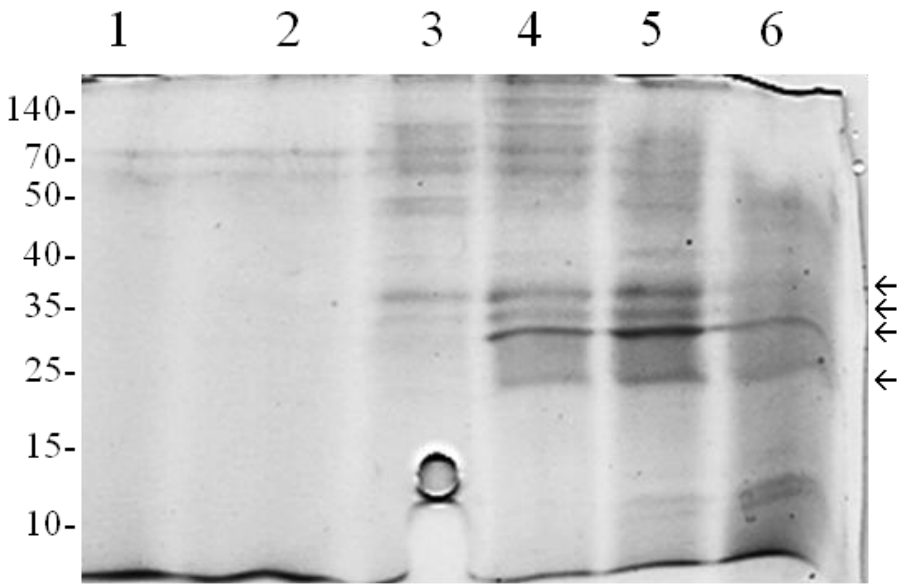

Figure 4.4 Protein banding pattern of CFF prepared from *B. bassiana* cultures grown in YPG. The SDS-PAGE was performed with a 15% w v^{-1} polyacrylamide gel. Lanes 1-6 were loaded with 0, 9, 14, 23, 25 or 33 µg of protein that was precipitated by an 80% saturated solution of AS from 1 mL of CFF prepared from cultures grown for 0, 1, 2, 3, 3.5 and 4 d, respectively. The masses (kDa) of the molecular ladder are indicated to the left of the photograph. The four arrows on the right of the photograph indicate locations of the major bands (< 40 kDa) that were correlated with elevated tolerance to UVR in CS.

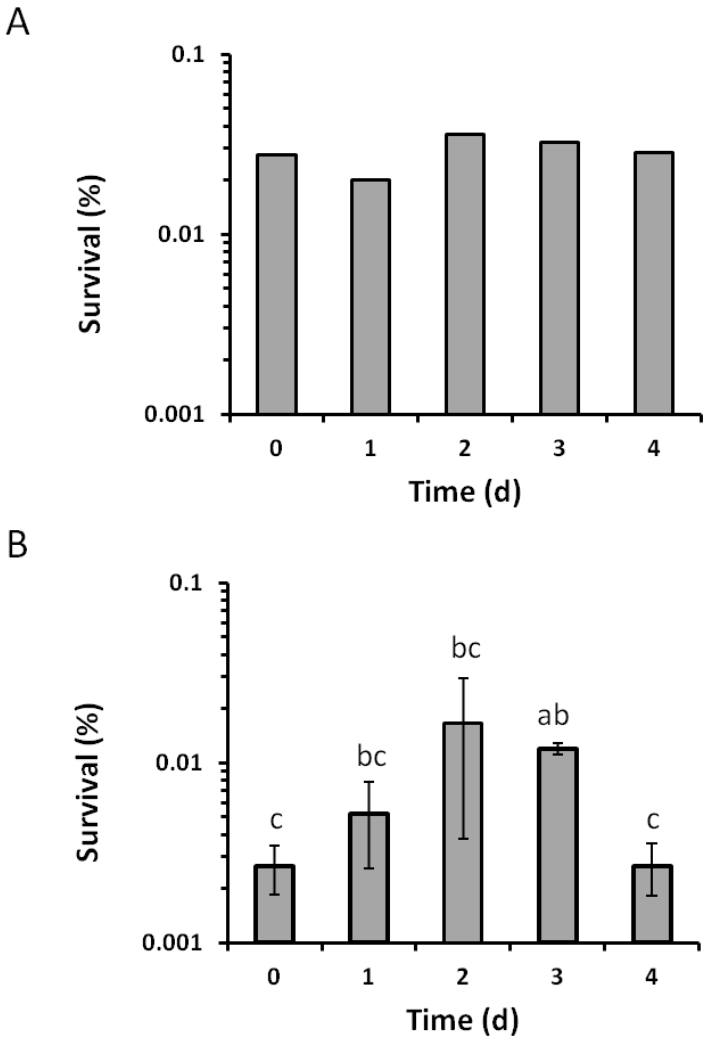

Figure 4.5 The effect of 55 °C preheated CFF on survival of CS challenged with UV-C. The assay to assess EIT to UVR was performed as in section 4.3.4 and sampled after receiving a dose of 90 (A) or 120 J m^{-2} (B) of UV-C. The CFF was prepared from cultures grown for zero (harvested immediately after inoculation) to 4 d in VM or YPG. The protein concentration of CFF was approximately 9, 14, 23 or 33 µg mL^{-1} after 1, 2, 3 or 4 d incubation time. The results are shown as bars in panel A and B represent the combined mean survival from two and four trials, respectively. An equal number of experiments were performed using CFF prepared from cultures grown in VM or YPG. The survival values obtained from CS treated with CFF prepared from either medium were combined because they were similar. For example, CS treated with CFF prepared from cultures grown in VM or YPG, yielded mean survivals of 0.0026% and 0.0028% from 0 d cultures or 0.013% and 0.011% from 3 d cultures, respectively. Bars in panel B containing a same letter in their label were determined to not be significantly different by Tukey's multiple comparison test (α=0.05). Error bars in panel B show SEM. Results in panel A were not analysed with Tukey's multiple comparison test or show SEM because were performed in duplicate.

It was apparent that an increase in survival was positively correlated with the age of the culture used to prepare the CFF (up to 3 d) and its protein content, particularly those < 40 kDa, until a maximum was reached after 3 d (Figure 4.4). Conversely, CFF prepared from cultures propagated for 4 d was not able to increase survival of CS above that of those treated with CFF prepared from a 0 d culture, despite possessing the highest protein content (33 μg mL^{-1}). In comparison, CFF from cultures propagated for 3 d contained less protein (23 μg mL^{-1}), but significantly higher CS survival. This difference in survival may be attributed to the presence of four major proteins that were < 40 kDa, but less present in CFF from a 4 d culture.

The above results suggested that the ELF(s) may only be produced during growth and therefore is potentially the product of primary biosynthesis and may be a protein of < 40 kDa. Moreover, the inability of CFF prepared from 4 d cultures to produce elevated tolerance to UVR may be due to: (i) reduced; or (ii) halted production of ELFs during fungal stationary phase; (iii) faster turnover/degradation; and/or (iv) loss of ELF activity (measured as its ability to increase survival rates in challenged spores). However, the potential contribution of each of these scenarios in reducing the ability of CFF prepared for a 4 d culture to induce elevated tolerance has not been determined experimentally. Nonetheless, the association between the presence of proteins in CFF that were < 40 kDa and the ability of CFF to increase survival in UV-C challenged CS provided further correlative evidence that CFF may contain putative ELFs, which may be proteins of < 40 kDa. The above results also indicated that CFF prepared from a 3 d culture provided the most consistent increase in survival values of UV challenged CS. Although the culture would be entering stationary phase by 3 d, fungal biosynthesis would still be occurring, which appeared to be correlated with ELF accumulation. A 3 d culture period was

chosen as optimal and used for all subsequent experiments to prepare CFF containing putative ELF.

The correlation between the OD of the culture and its ability to produce elevated tolerance resembles responses that involve quorum sensing, which are also cell population dependent. Quorum responses have been found to occur in fungi but are controlled by aromatic alcohols, such as farnesol in known instances (Reviewed in Albuquerque and Casadevall, 2012). Furthermore, farnesol may also be involved in the response to particular stresses since it was found to induce the upregulation of proteins involved in oxidative stress in *C. albicans* (Shirtliff *et al.*, 2009). In addition, the observation that a phenomenon resembling EIT to UVR is linked to cell density may imply that this response is energetically costly to the cells and as a result may improve survival fitness after a threshold number of cells are present, which is similar to quorum sensing in other microorganisms. However, ESC/ELF and conventional quorum molecules differ by one key characteristic; the formers' requirement for environmental stress to be present for them to be activated (Rowbury, 2001a).

It was also important to determine if CS also secreted a putative ELF. Structurally, CS differ from BS in that they have a thicker cell wall (Bidochka *et al.*, 1987). In addition to their reduced overall metabolism, CS also require hydration to promote germination and the prerequisite steps, including cell wall weakening at the apex once polarity is established (Reviewed in Shaw *et al.*, 2011). Furthermore, CS are dormant bodies and their transcriptional functioning requires much more nutritional conditions and time than that investigated here (Bidochka *et al.*, 1987). For example, CS in YPG will hydrate and become fully swollen within 6 h, germinate within 6-12 h, exhibit polar growth as hyphae in 12 h and the culture will have mostly BS present, as a proportion of total propagules, within 24 h of inoculation (Bidochka *et al.*, 1987).

The precedent for CS potentially being able to secrete proteins, including ELF, was that proteins, such as proteases have been found to be secreted by CS upon hydration (Qazi and Khachatourians, 2007); therefore it was important to determine if a putative ELF(s) was also secreted by assaying for increased tolerance to UVR in CS. This was performed by incubating CS with CFF that was prepared from either 0.02% (v v^{-1}) Tween 80, which was used to harvest the CS or sterile distilled water that was used to rinse the same CS. Prior to filtration, these CS suspensions contained ~ 10^9 CS mL^{-1}, which were approximately 10-fold more propagules than was found in a 3 d culture. The resulting survivals of UVR challenged CS (120 J m^{-2}), treated with Tween 80 or sterile distilled water were 0.0006% and 0.0005%, respectively. These values were both lower than those obtained from CS similarly treated with VM or CFF produced from a culture grown for 3 d, which were 0.005% and 0.022%, respectively. The fact that neither CFF prepared from Tween 80 nor sterile distilled water used to rinse CS produced survival values similar to that of CFF prepared from a 3 d culture indicated that ELFs may not be secreted by CS, at least not in the quantities needed to produce a biological response in CS. This observation provided another line of evidence suggesting that putative ELF(s) may be secreted by *B. bassiana* during vegetative growth.

Treatment of CS with preheated CFF did not influence their survival when challenged with 120 or 180 J m^{-2} of UV-C under photoreactivating conditions (Figure 4.6). Therefore, it appeared that the phenomenon which resembles EIT to UVR in CS likely occurred independent of enzymatic photoreactivation, perhaps through NER pathways. To provide another line of evidence for the confirmation of this finding, molecular data was used to determine if regulatory elements that are known to be associated with genes involved in heat tolerance acquisition may also be involved in *phr-1* regulation. This was performed by inspecting the first 1000 nts found

directly upstream of the predicted ORF of the putative *phr-1* from *B. bassiana* ARSEF 2860 (JH725152; nts 1380307 to 1382122), as per Gasch *et al.* (2000), for the presence of particular sequence elements. These elements included those involved in the HSR [GAANNTTCNNGAA (Sorger and Pelham, 1987)], general stress response [CCCCT or AAAAG (Martinez-Pastor *et al.*, 1996)] and those correlated with the ESR [GCGATGAG and AAAAWTTTT (Reviewed in Gasch, 2007)]. This analysis indicated that *B. bassiana* lacked these elements in the analysed sections. This was consistent with the above finding since preheated CFF did not appear to influence photoreactivation in UVR challenged CS. Although, it is yet to be determined what specific genes may be respond to ELF(s) or ESC(s), they would be expected to be involved in the response to stress. Therefore, *cis*-elements known to control the expression of genes that are responsive to stress were selected for the analysis described above.

Treatment with CFF was not found to influence the heat tolerance of CS as determined by their survival rates following challenge at 55 °C for 10 or 20 min (Figure 4.7). The observation that preheated CFF can increase tolerance in CS to UVR (under non-photoreactivating conditions) but not likely heat, may indicate that UVR and heat tolerance systems differ in their response to putative ELF(s). These outcomes indicated that CS were responsive and unresponsive to preheated CFF, respectively, with regards to its ability to promote elevated tolerances to UVR or heat. Tolerance to UVR was also found to be induced by preheated CFF in *E. coli*, but this treatment also induced tolerance to heat (Rowbury, 2003a). Therefore differences in EIT-like response may exist between *B. bassiana* CS and *E. coli* and may be connected for example to their eukaryotic/prokaryotic origins, differing ecological niches and/or genetic regulation.

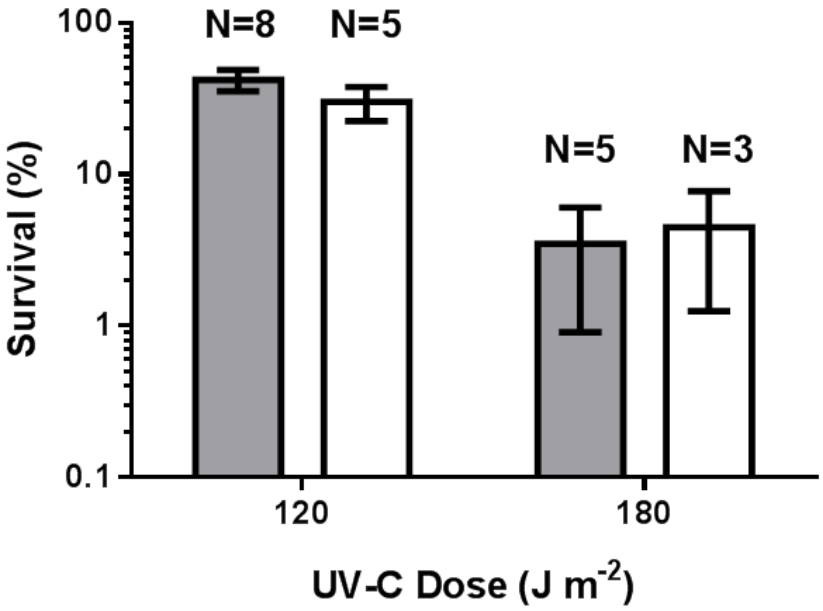

Figure 4.6 The effect of 55 °C preheated CFF or growth media on survival of CS challenged with UV-C under photoreactivating repair conditions. Preparation of the CFF, preheating and execution of the bioassay with CS was as specified in sections 4.3.2, 4.3.3 and 4.3.4, respectively. Grey or white bars show the mean survival of CS treated with preheated CFF or growth medium, respectively, and sampled after a UV-C dose of 120 and 180 J m^{-2}. Error bars show SEM and the number of experiments analysed is indicated above each bar. The effect of treatment was not found to be significantly different by Tukey's multiple comparisons test (α=0.05) at either dose.

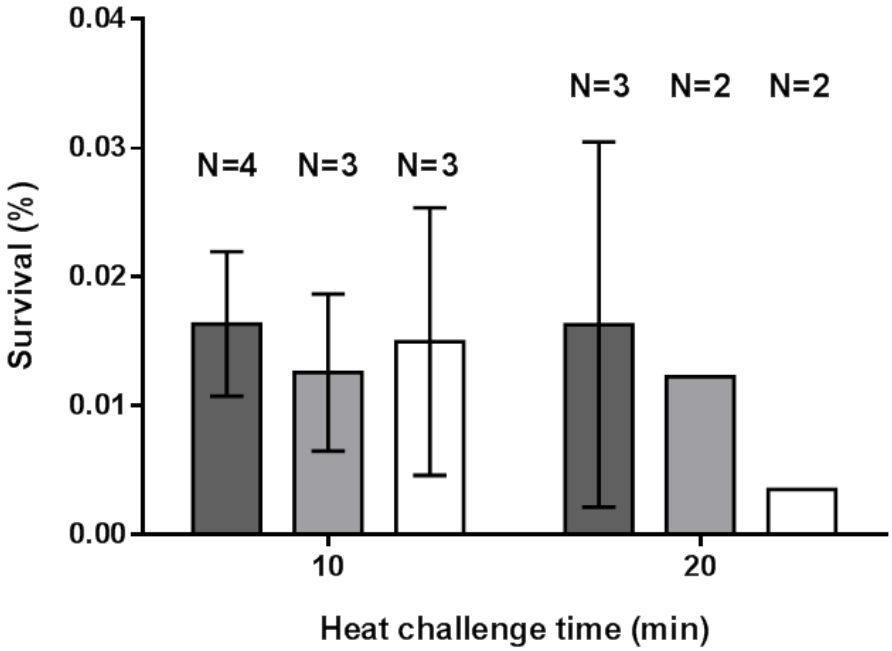

Figure 4.7 The effect of preheating CFF on the survival of CS challenged at 55 °C. Preparation of CFF, preheating and execution of the bioassay to asses EIT to heat was as in section 4.3.2, 4.3.3 and 4.3.5, respectively, except that CFF prepared from *B. bassiana* grown in VM was preheated at either 55 °C (dark grey bars) or 22 °C (light grey bars) and VM was preheated at 55 °C (white bars) before CS were added and incubated together for 4 h. Error bars show SEM (when N > 2) and bars show the mean survival calculated from the number of experiments indicated above each bar, which was measured in quadruplicate. Tukey's multiple comparison test was performed for those which N > 2, however, none were found to be significantly different following the same heat challenge time (α=0.05).

Protein content of CFF and the presence of proteins < 40 kDa were correlated with the ability of preheated CFF to produce elevated tolerance to UVR in CS. Due to this correlation, it was reasoned that if ELFs were present within CFF, they may likely be proteins or possessed a proteinaceous constituent and should be susceptible to proteolysis by trypsin, which could lessen their ability to increase tolerance to UVR. Cell-free filtrate was treated with pancreatic trypsin from porcine at approximately 10-fold greater than was required (according to the manufacturer's directions) to hydrolyze 23 $\mu g\ mL^{-1}$ of unpurified protein under the experimental conditions, to ensure that nearly all of the proteins within the CFF were proteolysed. Although protease degradation of extracellular proteins was not assessed in this experiment, it was in section 5.4.1 and was found that trypsin reduced the staining of protein bands, indicating their degradation. Incubation of CFF with trypsin significantly (19-fold) reduced its ability to increase survival of UVR challenged CS, compared to CS treated with CFF without trypsin (Figure 4.8). Furthermore, incubating VM with trypsin prior to preheating did not affect survival in CS, compared to those treated with VM without trypsin. Therefore, the addition of trypsin to CFF appeared to abolish its ability to increase UVR tolerance in CS. This suggested that putative ELF(s) may be present in CFF and is likely a protein or has a protein component. Similar findings have been reported in *E. coli* (Rowbury and Goodson, 2001), *C. jejuni* (Murphy *et al.*, 2003) and *L. japonicus* (Vorob'eva *et al.*, 2003). These studies showed that a phenomenon resembling EIT, possibly controlled by secreted proteins > 10 kDa, could also be abolished by treating the CFF with protease.

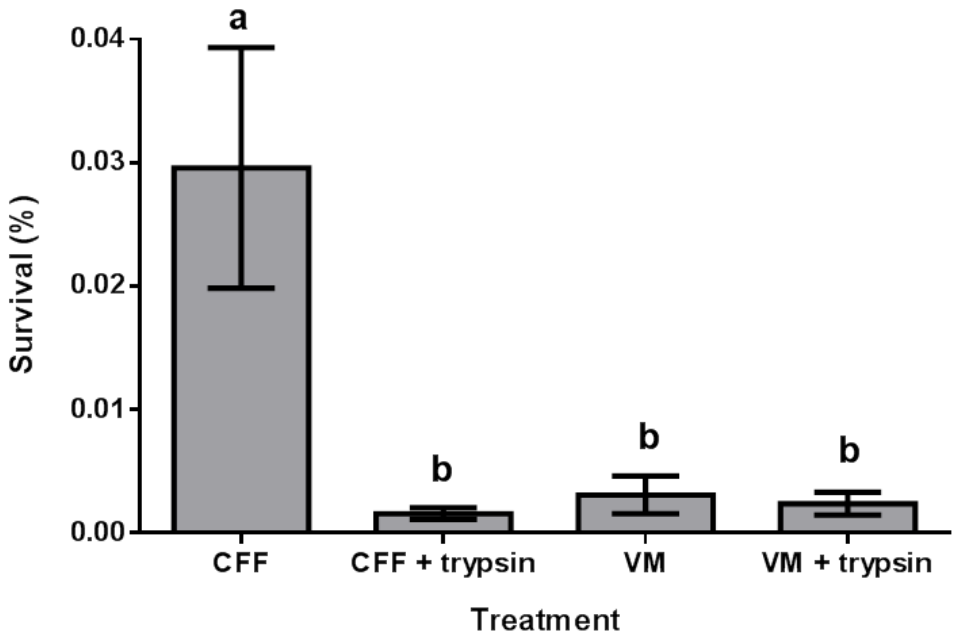

Figure 4.8 The effect of treating CFF or VM with trypsin on its ability to increase survival of CS challenged with 120 J m^{-2} of UV-C. Preparation of CFF, preheating and execution of the bioassay to asses EIT to UVR was as in section 4.3.2, 4.3.3 and 4.3.4, respectively, except that CFF or VM were supplemented with or without 24 μg mL^{-1} trypsin, before and after 30 min incubation at 22 °C. The CFF was then preheated at 55 °C and inoculated. Bars show the mean survival calculated from three trials that were measured in quadruplicate, except for those treated with CFF or CFF + trypsin, which were from four and five trials, respectively. Error bars show SEM and bars labeled with a same letter were determined to not be significantly different by Tukey's multiple comparison test (α=0.05).

Another characteristic shared by ESCs/ELFs is their heat stability. The factors produced by *E. coli* (Rowbury and Goodson, 1999a), *S. cerevisiae* (Vovou *et al.*, 2004) or *C. jejuni* (Murphy *et al.*, 2003) remained active following an incubation of 75 °C for 15 min, 100 °C for 5 min or 100 °C for 10 min, respectively. To determine if putative ELFs produced by *B. bassiana* were heat stable, CFF was incubated at 121 °C for 15 min in an autoclave, prior to being treated as specified. The result from this single experimented showed that CS treated with CFF had higher survival values of 0.046%, compared to 0.009% in those treated with growth medium. Therefore, the putative factor in CFF apparently remained responsive to heat activation, following the high heat treatment. Other examples of heat stable proteins have been found and exhibit reversible thermal denaturation. For example, ribonuclease-A does not lose activity following incubation at 121 °C for 20 min (Miyamoto *et al.*, 2009). Therefore, the apparent heat stability of putative ELF is not in opposition to the known limitations imposed by biology; however more research is required to provide a better understanding of the heat stability of the putative ELF(s) from *B. bassiana*.

4.4.2 Parameters required for the induction of tolerance to UVR in CS by CFF

Activated ELF was defined as that which could cause EIT in the test organism. High heat was tested as a potential activator of putative ELF in CFF because it could be easily manipulated. This was done by assaying the thermal activation of the putative ELF acquired by preheating at various temperatures, through its ability to increase the survival rates of UV-C challenged CS, which is characteristic of EIT in other organisms (Figure 4.9). At 22 °C, CFF was unable to increase UVR survival in CS over similarly treated growth media (either VM or YPG). Heating CFF to 45 °C increased survival of CS by approximately four-fold compared to

those treated with growth medium heated at 45 °C, but was not significantly different. Cell-free filtrate preheated to 55 °C provided a significant ($p=0.0254$) increase in survival to treated CS that was approximately nine-fold higher than in CS treated with growth medium preheated to 55 °C. Preheating CFF at 65 °C for 30 min was not conducive for the activation of the putative ELF. This was evident by the similar survivorship of UV-C challenged CS treated with 65 °C preheated CFF, compared to those treated with 65 °C preheated growth media. This result suggests that the activity of ELF may have been lower when CFF was preheated at 65 °C, compared to 55 °C.

Another observation was that survival of CS treated with growth medium appeared to be positively correlated with the temperature the growth medium was preheated to (Figure 4.9). A similar finding has been documented in other systems and has been attributed to the HSR, which is known to elevate UV tolerance (Mishra *et al.*, 2009). However, this increase in survival by heated growth medium was minimal, compared to the increase in survival observed in CS treated with 55 °C preheated CFF.

With regards to EIT to UVR, ESC produced by *E. coli* can also be activated by thermal stress and increase UV tolerance (Rowbury, 2003b). Therefore, it is possible that the physiological responses to activated putative ELF and ESC in *B. bassiana* and *E. coli*, respectively, may share common features. For example, increased DNA repair likely contributes to the increase in tolerance to UVR in *B. bassiana* and *E. coli*, since the biocidal effects of short wave UVR have been attributed to the DNA damage they induce, which are mainly CPDs and (6-4)PPs (Wang, 1976). More specifically, it was shown here that photoreactivation is not likely involved in this tolerance, therefore NER is a mechanism which is potentially positively affected by the EIT-like phenomenon in *B. bassiana*. Since the conditions of repair were not provided by Rowbury

(1999) it was not possible to speculate on the role that photoreactivation plays in EIT to UVR in *E. coli*.

In addition to temperature, the duration the CFF was preheated at 55 °C also affected its ability to increase survival of CS challenged with UV-C, perhaps through the activation of putative ELF within the CFF and the promotion of EIT. Survival of CS was positively correlated with the duration of CFF preheating (Figure 4.10). A maximal increase in survival was observed in CS treated with CFF preheated for 30 min, which was approximately ten-fold higher than CS incubated with similarly treated growth media. Continued heating was observed to decrease the survival of CS from that obtained after 30 min, although their survival was somewhat elevated compared to similarly treated growth media. As noted above, the time dependence of putative ELF activation within CFF leading to EIT and increased survival, could likely be influenced by temperatures, but this has yet to be determined experimentally in *B. bassiana*. However, it is possible that the lower UVR survival in CS treated with either 45 or 65 °C preheated CFF may be due to the fact that the putative ELFs may have not been heated for long enough or for too long, respectively and may influence the activity of ELF. This potential temperature/time interaction on the activation of putative ELF is consistent with findings in *E. coli* (Rowbury, 2003a; Rowbury, 2005) and is supported by the fact that biochemical reactions occur at increasingly rapid rates as temperatures are increased. Nonetheless, 30 min at 55 °C were chosen as the optimal time and temperature for activation of putative ELF.

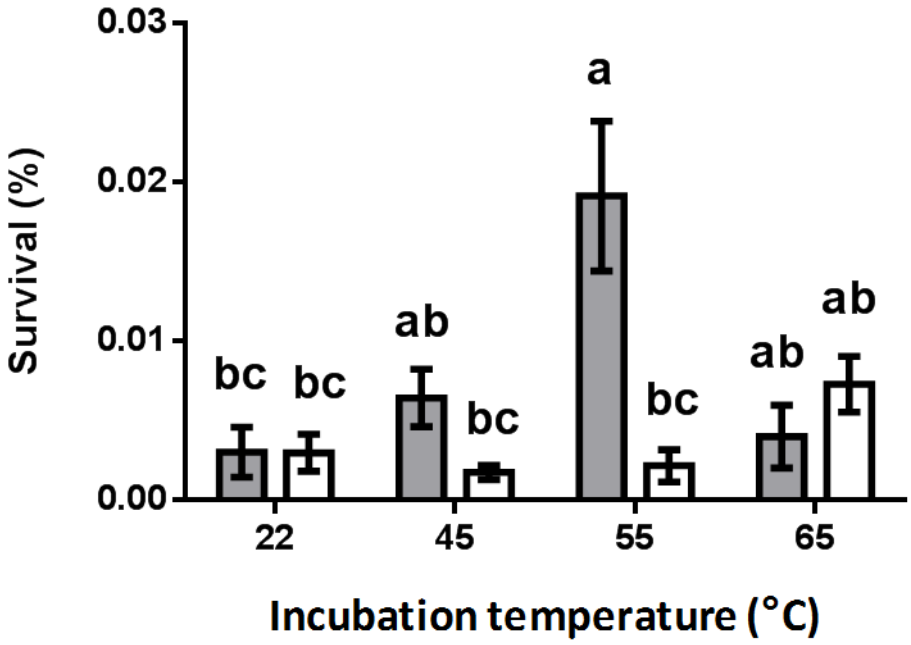

Figure 4.9 The effect of preheating temperature of CFF or growth media on survival of CS challenged with 120 J m^{-2} of UV-C. Preparation of CFF, preheating and execution of the bioassay to asses EIT to UVR was as in section 4.3.2, 4.3.3 and 4.3.4, respectively, with the exception that CFF (grey bars) or growth media (white bars) were incubated at the temperature indicated on the x-axis before CS were added. The bars represent the mean survival from 6, 5, 13 and 5 trials for CFF or 7, 5, 5 and 6 for growth media treated samples heated at 22, 45, 55 or 65 °C, respectively. The CFF and growth media were incubated for 30-50 min, however the number of trials performed with a particular duration of incubation differed. The number of trials performed for each treatment/temperature combination with a particular duration of incubation was: CFF/22 °C at 30 min =2, 40 min =2, 50 min =2; CFF/45 °C at 30 min =2, 40 min =2, 50 min =1; CFF/55 °C at 30 min =8, 40 min =3, 50 min =2; CFF/65 °C at 50 min =5; growth media/22 °C at 30 min =3, 40 min =2, 50 min =2; growth media/45 °C at 30 min =2, 40 min =2, 50 min =1; growth medium/55 °C at 30 min =3, 40 min =2; and growth medium/65 °C at, 50 min =6. Error bars show SEM and bars containing a same letter in their label were determined to not be significantly different by Tukey's multiple comparison test (α=0.05).

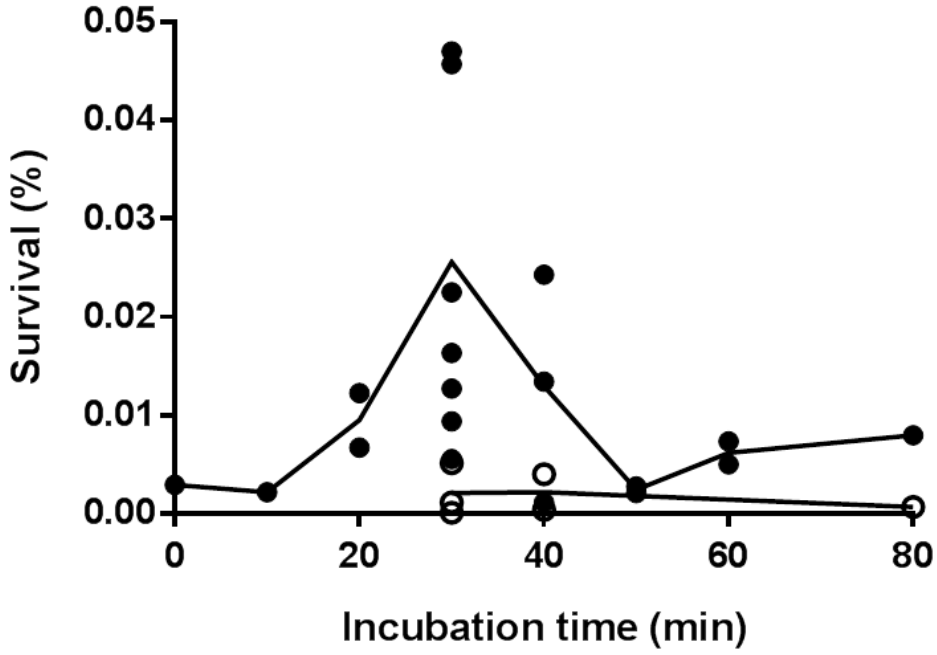

Figure 4.10 The effect of preheating duration of CFF or growth medium on survival of CS challenged with 120 J m^{-2} of UV-C. Preparation of CFF, preheating and execution of the bioassay to asses EIT to UVR was as in section 4.3.2, 4.3.3 and 4.3.4, respectively, except the CFF (●) or growth medium (○) were incubated at 55 °C for the duration indicated on the x-axis before CS were added. Each datum point represents the mean survival obtained from a single experiment, sampled in quadruplicate and the curve was generated (using GraphPad Prism 6) by connecting the means from ≤ 7 experiments, depending on the incubation time. The total number of datum points analysed were 20 and 6 for CFF and growth medium treated samples, respectively.

The results of preliminary experiments that were conducted to study the time required for CFF to induce an elevated tolerance to UVR in CS will be discussed here. This was performed by preheating CFF or growth media at 45 °C for 30-50 min, before CS were added and incubated at 27 °C to promote elevated tolerance to UVR. Although these temperatures and durations of preheating had been shown to be non-optimal for activation of putative ELF they provided additional insight into these potential requirements for EIT to UVR in CS. It was found that the duration of incubation of CS with the treatment may be positively correlated with an increase in survival in CFF treated, but not growth medium treated CS. Treatment with CFF produced CS survivals of 0.0029%, 0.0063% and 0.0064 ± 0.0018% SEM, while CS treated with growth medium had survivals of 0.0019%, 0.0009% and 0.0017 ± 0.0004% SEM, after 1, 3 and 4 h of induction, measured from one, two and five experiments, respectively. The survivals provided by a 3 or 4 h induction (0.0063% and 0.0064%, respectively) were similar, but 3.7-fold and 7-fold greater than those provided by similarly treated growth medium. As a result, 4 h was chosen as optimal for the induction of tolerance to UVR in CS using preheated CFF, preferably at 55 °C. Also, the time required for the response that resembles EIT to potentially occur may not differ due to the thermal conditions that may have activated the putative ELFs. In other words, ELFs may be functionally similar regardless of the temperature that activated them, *ceteris paribus*. If ELF activity varied due to the temperature, so too would the level of protection provided through EIT, if the response was correlated with changes in gene expression. This is because the expression of genes that are responsive to a stimulus is positively correlated with dose (Forrester *et al.*, 2012) assuming EIT is affected by gene expression.

Although the mechanism(s) which provided an elevated tolerance to UVR in cells treated with preheated CFF is unknown, tolerance to UVR in fungi can be achieved generally by two

well-known means. Firstly, repair of damage, such as that induced in DNA by UVR can increase the ability of an organism to tolerate a dose of UVR. This has been shown to be primarily through photoreactivation and/or NER (Chelico *et al.*, 2005). Secondly, physical shielding can also increase UVR tolerance and survival, and has been found to occur in pigmented fungi, such as *M. anisopliae* (Braga *et al.*, 2006; Rangel *et al.*, 2006). Therefore, it is possible that an EIT-like response in *B. bassiana*, directly or indirectly, mediates DNA repair pathways, but not likely melanin disposition, since the fungus is not pigmented.

A single result showed that the survival of UVR challenged CS was also found to be influenced by the timing of their exposure to preheated CFF. Following a 2 h incubation with CS, CFF that was previously preheated at 55 °C was replaced with similarly treated VM and allowed to incubate for an additional 2 h. This treatment produced a survival value of 0.004% in CS exposed to 120 J m^{-2} of UV-C, compared to that of CS which received the positive control treatment (treated with CFF as standard) and had a survival of 0.047%. This result suggested that the continued presence of CFF prior to the insult may be a requirement for it to increase tolerance to UVR in CS. Rowbury (2001a; 2003a; 2005) has speculated that the requirements for EIT to be established could include signal transduction, gene expression and/or enzyme activation which can also proceed following UV challenge, which is the case in other stress responses. As a result the use of tracking the potential acquisition of EIT by CS, survival may be limited to determining the requirements to provide a biological response, measured through the bioassay. Therefore, determination of molecular indicators of EIT, such as reporter genes, would be useful to follow the physiological events required for the establishment of EIT. However, this required an understanding of the molecular biology of EIT that is beyond the current state of knowledge.

4.4.3 Screening for EIT-like responses in BS

In addition to EIT-like responses in CS, it was important to determine if they also occurred in BS following treatment with preheated CFF. Such a finding was suspected to be useful in detecting candidate protein(s) that possessed ELF activity. This is because BS are morphologically different and more metabolically active than CS and may be able to respond to active ELF in a more consistent manner and therefore better suited to detect ECs.

Initial tests revealed that BS were not responsive to the method which produced elevated tolerance to UVR in CS, with the exception that CFF was preheated at 45 °C prior the addition of BS (Figure 4.11). These results showed that BS incubated with preheated CFF had similar survival rates following a UV-C dose of 36, 60 or 120 J m^{-2}, compared to those incubated with similarly treated growth medium, or CFF preheated at 22 °C. These findings suggested that EIT to UVR likely does not occur in BS, under these conditions.

The same protocol was tested for its ability to induce elevated tolerance to heat in BS. The results of an experiment performed in duplicate showed that 0.011% and 0.013% of BS treated with preheated VM or CFF, respectively, survived a 30 min challenge at 55 °C in PBS. Therefore, BS were likely not responsive to the method which produced an EIT-like response to UV in CS.

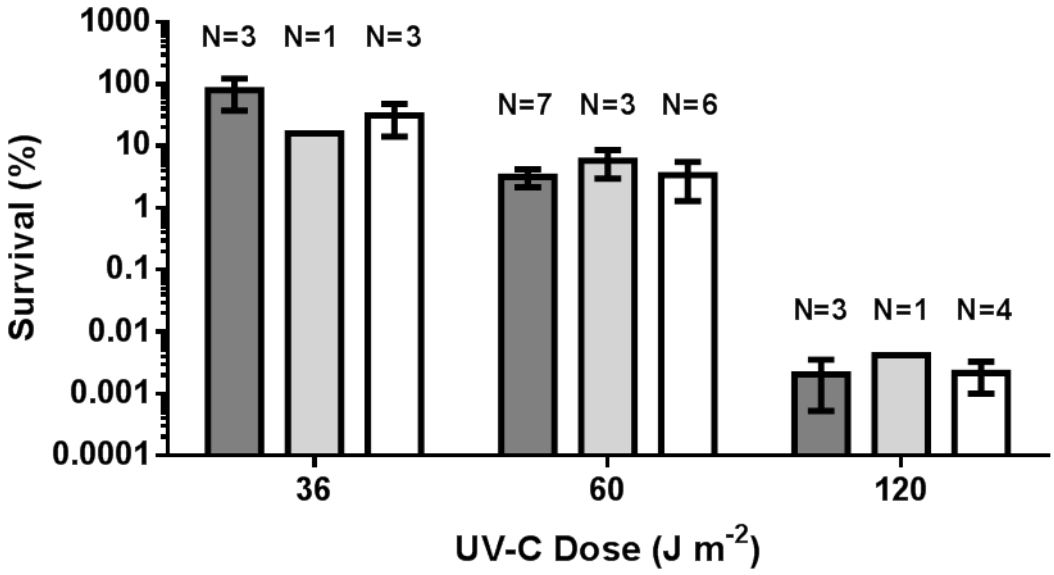

Figure 4.11 The effect of preheating CFF on survival of BS challenged with UV-C, under non-photoreactivating conditions. Preparation of the CFF, preheating and execution of the bioassay were as specified in sections 4.3.2, 4.3.3 and 4.3.4, respectively, except that CFF was preheated at either 45 °C (dark grey bars) or 22 °C (light grey bars) and the media was preheated at 45 °C (white bars) for 30 min before BS were added. Bars show the mean of like treatments at each dose and the number of experiments analysed is indicated above each bar. Error bars show SEM (for N > 2) and Tukey's multiple comparison test was performed on treatments that received the same dose, when N > 2, however none were found to be significantly different (α=0.05).

In light of these results, other parameters were tested to determine if BS could be prompted to acquire an EIT-like response. In a preliminary experiment, BS were challenged directly in CFF at 55 °C for 30 min that was treated with various heating regimes. This single result showed that BS challenged in CFF that was preheated at 55 °C for 3 or 100 min had the highest survival values of 0.139% and 0.067%, respectively. In comparison, BS challenged in CFF that was preheated at 22 °C for either 3 or 100 min had similar survivals of 0.018% and 0.025%, respectively. Interestingly, only 0.018% of BS survived when they were challenged in CFF that was preheated for 100 min at 55 °C then cooled to 22 °C (required ~ 5 min) before BS were added to the vial and incubated at 55 °C for heat challenge. The survival rates of BS treated with 22 °C preheated CFF (0.018% and 0.025%) were similar to those obtained in the previous experiment (0.011-0.013%; see above paragraph), relative to BS treated with 55 °C preheated CFF. This may indicate that the baseline survival rate of BS challenged at 55 °C was consistent when not stimulated to produce an EIT-like response to heat. This is an important characteristic, since high variation within untreated BS would increase the difficulty in distinguishing between a biological response to ELF and a null response with statistical tests. Historically, the research of many other distance interactions has been hindered due high variability of the responses (Reviewed in Nikolaev, 2000). As a result of its ability to increase heat tolerance in BS, preheating CFF for 3 min at 55 °C was chosen as the optimal time and temperature to provide elevated tolerance to heat in BS and was used to study the EIT-like in these propagules.

As noted above, the survival of BS challenged in CFF preheated at 22 °C was lower than those challenged in CFF preheated to 55 °C. This effect may provide clues for the temporal requirements for the potential activation of putative ELF by heat with respect to its ability to increase heat tolerance in BS. To elaborate, it appeared that CFF required preheating prior to the addition of BS in order to increase survival rates in heat challenged BS. Conversely, BS which were heat challenged in CFF that was either previously held at 22 °C or cooled to 22 °C following 55 °C

preheating, before being incubated at 55 °C for challenge, had lower survivals than BS challenged in CFF that was preheated at 55 °C (not cooled) prior to inoculation. This was an interesting result because at 22 °C, CFF would require ~ 3 min to equilibrate to 55 °C once was placed in the 55 °C water bath (contained in a glass vial). Therefore, the duration BS in 22 °C preheated CFF were exposed to 55 °C, would be less than BS added directly into CFF that was preheated to 55 °C, yet they had less survival. Therefore, something other than heat challenge duration must have affected the survival of the BS, since a decrease in survival is a function of both the duration and the temperature of challenge. These results suggest the presence of active ELF within the preheated CFF and could be responsible for the difference in survival.

Furthermore, the apparent requirement for the suspected ELF to be held at 55 °C may be required for it to achieve and maintain activation within CFF. This may be a fundamental difference in the functioning of the putative ELF in *B. bassiana* compared to ESC in *E. coli*, which can remain active for at least a few minutes once the stress is removed (Rowbury, 2005). Furthermore, Rowbury (2005) has suggested that active ESCs may be able to diffuse from an area exposed to heat stress, to cells not yet exposed to the stress and remain active, allowing it to cause EIT to heat and other stresses. However, in the case of elevated tolerance to heat in BS, it appeared that heat stress and the putative ELF may be required in concert for it to occur. Therefore, it is possible that the putative ELFs studied here may be inactivated more rapidly than ESC(s) produced by *E. coli*, in the absence of thermal stress conditions.

This work was extended to compare the protective effect provided by preheated CFF to that of a conventional heat shock as per Xavier (1998) (Figure 4.12). After being challenged with heat for 15 min, the survival of BS that were challenged (55 °C) in CFF that was preheated at 22 °C or 55 °C were similar, but higher than those challenged in VM. Also, the survival of BS challenged in VM preheated at 55 °C were similar to those treated with a heat shock by incubating at 45 °C for 1h prior

to being challenged. After a 30 min challenge the survival of BS, regardless of treatment, were quite similar and ranged from 0.059% to 0.095%. The effect of 55 °C preheated CFF on BS survival was strongest after a 45 min heat challenge. The survival of BS that received this treatment was 2.7, 3.5 and 6.8-fold higher than those that received a heat shock or were incubated in VM or CFF that was preheated at 22 °C, respectively, but was not significant. Since the apparent EIT-like response was most pronounced in BS that were challenged at 55 °C for 45 min, this was chosen as the standard heat challenge to asses EIT to heat in BS.

It appeared that the survival of BS that were treated with a heat shock then challenged in VM preheated at 55 °C compared to those challenged in CFF preheated at 55 °C may be similar, however more research is required to extend these findings. Nonetheless, a similar finding has been reported in *S. cerevisiae* where the survival rates of heat challenged cells that received a heat shock or preheated CFF treatment were similar but elevated compared to those challenged in fresh growth medium (Vovou *et al.*, 2004). This observation may indicate that the mechanisms which provided heat tolerance and occur in response to active ELF or heat shock may provide a similar level of tolerance, possibly through shared or similar responses; however no specifics are known. Clearly, a better understanding of the events that lead to EIT would provide insight into the molecular biological events that control it. As noted by Morano (2012) a true sensor of heat, needed to elicit the HSR remains to be found. Therefore, it is possible that ESC(s) and/or ELF(s) may function in this manner; as sensors of heat stress which may function with intracellular sensors of heat, rather than as substitutes (Rowbury, 2001a; Rowbury, 2003a), however more research is needed in this area.

Cell-free filtrate prepared from *B. Bassiana* cultures grown in YPG, also increased heat tolerance of BS when challenged in the preheated CFF (Figure 4.13). In CFF prepared from either cultures grown in YPG or VM, BS survived best when they were heat challenged in CFF preheated to 55 °C, compared to those challenged in preheated growth media, or CFF that was not preheated to

55 °C. Furthermore, the survival of BS challenged in 55 °C preheated CFF, prepared from cultures grown in YPG, was significantly higher than all except 55 °C CFF prepared from VM cultures. While 55 °C preheated CFF prepared from VM cultures provided survival that differed significantly to only BS provided the same CFF preheated at 22 °C. In addition, BS challenged in preheated PBS had survivals rates that were similar to all except those challenged in 55 °C preheated CFF from YPG cultures, which were 4.4-fold greater. Here it was shown that CFF prepared from *B. bassiana* cultures grown in complex (YPG) and possibly defined media (VM), were able to increase heat tolerance in BS, which resembles the EIT phenomenon. Therefore, the factor(s) responsible for this phenomenon are likely not intrinsic constituents of the media; but are produced by the fungus.

It may be possible that the local environments where BS and CS are found in nature may influence their response to ELF. While BS can be exposed to solar UVR in environments, such as in soil, they are shielded from UVR within a host insect. In contrast, during the infection cycle, aerial CS are produced outside of the insect cadaver and thus are not shielded from solar UVR, but also are not exposed to the elevated temperatures within the insect that occur as a result of the behavioral fever. The fact that CS do not generally encounter an insect's fever may help explain their apparent lack of responsive which resembles EIT to heat, since it may not provide additional fitness to the fungus. However, preheating of CFF was required for elevated tolerance to UVR in CS and suggested that activation of the suspected ELF may occur in liquid. Therefore, it is difficult to speculate on the functioning of ELF(s) with respect to CS, since this cell type appears to be adapted to non-liquid environments (Jeffs *et al.*, 1999), although CS can also enter the host through ingestion, in chewing insects (Reviewed in St Leger and Wang, 2010).

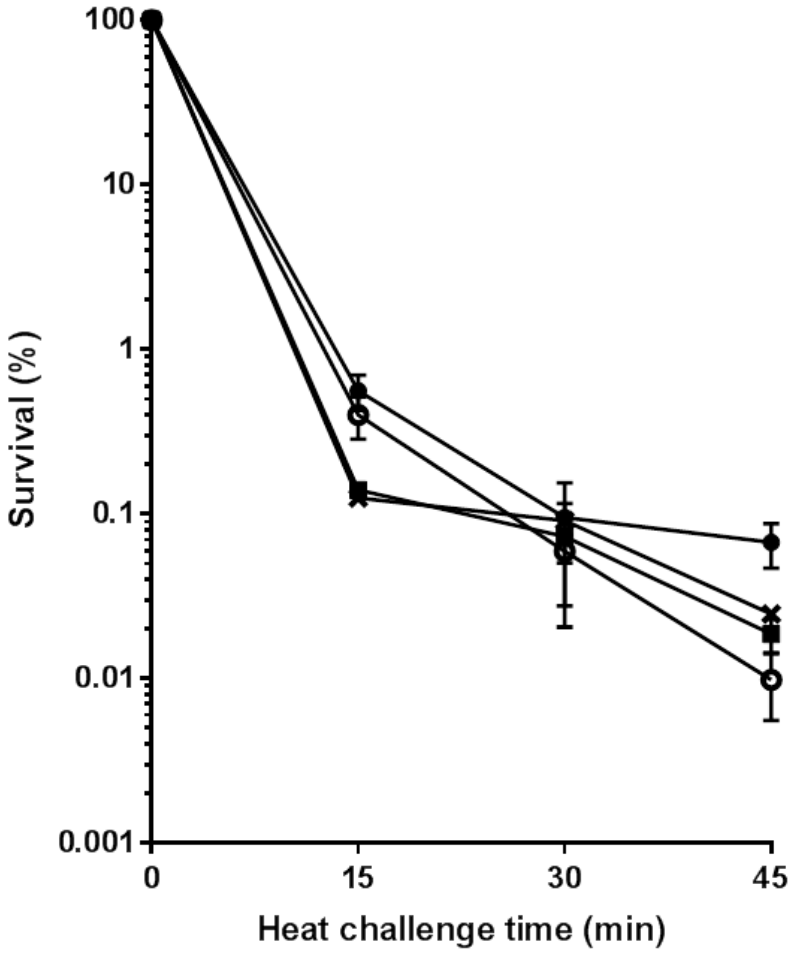

Figure 4.12 The effect of preheating CFF and heat shock on survival of BS challenged at 55 °C. Before BS were added, CFF (prepared from cultures grown in VM) was incubated for 3 min at 55 °C (●) or 22 °C (○) and VM was incubated at 55 °C (■). Blastospores were also treated with a heat shock at 45 °C for 1 h in VM (**X**), before they were transferred to VM preheated to 55 °C and challenged. Symbols show the mean survival of samples taken at the times indicated on the x-axis. For both CFF treatments N=3, 4 and 4 at 15, 30 and 45 min, respectively. The mean survival of BS that were or were not treated with heat shock prior to challenge in VM were calculated from N=2, 3 and 2 or 1, 3 and 3 at 15, 30 and 45 min, respectively. Error bars show SEM (for N > 2) and Tukey's multiple comparison test was performed with data points with N > 2, however none were found to be significantly different following the same heat challenge duration (α=0.05).

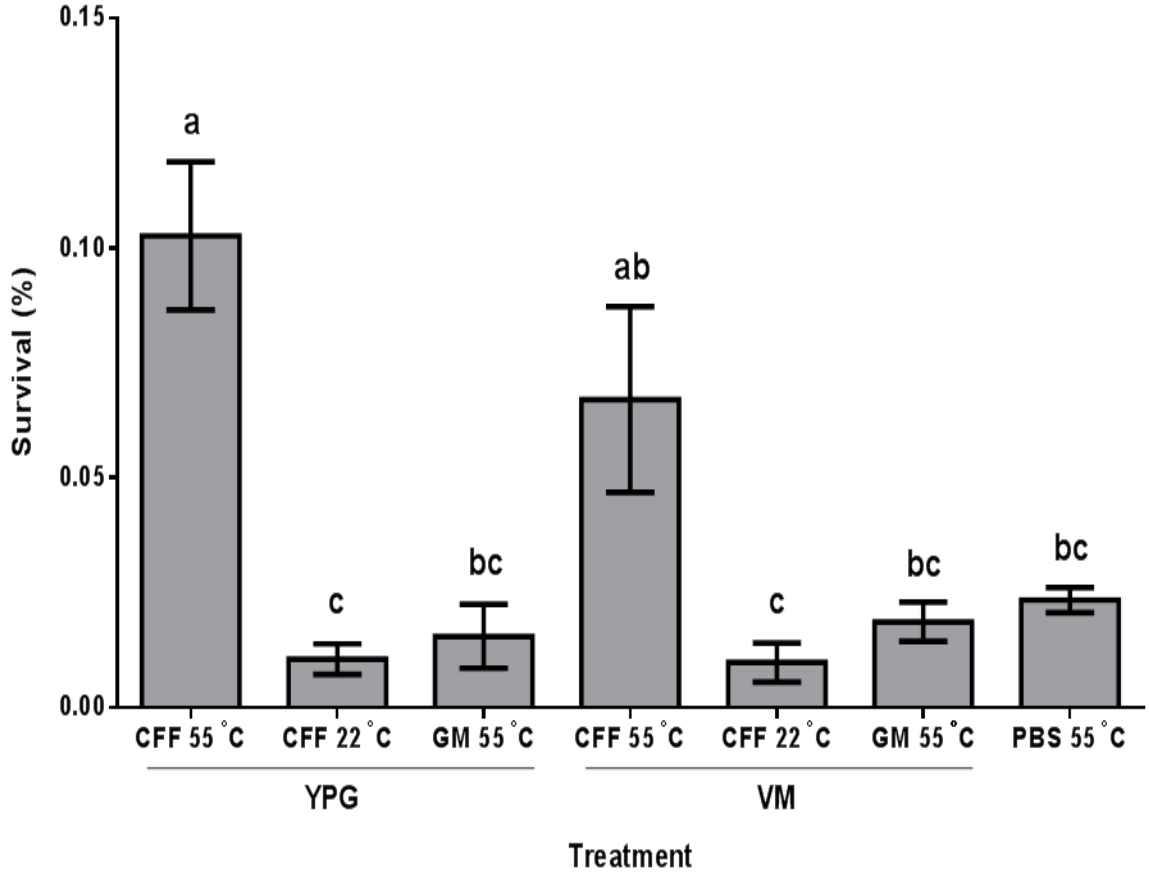

Figure 4.13 The effect of preheating CFF on the survival of BS challenged at 55 °C for 45 min. The heat tolerance assay was performed as specified in section 4.3.5. The heat challenge medium used was either PBS or CFF or growth medium (GM) which was YPG or VM as indicated. Prior to BS addition, the CFF was preheated at either 55 °C or 22 °C as indicated below the x-axis, while YPG, VM and PBS were preheated at 55 °C only. The values from BS treated in CFF or VM are the same as those shown in Figure 4.12, after a 45 min challenge. Bars represent the mean survival, calculated from three trials sampled in quadruplicate, except for those treated with CFF prepared from cultures grown in VM, which were calculated from four trials. Error bars show SEM and bars containing a same letter in their label were determined to not be significantly different by Tukey's multiple comparison test (α=0.05).

As shown above, preheated CFF has the ability to increase tolerance to lethal heat temperatures in BS. However, it still remained to be established if a similar effect also occurred in the presence of supra-optimal but sub-lethal temperatures. To determine this, the growth and viability of *B. bassiana* cultures was measured. These were incubated in YPG with (1:1; CFF:YPG) and without CFF at optimal growth (27 °C) or sub-lethal (34 °C) temperatures. It was found that the media treatment did not influence the growth rate or development of cultures (Figure 4.14). Differences were found due to incubation temperatures. As expected, the optimal growth temperature promoted faster growth and development, compared to the supra-optimal temperature. After a 5 h incubation at 27 °C or 34 °C, 20-26% or 92-94% of propagules remained not swollen CS, respectively. Following 22 h of incubation 0-6.5% and 36.5-47% of propagules remained not swollen CS at 27 °C and 34 °C, respectively. After 5 h those incubated at 27 °C entered log growth and reached the greatest observed cell numbers and viable counts after 27 h. In contrast, cultures incubated at 34 °C had a constant reduction in viable counts and no increase in cell numbers over time. Although, CS were able to swell and germinate at 34 °C, this development did not progress into sustained polarized growth.

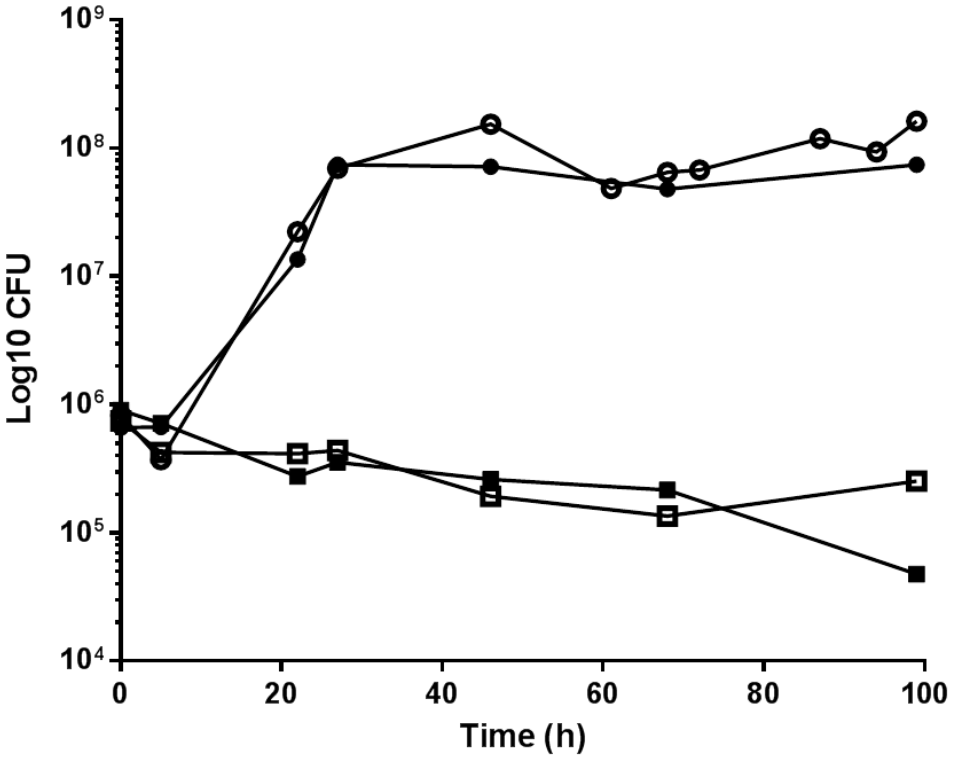

Figure 4.14 The effect of CFF on growth of *B. bassiana* during optimal and supra-optimal temperatures. In 250 mL Erlenmeyer flasks with 50 mL of media containing of YPG (open symbols) or an equal ratio of YPG and CFF (closed symbols) were inoculated to 10^6 CS mL^{-1} and incubated at 27 °C (circles) or 34 °C (squares). Samples were taken at the indicated times, diluted in PBS and plated on YPGA to measure CFUs. The curves were produced from the means of single experiments that were sampled in triplicate.

The above results showed that CFF prepared from *B. bassiana* culture was not able to alter growth or development of *B. bassiana* cultures at optimal or sub-lethal temperatures, under the experimental conditions. This indicated that the putative ELF within CFF, likely does not have a role in growth and development of *B. bassiana* during optimal and sub-lethal temperatures under the condition tested, but instead may strictly affect survival at lethal temperatures. Although, the internal temperature of the insect that is reached during behavioural fever is sub-lethal to the fungi, it is sufficient to contribute to reduce mycosis in the host (Carruthers *et al.*, 1992). As a result, the interaction between temperature and the ability of the fungus to cause insect infection is not simple and likely involves additional factors controlled by the insect, fungus and environment. Therefore, it is not possible to exclude the potential role of ELF during insect infection. For example, 35 ºC is approaching the T_{max} of *B. bassiana*, but infected grasshoppers do not develop mycosis when incubated at this temperature, but do at lower temperatures (Carruthers *et al.*, 1992). While it is neither possible nor practical to totally mitigate detrimental field conditions, it is possible to acquire the knowledge of correlations between heat and induced stress responses. Ultimately, this fundamental understanding can be used for applied research and development, improving the ability of *B. bassiana* and other EPF to be used as biopesticides, perhaps by improvement of their ability to mitigate the detrimental effects of their environment.

The apparent difference between growth rates of *B. bassiana* shown in Figure 4.3 compared to Figure 4.14 can be attributed the differing method of measurement, as OD measures total cell density, which can be influenced by cell size. In the case of *B. bassiana*, the presence of hyphae will cause a discrepancy between OD and viability measurements since will only

produce a single CFU but are significantly larger than BS and as a result will produce a proportionally larger increase in OD.

4.5 Connection to the next study

The increased tolerance to UVR and heat in CS or BS, respectively, provided by preheated CFF, resembles EIT-like responses. The establishment of such phenomena marked important discoveries required to extend its research and verify the hypothesis proposed in this thesis. The experimental parameters required to induce this response were partially characterized and provided an operational foundation that enabled the established assays to be modified. It remained to be determined if the putative ELF(s) which affect CS and BS are different molecules. Nonetheless, it was shown that UVR tolerance, in CS, was correlated with extracellular proteins that were < 40 kDa, but tolerance was not established in CS when the CFF was pretreated with trypsin. Therefore, the putative ELF(s) involved here is likely proteinaceous and could be genetically encoded**.** In the following section, the understanding gained here of the response that resembles EIT and the putative ELF(s) was employed to screen for EC proteins through a combination of microbial and electrophoretic techniques.

5.0 SCREENING FOR AND CHARACTERIZATION OF ELF CANDIDATES

5.1 Abstract

In this section it is reported that *B. bassiana* BS respond to elevated lethal temperatures (55 °C) potentially through a secreted protein, which is considered a putative ELF. This protein requires heat to activate it and promote elevated tolerance to heat in BS; a phenomenon that resembles EIT in *E. coli*. Several novel assays that were required to screen for and characterize the putative ELFs in *B. bassiana* are described here. Stepwise, a polyacrylamide-based *in situ* bioassay is reported that implicated several extracellular proteins, which were considered EC proteins. These ECs were further resolved as two separate species by two-dimensional clear native/sodium dodecyl sulfate polyacrylamide gel electrophoresis (2D-CN/SDS-PAGE). These ECs were also purified by elution following clear native polyacrylamide gel electrophoresis (CN-PAGE) and were termed EC1 and EC2 with an estimated relative molecular mass (M_r) of ~ 28 and 26 kDa, respectively. In addition, EC1 was found to be a glycoprotein and upon deglycosylation its M_r was reduced to a size very similar to that of EC2, ~ 26 kDa. Secondly, structure function relationships were demonstrated through a whole cell, pull-down assay, indicating that BS may interact specifically with the heat activated EC1 protein. Furthermore, bioassays with both purified ECs revealed that only glycosylated EC1 possessed the ability to cause elevated tolerance to heat in BS. The elucidation of EC1 as the most likely candidate to be involved in EIT to heat in BS warranted its continued study through the determination of its amino acid sequence, leading to the discovery of a gene encoding this candidate protein.

5.2 Introduction

Beauveria bassiana is a commercially important EPF that can be employed as an alternative to chemical pesticides for the control of insect pests in agriculture and forestry (Khachatourians *et al.*, 2002; Shah and Pell, 2003; Khachatourians, 2009; Hajek and Delalibera, 2010). However, its dependence on a narrow range of environmental conditions has limited its widespread adoption (Fargues, 2003). One such factor is heat stress. This is important when EPF are applied during daylight hours since prolonged high temperatures can cause inactivation of fungal spores leading to decreased insect mortality (Vestergaard *et al.*, 1995; Inglis *et al.*, 1997). Furthermore, insects, such as grasshoppers when infected by an EPF will commonly bask in sunlight to increase their internal body temperature and induce a so called behavioral fever, in an attempt to inactivate or suppress the pathogen (Roy *et al.*, 2006). During a behavioral fever it is possible for the insect to raise its body temperature to greater than 10 °C above the ambient temperature, depending on available sunlight (Carruthers *et al.*, 1992). Both the environment and the insect's ability to tolerate higher temperatures will determine how effective behavioral fever is at suppressing the fungal infection. Often the temperature reached during the fever is sub-lethal to the fungus, but is sufficient to reduce mycosis in the host. For example, 35 ºC is approaching the T_{max} of *B. bassiana*, but infected grasshoppers do not develop mycosis when incubated at this temperature but do at lower temperatures (Carruthers *et al.*, 1992). Therefore, the interaction between temperature and the ability of the fungus to cause insect infection is not simple and likely involves additional factors. While it is neither possible nor practical to totally mitigate detrimental field conditions, it is possible to acquire the knowledge of correlations between heat and induced stress responses. Ultimately, this fundamental understanding can be used for applied research and development, improving the ability of *B. bassiana* and other EPF

to be used as biopesticides, perhaps by improvement of their ability to mitigate the detrimental effects of their environment.

Xavier *et al.* (1999) characterized the cellular response to heat stress in several EPF. Although its role in the HSR or ESR is not yet established, extracellular stress sensing in *E. coli*, through ESCs may play a pivotal role in tolerance to environmental stressors, such as heat, UVR and pH (Hussain *et al.*, 1998; Rowbury and Goodson, 1999a; Rowbury and Goodson, 1999b; Lazim and Rowbury, 2000; Rowbury, 2003b). The EIT phenomenon was discovered 15 years ago in *E. coli* (Hussain *et al.*, 1998). It was thought to be controlled by secreted, diffusible proteins termed ESCs (Rowbury and Goodson, 1999a). The ESCs are activated external to the cell by various chemical and physical stresses (Rowbury and Goodson, 1999b), which enables them to promote an elevated tolerance to stresses in the target cell. This was characterized by an increase in survival as measured by the number of CFU produced by stress challenged cells compared to those not treated with activated ESC (Rowbury, 2001a). This system is reported to allow *E. coli* to detect a variety of stressors through the ESC(s), and thought to enable the cell to pre-emptively induce responses necessary to better survive the impending insult. Similar phenomena have also been found to occur in *C. jejuni* (Murphy *et al.*, 2003) and *S. cerevisiae* (Vovou *et al.*, 2004). Some physiological characterization has been performed with regards the effect of EIT on survival, with a vast majority of this being performed in *E. coli*. However, very little is known about the ESC and ELF molecules, including their amino acid composition and identification of a corresponding gene.

It was hypothesized that like in other systems (Rowbury and Goodson, 2001; Murphy *et al.*, 2003), the ELF phenomenon in *B. bassiana* is controlled by a secreted protein. However, selective assays were not present in the literature to screen for a protein with such an activity.

Assays for the study of stimulus-cell interactions, signal transduction or their downstream effects while commonplace and available, are generally exclusive to well-defined systems whose components have been thoroughly characterized. For example, specific knowledge pertaining to physiology and/or molecular biology of the receptor (Yu *et al.*, 1998; Suska *et al.*, 2005) and either the cellular response or the protein/stimulus are common perquisites (Raponi *et al.*, 1997). Although the recent elucidation of the genome of *B. bassiana* marks the availability of a powerful resource, specific information regarding ELF and its physiological effects remained unknown at this time. This necessitated the development of novel bioassays to screen and characterize extracellular proteins secreted by *B. bassiana* for ELF activity and other potential characteristics. This was achieved through a combination of microbiological and polyacrylamide electrophoresis based techniques that permitted the direct identification and characterization of an EC for the first time in any organism.

5.3 Materials and methods

5.3.1 Preparation of *B. bassiana* cultures and spore suspensions

Preparation of *B. bassiana* cultures and spore suspensions was performed as described in sections 3.3.1 and 4.3.1.

5.3.2 Preparation and storage of CFF

Cultures were grown for 68-72 h at 27 °C on YPG and vacuum filtered through a 10 cm diameter Whatman #1 filter per 200 mL of culture to remove a majority of the biomass. This fluid was then filtered with vacuum through a Millipore filter (5 cm diameter, 0.45 µm pore size) per 200 mL filtrate to remove the remaining biomass, which was primarily BS. Filters were changed for every 200 mL of filtrate to limit clogging. The resulting sterile CFF was used in the

following assays (used fresh or stored -30 °C and used within 4 d) and protein concentration protocols (used fresh). Filtrate preparation and all subsequent manipulations required to concentrate the protein were performed at 4 °C.

5.3.3 Salt mediated precipitation

Fine ground ultra-pure AS (MP Biomedical, Solon, Ohio) was added to the CFF to facilitate precipitation of proteins. The appropriate amount of AS required to achieve 40% AS saturation was added over 30 min with constant stirring (setting 3-4 on a Corning stirrer/hot-plate, model PC-320) and was allowed to equilibrate with stirring for an additional 30 min to achieve homogeneous distribution of the solubilized AS throughout. The filtrate was then centrifuged at 10,000 x*g* for 20 min at 4 °C and the pellets were solubilised in 0.2 M, phosphate buffer, pH 6.5 with 10% (v v^{-1}) glycerol and stored at -30 °C and used within 4 d. This process was repeated on the remaining supernatant to produce additional protein fractions from the CFF that was up to 95% saturated with AS. The protein fractions were recovered from CFF that had AS added to 40%, 60% or 80% saturation are referred to as fraction 40 (F40), 60 (F60), 80 (F80) or 95 (F95).

5.3.4 Acetone mediated precipitation

Acetone chilled to -30 °C was added with stirring to CFF placed in a glass beaker on ice over 10 min until a final concentration of 80% (v v^{-1}) acetone was achieved. This solution was then stirred at setting 4.5 with a Corning hotplate stirrer (model PC-320) for an additional 10 min and stored at -30 °C overnight. This liquid was then decanted into several tubes and centrifuged at 10,000 x*g* for 20 min at 4 °C to recover the precipitated protein contained in the CFF. The supernatant was decanted and the remainder was removed by evaporation at 22 °C and solubil-

ized in phosphate buffer with 10% (v v^{-1}) glycerol and stored at -30 °C.

5.3.5 Dialysis

Dialysis was performed with 2 kDa cut-off membrane tubing (Spectra/Por, Laguna Hills, CA). Tubing was filled with 2-5 mL of F80 and clamped to allow approximately two-fold expansion of the volume of the tube to ensure leaks did not occur. Fraction eighty was dialysed against 40x volumes of PBS over 24 h at 4 °C with stirring at approximately 90 RPM and the buffer was changed approximately every 8 h. Samples of the dialysate were taken before every change and assayed for protein content, which was not detectable (< 5 µg mL^{-1}) when concentrated with AS by 20-fold.

5.3.6 Assay for EIT to UVR in CS

Preheating of AS fractions/other treatments and UV-C tolerance assays with CS were performed as described in sections 4.3.3 and 4.3.4, respectively. Conidiospores were incubated in YPG supplemented with the indicated treatment, prior to UV-C challenge.

5.3.7 Assay for EIT to heat in BS

The assay for EIT to heat in BS was performed as described in section 4.3.5 except that assays that included purified protein, eluted following CN-PAGE were performed in smaller 5 mL glass vials and contained a final volume of 1 mL with average protein concentrations of 12 to 19 µg mL^{-1}. Assays containing treatments that were not gel purified were performed in vials containing 3-5 mL of PBS in 15 mL glass vials. Gel purified protein, AS fractions or other treatments as indicated were added to PBS that was preheated to 55 °C and incubated for 3 min to allow the temperature to become fully equilibrated to 55 °C, before the addition of BS. Prior to this heating, when stated, trypsin was added to a final concentration of 24 µg mL^{-1} and incu-

bated at 27 °C for 30 min to determine if protein hydrolysis affected EIT to heat in BS.

To determine the effect of treating BS with F80, post-heat challenge, BS were heated in PBS and samples were either plated immediately or 0.1 mL of challenged BS suspension was added to 0.4 mL YPG supplemented with 0.5 mL PBS with or without 50 µg of F80 protein mL^{-1} that was preheated at 55 °C for 3 min. The BS were incubated at 27 °C for 4 h with shaking at 150 RPM before being plated and enumerated. Survival was calculated relative to unchallenged BS.

5.3.8 Sodium dodecyl sulphate polyacrylamide gel electrophoresis

The SDS-PAGE method was performed (as described in section 4.3.6.) with the samples that are indicated in the appropriate figures being combined 1:1 with sample buffer.

5.3.9 Clear native polyacrylamide gel electrophoresis

The CN-PAGE method was utilized to separate peptides in a non-denatured state to promote the retention of their biological activity as per Qazi and Khachatourians (2007). The protocol and buffers used to perform CN-PAGE were similar to those used for SDS-PAGE, except that 10-fold higher concentrations of Triton X-100 were used instead of SDS in all buffers and samples were incubated at 22 °C for 5 min after being combined 1:1 with sample buffer, which did not contain β-mercaptoethanol. Aliquots of 30 µL containing between 5 – 15 µg of protein were loaded into each well and samples were subjected to electrophoresis at 15 mAmp for 3.5 h at 4 °C until the dye front was 2-5 mm from the gel edge. The amount of protein loaded was dependent on the gel's downstream application and is stated in the figure's legend. When required, gels were stained with blue silver and visualized as standard or prepared for or 2D-CN/SDS-PAGE (see section 5.3.10) or *in situ* EIT assay (see section 5.3.11). In preparation for

in situ EIT assay, gels were pre-electrophoresed for 30 min before samples were loaded. This was performed to remove molecules which may interfere with the bioassay, such as ammonium persulfate and N,N,N',N'-tetramethylethylenediamine.

5.3.10 Two-dimensional clear native/sodium dodecyl sulfate polyacrylamide gel electrophoresis

The 2D-CN/SDS-PAGE method was employed, as described by Wittig *et al*. (2006), to determine the number of protein species present within the area of the CN-PAGE gel that was determined to contain ECs by the *in situ* EIT to heat assay. Through 2D-CN/SDS-PAGE proteins are initially separated based on their mobility under non-denaturing conditions using CN-PAGE as the first dimension and followed by SDS-PAGE in the second dimension, performed as below. Following CN-PAGE a vertical strip of the polyacrylamide gel which contained the separated F80 proteins was removed with a sterile scalpel, then incubated with 15 mL of denaturing solution which contained 10% (w v^{-1}) SDS and 1% (w v^{-1}) β-mercaptoethanol at 55 °C for 30 min, followed by a similar incubation with 10% (w v^{-1}) SDS, to facilitate dilution of β-mercapto-ethanol and help maintain the proteins in a denatured state. The strip was then placed over a standard pre-cast 15% (w v^{-1}) polyacrylamide gel containing SDS that had a 1 cm layer of stacking gel. The gel strip was then covered with the stacking gel solution. Following polymer-ization, the proteins contained in the polyacrylamide strip were subjected to electrophoresis and visualization as standard, except the sample was initially electrophoresed at 60 V until the sample completely entered the resolving gel, followed by an increase in current to 120 V.

5.3.11 *In situ* EIT to heat assay

The *in situ* EIT to heat assay was adapted from a method used in a zymography based study (Qazi and Khachatourians, 2007). A 50 µL aliquot containing 12.5 µg of F80 protein was separated through a 1.5 mm thick, 10% (w v^{-1}) polyacrylamide gel, under non-denaturing conditions as described in section 5.3.9. Following electrophoresis a strip of gel containing the lane with F80 was removed with a sterile razor blade and placed in 30 mL PBS, pH 6.5 for 30 min at 27 °C, then again at 55 °C to activate the ELF proteins(s) that were potentially in the gel. Incubating the strip in PBS adjusted the pH within the polyacrylamide to ~ 6.5, a pH that is conducive to both the activity of putative ELF and germination. Furthermore, soaking allowed the impregnated proteins time to diffuse through the gel to some degree. It has been shown that a protein of ~ 13 kDa can diffuse ~ 0.4 mm through a 20% (w v^{-1}) polyacrylamide gel in 1 h (Lewus and Carta, 1999). Therefore, it was predicted that a protein of ~ 30 kDa impregnated in a 10% (w v^{-1}) polyacrylamide gel could diffuse > 0.4 mm in 1 h. This is because the relative diffusion rates of the ~ 30 kDa ECs would be increased by a reduction in polyacrylamide concentration more than it would be decreased by an increase in protein mass, compared to the parameters studied by Lewus and Carta (1999). As a result, BS overlaid nearest to the ECs would encounter them most quickly and survival should be highest in BS that are within closest proximity to ELF(s).

Gel strips were overlaid with 10 mL of molten YPG containing 0.9% (w v^{-1}) agar, which was inoculated with heat challenged BS to 10^6 mL^{-1} and mixed by vortex immediately before being poured over the polyacrylamide gel impregnated with F80. Following a 36 h incubation at 27 °C in sealed Petri dishes, overlaid gels were viewed at an objective of 35x with a dissecting microscope and CFUs were enumerated per 0.7 cm along the length of the overlaid polyacryl-

amide gel strip, which corresponded to 0.1 retention factor (R_f). The survival of BS was calculated as the percent CFU within each 0.1 R_f section relative to the total number of CFU along the entire length of the gel strip.

5.3.12 Protein elution following CN-PAGE

The ECs identified in F80 were purified by first resolving up to 1.5 mg of F80 protein by CN-PAGE through a 12% (w v^{-1}) gel that contained one lane which was the entire width of the slab gel and eluted as described by Castellanos-Serra *et al*. (1996). Briefly, a non-denaturing reverse stain using zinc and imidazole was used to visualize the protein bands. After staining the protein bands corresponding to the two EC bands or BSA (control) were removed separately with sterile scalpels and the mass of the gels was recorded. The gels were then rinsed sequentially once each with 50 mM ethylenediaminetetraacetic acid, 10 mM ethylenediaminetetraacetic acid and thrice with phosphate buffer for 5 min with a 2:1, rinse solution:gel volume ratio, to remove the remaining zinc and ethylenediaminetetraacetic acid. The rinsed gels were then suspended in fresh phosphate buffer and extruded through plastic pipette tips that were cut to provide progressively smaller gel particles. It generally took 5-10 min to process each protein sample into a suspension containing gel particles of ~ 0.2 mm in diameter. This processing increased the surface area of the gel to improve the recovery of the protein. The extruded gel was then agitated overnight at 22 °C using an orbital shaker set at 240 RPM. This protocol was tested using purified BSA and was able to recovery approximately 90% of the BSA applied to the preparative CN-PAGE.

5.3.13 Deglycosylation experiments

Gel purified ECs were tested for the presence of glycosylation using a deglycosylation kit (New England Biomedical) using the manufacturer's directions, but scaled-down to accommodate the amount of EC protein recovered by elution. The 50 µL deglycosylation reactions contained 3.9 and 0.3 µg of gel purified EC1 and EC2, respectively. This was followed by separation of the proteins with SDS-PAGE and deglycosylation was determined by SDS-PAGE mobility assays and staining with blue silver dye. Samples containing EC2 were stained with the Bio-Rad silver stain as per the manufacturer's direction (Biorad, Hercules, USA) because the amount of EC2 present was too low to be detected with blue silver.

5.3.14 Pull-down assay to detect interaction between ECs and BS

To determine if extracellular proteins within CFF interacted with BS a modified version of the conventional pull-down assay as described by Sambrook and Russel (2001) was developed. The rationale was that ESCs produced by *E. coli* have been speculated to interact with cells (Rowbury, 2001a; Rowbury, 2001b). Therefore, such an event may occur through an interaction between ELF and BS, through their cell surface. In a plastic centrifuge tube, 300 µL of protein (300 µg protein mL^{-1} of PBS) precipitated with acetone from CFF or 1 mg mL^{-1} solution of BSA was preheated at either 55 °C or 25 °C for 30 min before being combined with 100 µL of unstressed BS to achieve a final concentration of 2×10^6, 2×10^7 or 2×10^8 BS mL^{-1}. Following a 20 min incubation at 27 °C with periodic mixing, the tubes were differentially centrifuged at 10,000 x*g* for 10 min to remove BS and proteins interacting with them from the suspension. A 50 µL aliquot was taken from the supernatant of each treatment and prepared as standard for SDS-PAGE to determine if the protein profile was altered.

This assay was scaled-down to 65 µL when gel purified protein was used. This assay was performed the same as above accept 50 µL of EC1 or BSA was preheated and 15 µL of BS suspension was added to this. The final concentrations in this scaled down assay were 10^7 BS mL^{-1} and 10 or 100 µg mL^{-1} of EC1 or BSA, respectively. Also, only 20 µL aliquots of the supernatant were taken so as to not disturb the pellet and subjected to SDS-PAGE analysis.

5.3.15 Protein concentration determination

This was performed as described in section 4.3.7.

5.3.16 Statistical analysis

Statistical analysis was performed as per section 4.3.8. Tukey's, Dunnett's or Student's tests were applied to compare all means against each other or to compare the means against a control group, or compare two means, respectively. All experiments were repeated at least three times, unless stated otherwise and the sample size used to calculate each mean is indicated within the text or figure legends.

5.4 Results and discussion

5.4.1 Recovery of ELF activity from CFF

In the previous section of this thesis it was established that heat and UVR tolerance in BS and CS, respectively, could be increased by a treatment with preheated CFF and may involve an ELF(s) and EIT. With regards to elevated tolerance to UVR in CS, this effect was correlated with the presence of extracellular proteins in the CFF that were < 40 kDa. Furthermore, treatment of the CFF with trypsin removed its protective effect, which implied the involvement of extracellular protein(s) and is consistent with findings in *E. coli* (Rowbury, 2003b). These extracellular proteins present in CFF prepared from *B. bassiana* cultures were fractionated by

salting out with AS and concentrated by resuspending in a smaller volume to improve their detection by the methods described here. The protein fractions that were recovered from CFF that had AS added to 40%, 60% or 80% saturation are referred to as F40, F60, F80 or F95. The total amount of protein in CFF that was recovered in F40, F60 or F80 was estimated to represent 0.2% ± 0.1% SEM, 4.0% ± 2.7% SEM and 2.0% ± 1.4% SEM of protein found in CFF, respectively, calculated from three representative trials. The CFF was not generally saturated to 95% AS since this fraction was not found to consistently increase survival of heat challenged BS (see below), but recovered 0.2 and 2.5% of CFF proteins in two trials.

Two prominent protein bands of < 40 kDa were visible in all fractions, while bands that correspond to proteins of Mr > 40 kDa were less prominent (Figure 5.1). A third protein of < 40 kDa was also visible in F60 and F80, but less so in F95 and not detectable in F40. The presence of this protein may be a function of its solubility at 60% and 80% AS saturation and likely was depleted from the CFF following fractionation with these concentrations of AS, thus was less visible in F95. Detection of the third species may also related to the total protein loaded, which was less in F40 an F95 than F60 and F80 and would also influence the detection of this protein band, since the total protein loaded contains a population individual proteins. Furthermore, the F95 supernatant, although diluted by roughly 36% due to the increase in volume as a result of AS addition, did not yield detectable bands using blue silver stain, which has a detection limit of ~ 1 ng per protein (Candiano *et al.*, 2004).

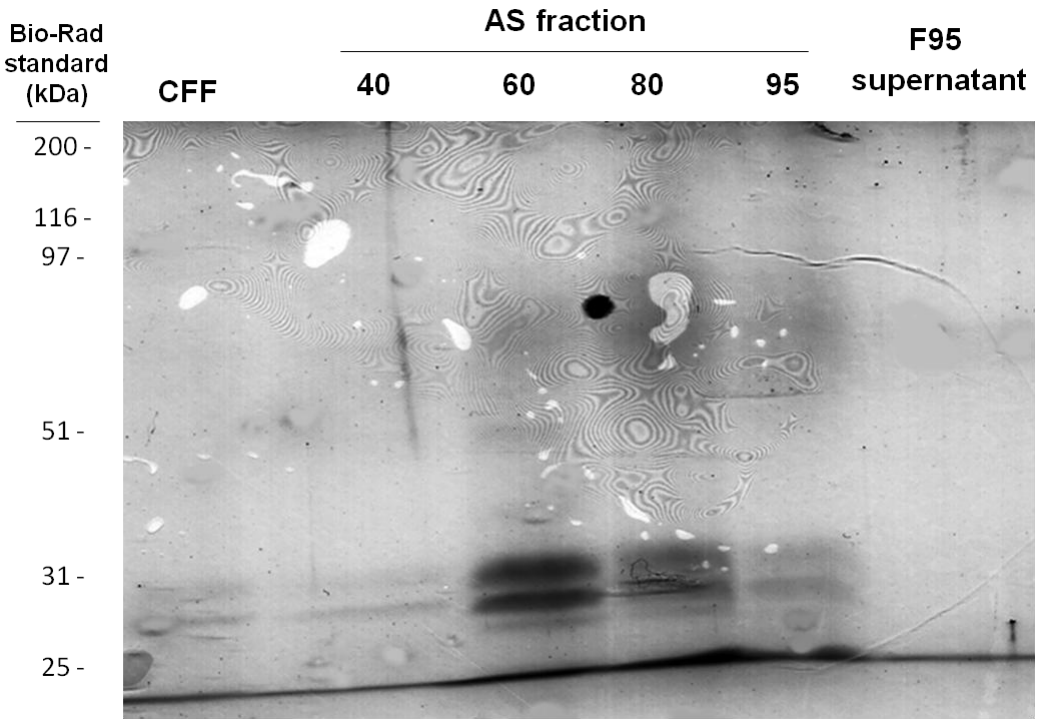

Figure 5.1 Protein banding patterns of CFF or AS fractions separated by SDS-PAGE through a 12% (w v^{-1}) polyacrylamide gel. All lanes were loaded with the indicated sample which contained an estimated 0.1, 9.5, 50, 17, 18 and 0.02 µg of protein for CFF, F40, F60, F80, F95 and F95 supernatant, respectively. Bio-Rad broad range standards (kDa) are indicated on the left.

These fractions were assayed for their ability to increase the tolerance of CS to UV-C challenge (Figure 5.2). Treatment of CS with F40 or BSA did not significantly alter survival, compared to those treated with PBS. Conversely, when treated with F60 or F80 the mean survival rates of CS was increased by approximately 2- and 4-fold, respectively, compared to BS treated with PBS alone, but were not significantly different than BS treated with PBS. Again, increased survival appeared to be correlated with the presence of proteins < 40 kDa, consistent with the findings shown in the previous section of this thesis. However, the survival values obtained from this experiment were > 20-fold lower compared to those discussed in section 4.4.1 where 0.15 to 0.3% of CS treated with CFF survived a similar challenge with UV-C. Although it is possible a biological effect occurred in CS treated with F80, the effect was small and quite variable as the standard deviation produced by this treatment was larger than the mean. Therefore, the biological effect in CS as measured by CFU may be too variable to be conducive for further study using this test system. As reviewed by Nikolaev (2000), other whole cell bioassays involving distant interactions have also shown substantial experimental variation and rarely did the reproducibility of the results reach 100%. Therefore, a different functional assay system was required to test for a response that resembles EIT and explore it.

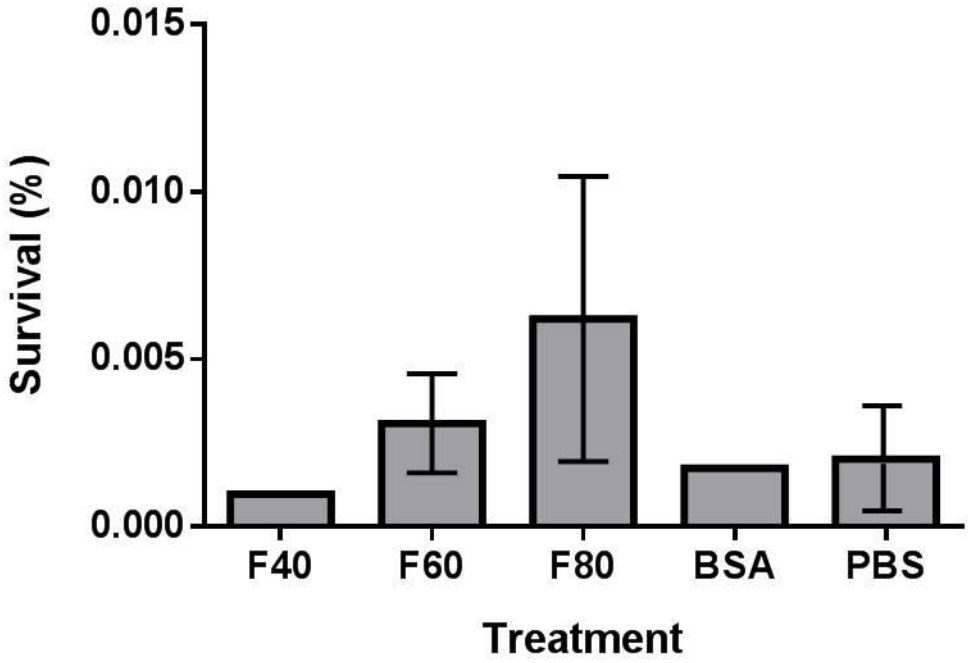

Figure 5.2 The effect of treating CS with AS fractions prepared from CFF on their survival when challenged with 120 J m^{-2} UV-C. The AS fractions were prepared from CFF obtained from cultures grown in VM. The AS fractions, PBS and BSA were all preheated and then incubated with CS in YPG as specified. The average protein concentration (µg mL^{-1}) for F40, F60, F80, BSA and PBS was 43, 47, 53, 75 and none detectable, respectively. The bars show the mean survival of CS, calculated from three trials except for F40 and BSA treated samples, which were from two. Error bars show SEM (for N > 2) and Dunnett's multiple comparison test was performed to determine if survival of BS treated with F60 or F80 were larger than those treated with PBS; however, none were found to be significantly different (α=0.05).

As established in the previous section, challenging BS in CFF that was preheated to 55 °C increased their ability to survive at 55 °C for 45 min, compared to those treated in preheated growth media. Ammonium sulphate fractions were used to determine if they could increase heat tolerance in BS and could be correlated with the proteins recovered in these fractions (Figure 5.3A). Blastospores treated with F80 showed a significant, 7.9-fold increase in survival compared to PBS (untreated control). Blastospores challenged in the presence of F40 or F60 also had increased survivorships compared to PBS treated BS and were 2.5 and 5.4-fold greater, respectively, but were not significant. The ability of F95 to increase heat tolerance in BS was tested, but it was not found to consistently effect survival of heat challenged BS and produced survivorships of 0.0006% and 0.074% in two trials. Variation in survival produced by the F95 treatment may be related to the variation in the protein recovered in this fraction; since 0.2% and 2.5% of total protein was recovered in two trials which may also effect the protein composition of F95 and could influence the consistency of the survival rates. The ability of F40, F60 and F80 to increase the heat tolerance of BS suggested that putative ELF(s) may have been recovered in these fractions. Furthermore, F60 and F80 provided BS with the largest increase in survival and also had the highest proportion of proteins with a M_r of < 40 kDa, particularly three between 25 to 31 kDa (Figure 5.1). This observation was similar to that of the apparent EIT-like response to UVR in CS (see section 4.4.1) where increased tolerance was correlated with the presence of proteins < 40 kDa. It was possible that putative ELF(s) recovered in F80 were present in greater amounts, relative to the total protein concentration, or possessed higher activity compared to the other fractions. Therefore, they may be involved in increasing heat tolerance in BS.

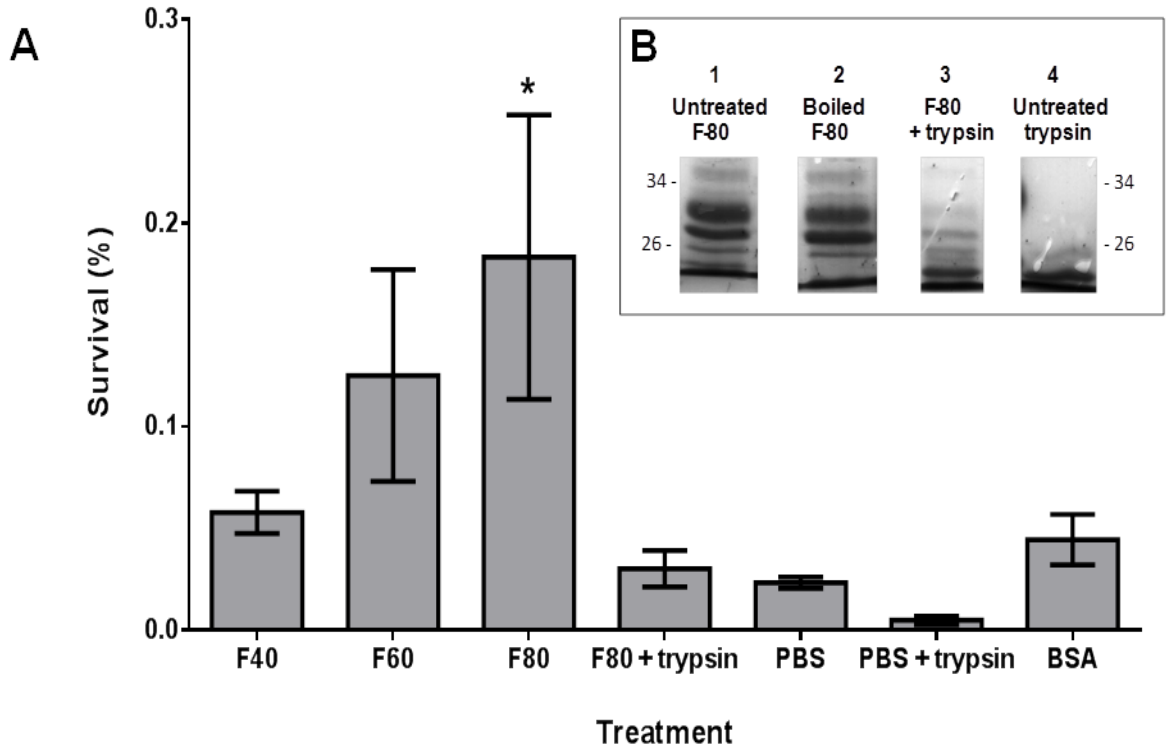

Figure 5.3 Effect of AS fractions and trypsin pretreatment on survival of heat challenged BS. Panel A shows the results of the assay to assess EIT to heat in BS. All AS fractions were prepared from CFF obtained from cultures grown in YPG for 3 d. Heat challenge was performed in PBS supplemented with the indicated treatment and had the following average final protein concentrations (μg mL^{-1}): F40 and F60, 47; F80, 23; F80 + trypsin, 52; PBS, not detectable; PBS + trypsin, 24; and BSA, 28. Bars represent mean survival, calculated from three trials sampled in quadruplicate. Error bars show SEM and the bars labeled with an asterix symbol were determined to be significantly different compared to PBS (no treatment control) by Dunnett's multiple comparisons test (α=0.05). Panel B shows the protein bands with M_r of < 40 kDa in F80 with and without trypsin pretreatment, separated by SDS-PAGE through a 12% (w v^{-1}) polyacrylamide gel. The gel sections shown were from lanes loaded with or without 5 μg of F80 protein that received the following treatments prior to SDS-PAGE sample preparation: 500 μg mL^{-1} of F80 protein was 1, untreated; 2, supernatant of F80 that was boiled for 5 min then centrifuged for 5 min at 10,000 x*g*; 3, treated with 24 μg mL^{-1} trypsin for 30 min at 27 °C; and 4 is the same as 3 without F80. The masses of the Fisher EZ-run prestained protein ladder (kDa) are indicated on the left and right.

Blastospores were challenged in the presence of BSA to determine if the general protective effect it may provide was greater than that provided by PBS, since BSA has been found to provide protein stabilizing effects on other proteins at elevated temperatures (Spiro *et al.*, 1983). Although BSA treated BS increased survivorship following heat challenge by 1.9-fold, compared to those treated with PBS, this increase was not significant (Figure 5.3A). It can be concluded from this that the protective effect provided by F80 was greater than that offered by solubilized BSA and provided support to pursue the EIT-like phenomenon.

As in the phenomenon that resembled EIT to UVR in CS, it was important to determine if fragments of the recovered extracellular proteins could affect heat tolerance in BS (Figure 5.3A). This was performed by pretreating F80 with trypsin. This eliminated the ability of F80 to significantly increase heat tolerance in BS and resulted in a 1.3-fold increase in survivorship compared to PBS treated BS. Similarly, the pretreatment of PBS with trypsin did not significantly affect the ability of BS to tolerate heat, compared to those challenged in untreated PBS. This implied that the tryptic activity which was present at the time the BS were introduced was insufficient to significantly reduce their ability to tolerate heat. As result, the reduction in survival of BS treated with F80 + trypsin is likely due to proteolytic degradation of putative ELF, which was recovered in F80. Proteolysis of proteins in F80 was confirmed using SDS-PAGE (Figure 5.3B) which demonstrated a reduction in the most abundant extracellular proteins between 20-35 kDa, as judged by stainability. However, boiled F80 did not produce a comparable reduction in these proteins following centrifugation. These data provided further evidence to support the presence of a phenomenon that resembles EIT to heat in BS, and similar to elevated UVR tolerance in CS it was correlated with proteinaceous molecules of < 40 kDa. Similarly, induced heat tolerance has also been attributed to extracellular proteins in *E. coli*

(Rowbury and Goodson, 2005) and *C. jejuni* (Murphy *et al.*, 2003) as their proteolysis decreased their ability to promote tolerance.

A single result suggested that ELF activity was retained in F80 following dialysis with a M_r cut-off of 2 kDa, without detectable loss decrease in survival of treated then challenged BS (or total protein) since 0.234% and 0.231% survived when treated with F80 that was or was not dialysed, respectively. In addition, an experiment was conducted and its result suggested that protein precipitation with acetone may also be able to increase heat tolerance in BS, but not to the same degree as F80, since only 0.079% of BS treated with acetone precipitated protein (75 µg mL^{-1}) survived the heat challenge, compared to 0.059% in BS treated with the same amount of BSA. However, more data is required to confirm if particular acetone precipitated proteins can increase heat tolerance in BS.

These data provided further evidence to support the hypothesis that ELF(s) is a proteinaceous molecule that is secreted by *B. bassiana* and warranted further efforts to isolate the causative molecule. Furthermore, the EIT-like response to heat in BS appeared to be less variable than the response to UVR in CS. As a result, heat tolerance in BS was chosen as the appropriate system to screen for ECs.

5.4.2 Screening extracellular proteins for ECs and their characterization

To screen the above proteins for ECs it was important to determine whether elevated tolerance to heat in BS was induced when preheated F80 was supplied to BS following heat challenge. To determine this, BS were heat challenged in PBS and transferred to YPG that was supplemented with either 55 °C preheated PBS or F80 and were incubated for 4 h at 27 °C before plating. The survivorship of BS were 3.5-fold greater in those supplemented with F80

compared to PBS (Figure 5.4). In addition, both treatments yielded increased survival values than if BS were plated immediately. This apparent difference in survival was not due to an increase in fungal propagules, caused by growth in the YPG containing treatments during the post-heat challenge incubation, which would positively bias the number of CFUs observed. This is because such an increase would first require the development of hyphae from the challenged BS prior to additional BS being created. However, microscopic observation of the suspensions showed a lack of hyphae present immediately after challenge or following a 4 h incubation. Furthermore, the conditions were not conducive for microcycle conidiation (Thomas *et al.*, 1987). Therefore, these results demonstrated that the BS produced by *B. bassiana* could also respond to F80 following heat challenge in the prolonged absence of the insult. It is undetermined whether other organisms, such as *E. coli* can respond to ESC following heat challenge, although *E. coli* is thought to respond to preheated CFF prior to the insult (Rowbury and Goodson, 1999a). Similar to *B. bassiana* are the findings in *S. cerevisiae* (Vovou *et al.*, 2004) which had greater heat tolerance when challenged in the presence of preheated CFF.

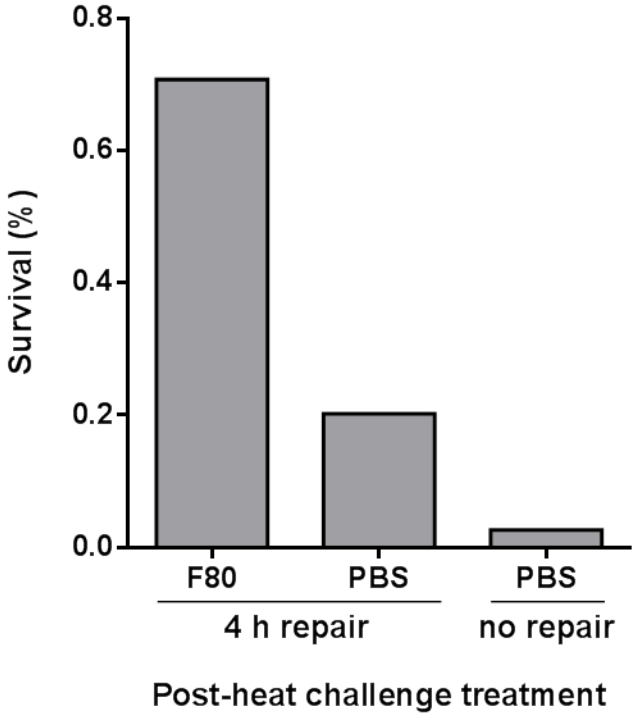

Figure 5.4 The effect of post-heat challenge treatment of BS on their survival following heat challenge. A 0.1 mL aliquot of undiluted, heat challenged BS was combined with 0.4 mL YPG and 0.5 mL of PBS, with or without 50 µg of F80 protein, and incubated at 27 °C for 4 h before being plated. Blastospores were also plated immediately following challenge (no repair). Bars represent means of a single experiment sampled in quadruplicate.

With the knowledge that heat challenged BS were responsive to F80 it was potentially possible to use them to detect ECs through an *in situ* assay to screen extracellular proteins produced by *B. bassiana* for the ability to promote elevated tolerance to heat. This assay was performed by first separating F80 proteins by CN-PAGE and incubating a strip of gel containing F80 at 55 °C to activate the putative ELF(s) contained within it. This strip was then overlaid with soft YPGA seeded with heat challenged BS. Following incubation, CFUs resulting from the surviving BS were enumerated per each 0.7 cm section of gel along the axis the proteins migrated. These enumerations were used to calculate the relative distribution of CFUs across the strip (refer to section 5.3.11 for more detail). Proteins within the polyacrylamide following electrophoresis were expected to not be denatured, remain diffusible and retain their functionality (Qazi and Khachatourians, 2007) (Figure 5.5A). It has been shown that a protein of ~ 12 kDa can diffuse ~ 0.4 mm through a 20% (w v^{-1}) polyacrylamide gel in 1 h (Lewus and Carta, 1999). Therefore, it was estimated that a protein of ~ 30 kDa impregnated in a 10% (w v^{-1}) polyacrylamide gel could diffuse > 0.4 mm in 1 h. As a result, it was predicted that heat challenged BS would come into contact with putative ELF and other proteins which diffused through the polyacrylamide matrix and into the YPGA overlay containing the BS during the incubation period, permitting an increase in CFUs in the areas closest to the where the putative ELF(s) migrated to during electrophoresis.

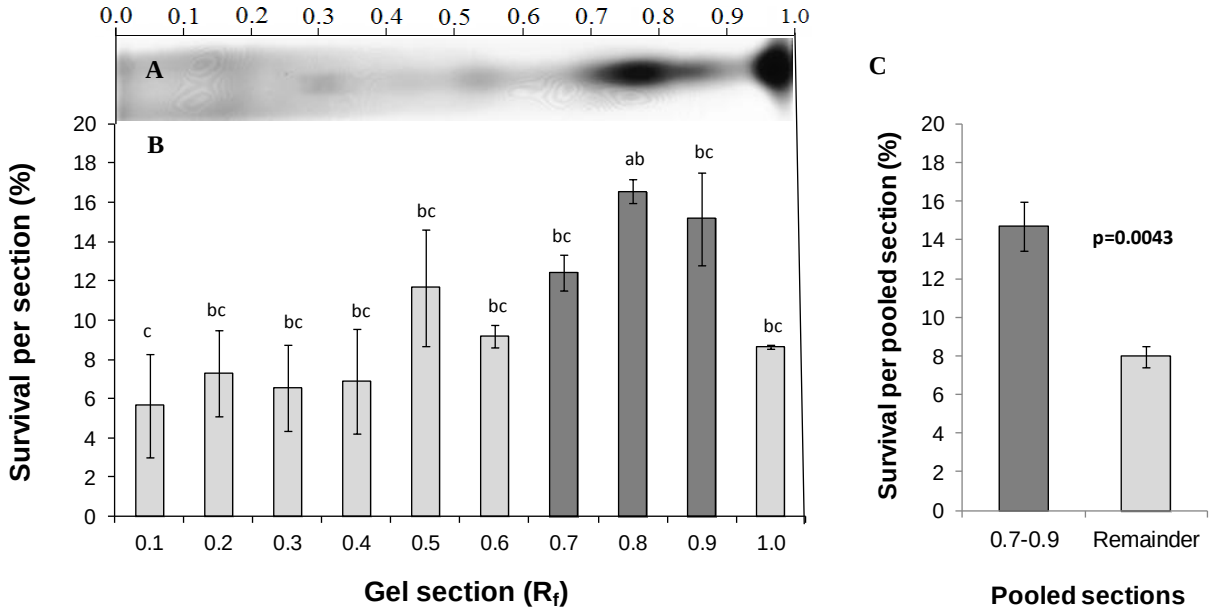

Figure 5.5 *In situ* EIT to heat assay. Panel A shows the protein banding pattern produced by 12.5 µg of F80 protein separated by CN-PAGE through a 10% polyacrylamide gel. Panel B shows the results of the *in situ* EIT to heat assay as a histogram. The bars represent the mean survival per 0.1 R_f section that formed from heat challenged BS which were overlaid on an unstained gel similar to panel A. Panels A and B are aligned so that the x-axis of B directly corresponds with locations on the polyacrylamide gel and 0.1 R_f represents a 0.7 cm section of gel. The bars in panel C show the pooled average survival from sections 0.7-0.9 (dark grey; three sections) and the remainder (light grey; seven sections). Sections 0.7-0.9 were chosen to be pooled because 0.7 and 0.9 were adjacent to 0.8 and contained the three highest survivals and the highest amount of stainable protein (excluding section 1.0, which had lower survival). The results were obtained from three trials. Error bars show SEM and bars containing a same letter in their label were determined to not be significantly different by Tukey's multiple comparison test (α=0.05), while the results of an unpaired t-test showed that the mean of sections 0.7-0.9 shown in panel C were significantly greater (p=0.0043) than the remaining sections.

Proteins in close proximity with the sections that had the most CFUs were correlated with an increase in survival and were considered ECs (Figure 5.5B). The ability of the ECs to increase survival of the closest BS suggested that functionality of the suspected ELF-BS interaction was likely maintained and may have led to EIT. The highest percentage of the total survivors were found at relative mobility (measured as R_f) 0.71 – 0.8, with a survivorship of 16.6%. The two adjacent segments, sections 0.61-0.7 and 0.81-0.9, had the second and third highest survival values of 12.4% and 15.2%, respectively. The remaining segments of the gel had between 5.8% and 11.7% of the total survivors per section.

It appeared that the EC molecules could diffuse and entered the nearest sections of the overlaid medium, as shown by an increase in survival of the BS in these sections. Therefore, to better represent the results of this experiment the survival values from R_f 0.71-0.8 were pooled with its two flanking regions (Figure 5.5C). This resulted in a mean survival value of 14.7% ± 2.9% SEM for the three sections covering R_f 0.61-0.9 which was significantly higher ($p=0.0043$) than that of the mean survival for the remaining sections (8.0% ± 3.7% SEM). The sections of the overlay identified to have the highest survival rates following the *in situ* assay were used to indicate which proteins may have ELF activity and were designated ECs. Two protein species which represented the majority of the F80 protein visualized following CN-PAGE were found between 0.71-0.85 R_f and were correlated with the highest survivorship. As a result, these two protein species were considered EC proteins and were studied further.

To resolve the ECs identified above, 2D-CN/SDS-PAGE was used to more accurately estimate their M_r and determine if they contained individual polypeptides in a multi-subunit protein complex (Wittig *et al.*, 2006). This method allowed an entire lane separated by CN-PAGE to be resolved under SDS-PAGE conditions and analyzed with greater handling ease and

better in gel visualization of proteins as opposed to eluting each protein of interest separately. To achieve this, proteins were separated by CN-PAGE (Figure 5.6A) in the first dimension then denatured and separated by SDS-PAGE as the second dimension (Figure 5.6B). Of particular interest were the species found in the second dimension that were separated from the EC proteins identified using the *in situ* ELF assay. These were visualized as two stainable distinct protein spots termed EC1 and EC2 (Figure 5.6B). Due to the greater stain binding, it appeared that there was relatively more EC1 than EC2. Both ECs had R_f values of approximately 0.36 correlating them with two proteins which migrated as 26 kDa and 28 kDa molecules under conventional SDS-PAGE (Figure 5.6C).

To purify EC1 and EC2 they were separated by CN-PAGE, visualized by reverse zinc staining then eluted (Figure 5.7). The reverse staining required ~ 30 min to complete and is superior to using a reference gel slice stained with Coomassie or other dyes with respect to speed and ease of processing (Castellanos-Serra *et al.*, 1996). This is especially important where several proteins with similar M_r are present in the sample, making direct visualization imperative for exact extraction of a pure sample. The non-denaturing condition also allowed functional assays to be performed with the eluted protein. This protocol was optimized using BSA and was able to recover approximately 90% of the BSA applied to the preparative CN-PAGE (Figure 5.8). With regards to elution of ECs, one experiment with 1500 µg of F80 protein yielded 107 µg and 44 µg of pure EC1 and EC2, respectively.

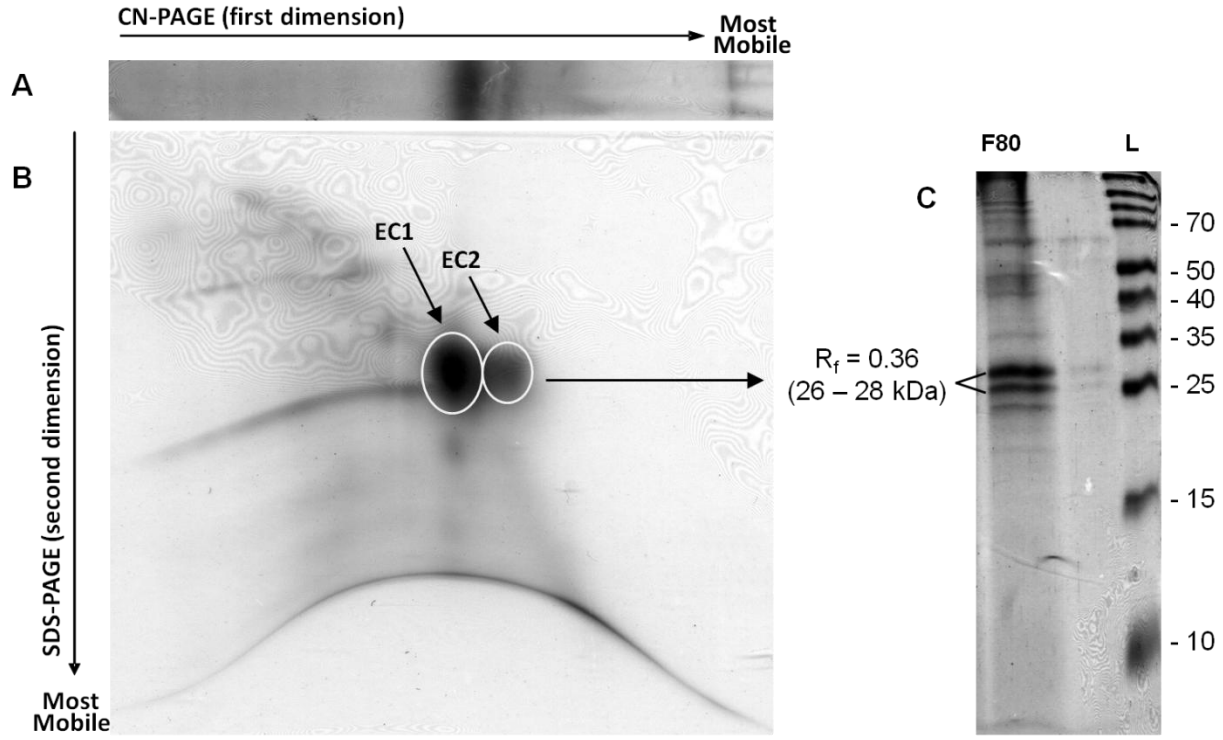

Figure 5.6 Resolution of EC1 and EC2 by 2D-CN/SDS-PAGE. Panel A shows a strip of polyacrylamide containing 10 µg of F80 protein separated by CN-PAGE, while Panel B shows the resolution of proteins in panel A separated through a second dimension using SDS-PAGE with a 15% (w v^{-1}) polyacrylamide gel. Panel C shows the resolution of 2.5 µg of F80 proteins by SDS-PAGE through a 15% (w v^{-1}) polyacrylamide gel. Lane L, contained 5 µL of Spectra™ multicolour broad range protein ladder and their masses (kDa) are indicated on the right.

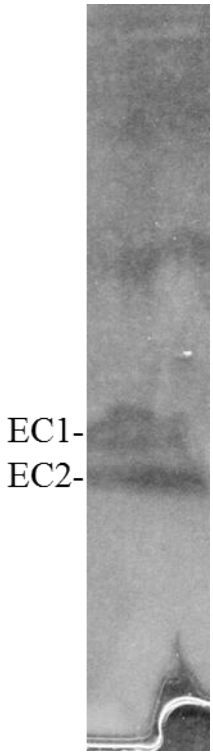

Figure 5.7 Separation of EC1 and EC2 by 12% (w v^{-1}) CN-PAGE and visualization with reverse zinc staining. The above photograph shows a lane containing 50 µg of protein.

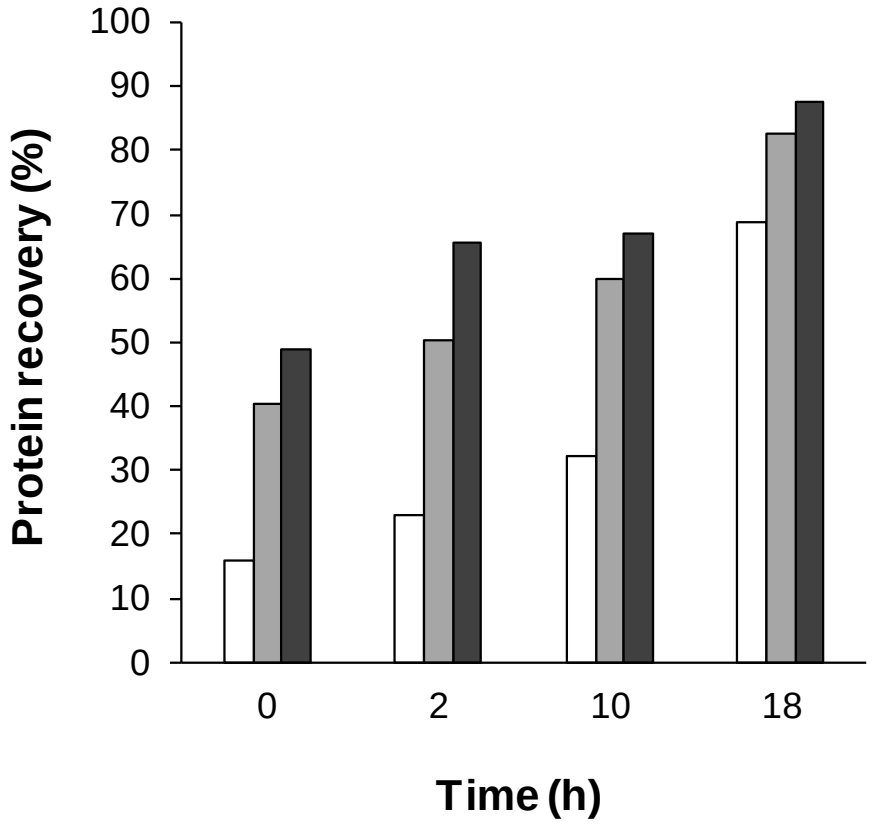

Figure 5.8 Optimization of BSA recovery by elution following 12% (w v^{-1}) CN-PAGE. Following the separation of 24 µg of BSA by CN-PAGE and reverse staining, three gel sections containing a single lane with BSA were removed and processed for elution. The white, light grey and dark grey bars show the recovery of BSA from gels that were processed to have gel particles with diameters of approximately 1 mm, 0.5 mm and 0.2 mm, respectively. Following processing, the protein content recovered was determined after 0 h (immediately after processing), 2, 10 and 18 h and were used to estimate protein recovery. These data were from a single experiment.

Gel purified EC1 and EC2 were estimated to have a M_r of 28 and 26 kDa, respectively, by SDS-PAGE analysis (Figure 5.9A). Both EC1 and EC2 corresponded with two extracellular proteins found in CFF that was prepared from a *B. bassiana* culture. Functional analysis of the purified ECs was required to serve as a conclusive determination of which molecule could induce increase heat tolerance in BS and therefore likely contained ELF activity (Figure 5.9B). The results of this experiment demonstrated that EC1 was able to increase the survival of heat challenged BS over those treated with BSA by 5-fold and was determined to be a significant increase ($p=0.0337$). Although EC2 increased BS survival over BSA by 2.1-fold, this treatment was not found to have a significant effect. In addition, a 1:1 combination of EC1 and EC2 was able to increase BS survival to a level comparable to EC1 alone and was found to be significant when compared to BSA treated BS ($p=0.0228$). Bovine serum albumin was selected as the control because it was found to not increase BS survival over PBS and was a protein whose purification could also be monitored and assessed for purity. Furthermore, BSA is not known to possess an activity that specifically influences BS and their tolerance to heat.

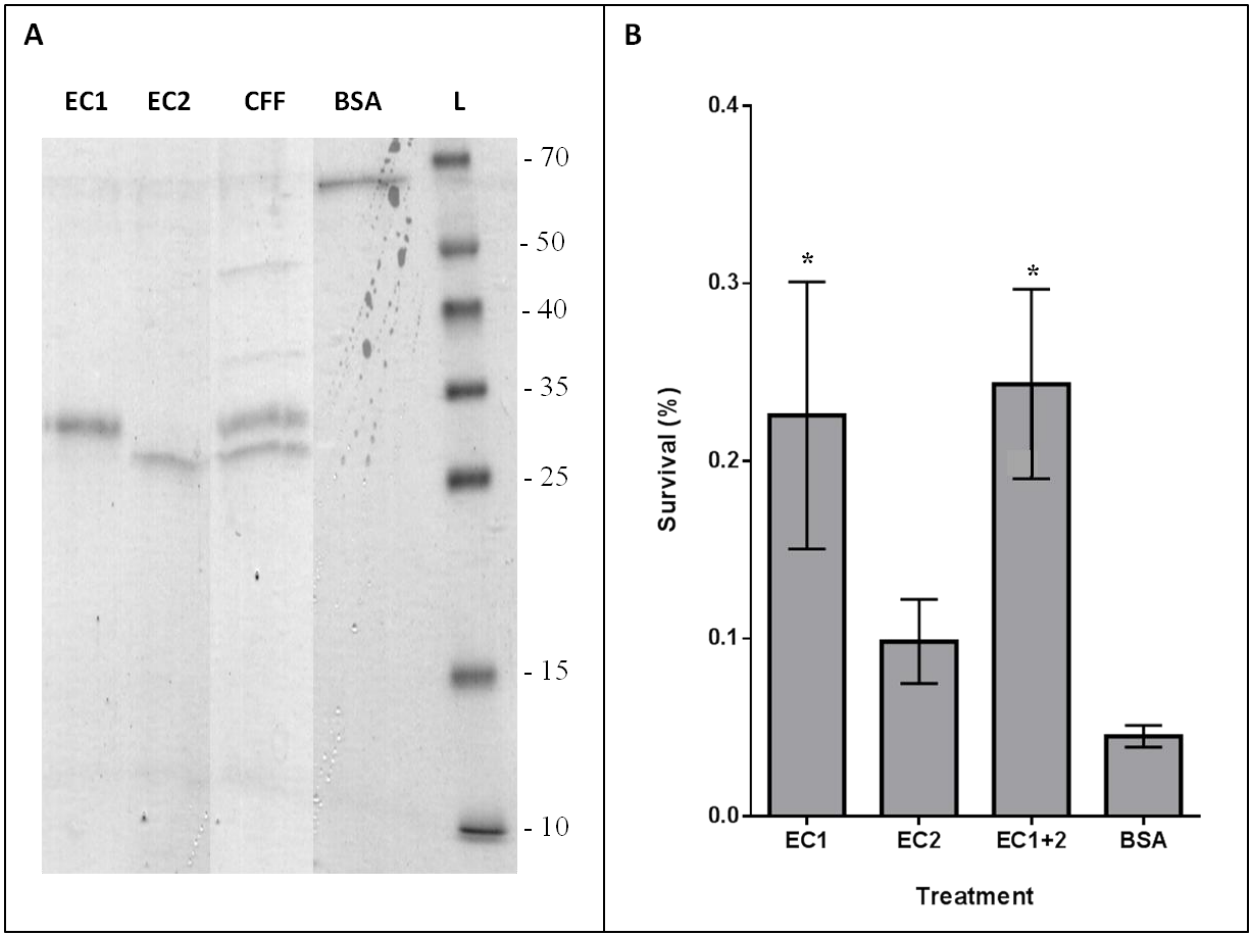

Figure 5.9 Visualization of purified EC1 and EC2 using SDS-PAGE and their effect on survival of heat challenged BS. Panel A shows the separation by SDS-PAGE through 15% polyacrylamide (w v^{-1}) of 1 µg, 1 µg, 3 µg and 1 µg of EC1, EC2, F80 and BSA protein, respectively, and lane L contained 5 µL of Spectra™ Multicolour broad range protein ladder and their masses (kDa) indicated on the right. Panel B shows the survival of BS following heat challenge, that were treated with gel purified EC or BSA. The heat challenge was performed as specified in 1 mL of PBS supplemented with an average of 19, 12, 15 and 13 µg mL^{-1} of EC1, EC2, EC1+2 (1:1) and BSA, respectively. Bars show the mean survival, calculated from triplicate experiments sampled in quadruplicate and error bars show SEM. Bars labeled with an asterix were determined to be significantly different compared to BSA by Dunnett's multiple comparisons test (α=0.05).

The reduced ability of EC2 to produce an increase in survival over BSA suggested that it may possess a decreased capacity to increase tolerance to heat in BS compared to EC1 and was perhaps effected by the presence of some post-translational modification (PTM). Glycosylation is known to be one of the most common PTMs present in proteins secreted by fungi (Reviewed in Peberdy, 1999). Since both ECs appeared to be secreted, glycosylation was implicated as a type of PTM that is potentially present on one or both of the ECs. Furthermore, both N- and O-linked glycosylation have been documented to influence many functional properties of proteins, such as binding, thermal stability, secretion and recognition by host immunity (Reviewed in Varki, 1993), all of which may be pertinent in the molecular biology of ELF produced by *B. bassiana*. Therefore, both ECs were assayed for the presence of these PTMs. This was determined by treating them with a cocktail of deglycosylation enzymes that would remove all N-linked and O-linked moieties, except those linked to mucin-like domains. Following enzymatic treatment, mobility assays via SDS-PAGE were used to determine if the M_r of treated ECs differed from untreated. A decrease in M_r following deglycosylation treatment would indicate that the protein was glycosylated. The results of this experiment showed that EC1 was glycosylated while EC2 did not appear to be (Figure 5.10). This was evident by the shift in M_r of untreated (native) EC1 from ~ 28 kDa to 26 kDa following treatment with deglycosylases, while the M_r of EC2 remained unchanged (26 kDa) following treatment.

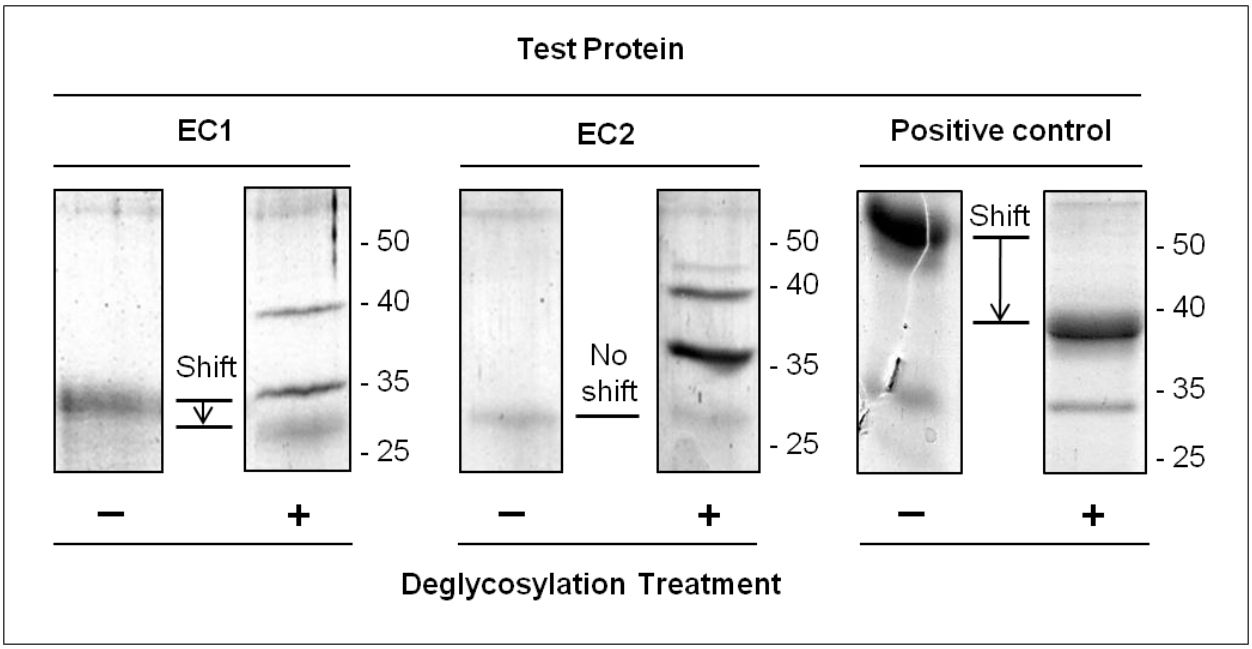

Figure 5.10 Effect of deglycosylation on the mass of ECs. The test proteins EC1, EC2 and positive control (fetuin) were treated with the protein deglycosylation mix as directed. The effect of deglycosylation was determined by mobility assays using SDS-PAGE and the shifts are indicated for each in the figure. Following treatment, EC1 and the known glycoprotein, fetuin shifted from ~ 28 and ~ 50 kDa to ~ 26 and ~ 38 kDa, respectively, while no shift was detected with EC2. Approximately 1.2 µg, 0.1 µg and 25 µg of EC1, EC2 and fetuin, respectively, were loaded. The EC1 and fetuin samples were electrophoresed through 12% (w v^{-1}) polyacrylamide and stained with blue silver and EC2 samples were electrophoresed through 15% (w v^{-1}) polyacrylamide and stained with silver nitrate. The bands resulting from the deglycosylation enzymes peptide -N-Glycosidase F and neuraminidase had M_r of ~ 37 kDa and ~ 35 kDa, respectively. The masses (kDa) of the Spectra™ multicolour broad range protein ladder are indicated to the right of the test protein groups.

The M_r of EC1 following its deglycosylation was indistinguishable from that of EC2 (26 kDa). The apparent size shift of ~ 2 kDa does not specifically indicate the presence of either O- or N-linked glycosylation, since their corresponding mechanisms attach sugar core groups of ~ 1.1 and 1.5 kDa, respectively, in *S. cerevisiae* and additional sugar and other molecules can be attached to these to further alter the mass of the glycoprotein (Reviewed in Peberdy, 1999). Glucoamylase I, a secreted protein, produced by *Aspergillus awamori* is one of the best studied glycoproteins in filamentous fungi and has been found to possess both N- and O-linked glycosylation which contribute > 8 kDa (Goto *et al.*, 1999) and > 13.2 kDa (Oka *et al.*, 2005) to the mass of the glycoprotein, respectively. As a result the ~ 2 kDa increase caused by glycosylation of EC1 appears to be within reason for both N- and O-linked glycosylation.

It appears that the presence of glycosylation in ECs is correlated with their ability to increase heat tolerance in BS, since EC2, which lacks such a PTM, has a decreased ability to increase tolerance (Figure 5.9B). The reason for this effect was not obvious. Glycoproteins produced by filamentous fungi are less studied compared to those in yeasts or higher eukaryotes; however it was apparent that this type of PTM provides a variety of structure-functions that differ from the nascent proteins. As a result, glycoproteins have been found to be involved in a variety of biological roles (Reviewed in Varki, 1993). In filamentous fungi, most secreted proteins are thought to be glycoproteins and their glycosylation may be a rate limiting step in their transport to outside of the cell (Reviewed in Peberdy, 1999). For example, it was found that glucoamylase and invertase required O-mannosylation or N-glycosylation, respectively, to be secreted properly (Perlinska-Lenart *et al.*, 2005). However, it does not appear that the secretory pathway of *B. bassiana* strictly discriminates against either EC based on the presence of glycosyl moieties, since both forms are present in the medium. This phenomenon appears to be common

and the presence of a quality control mechanism in the protein secretion pathway could suggest that misfolded proteins may be produced by the cell (Peberdy, 1999). Furthermore, it is logical to expect that a misfolded protein would likely have reduced functional activity. In this regard, it has been found that glycosylation is needed for activity in some enzymes. For example, glycosylation was required for activity in human acid beta-glucosidase as this enzyme was not functional when expressed in bacteria (Grace and Grabowski, 1990). This observation is consistent with findings discussed here, as EC2 was not determined to be glycosylated and had a reduced ability to increase survival in heat challenged BS, compared to EC1 which was glycosylated. However, in the case of ESC/ELF its true activity is unknown and is only manifested through the generation of CFUs; a very complex process.

Following activation of ESC/ELFs, an interaction with cells is thought to be a subsequent step in the process required to generate stress tolerance via EIT (Rowbury, 2001a; Rowbury, 2001b). The binding characteristics of a nascent protein have the potential to be modified by their glycosylation. This has been studied extensively in glycoproteins found in the extracellular matrix produced by mammalians cells (Reviewed in Hynes, 2009). Proteins, such as heparan sulfate proteoglycans are involved in cell-cell signaling through an interaction with extracellular growth factors. Since EC1, a possible ELF, is a glycoprotein with potential for the involvement in cell-cell signaling it is possible that glycosylation may influence the suspected interaction between it and the cell.

An assay for this was developed from a modified pull-down assay to determine if ECs could interact with BS. In contrast with the conventional pull-down system that employs a bait protein, tagged with glutathione *S*-transferase (or other protein with known binding properties) and an appropriately tagged prey protein (Sambrook and Russell, 2001); unchallenged BS were

used as bait for the EC proteins. Following incubation, BS were removed from the bait/prey suspension by differential centrifugation, which was expected to also remove proteins interacting BS from the supernatant. Potential protein-BS interactions were assessed by SDS-PAGE analysis and were indicated by a relative reduction in the intensity of their corresponding protein bands in supernatants with BS compared to those without.

The pull-down assay revealed that when preheated at 55 °C, a potential interaction occurred between BS and the 28 kDa EC1, but was not detected to occur with EC2 (Figure 5.11). This was evident because EC1 was no longer detectable in the supernatant following SDS-PAGE analysis, due to its co-sedimentation with the BS following differential centrifugation. None of the protein species, including EC1, were detected to interact with BS when the protein containing fractions were preheated at 25 °C. This was concluded by their presence in the polyacrylamide gel following the above treatment and pull-down with BS. This result was consistent with previous data (Figure 4.13) since it was found that CFF required to be heated at 55 °C to produce elevated tolerance to heat in BS, which did not occur at 22 °C. Furthermore, extracellular proteins preheated at 55 °C then incubated and centrifuged without BS did not show an altered protein banding pattern. This indicated the removal of EC1 from the supernatant was not due to heating alone. The selective nature of the potential interaction between the 28 kDa EC1 and BS is supported by the observation that both the 26 kDa EC2 and a 21 kDa protein species remained in the suspension and were not affected by the preheating temperature or the presence of BS, indicating non-interactivity with BS.

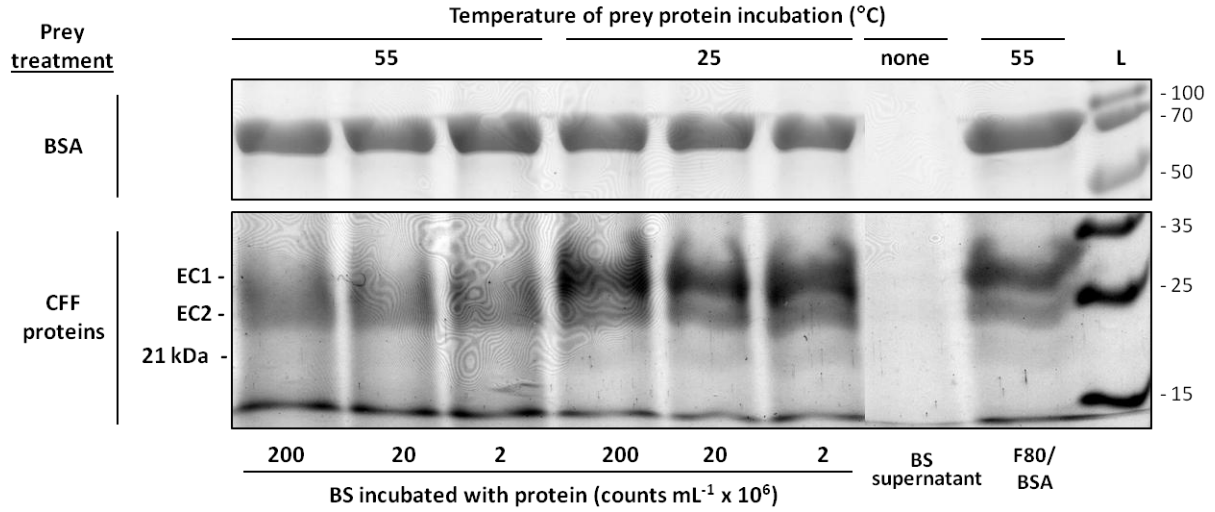

Figure 5.11 Pull-down assay to detect interaction between BS and extracellular proteins. Prior to being combined with the BS, prey proteins were incubated at 25 or 55 °C (indicated above the gel photograph), while the three concentrations of BS that were combined with the prey proteins are indicated below the gel photograph. Also shown is the supernatant from the same assay as above that contained only BS (BS supernatant) or prey protein (F80/BSA). Prey proteins used are indicated to the far left of the photograph and to the right of those the protein bands containing EC1, EC2 and a 21 kDa species are indicated. Lane L contained 5 µL of Spectra™ Multicolour broad range protein ladder and their masses (kDa) are indicated on the right. Lanes contained a maximum of 7.5 µg for both prey treatments.

Furthermore, performing the pull-down assay with BSA, as an external negative control with 55 or 25 °C preheating step, did not cause a detectable change of the intensity of the BSA protein band. Also, no polypeptides were visualized in the supernatant which contained only BS, which provided confidence that the proteins visualized in the other treatments were only from the protein fractions added to the assay.

Another pull-down experiment was conducted to help confirm the interaction that may have occurred between purified EC1 and BS (Figure 5.12). In spite of the interaction between EC1 and BS which was apparent, in this case, the EC1 band was not totally removed following pull-down with BS. Possibly, purified EC1 may have been depleted from the supernatant following pull-down with BS when it was preheated at 25 or 55 °C. This differed from the results shown in Figure 5.11, where EC1 was only removed following a 55 °C preheating. However, in both pull-down experiments EC1 was apparently depleted following incubation with BS suggesting that they do interact. However, a more sensitive quantitative measure is needed to assess the potential interaction between EC1 and BS, and how it may be involved in the establishment of EIT.

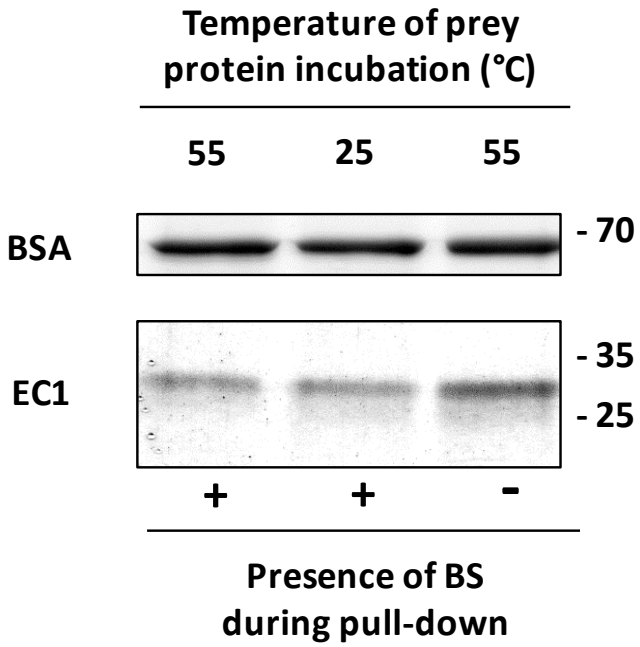

Figure 5.12 Pull-down assay to detect interaction between BS and gel purified EC1. Sections of the gel that contained the prey proteins BSA or EC1 are indicated to the left of the photograph and the masses (kDa) of the Spectra™ Multicolour broad range protein ladder are indicated on the right. Prior to being combined with BS the prey proteins were incubated at 25 or 55 °C (indicated above the gel photograph) for 30 min before being combined with 10^7 BS mL^{-1} or PBS without BS (indicated above the gel photograph). Lanes contained 1 and 0.1 µg of protein for BSA and EC1 treatments, respectively.

With regards the results shown in Figure 5.11, some depletion of an EC was expected following a pull-down in samples that were preheated to 55 °C and included BS, since a potential interaction between ELF and BS was thought to be required to produce EIT and was consistent with the results of previous bioassays. It was unexpected however, that nearly all of the EC1 would be removed from the supernatant, as was found in a pull-down assay with unpurified prey proteins. This was because many protein-cell surface interactions are transient, although some stable interactions are known to occur in the extracellular matrix of mammals (Reviewed in Hynes, 2009). A sufficient number of these interactions would decrease the amount of free ligand available in the solution and would manifest itself as a depletion of a particular protein band following SDS-PAGE analysis. This posed a quandary since the molar ratio of EC1 molecules to BS was estimated to be > 10^7:1. This estimation was based on the amount of BS and EC1 in the assays, its M_r and that EC1 was ~ 50% of the total protein in the CFF, which was estimated from the banding profiles the fractions produced. Furthermore, an estimate of > 10^5 receptors per cell (for a single receptor) (Hendriks *et al.*, 2003) is near the known upper limits. Even if a receptor for ELF was present at this number the EC1molecules would still be in ~ 30-fold molar excess (compared to their receptor) if 100% of EC1 molecules were bound 1:1. Therefore, due to the stoichiometrics suspected to be required for such a substantial removal of EC1 to occur in the pull-down assay it is possible that: 1) non-specific interactions are occurring, 2) the potential ELF can bind to multiple targets and/or 3) that this interaction does not follow mass action kinetics.

The first scenario cannot be ruled out entirely, however, there would likely be concurrent depletion of BSA or other extracellular proteins present in the CFF, but this was not observed. Also, physical entrapment of EC1 by BS would not be a significant source of its depletion at

these BS concentrations. In addition, binding artifacts more commonly arise from nonspecific binding in reconstituted systems using recombinant proteins, than in ones using proteins from tissue or cell lysates in conventional pull-down assays (Wissmueller *et al.*, 2011). Since the proteins were not recombinant, non-specific binding artifacts are less likely to be a major source of EC1 depletion. Therefore, the effect of scenario one may be negligible, but likely consistent between the proteins species present in the CFF and BSA.

With regards to the second scenario, receptors are functionally silent when they are unbound, and in this state they will specifically bind to a particular ligand. This specificity becomes relative under high concentrations of a particular ligand since in some cases a receptor can bind different ligands (Lambert, 2004). Therefore, scenario two may contribute to depletion of EC1, especially since BS were rinsed multiple times to promote their surface receptors to be in an unbound state, in addition to removing interfering material, prior to being combined with the ECs. Although, the total number of targets/receptors per BS that could potentially interact with EC1 is unknown in *B. bassiana*, the number of binding targets would be many fold greater if several distinct receptors could interact with EC1, compared to if just one receptor interacted. In *E. coli* an interaction between ESC and the cell's surface through a receptor has not been established, but has been suspected to occur since ESCs are extracellular and produce a cellular response (Rowbury and Goodson, 2001; Rowbury, 2001a). However, due to the lack of specific information regarding the potential/confirmed binding targets of ESCs and others ELFs it is not possible to determine how many receptors may be involved, but such an interaction cannot be excluded from possibility either.

The third scenario suggests that receptor recycling may potentially occur. A ligand that is able to bind with a free target, dissociate, remain in an active state and bind again can be de-

scribed as adhering to mass action kinetics. In this model only a proportion of targets can be occupied by a ligand at equilibrium. However, it is possible that the apparent interaction between EC1 and BS may not adhere to this model, unless a substantial amount of EC1 interacted with the cell in a nonspecific manner or bound to a variety of targets. This is due to the observation that nearly all EC1 was depleted following pull-down, which supports that the potential interaction between EC1 and BS may not follow mass action kinetics. Nonetheless, it may be possible that the apparent interaction between EC1 and BS may be explained by a different interaction model, for example through its endocytosis following interaction with the cell. Endocytosis has been studied in receptor tyrosine kinases, such as ERB-1 (eukaryotic ribosome biogenesis protein 1) in humans (Waterman and Yarden, 2001) and the G-protein coupled receptors, such as the mating a-factor receptor in *S. cerevisiae* (Chen and Davis, 2000). In both examples, upon binding with their proteinaceous ligand, the ligand-receptor complex is activated and is translocated into the cell via endocytosis and the receptor is recycled back to the cell surface where it is free to interact with another ligand and repeat the cycle. In the case of receptor tyrosine kinases this process required ~ 15 min in human models (Hopkins *et al.*, 1990). This type of receptor is also known to be present at very high numbers ($> 10^5$) per cell in humans (Hendriks *et al.*, 2003). Therefore, the direct uptake, speed of receptor recycling and number of receptors may all be conducive for explaining the possible interaction between EC1 and BS, since each would contribute to the depletion of EC1 following the pull-down assay.

To summarize the above; all extracellular polypeptides, including the 28 kDa EC1 remained in the supernatant following heating at 55 °C and centrifugation without BS. While, in the presence of BS, only EC1 was depleted from the supernatant (in one experiment; Figure 5.11) following pull-down and only after it was preheated to 55 °C. This indicated the tempera-

ture effect on binding to BS is may be specific to EC1; however, the specific details of this potential interaction are unknown. In addition, the apparent heat requirement of EC1 to interact with BS is consistent with the requirement of CFF, containing EC1, to be preheated in order for it to confer elevated heat tolerance to heat in BS. This provided additional evidence to suggest that EC1 may have ELF activity and could be involved in EIT to heat in BS. However, in a second pull-down experiment, an interaction between purified EC1 and BS appeared to occur, but did not deplete EC1 to the same level as the first experiment, nor did it reveal the same requirement for the preheating of EC1to elicit the apparent interaction with BS. Therefore, confirmation of the apparent interaction between EC1 and BS may be required since false positives are not uncommon findings in studies of protein-protein interactions, even though they are more likely in heterologous systems (Wissmueller *et al.*, 2011). For example, localization and mutation studies would be useful in confirming the potential interaction and determining which receptors may be involved. Also, additional studies are required to elucidate the kinetics of the potential interaction between EC1 and BS, which would provide additional clues for the receptors or other targets that may be candidates to interact with the likely ELF. Furthermore, the elucidation of the direct molecular target(s) of ELF may provide insight into how EIT is involved in the response to heat in *B. bassiana*.

5.5 Connection to the next study

In this section it was established that the phenomenon which resembles EIT to heat in BS was an appropriate system to exploit for the detection of ECs because the response appeared to be less variable than in CS. Through this system, two ECs were revealed with M_r of ~ 26 and 28 kDa. The larger EC1 was found to be glycosylated and appeared to interact with BS upon

heating and purified EC1 was shown to increase heat tolerance in BS. These results provided further confidence to support the claim that EC1 likely possesses ELF activity and is involved in EIT to heat in BS. In the next section purified EC1 and EC2 were subjected to mass spectrophotometry to determine portions of their amino acid sequences. These experiments produced results that were crucial for the discovery of their likely encoding gene *elf* and to elucidate the sequence of the full-length ELF.

6.0 MOLECULAR CHARACTERIZATION OF ELF

6.1 Abstract

The ability of EPF to control various pest insects important to agriculture can be negatively impacted by various stressors and hence are economically and commercially consequential. A novel phenomenon has been discovered in *B. bassiana* that appears to be involved in the establishment of tolerance to heat and likely requires a secreted protein, ELF. It was found that EC1 as identified in section five of this thesis has been shown to be involved in the establishment of tolerance to heat in BS, which is a response that resembles EIT. As a result, EC1 is likely an ELF produced by *B. bassiana*, based on its ability to increase heat tolerance. A second protein, EC2 has also been correlated with the presence of EC1 but was not able to increase the ability of BS to survive heat challenge. Both of these proteins were purified, then analysed using ESI-MS/MS. This generated 86 unique *de novo* peptide sequences in total from EC1 and EC2. Many of these peptides and the parent ions they were deduced from were found in both ECs. From this it was concluded that EC1 and EC2 had the same amino acid sequence and differed by the presence of glycosylation on EC1.

An EST from *B. bassiana* was identified in the data base and encoded amino acid sequences found in 6 of the 11 parent ion peptides. As a result this cDNA clone was considered to be a candidate to partially encode for EC1 and EC2 in *B. bassiana* and was used to amplify the remaining sequence using PCR based methods. This revealed a 741 bp ORF that encoded the six peptides encoded by the EST, in addition to two more, for a total of eight out of the possible eleven peptides identified in EC1 and EC2. Furthermore, this ORF encoded a protein with other

predicted features that were consistent with those observed in the two ECs, including glycosylation sites, secretion signal peptide and its deduced size before (27.4 kDa) and after (25.9 kDa) signal peptide cleavage. The entire ORF of the candidate gene (*elf*) was identified in *B. bassiana* and was inserted into an expression cassette and introduced into the methylotrophic yeast, *P. pastoris*, where its expression could be controlled by the presence of methanol through a methanol responsive promoter. This strategy was successful and yielded a cell line able to produce an extracellular protein that was able to increase heat tolerance in BS, which resembled the EIT response and as a result was considered TG-ELF, since elevated stress tolerance, is the only known effect of ESCs. This provided additional evidence that that the candidate *elf* encoded a functional ELF. However, neither CS, hydrated (swollen) CS and hyphae produced by *B. bassiana* nor BS produced by *I. farinosa* or *T. inflatum* appeared to be responsive to TG-ELF.

The molecular function(s) of ELF remained elusive as none of the most similar sequences in the database possessed a known function. Furthermore, structural models were unable to provide confident prediction of potential functions for ELF. It was likely that ELF is a SSCP due to its size, abundance of cysteine and was secreted. Three internal repeats of 63 aa were also found in the deduced ELF sequence. Although not well understood, internal repeats have also been found in proteins produced by fungal phytopathogens and are thought to play a role in rapid protein evolution. In addition, correlative clues suggest that the potential ELF-BS interaction is of low affinity, which is consistent with agonist-receptor interactions required for signal transduction, which had been previously suspected to be required for EIT to occur. This work has revealed for the first time the sequence of a likely ELF and its candidate encoding gene, *elf*.

6.2 Introduction

The ELF likely produced by *B. bassiana*, specifically corresponding to EC1 identified in section five of this thesis, has been shown to be likely involved in the establishment of EIT to heat in BS. A second protein, EC2 has also been correlated with the presence of EC1. In this study, both of these candidate proteins were analysed using ESI-MS/MS to identify *de novo* sequences from the tryptic peptides produced from the ECs (Reviewed in Seidler *et al.*, 2010; Walther and Mann, 2010). This and other mass spectrometry based strategies have become the gold standard for protein sequencing because of its ease of automation and accuracy, compared to Edman degradation (Domon and Aebersold, 2006). Genetic methods can be used to identify the encoding gene through the generation of *elf* mutants, but *de novo* peptide sequencing was selected because the ECs have been identified and could be purified in the amounts required for ESI-MS/MS, and would provide direct amino acid sequence information. The resulting peptide sequence information can be used to identify a candidate DNA sequence(s) that may encode ELF. The candidate *elf* sequence(s) can then be employed in many conventional molecular biological techniques, such as heterologous protein expression, to confirm the encoded gene product was involved in EIT through the established bioassay.

In the case of proteins with unknown functions, additional analysis is required to help elucidate or rule out some potential activities. In this regard, various *in silico* techniques for sequence analysis can be quite useful. With the availability of powerful structural modeling tools it is possible to add an additional level of complexity to this analysis and imply functions for these sequences based on their predicted structure. There are ~ 16,000,000 unique peptides in the public data banks and only ~ 80,000 solved protein structures, creating a need to predict structure/function from sequence alone. Homology modeling, relies on the observation that the

number of protein folds in nature are limited and many distant homologues adopt remarkably similar structures even though a relatively large degree of sequence dissimilarity exists between them (Baker and Sali, 2001). These methods extend the protein fold library obtained from experimentally solved structures by comparing known structures and folds to peptides in data banks with similar sequences, but with unsolved structures. Those deemed a sufficient match are used to expand the protein fold library to improve fold prediction for the query sequences. This enables proteins with only limited sequence similarity (~ 20%) to proteins with known structures to be modeled accurately (Kelley and Sternberg, 2009). In contrast, *ab initio* structural modeling is less accurate than homology modeling, but it does not require close sequence or structural homologues to the protein of interest. This method of modeling can allow structure/function relationships to be predicted in proteins of interest that do not have sequence of structural homologues available for comparison, but is less accurate than homology modeling (Roy *et al.*, 2010).

Here both EC1 and EC2 were analysed with ESI-MS/MS to determine a portion of their amino acid sequences to aid in identifying and cloning the candidate *elf*. The intent of this was to: a) determine if ELF was genetically encoded, b) confirm that the candidate *elf* encoded a protein with ELF function by expressing it transgenically in *P. pastoris* and assaying for its ability to produce elevated tolerance to heat stress in BS and c) gain insight into ELFs structure/ function through sequence analysis and structure modeling.

6.3 Materials and methods

6.3.1 Preparation of cultures and fungal propagule suspensions

The cultivation of *E. coli*, *B. bassiana* and other EPF was performed as described in sections 3.3.1. Preparation of CS and BS from *B. bassiana*, *I. farinosa* and *T. inflatum* were performed as in 4.3.1, except that *I. farinosa* and *T. inflatum* cultures were incubated at 24 °C.

Swollen CS and hyphal cell types were recovered from *B. bassiana* grown in YPG as per section 4.3.1 except that the cultures were inoculated to 10^8 CS mL^{-1}, which was required to produce a sufficient number of propagules of the desired cell types to assay for EIT to heat (~10^7 mL^{-1}). Also, swollen CS and hyphal cell types were harvested after 8 and 22 h, respectively, as per Bidochka *et al.* (1987), by centrifugation at 6,000 x*g* for 2 min and rinsed twice with PBS. These incubation times were chosen to obtain the greatest proportion of the desired cell type without the presence of more advanced stages of development. Swollen CS has been defined as the second developmental stage of *B. bassiana* grown in liquid culture and are spherical and 3-5 µm diameter (Bidochka *et al.*, 1987). Hyphae included the third, fourth and fifth stages of development which exhibit polar growth and were defined as possessing an emerging germ tube that was less than 10 µm length, 10-30 µm and > 30 µm in length, respectively (Bidochka *et al.*, 1987). The swollen CS and hyphal suspension contained 24% and 47% of the desired cell types, respectively (CS and BS contained ~ 100%). These propagules were assayed for EIT to heat with the same method that was used for BS, except were supplemented with 10 µg mL^{-1} of TG-ELF (see section 5.3.7).

Pichia pastoris strain GS115 (Invitrogen, Carlsbad, USA) was cultured according to the manufacturer's directions, see sections 6.3.7 and 6.3.8.

6.3.2 Protein sequencing

In-gel sample digestion, liquid chromatography with tandem mass spectrometry and manual nanospray analysis were performed as per Parker *et al*. (2005) at the University of Victoria Genome BC Proteomics Centre (Victoria, Canada). An overview of the ESI-MS/MS protocol is shown in Appendix I.

6.3.3 Sequence analysis

Sequence analysis was performed with candidates for ELF and *elf* sequences as per section 3.3.6 with the following exceptions.

Mass spectrometry BLAST was performed as per Shevchenko *et al.* (2001) using the default settings to determine if the *de novo* peptide sequences identified from EC1 or EC2 had sequence that were homologues of others in the data base. Mass spectrometry BLAST was designed for matching relatively short peptide sequences with other sequences with that are closely related (Shevchenko *et al.*, 2001). PEAKS, which was kindly provided on a trial by Bioinformatics Solutions Inc. (Waterloo, Canada) was also used to query the database for sequences with similarities to those generated by de novo sequencing, using the default settings.

Homology searches and alignments for phylogenetic analysis of the putative ELF sequence were performed as described in section 3.3.6. Briefly, ten hits were returned with E-values cut-offs of $\leq 10^{-5}$ when the product encoded by the *elf* candidate was used as the input. Also, the 'allow smaller final blocks' option was enabled for sequence curation with Gblock to allow for a less stringent alignment between the 13 sequences analysed (1, 3 and 9 were out-group, putative ELFs and related sequences from EPF, respectively) which was required to perform phylogenetic analysis with curation (Castresana, 2000).

Signal peptides were predicted using SignalP 4.0 (Petersen *et al.*, 2011) with the default settings.

N-glycosylation sites were predicted by the NetNGlyc 1.0 server using the default settings (available at http://www.cbs.dtu.dk/services/NetNGlyc/) as per Tomar *et al.* (2011).

The ELF sequence was analysed for internal repeats using rapid automatic detection and alignment of repeats (available at http://www.ebi.ac.uk/Tools/pfa/radar/) with the default settings and a multiple alignment of the repeats was performed as per section 3.3.6.

Amino acid composition was calculated using ProtParam (available at http://web.expasy.org/protparam/).

6.3.4 Nucleic acid isolation and analysis

Nucleic acid isolation and analysis was performed as per section 3.3.3.

6.3.5 Agarose gel electrophoresis

Agarose gel electrophoresis was performed as per section 3.3.4.

6.3.6 Sequence identification by PCR and RACE

Sequence identification by PCR and RACE was performed as per section 3.3.5 with the following changes. Oligonucleotide primers were designed from the EST GT894226.1, which was deduced to encode six *de novo* sequences identified in EC1 and EC2 and was a candidate to encode the entire ELF protein. These primers (Table 6.1) were designed to have a T_m of ~ 68 °C, which was recommended by the manufacture of the RACE kit (FirstChoice® RLM-RACE Kit, Invitrogen, Carlsbad, USA). Confirmation that ELF primers could amplify sections with the predicted sizes was assessed by performing 25 µL PCRs and products were resolved by 1.5% (w v^{-1}) agarose gel electrophoresis. These reactions included 1 µg of genomic DNA from *B.*

bassiana as template and 1 u of Taq DNA polymerase (Invitrogen, Carlsbad, USA) as per the manufacturer's directions. Four annealing temperatures of 63, 61, 59 or 57 °C were tested to determine which was optimal for generating the predicted amplicon. The temperature cycles used were: 300 s at 95 °C x1; 60 s at 95 °C, 30 s at 63, 61, 59 or 57 °C, 60 s at 72 °C x35; and 15 min at 72 °C x1.

The ELF primers were employed in RACE to amplify the 5' and 3' regions that are adjacent to the sections of cDNA that they anneal to. The expected sizes of the predicted RACE products were estimated using the sequence information of the EST and the knowledge that the nascent size of EC2 is estimated to be ~ 26 kDa. A protein of this size was estimated to contain ~ 236 amino acids by considering an average amino acid mass of ~ 110 Da and would require a coding DNA of ~ 700 bp. In addition, consideration was given to the size of the oligonucleotide adaptor and amount of polyadenylation, which would also influence the size of the RACE products (see Section 3.4.2).

The RNA extracted from *B. bassiana* was used to create a cDNA containing 5' or 3' adapters using the FirstChoice® RLM-RACE Kit as directed (Invitrogen, Carlsbad, USA). Products were amplified in 25 µL PCRs with Platinum® Taq High Fidelity DNA polymerase (Invitrogen, Carlsbad, USA) as per the manufacturer's directions with the exception of using 1 µL of cDNA prepared for RACE with 0.4 mM of the appropriate ELF primer and 0.6 mM of outer 5' or 3' RACE primer supplied by the manufacturer. Touchdown PCR (Don *et al.*, 1991) was used to amplify the candidate *elf* sequences with the following temperature cycles: 120 s at 94 °C x1; 30 s at 94 °C, 100 s at 68 °C x10; 30 s at 94 °C, 30 s at 61 °C, 100 s at 68 °C x25; and 20 min at 68 °C x1. The presence of amplicons were determined by electrophoresis through a 1.0% (w v^{-1}) agarose gel.

Table 6.1 Important characteristics of oligonucleotide primers for the amplification of GT894226.1 sequence in *B. bassiana* using 3' and 5' RACE.

Primer name	Sequence	GC %	Tm (°C)
ELF-F1	CGGAGTGCTACGCTGGCCAC	70	68.3
ELF-F1.1	TGGCTCCTGCCACGACGTTG	65	66.0
ELF-F2	GCACCGACAGCCTTGAGCGA	65	68.2
ELF-F2.1	TGAGGCCGGTTGTGGCACTG	65	68.4
ELF-R1	ATGCAGTCCGCGACGGTAGC	65	67.9
ELF-R1.1	TCGCTCAAGGCTGTCGGTGC	65	66.0
ELF-R2	CAGTGCCACAACCGGCCTCA	65	68.4

The above RACE reactions were used as templates for nested PCRs utilizing the inner RACE and nested ELF primers to anneal to internal priming sites on the 5'or 3' RACE adapters and *elf* sequences, respectively (Table 6.1). These 25 µL reactions were catalysed by 1 u of recombinant Taq DNA polymerase (Invitrogen, Carlsbad, USA) as per the manufacturer's directions with the exception of using 2 µL of the initial RACE reaction as template and 0.3 mM and 0.6 mM of the appropriate ELF and inner RACE primer, respectively. Touchdown PCR was also used for these reactions with the same temperature cycles as the first RACE reactions, as shown above. The presence of PCR products was determined by electrophoresis through a 1.0% (w v^{-1}) agarose gel.

The RACE products generated in reactions that contained the ELF-F1, ELF-F1.1, ELF-R1 and ELF-R1.1 primers with the appropriate outer RACE primers were inserted into pCR 4-TOPO (Invitrogen, Carlsbad, USA) and used to transform chemically competent *E. coli* DH5α (Invitrogen, Carlsbad, USA) as directed by the manufacturer. Transformants were selected using ampicillin (100 µg mL^{-1}) and X-gal (50 µg mL^{-1}) to screen the colonies for plasmid and insert presence, respectively. No antibiotic resistant colonies grew from ELF-R1.1 clones. The vectors were named for the gene specific primer used to create their insert; PCR4:ELF-F1, PCR4:ELF-F1.1 and PCR4:ELF-R1.

The method termed colony PCR, as described by Sambrook and Russel (2001), was used to confirm that the PCR4:ELF-F1, PCR4:ELF-F1.1 and PCR4:ELF-R1 transformants contained regions from the candidate *elf*. This was performed using Taq DNA polymerase with the gene specific primers pairs ELF-F2.1/ELF-R1 for PCR4:ELF-F1 and PCR4:ELF-F1.1 clones or ELF-F1/ELF-R2 for PCR4:ELF-R1 clones and the following temperature cycles: 180 s at 94 °C x1; 45 s at 94 °C, 30 s at 61 °C, 60 s at 72 °C x20; and 10 min at 72 °C x1. Plasmids were extracted

and the inserts were sequenced using M13 forward (-20) and M13 reverse priming sites by the National Research Council Plant Biotechnology Institute (Saskatoon, Canada).

The sequences obtained from the PCR4:ELF vectors overlapped with the EST from *B. bassiana* which contained the candidate *elf* sequence and appeared to represent a contiguous sequence. The primers ELF-Fa (5'-GAAAACCGCCTCCTTCTTCCT-3') and ELF-Ra (5'-CGTTACGAGCCCATGCACAT-3') were designed from the apparent contiguous sequence to confirm its presence by PCR and was predicted to anneal upstream and downstream of the predicted ORF found in the candidate *elf* sequence, respectively. These 25 µL reactions included 1 µg of genomic DNA or 1 µL of previously prepared cDNA from *B. bassiana* GK2016 and *B. bassiana* ARSEF3113 or 1 µg of genomic DNA from *L. longisporum, M. anisopliae* or *T. inflatum* as template and 1 u of Taq DNA polymerase (Invitrogen, Carlsbad, USA) as per the manufacturer's directions. The temperature cycles used were: 180 s at 94 °C x1; 60 s at 94 °C, 30 s at 59 °C, 60 s at 72 °C x35; and 15 min at 72 °C x1.

Following resolution of the three resulting ELF-Fa/ELF-Ra products by 1% (w v^{-1}) agarose gel electrophoresis they were purified and cloned into pCR 4-TOPO. The transformants were confirmed to contain the insert by colony PCR using the primer set ELF-F1/ELF-R1 with the following the temperature cycles: 300 s at 95 °C x1; 60 s at 95 °C, 30 s at 61 °C, 60 s at 72 °C x35; and 15 min at 72 °C x1, followed by 1.5% (w v^{-1}) agarose gel electrophoresis. The inserts were sequenced and the plasmid containing insert derived from GK2016 was termed PCR4:ELF-Fa-Ra.

6.3.7 Assembly of PicZ*α*:ELF and PicZ:ELF cassettes and transformation of *P. pastoris*

The resulting sequence obtained from *B. bassiana* GK2016 was used to design the following three primers, shown below with *EcoRI* and *XbaI* sites underlined in ELF-F and ELF-R primers, respectively:

1) ELF-Fb (5′-CGAATTC*AAAAA***ATG**GAGACTGCTGTTGGTATTG-3′)
2) ELF-Fc (5′-CGAATTCTTGCCCCATGCTGATAAATCAAC-3′)
3) ELF-Rb (5′-CTCTAGA**TTA**AGGCTGTGGCTCATGGTC-3′)

Both ELF-F primers were designed to be used with ELF-Rb to amplify the entire ORF including the in-frame stop codon (bolded TTA in the above ELF-Rb sequence) which encoded *de novo* peptide sequences identified in EC1 and EC2. Primers ELF-Fb and ELF-Fc differed in that the former's annealing location included the predicted start codon of the candidate *elf* (bolded ATG in the above ELF-Fb sequence) to and was expected produce an amplicon that would encode ELF with its predicted secretion signal peptide, while the latter was designed to anneal to the next nucleotide downstream of the encoded signal peptide to produce a product without its native signal peptide. Furthermore, ELF-Fb also included an in-frame Kozak sequence (italicized AAAAA in the ELF-Fb above sequence). These products were amplified using the above primers as 25 µL reactions and included 1 µL of extracted PCR4:ELF-Fa-Ra as template and 1 u of Taq DNA polymerase (Invitrogen, Carlsbad, USA) as per the manufacturer's directions. The temperature cycles used were: 180 s at 94 °C x1; 60 s at 94 °C, 30 s at 59 °C, 60 s at 72 °C x35; and 15 min at 72 °C x1. The amplicons were then resolved by 1% (w v^{-1}) agarose gel electrophoresis, purified, inserted into pCR 4-TOPO, used to transform *E. coli*,

confirmed by colony PCR with ELF-F1/ELF-R1 and electrophoresis through 1.5% (w v^{-1}) agarose gel and were sequenced as per the manufacturer's directions. The resulting constructs were termed PCR4:ELF-Fb-Rb and PCR4:ELF-Fc-Rb, which contained the candidate *elf* with and without its predicted secretion signal peptide encoded, respectively.

The expression vectors pPicZB and were used for the overexpression of the candidate *elf* and were selected to ensure that the predicted ORF remained in-frame. Both of these possess the *P. pastoris* alcohol oxidase promoter which allows the induction of gene expression when methanol is present in the medium. These vectors differ by the presence of the *S. cerevisiae* α-mating factor signal peptide in pPicZαA, which is incorporated with the protein of interest when it is synthesized *in vivo*, to promote its secretion while a protein of interest produced under the direction of pPicZB would remain in the cytosol unless a native signal sequence was included. The restriction enzymes *EcoRI* and *XbaI* were used to remove the candidate *elf* inserts from PCR4:ELF-Fb-Rb and PCR4:ELF-Fc-Rb and were then directionally subcloned using a 1:6 (vector:insert) molar ratio into the same sites of pPicZB and pPicZαA, respectively, with T4 DNA ligase, as directed by the manufacturer (Invitrogen). The resulting constructs were named PicZ:ELF and PicZα:ELF.

These constructs were used to transform chemically competent *E. coli* DH5α (Invitrogen, Carlsbad, USA) as per the manufacturer's directions and transformants were screened on Lysogeny broth with 0.5% (w v^{-1}) NaCl, 1.5% (w v^{-1}) agar and 50 µg mL^{-1} of the antibiotic Zeocin. Transformants were confirmed to contain the desired insert by colony PCR with ELF-F1/ELF-R1 and electrophoresis through 1.5% (w v^{-1}) agarose gel. Three clones from each construct were grown in Lysogeny broth with 0.5% (w v^{-1}) NaCl and 50 µg mL^{-1} Zeocin. The plasmids were extracted from these clones and their inserts were sequenced using the primers

5’Aox (5’-GACTGGTTCCAATTGACAAGC-3’) and 3’Aox (5’-GCAAATGGCATTCTGA CATCC-3’) to ensure the predicted ORF was in-frame. One clone with the correct frame was selected for each and grown in 100 mL of Terrific Broth [1.2% (w v^{-1}) tryptone, 2.4% (w v^{-1}) yeast extract, 0.4% (v v^{-1}) glycerol, 0.017 M KH_2PO_4, 0.072 M K_2HPO_4] with 25 µg mL^{-1} Zeocin (Invitrogen, Carlsbad, USA) in preparation for midi-prep by the alkaline plasmid extraction method as described in (Sambrook and Russell, 2001). Twelve micrograms of each construct were linearized separately with *PmeI* or *SacI* using the manufacturer’s directions (Thermo Scientific). Linearization was assessed by agarose gel electrophoresis and the appropriate bands were removed with a sterile scalpel and the DNA was extracted as per section 3.3.5. Six micrograms of each linearized vector was used to transform competent *P. pastoris* cells (performed in duplicate) using the electroporation method as directed by the manufacturer (Invitrogen).

Transformants were screened using antibiotic selection with several concentrations (0, 200, 600 and 1000 µg mL^{-1}) of Zeocin in 1% (w v^{-1}) yeast extract, 2% (w v^{-1}) peptone, 2% (w v^{-1}) glucose, 1 M sorbitol and 2% (w v^{-1}) agar. The most resistant colonies were selected as directed by the manufacturer, since this phenotype has been shown to be correlated with expression of the gene of interest. Transformants were screened by colony PCR supplemented with 5% (v v^{-1}) glycerol using primer sets ELF-Fc/ELF-Rb and 5’Aox/3’Aox to confirm they possessed the candidate *elf* insert and that it was within the expression cassette, respectively. Glycerol was required because there were sections of the candidate *elf* that had higher than 70% GC, which hinders denaturation and impedes primer annealing (Hube *et al.*, 2005). The temperature cycles used were: 180 s at 94 °C x1; 60 s at 94 °C, 30 s at 59 °C, 60 s at 72 °C x35; and 15 min at 72 °C x1, except that the reactions with Aox primers were performed with an annealing

temperature of 54 °C. The products were then separated by electrophoresis through 1.0% (w v^{-1}) agarose gel.

6.3.8 Expression of *elf* by *P. pastoris*

Twelve and seventeen transformants that were confirmed to contain PicZ:ELF and PicZα:ELF, respectively, were screened for production of putative TG-ELF. Induction was performed as directed by the manufacture but was scaled-down to 10 mL in test tubes. Briefly, the 29 clones were cultured separately in 10 mL of buffered glycerol-complex medium over night to achieve an $OD_{600\ nm}$ of 2-6. These cells were harvested by centrifugation and resus-pended in buffered complex methanol medium which contained 0.5% (v v^{-1}) methanol and used to inoculate 10 mL of the same medium to an $OD_{600\ nm}$ of ~ 1. Cultures were incubated at 28 °C with shaking at 300 RPM and a 1 mL sample was collected after 2, 3 and 4 d. The samples were centrifuged at 10,000 x*g* for 1 min and the supernatant and cell pellet were separated and stored at – 20 °C. Cultures were also supplemented with 50 µL of methanol daily, as directed by the manufacturer. The protein content of these samples was quantified by Bradford reaction to assess the ability of the cultures to accumulate protein in the medium, which may indicate secretion and accumulation of TG-ELF. The CFF from transformants that produced the highest extracellular protein content was further analysed by SDS-PAGE to determine if a protein with the expected size of ~ 30 kDa was present.

The two best performing transformants were selected for scaled-up over expression experiments. These were αELF2 and αELF14 for PicZα:ELF and ELF4 and ELF5 for PicZ:ELF. Over expression experiments were performed as directed by the manufacturer (similar to the scaled-down version above), with the exception that 100 mL cultures were grown in 500 mL

spinner flasks instead of a baffled flask. Cells were incubated at 28 °C and the spinner was propelled by a magnetic stir plate (Corning) and 0.5 mL of methanol was added daily as directed by the manufacturer. Samples of 1 mL were removed daily and the OD at 600 nm was measured to monitor cell growth. One millilitre samples were also centrifuged at 10,000 x*g* for 1 min to remove the cells and the supernatant was immediately frozen at -20 ºC and used to estimate their protein content and accumulation of an overexpressed protein.

6.3.9 Preparation and storage of CFF for bioassays

Cell-free filtrate was prepared from *B. bassiana* culture as described in section 5.3.2. For the preparation of CFF from *P. pastoris* cell lines (αELF2, αELF14, ELF4 and ELF5) were grown for 48 h as per section 6.3.8 and were centrifuged at 10,000 x*g* for 1 min to remove the cells and the supernatant was recovered. The supernatant was then filtered with vacuum through a Millipore filter (5 cm diameter, 0.45 µm pore size) to remove the remaining biomass to produce CFF. The resulting sterile CFF was employed in bioassays (used fresh or stored -30 °C and used within 4 d) and/or protein concentration protocols (used fresh). Filtrate preparation and all subsequent manipulations required to concentrate the protein were performed at 4 °C.

6.3.10 Salt mediated precipitation

Salt mediated precipitation was performed as described in section 5.3.3, except that only F80 was prepared and recovered. Following precipitation, F80 was dialysed as in section 5.3.5.

6.3.11 Assay for EIT to heat

The assay for EIT to heat was performed as described in section 5.3.7, with the following exception. Assays that included CS, swollen CS and hyphae were performed as per BS, but CS and swollen CS were challenged in PBS with 0.02% (v v^{-1}) Tween 80 and all were supplemented

with 10 µg mL^{-1} of gel purified TG-ELF or BSA. The BS produced by *I. farinosa* and *T. inflatum* were also assayed for EIT to heat as described in 5.3.7, except that they were supplemented with 100 µg mL^{-1} of gel purified TG-ELF or BSA and *T. inflatum* was incubated at 24 °C, rather than 27 °C, to produce CFUs.

6.3.12 Protein concentration determination

Protein concentration determination was performed as described in section 4.3.7.

6.3.13 Sodium dodecyl sulfate polyacrylamide gel electrophoresis

The SDS-PAGE method was performed as described in section 4.3.6. with the samples that are indicated in the appropriate figures being combined 1:1 with sample buffer. In addition, intracellular fractions from *P. pastoris* were prepared as per Xavier (1998) with the following modifications. Cells were harvested from 1 mL samples of media and agitation was supplied by vortex at maximum setting for 30 s, followed by cooling on ice between agitations and was repeated for a total of six cycles. Microscopy at 400x was used to assess cell lysis.

6.3.14 Clear native polyacrylamide gel electrophoresis

The CN-PAGE was performed in preparation for protein elution as per 5.3.9., with the exception that up to 2.5 mg of F80 protein was separated per gel. These fractions were prepared from ELF4 and αELF2 *P. pastoris* cultures grown in the presence of methanol.

6.3.15 Protein elution

Protein elution was performed as per 5.3.12.

6.3.16 Protein structure/function prediction

Structure/function prediction was performed as per section 3.3.7, except that CombFunc was not used because it is not able to perform *ab initio* modeling since no structural or sequence homologues to known ELFs existed in the protein data bank. The ELF sequence was not predicted to possess multiple protein domains, therefore the entire sequence, with and without the predicted signal peptide removed, was used as the input.

6.3.17 Statistical analysis

Statistical analysis was performed as per section 4.3.8. Tukey's, Dunnett's or Student's tests were applied to compare all means against each other or to compare the means against a control group, or compare two means, respectively. All experiments were repeated at least three times, unless stated otherwise and the sample size used to calculate each mean is indicated within the text or figure legends.

6.4 Results and discussion

6.4.1 *De novo* sequencing of the likely ELF, EC1 and a related protein, EC2

It would be expected that information regarding the amino acid sequence of EC1 and EC2 would provide insight into the structure/function relationship of these proteins. Previous attempts to identify the ECs using mass spectrometry and peptide mass fingerprinting were unsuccessful. This was likely due to the lack of available sequence data from filamentous fungi in public data bases, such as those provided by the National Center for Biotechnology Information or European Bioinformatics Institute. This obstacle is not uncommon for studies in organisms with unsequenced genomes (Shevchenko *et al.*, 2001) as the full genome of *B. bassiana* (Xiao *et al.*, 2012) was not available when the EC sequencing and identification was performed

(subsequent scans of the genome revealed one copy of a putative *elf*; see section 6.4.2). As a result, the use of peptide mass fingerprinting was not a suitable method for the acquisition of ELF sequence data. Therefore, a bottom-up proteomics approach was selected to aid in the identification and function determination of ELF. Specifically, ESI-MS/MS was chosen to deduce *de novo* amino acid sequences from tryptic peptides produced from EC1 and EC2. This strategy has been widely used for *de novo* sequencing of peptides (Reviewed in Seidler *et al.*, 2010; Walther and Mann, 2010). The University of Victoria Proteomics Centre (Victoria, Canada) was chosen to perform the *de novo* sequencing and analysis of raw data.

Survey scans of EC1 and EC2 with electrospray ionization mass spectrometry following tryptic digestion are shown in Figures 6.1 and 6.2, respectively. The peaks that did not match those produced by trypsin or keratin (common protein contaminant) were selected for ESI-MS/MS (Figures 6.1 and 6.2). In total, 11 precursor ions produced from EC1 and EC2 were analyzed (Table 6.2). All eleven were detected in EC1 and only seven in EC2. However, the four precursor ions not found in EC2 were of low intensity in EC1 and may explain why they were not present at the levels required for *de novo* sequencing in EC2 samples, which contained less protein. The ESI Analyst program was used to predict possible amino acid sequences from the collision-induced dissociation spectra (performed by the Proteomics Centre) (Table 6.2). In total, 86 unique *de novo* peptide sequences with a prediction score $\geq$ 90% were selected for further analysis. Alignments of the sequences predicted from an individual precursor ion generally had similar sequences and rough consensus sequences are shown as where possible to indicate common amino acids that were predicted. Furthermore, seven parent ions, found in both EC1 and EC2, were predicted to share the same amino acid sequences, which provided very strong evidence that they were the same protein (personal communication with Derek Smith, University of Victoria Proteomics Centre).

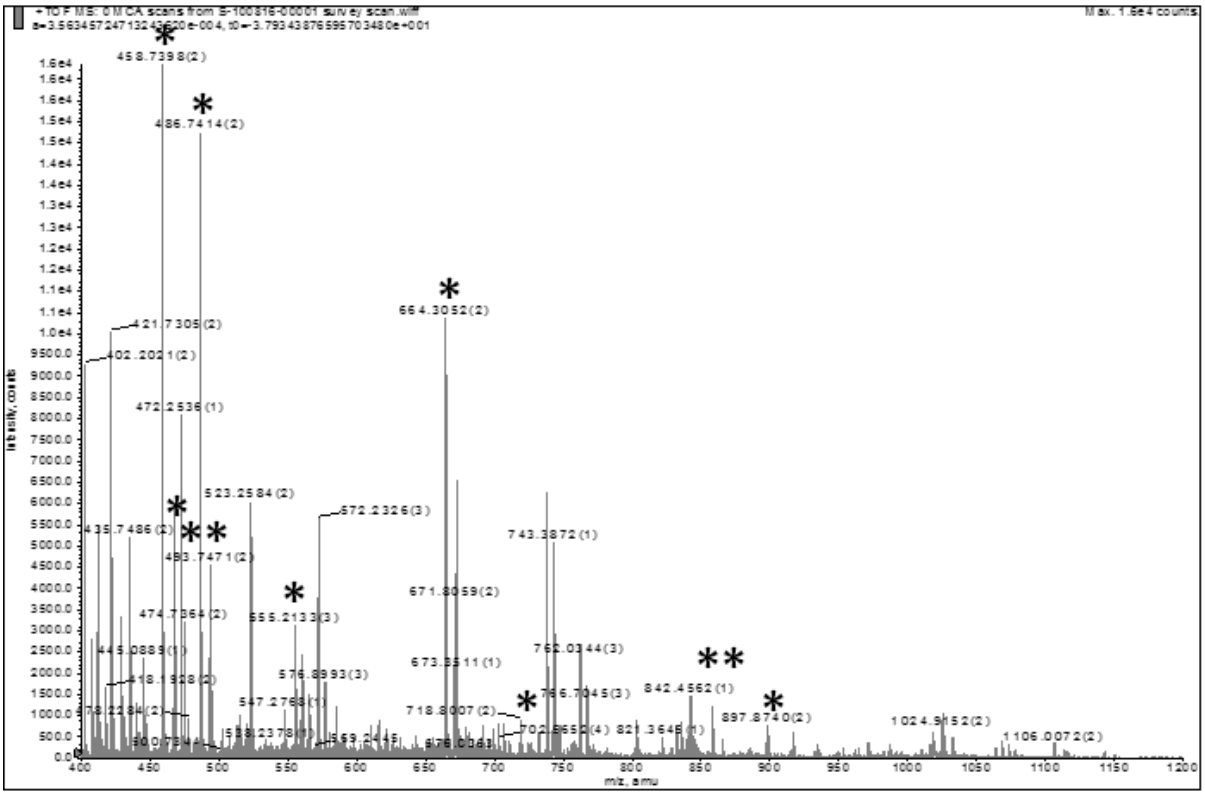

Figure 6.1 Survey scan of EC1 with electrospray ionization mass spectrometry. The above shows a screen shot of the survey scan, provided by the University of Victoria Proteomics Centre. The X- and Y-axes show the mass to charge ratio of the tryptic peptides, reported as (m/z) and the relative abundance of each peptide reported as intensity counts, respectively. The asterisks show which peaks were selected for ESI-MS/MS.

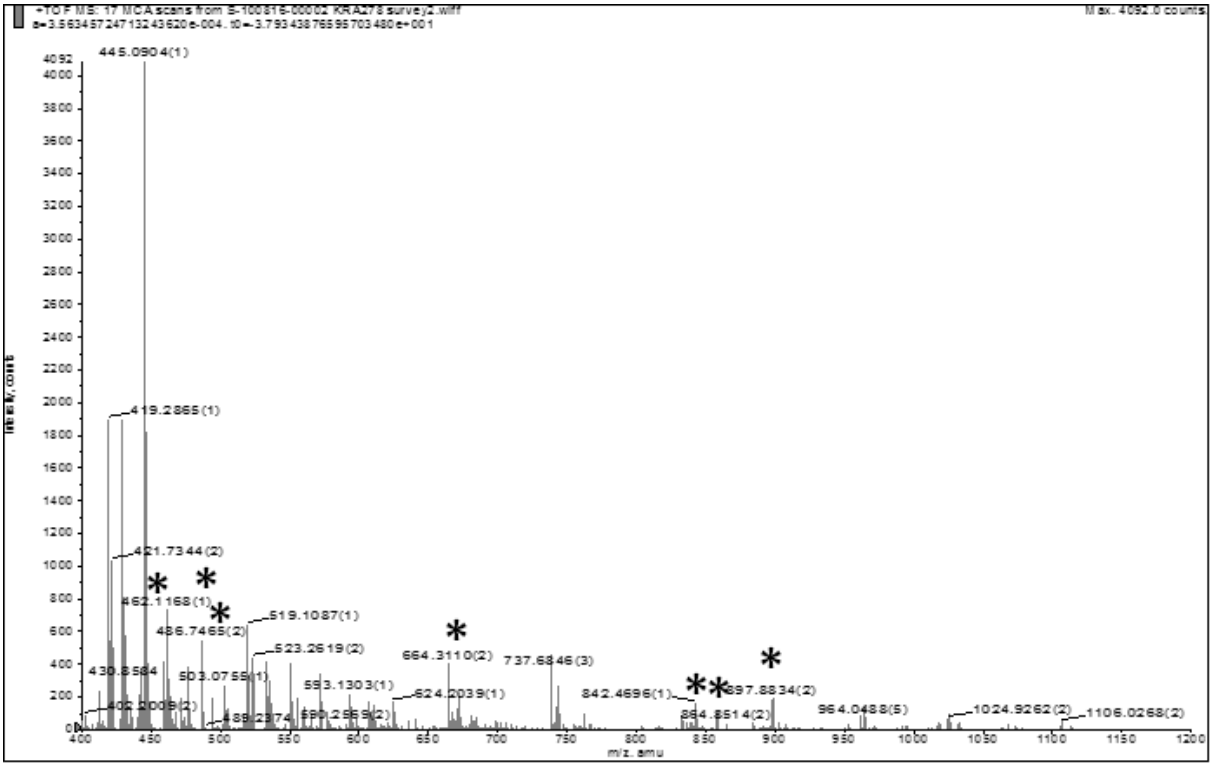

Figure 6.2 Survey scan of EC2 with electrospray ionization mass spectrometry. The above shows a screen shot of the survey scan, provided by the University of Victoria Proteomics Centre. The X- and Y-axes show the mass to charge ratio of the tryptic peptides, reported as (m/z) and the relative abundance of each peptide reported as intensity counts, respectively. The asterisks show which peaks were selected for ESI-MS/MS.

Table 6.2 Summary of unique *de novo* peptides proposed for each precursor ion following ESI-MS/MS of EC1 and EC2.

Precursor ion (m/z)[a]	Presence in sample[b]		Unique sequences[c]	Consensus sequences[d]	Most probable *de novo* sequences				
					Sequence[d]	Score (%)[e]	Mass (Da)		
	EC1	EC2					Observed	Expected	Δ
898	WP	✔	7	L/G--GADGNTR	QVAAMDCLLSGADGNTR	99.7	1796	1722	74
864	✔	WP	5	DYGSA**CHDVAY**SV--R	DYGSA**CHDVAY**SVVSR	99.9	1728	1729	-1
857	✔	✔	11	DYGSG**CHDVAY**S/AV/DV/D-R Y/D---**CHDVAY**ADVSR	DYGSG**CHDVAY**SVVSR	98.8	1714	1715	-1
719	✔	X	4	GS**CHDVAY**S/GV/E--R	GS**CHDVAY**SVGER	98.9	1438	1380	58
664	✔	✔	13	**VLET**-----Y/HGMK **VLET**AD---YGFK	**VLET**ADGGAYGMK	99.2	1329	1311	18
555	✔	X	5	GGAVHGDAAK	QVGGAVHGDAAK	96.0	1110	1109	1
494	✔	✔	12	--PDALESVK --PEGLE-K GAPD/W---GASVK	GAPDALESVK	99.9	987	986	1
486	✔	✔	8	--PEGVEWK GA/QPWVE--K	GAPEGVEWK	99.9	972	972	0
474	✔	X	5	None	LDGAANPYK	99.8	948	948	0
467	✔	X	5	None	GGPVSNGGYK	95.3	934	935	-1
458.7	✔	✔	11	LP--LPYK	LPWLPYK	97.7	917	916	1

a) The m/z was measured following electrospray ionization mass spectrometry and rounded to the nearest integer.
b) The symbols "✔"and "X" indicate if the precursor ion was present or absent, respectively. If the precursor ion was present but the count was too low for ESI-MS/MS it is indicated as having a weak peak (WP).
c) Only unique peptide sequences predicted with a score of ≥ 90% by ESI Analyst were counted.
d) Consensus sequences were generated by manual inspection of amino acid alignments. Bolded sequence represented sequences present in all predicted peptides from 865, 858 and 719 or 664 m/z parent ions.
e) Scores were determined by ESI Analyst.

The difference between the observed and expected masses of peptides can be used to detect PTMs, such as glycosylation (Reviewed in Larsen *et al.*, 2006). However, none of the peptides had differences great enough to indicate glycosylation or other large PTMs and were attributed to other types of chemical modifications, which may have been introduced *in vitro* or *in vivo*.

Initial searches performed using PEAKS software and collision-induced dissociation spectra data did not yield hits considered to be positive, as performed by the Proteomics Centre (Victoria, Canada). While *de novo* peptide sequencing is an important step in protein identification, it is not entirely useful without biological context, especially for proteins, such as ELF where very little is known about their molecular and functional characteristics (personal communication with Derek Smith, Proteomics Centre).

It was apparent that the lack of fungal genomic information and ESC/ELF sequence data was again a major obstacle, in spite of the identification of EC derived *de novo* peptide sequences, and prompted a change in strategy (at the time of this analysis still no genomes from EPF were publicly available). It was clear that strong positive hits, generally required to assign protein function/identity, would not be found. Therefore, hits on the borderline of positive and occasionally negative were needed also to be considered. A limitation of this strategy was the increased chance of false positives, but only fungal proteins were considered to help alleviate this. The programs used were PEAKS, which was kindly provided on a trial by Bioinformatics Solutions Inc. (Waterloo, Canada), and the publicly available BLAST (Altschul *et al.*, 1997) and mass spectrometry BLAST (Shevchenko *et al.*, 2001) tools provided by NCBI and the Bork Research Group at the European Molecular Biology Laboratory (Heidelberg, Germany), respectively. Each of the 86 unique *de novo* sequences were queried for homology using the

respective algorithms and the top hit for each was recorded and categorized. Identical hits were recorded once per parent ion, per search type, to limit biasing the results due to the variable number of unique sequences predicted for each. The general protein functions of binding (34 hits), signal transduction (27 hits) and anabolic/catabolic enzymes (21 hits) were categories that most commonly matched with the input sequences. To a lesser extent those involved with unknown (7 hits), enzyme regulation (4 hits) or transport functions (3 hits) were also observed.

The 34 hits found representing proteins with putative/known binding functions belonged to four sub-categories and were specifically involved in protein-membrane (14), protein-protein (13), protein-nucleotide (6) and protein-ligand (1) interactions. The 27 hits representing proteins involved in signal transduction were specifically involved in protein kinase (21), general signal transduction (3), G protein couple receptor (2) and cell-cell communication (1) functions. This analysis of the EC derived *de novo* sequences revealed a clear pattern with regards to the clustering of their respective binding and signal transduction mechanisms within the above sub-categories. Conversely, such a pattern was not apparent for the hits considered anabolic /catabolic enzymes. These 21 hits were scattered over 19 sub-categories, with only DNA helicase and tRNA synthetases containing more than one hit each. Furthermore, 19 of the 21 hits were found to be cytosolic proteins, which was in contention with the fact that ECs are secreted proteins.

Although these trends provided confidence that the research was progressing in the right direction to provide clues for protein identification/function prediction using the above strategy, more data was required for additional confirmation. Nonetheless, this type of analysis was very useful in providing insight into the likely structure/function of the ECs. Cross analysis of these results with the working hypothesis regarding ELF and its role in the physiology of *B. bassiana*

provided a more defined context to assess the findings. It was hypothesized that the ELF protein is secreted and involved in the establishment of an elevated tolerance to environmental stress conditions called EIT, for instance to heat in BS. Such a response would likely require an interaction between ELF and BS, which may be mandatory for transduction of the signal suspected to be carried by activated ELF. With this in mind, the binding and signal transduction functions, representing the majority of the hits, appear to be in agreement with the hypothesis. Furthermore, the other hits namely those associated with anabolic/catabolic enzymes may be false positives and were not included in the candidate function list. The scattering of hits within this group also provided credence to this.

A completely different strategy was to search for fungal ESTs using the NCBI database and the tBLASTn tool, which allowed translated nucleotides to be searched against protein input sequences. This resulted in hits from many different ESTs, the majority of which encoded for proteins which had functions that were unknown or unrelated to the suspected function(s) of ELF. Parent ions with an m/z of 865, 858, 719, 664, 494 and 487 generated ≥ 1 sequence that matched to a cDNA clone from *B. bassiana* (GT894266.1) (Figure 6.3). This EST contained 284 nts and appeared to encode several of the *de novo* sequences when it was translated using the -2 frame (i.e. translated from the mRNA produced from the reverse complement of the EST starting with the second nt from the 5' end). It was likely that some of the remaining *de novo* sequences were encoded by the full-length *elf*. Although the function of the protein deduced using the -2 frame was unknown, search results using the encoded peptide sequence with BLASTp and mass spectrometry BLAST had the best matches with a signal transduction/protein-protein interaction motif from *Podospora anserina* (Blast score = 33) and an unknown protein from *N. crassa* (Blast score = 69), respectively.

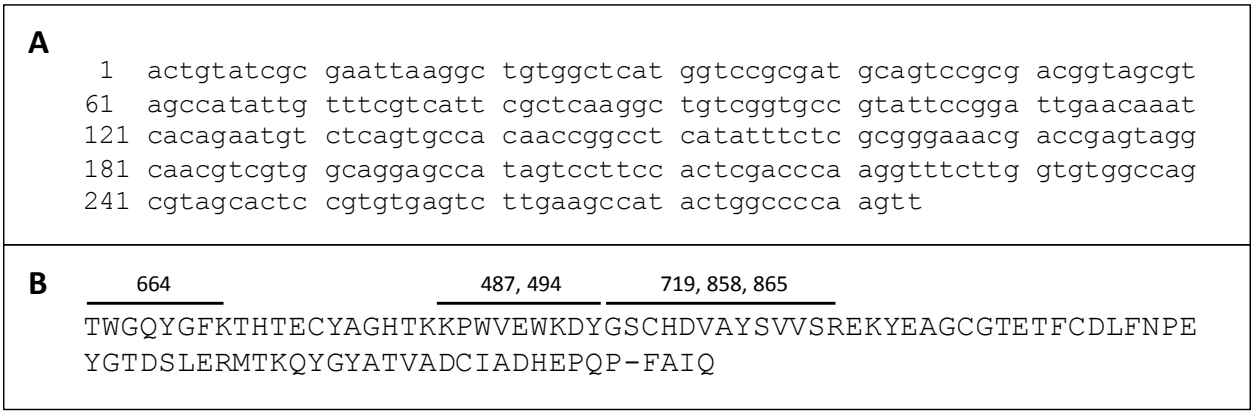

Figure 6.3 Sequence of *B. bassiana* cDNA clone GT894226.1 and its -2 translation frame. Panel A shows the DNA sequence of the cDNA clone. Panel B shows the amino acid sequence deduced from the DNA sequence when read using the translation -2 frame. The bold lines indicate the peptide sequences encoded by GT894226.1 that correspond with the *de novo* sequence identified in the respective parent ions, indicated by their m z^{-1} value. The dash symbol in panel B, before the ending FAIQ, indicates that an amino acid was not encoded at this location due to the presence the TAA stop codon.

Another search using the BLASTn tool to scan the EST and nucleotide databases had best matches with an encoded peptide of unknown function in the EPF *M. anisopliae* (Blast score = 38) and again with the putative signal transduction motif from *P. anserina* (Blast score = 33). Although the presence of the specific EST was not specifically mentioned by the authors, it is possible that it was produced by *M. anisopliae* BS, within the hemocoel of migratory locust (*L. migratoria*) (Zhang and Xia, 2009). Furthermore, the EST that was predicted to partially encode ELF was detected in *B. bassiana* mycelia (which also likely contained BS) during growth in liquid media that was supplemented with cuticular extracts from coffee berry borer (*Hypothenemus hampei*) (Mantilla *et al.*, 2012). These observations may be consistent with the production of ECs, which is correlated with the presence of BS in *B. bassiana*. The sequence information from the cDNA clone, from *B. bassiana*, which potentially corresponded to a section of *elf* will be exploited in the next section for the elucidation of its entire ORF.

6.4.2 Discovery and cloning of *elf*

The PCR techniques 3' and 5' RACE were chosen to amplify the sections that flank the sequence corresponding to GT894226.1. The oligonucleotide primers were designed to specifically anneal to GT894226.1 derived sequences, as directed by the RACE kit vendor (Figure 6.4). The expected sizes of the predicted RACE products were estimated using the sequence information of the EST and the knowledge that the nascent size of EC2 is predicted to be ~ 26 kDa. A protein of this size was estimated to contain ~ 236 amino acids by considering an average amino acid mass of ~ 110 Da and would require a coding DNA of ~ 700 bp. In addition, consideration was given to the size of the oligonucleotide adaptor and amount of polyadenylation, which would also influence the size of the RACE products (see Section 3.4.2).

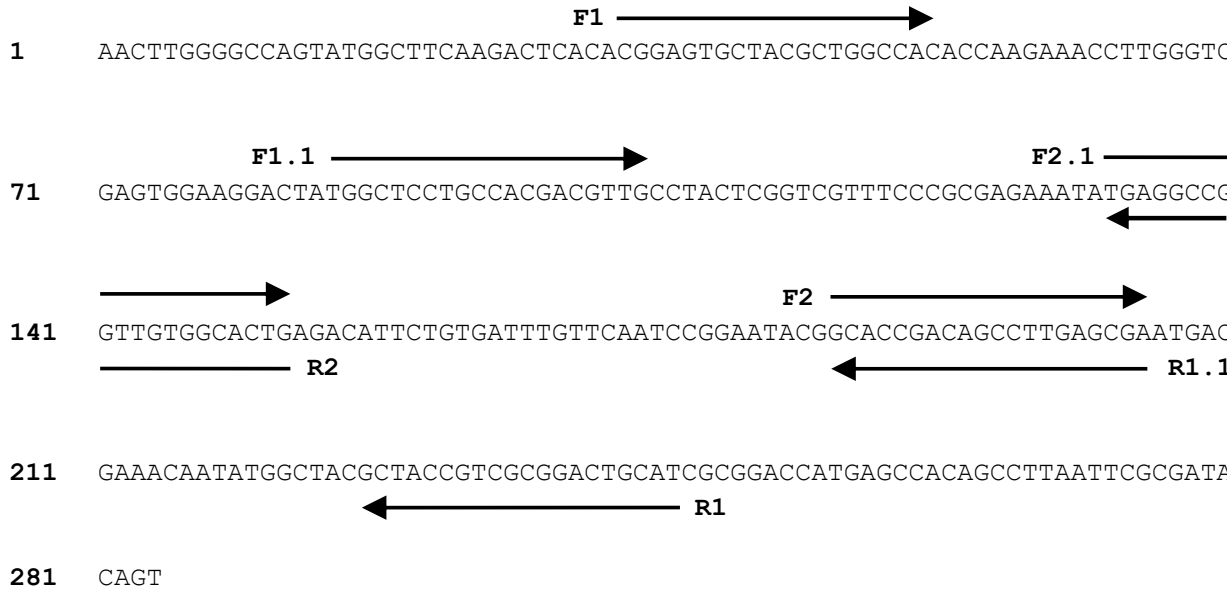

Figure 6.4 Overview of primer templates for RACE to amplify the sections that flank *B. bassiana* cDNA clone GT894226.1. The above shows the reverse complement sequence of clone GT894226.1, which was suspected to encode *de novo* peptides identified in EC1 and EC2. The arrows show where the ELF primers were designed to anneal. The F and R primers were designed for 3' and 5' RACE, respectively, in addition to product confirmation.

The optimal annealing temperature of these primers was tested empirically. This was by performing PCR using genomic DNA as template and annealing temperatures of 63, 61, 59 and 57 °C (Figure 6.5). Due to the locations the ELF primers were designed to anneal, amplicons of ~ 210, 170 and 160 bp were expected. All reactions produced amplicons of the expected sizes, but some non-specific products were present in reactions with an annealing temperature of 61 °C (Figure 6.5; lanes 2 and 6). However, reactions with a 61 °C annealing temperature provided the highest degree of amplification of the expected products. Therefore, this annealing temperature was chosen as optimal for amplification of the candidate *elf* using RACE. It was reasoned that increased amplification of products derived from the candidate *elf* was desired and their predicted sizes and size shifts following nested RACE could be used to differentiate them from non-specific products.

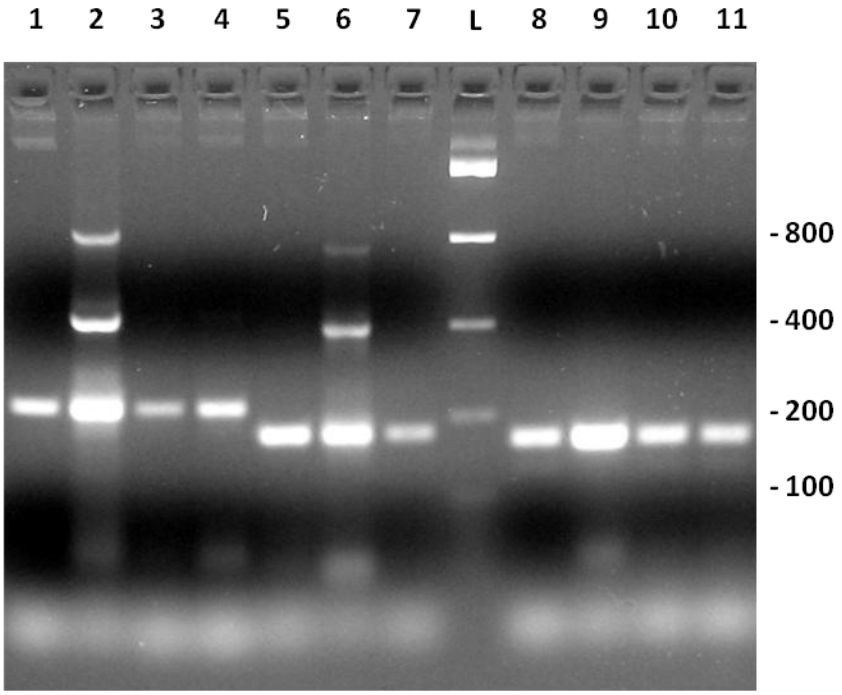

Figure 6.5 Effect of annealing temperature on amplification of sections of the candidate *elf* with PCR. The above shows the results of PCRs to amplify sections of candidate *elf* from *B. bassiana* DNA and separated by 1.5% (w v^{-1}) agarose gel electrophoresis. Primer sets ELF-F1/-R1, ELF-F1/-R1.1 and ELF-F1.1/-R1 were included in PCRs shown in lanes 1-4, 5-7 and 8-11, respectively. The annealing temperatures used for these reactions were 63 °C for lanes 1, 4 and 8; 61 °C for lanes 2, 6 and 9; 59 °C for lanes 3, 7 and 10; and 57 °C for lanes 4 and 11. Lane L indicated the DNA ladder and their masses are shown (bp) to the right.

With the knowledge that the ELF primers could amplify products of the expected size, RACE was employed to amplify the 5' and 3' ends of the candidate *elf* gene. The RNA extracted from *B. bassiana* was prepared for RACE and used as the template for the initial reactions. Touchdown PCR (Don *et al.*, 1991) was performed using the appropriate ELF and RACE primers that would specifically anneal to the candidate *elf* and RACE adaptor sequences, respectively (Figure 6.6A). The 3' and 5' RACE reactions produced amplicons of ~ 500 and ~ 800 bp, respectively, and non-specific products were also present. These reactions were then used as templates for nested RACE reactions to gain additional confidence in which products were likely derived from the candidate *elf* (Figure 6.6B). The nested reactions using the primers ELF-F2, ELF-F2.1 and ELF-R2 with their appropriate nested RACE primer, produced amplicons of ~ 320, 380 and 700 bp, respectively, in addition to non-specific products. These sizes were within the range that was expected, since the nested reactions were anticipated to produce specific products of ~ 80-180 bp less than those produced by the initial RACE reactions, depending on the primer used. These results provided confidence that the RACE products generated in reactions with the ELF-F1, ELF-F1.1, ELF-R1 and ELF-R1.1 primers were derived from the candidate *elf* sequence. These products were inserted into pCR 4-TOPO and used to transform *E. coli* DH5α. All transformations except those with PCR4:ELF-R1.1, produced white, antibiotic resistant colonies. However, this did not limit the sequence information generated since PCR4:ELF-R1 was expected to contain a larger insert with additional sequence information compared to PCR4:ELF-R1.1.

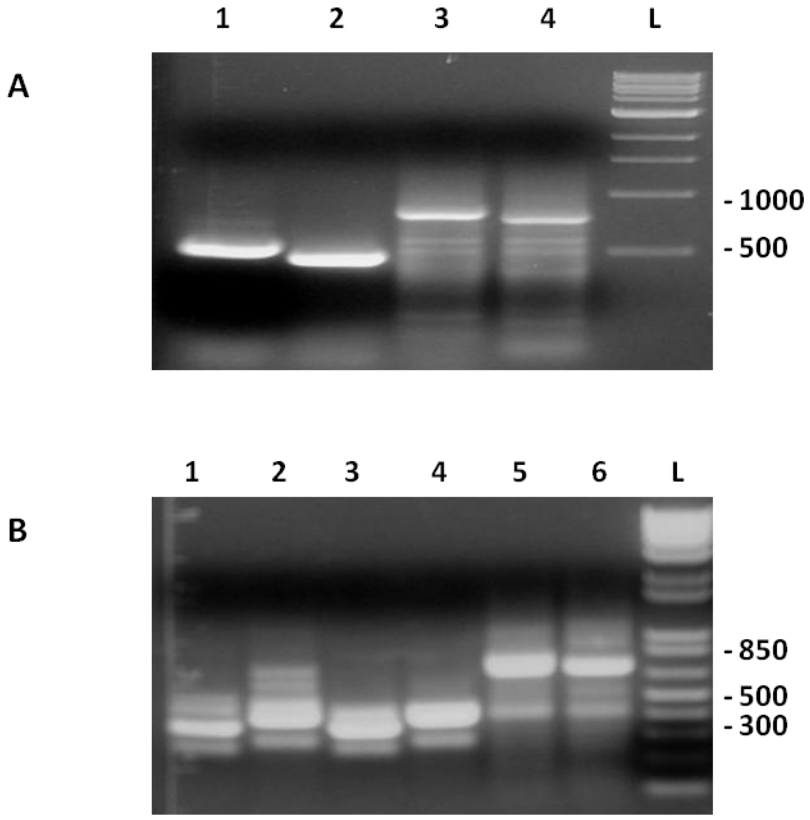

Figure 6.6 Amplification of 5' and 3' regions of the candidate *elf* with RACE. Panel A and B show the results of RACE with outer and inner RACE primers, respectively, to amplify the regions of candidate *elf* flanking those in GT894226.1 from *B. bassiana* separated by 1% (w v^{-1}) agarose gel electrophoresis. Panel A shows the reactions performed with cDNA as template with outer 3' RACE or 5' RACE primers in lanes 1-2 and 3-4, respectively. The ELF specific primers used in these reactions were ELF-F1, ELF-F1.1, ELF-R1 or ELF-R1.1 as shown in lanes 1, 2, 3 and 4, respectively. Panel B shows the nested reactions performed with inner (nested) 3' RACE or 5' RACE primers in lanes 1-4 and 5-6, respectively. The reactions shown in the lanes 1, 2, 3 and 4 of panel A were used as templates for the reactions shown in lanes 1-2, 3-4, 5 and 6, respectively, in panel B. The gene specific primers used in these reactions were ELF-F2 for lanes 1 and 3; ELF-F2.1 for lanes 2 and 4; and ELF-R2 for lanes 5 and 6. In both panels, lane L indicated the DNA ladder and their masses are shown (bp) to the right.

Colony PCR was performed on PCR4:ELF-F1 clones with primers set ELF-F2.1/-R1 and on PCR4:ELF-F1.1 and PCR4:ELF-R1 clones with primer set ELF-F1/-R2 primers to confirm that they contained the insert derived from the candidate *elf*. These reactions produced amplicons of ~ 110 bp, which was the expected size for both (not shown). In addition, the 110 bp product was only present when the candidate *elf* inserts were present as template, since non-transformed *E. coli* did not produce this amplicon. Sequencing of the inserts containing sections of the candidate *elf* confirmed they contained sequences that were identical to GT894226.1 (Figure 6.7). Furthermore, the sequences amplified by 5' and 3' RACE overlapped and contained an in-frame start and stop codon, respectively. It was apparent that GT894226.1 was derived from the 3' end of the mRNA transcript since it aligned with sequence found with 3' RACE, which had a poly-A tail, indicating that it was derived from the 3' end of mRNA (not shown). However, no poly-A site was found in any of the candidate *elf* sequences using the predictive sequences of ATTAAA or AATAAA and the predicted 3' untranslated region also lacked sequences indicative of AUUUA repeats on its corresponding mRNA.

Additional PCRs were performed to confirm the presence of the full-length candidate *elf* and reverse transcript using genomic DNA and cDNA, respectively, in *B. bassiana* GK2016 and ARSEF 3113. This was performed with the ELF specific primers ELF-Fa and ELF-Ra, which were designed to anneal upstream and downstream of the predicted ORF, respectively. These reactions yielded a product of ~ 900 bp from both genomic DNA and cDNA templates prepared from *B. bassiana* GK2016 and genomic DNA from the ARSEF strain, respectively (Figure 6.8; the product from *B. bassiana* GK2016 genomic DNA was not photographed). These products were of the expected product size since the forward and reverse primers bound 53 nts upstream and 86 nts downstream of the 741 nt ORF, respectively. These reactions were also performed

with genomic DNA templates prepared from *L. longisporum*, *M. anisopliae* or *T. inflatum*, but no products were detected, suggesting that if these EPF encoded *elf*, the primers used were not specific enough to yield a product derived from the respective fungus, or that these fungi may not contain an *elf* or a similar sequence.

Sequencing of the three above products confirmed that the candidate *elf* was present as a contiguous sequence in both genomic DNA and cDNA from *B. bassiana* GK2016 and shared ~ 97% sequence identity with that from the genomic DNA from the ARSEF strain (Figure 6.9). Furthermore, the sequences from GK2016 in both cDNA and genomic sources were identical; therefore the candidate *elf* lacked an intron. Similarly, the sequence from the ARSEF3113 strain had an ORF of the same size as that found in GK2016 with no sites indicative for intron splicing (Kupfer *et al.*, 2004). Therefore, it was likely that this sequence also lacked an intron. In addition, the predicted start codons in the candidate *elf* from either strain had adjacent sequences that corresponded with a Kozak sequence (ACAAUGG; start codon underlined). Kozak sequences are required in mRNA for efficient initiation of translation by ribosomes, which provided further confidence that these Met codons are truly start codons for the ORF (Kozak, 1986).

Figure 6.7 Sequence of the sections of the candidate *elf* that were produced by RACE. Panel A and B show the DNA sequences (5' to 3' order one the predicted coding strand) of the cDNA sections which were identified using 5' and 3' RACE, respectively. The underlined sequences denote those which match to the EST GT894226.1. The bolded font in panels A and B show the in-frame start (ATG) and stop (TAA) codons, respectively. In Panel B the next nts in the 3' direction from those shown were a consecutive run of adenosine residues, indicating the poly-A tail.

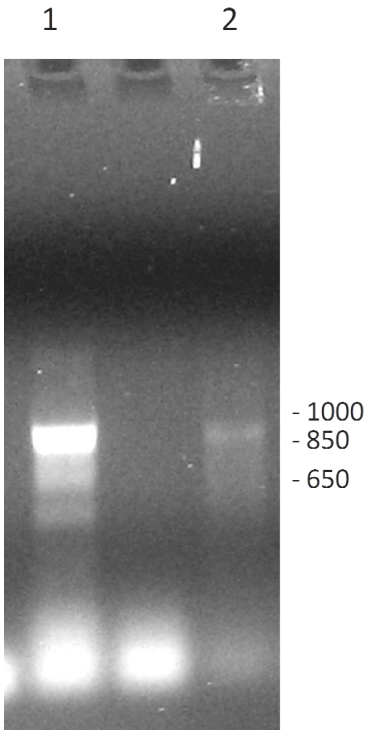

Figure 6.8 Results of PCR to amplify the candidate *elf* as a single product from two strains of *B. bassiana*. The above shows the PCRs separated by 1% (w v^{-1}) agarose gel electrophoresis. The PCRs shown in lanes 1 and 2 were performed with the primer set ELF-Fa/-Ra and the templates used were cDNA from *B. bassiana* GK2016 or genomic DNA from *B. bassiana* ARSEF3113, respectively. The sizes of the DNA ladder are shown (bp) to the right of the photograph.

Figure 6.9 The DNA sequence of the candidate *elf* from two *B. bassiana* strains. The sequences were amplified with PCRs using the primer set ELF-Fa/-Ra from the genomic DNA of *B. bassiana* GK2016 (GK) and ARSEF3113 (AR). Sequence obtained from cDNA prepared from *B. bassiana* GK2016 was identical to that from genomic DNA, but not shown. The in-frame start and stop codons are indicated in the sequence with a line and label.

The amino acid sequences deduced from the ORFs in both examples, candidates for *elf* had 97.6% similarity (Figure 6.10). The subsequent sections of this thesis were concentrated on the candidates for ELF/*elf* from *B. bassiana* GK2016 and will be the focus of the following analysis. Several molecular features of the candidate *elf*'s deduced gene product were consistent with previous findings were observed.

Firstly, two additional *de novo* sequences (459 and 555 m/z) were found within the sequence of the predicted protein, in addition to the six previously identified, for a total of eight of the possible eleven peptides found in EC1 and EC2. It is possible that the remaining three sequences were from contaminants, which is common in protein sequencing. It is also possible that the sequence prediction was not accurate, which can be complicated by the presence of PTMs which can influence the size and charge of the parent ions (Larsen *et al.*, 2006). Nonetheless, matching eight peptide sequences to a single ORF is more than sufficient to confirm that EC1 and EC2 are encoded by it.

Secondly, a secretion signal peptide was identified in the deduced product encoded by the candidate *elf* (Figure 6.10). This was consistent with the localization of EC proteins with ELF activity, which accumulated in the extracellular fraction of growing *B. bassiana* cultures (see sections 4.4 and 5.4). Secretion specific signal peptides are required for their translocation to the extracellular environment and changes to the signal peptide can influence its cellular destination (McKinnon *et al.*, 2009). Furthermore, secretion of a protein is often linked with its glycosylation (Reviewed in Peberdy, 1999).

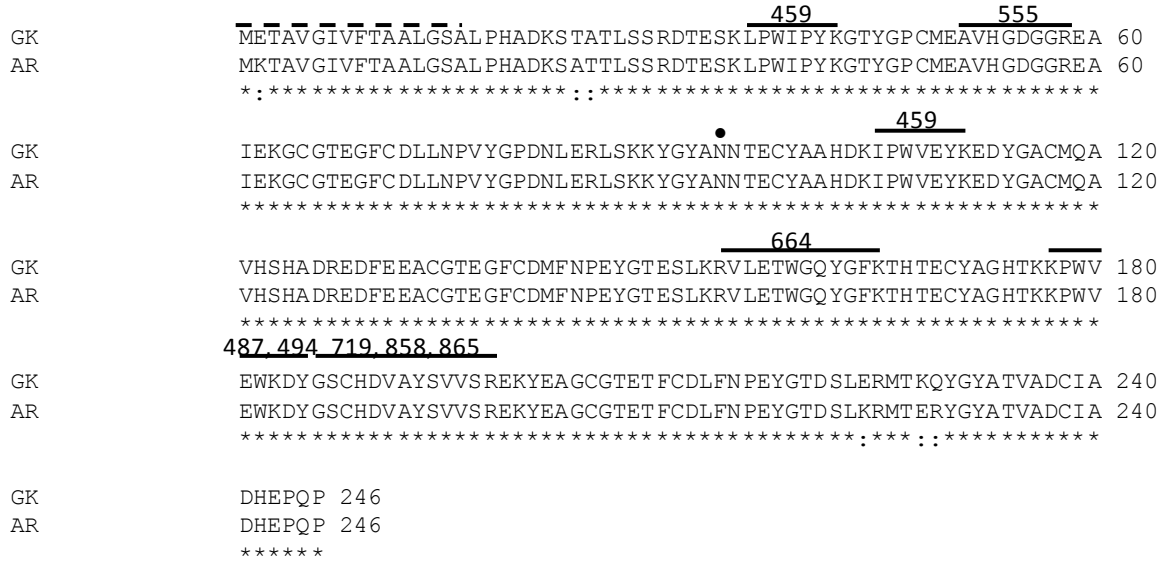

Figure 6.10 Deduced amino acid sequence of the predicted ORF encoded by the candidate *elf* sequences from the *B. bassiana* strains GK2016 (GK) and ARSEF 2860 (AR). The first 17 aa were predicted to possess a secretion signal and is indicated with a dashed line. The filled circle (●) indicates the location of a predicted N-glycosylation site. The solid lines show the sequences that matched to those identified in EC1 and EC2 through *de novo* sequencing and the m z^{-1} value of corresponding parent ions are also indicated.

This prompts the third similarity, which is the presence of an N-linked glycosylation site in the sequence encoded by the candidate *elf* (Figure 6.10). This type of glycosylation occurs at asparagine residues and potential glycosylation sites can be predicted by the sequence N-X-S/T (X can be any aa) (Bause, 1983). Potential O-linked glycosylation sites are also present, but possibly any serine or threonine can possess this PTM, therefore its prediction by sequence analysis is less certain than with N-linked types (Reviewed in Goto, 2007). However, if ELF possessed both an N- and an O-linked group, they would average 1 kDa each, since this PTM was found to account for ~ 2 kDa of the mass of EC1 (see section 5.4.2). Therefore, both types of glycosylation may be possible to exist together, but would be near the minimum size possible for these types of PTMs (Reviewed in Peberdy, 1999).

Lastly, the ORF encoded 246 aa, corresponding to a nascent protein with a mass of ~ 27.4 kDa. Following cleavage of the predicted signal peptide the mass of the unmodified ELF would be ~ 25.9 kDa, which is nearly identical to that of the non-glycosylated EC2.

In summary, the candidate *elf* encoded a protein that possessed: 1) 8 of the 11 *de novo* peptide sequences found in EC1 and EC2; 2) a potential secretion signal peptide; 3) predicted N- and O-linked glycosylation sites; and 4) a molecular mass consistent with previous experimental findings shown in the previous two sections of this thesis (see sections 4 and 5). These provided additional confidence that the candidate *elf* encoded a product with molecular features that are consistent with EC1; a protein that has the ability to increase heat tolerance in BS, which is the only currently known measureable effect of EIT.

It was important to determine if the putative ELF had sequence similarity with other proteins with known functions. A BLASTp search using the putative ELF sequence from *B. bassiana* GK2016 as the input and an E-value cut-off of $< 10^{-5}$ returned 10 hits, all from EPF;

five each from *B. bassiana* ARSEF 2860 and *M. anisopliae* ARSEF 23 (also referred to as *M. robertsii*) (Figure 6.11A). One of the hits from *B. bassiana* ARSEF 2860 was an apparent homologue of the putative ELF sequence and like that from *B. bassiana* ARSEF 3113 had 97% sequence identity with that from GK2016. However, this protein had no function assigned, nor did any of the others. The remaining nine hits had estimated masses of 20.1 to 45.5 kDa and sequence similarities with the putative ELF from GK2016 that ranged from 26% to 56%, which can be similar enough to possess a common structure (Kelley and Sternberg, 2009); however none had solved structures. As expected due to their sequence conservation, the three putative ELFs segregated into the same clade when their phylogenetics were modelled, while the other nine similar sequences were segregated into different clades (Figure 6.11B).

Three of the sequences [two (GI 400592848 and 400593516) and one (GI 322702275) from *B. bassiana* and *M. anisopliae*, respectively] had considerable sequence conservation in their N-terminal regions (up to 50% more conservation) with the putative ELF sequences compared to the six other similar sequences (Figure 6.11B, that from GK2016 is shown as a representative putative ELF sequence). Sequence conservation between the putative ELFs and their potential homologues may imply a conserved structure/function amongst these sequences. All of the putative ELF sequences and the nine homologues were analysed against the Prosite database (de Castro *et al.*, 2006), but did not reveal any known domains or signatures, other than for a hypothetical 25 kDa protein from *M. anisopliae* (322702864) which matched weakly to a prokaryotic membrane lipoprotein lipid attachment site profile. All of the sequences were predicted to have a secretion signal peptide (16 to 23 aa in length), suggesting that they may all be secreted. But other than this similarity it was apparent that the molecular function(s) of the putative ELFs and similar sequences could not be elucidated by sequence analysis alone. The

finding that the most similar sequence homologues were all found in EPF suggested that putative ELF and the potentially related proteins may possibly possess conserved functions that are import in the lifecycle of this group. Heat tolerance acquisition has been considered an important response in many organisms, including EPF. In addition to being potentially exposed to supra-optimal temperatures while subsisting as an saprophyte, when behaving as a pathogen this group of fungi can be exposed to temperatures that are elevated above the ambient by the host insect's behavioral activity and ability to thermal regulate their body temperature (Inglis *et al.*, 1997). Therefore, it is important to establish that the candidate *elf* encoded a functional ELF that is able to promote EIT to heat in BS.

6.4.3 Transgenic expression of *elf*

To determine if the candidate *elf* from *B. bassiana* GK2016 encoded a functional gene product it was expressed heterologously. The pPicZ system was chosen for this because it allowed controlled overexpression in the yeast *P. pastoris*. These vectors possess the alcohol oxidase promoter which allows the induction of genes under its control when methanol is present in the medium. Furthermore, this system has been employed to heterologously express and secrete glycosylated proteins at high concentration (up to 2.5 g L^{-1}) (Tschopp *et al.*, 1987). Extracellular accumulation of ELF was expected to be an asset for downstream experimentation, since the number of contaminating proteins would be less than in a system that directed the expressed protein to the cytosol or other cellular location, which would require more extensive purification.

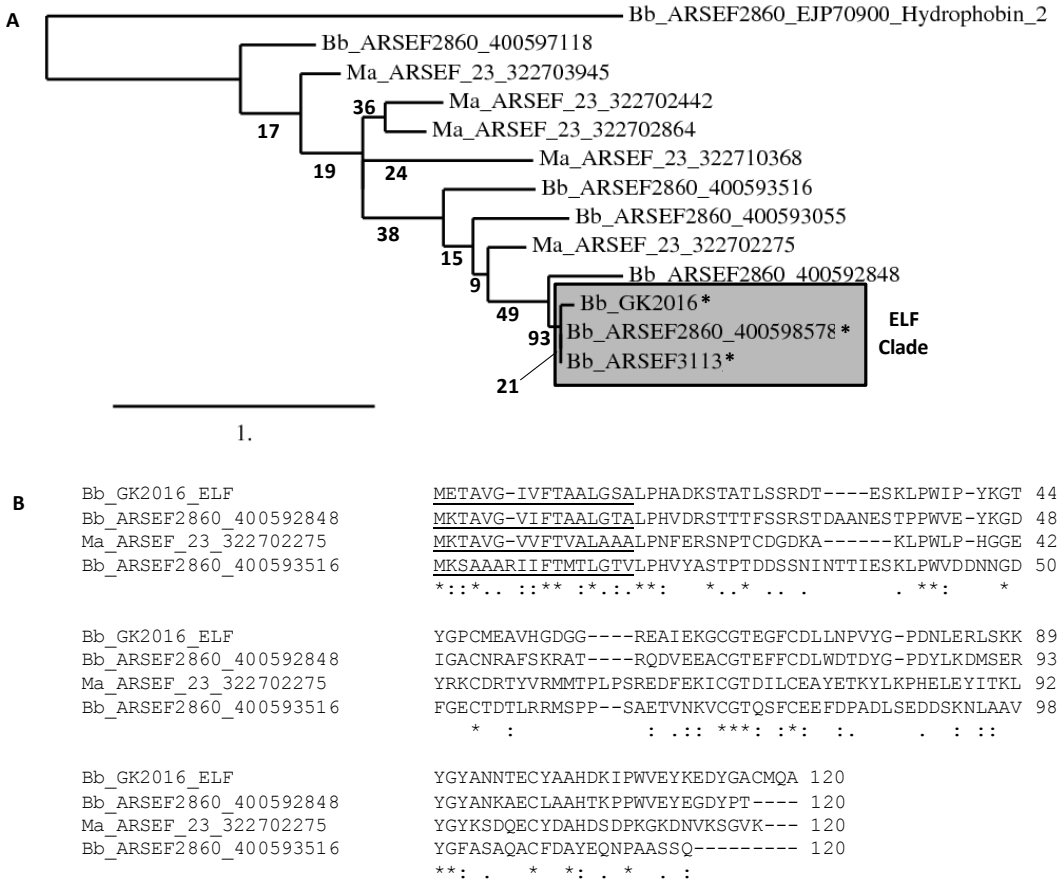

Figure 6.11 Phylogenetic and sequence analysis showing relationships between three putative ELFs from *B. bassiana* (Bb) and their most similar sequences from *B. bassiana* ARSEF 2860 and *M. anisopliae* (Ma) ARSEF 23. The taxon labels indicate the organism and strain that the input sequences were derived from and the Geninfo identifier numbers (when available), separated by an underscore. Panel A shows the predicted phylogenetic relationship between thirteen sequences. Two were homologues of putative ELF from *B. bassiana* GK2016 and were found in *B. bassiana* ARSEF 2860 and ARSEF 3113 and all three are indicated with an asterix (*) and ELF clade label. Of the remaining 10 sequences analysed, 4 and 5 were from *B. bassiana* and *M. anisopliae*, respectively. Support values (%) are provided for each branch; the scale conveys branch lengths to the number of substitutions per site and hydrophobin-2 from *B. bassiana* ARSEF 2860 was selected as the outgroup because its deduced size was approximately the same as putative ELF (29 kDa) and is extracellular. This analysis was performed using the service provided by Dereeper *et al*. (2008). The maximum likelihood method in the PhyML program (v3.0 aLRT) was used to reconstruct the phylogenetic tree. Support for internal branching was evaluated using the bootstrap method with 500 replicates (Guindon and Gascuel, 2003). The substitution models were selected assuming an estimated proportion of invariant sites equal to 0.072 and the gamma shape parameter was estimated to be 2.269. Panel B shows an alignment of the first 120 N-terminal amino acids of putative ELF from GK2016 and three other sequences which shared sequence similarity in this region with putative ELF. The underlined sequences indicate the predicted signal peptide.

The strategy was to insert the candidate *elf* with and without the encoded signal peptide into pPicZB and pPicZαA, respectively. These vectors would then be used to transform *P. pastoris* to create a transgenic yeast strain that could overexpress the candidate *elf*. The translocation of its gene product would be under the direction of its native signal peptide or the α-mating factor in pPicZB and pPicZαA, respectively. The PCRs using PCR4:ELF-Fa-Ra as the template and the primers sets ELF-Fb/-Rb and ELF-Fc/-Rb were used to produce amplicons containing the predicted ORF of candidate *elf* with and without the encoded signal peptide, respectively, and were of the expected size of ~ 740 and ~ 690 bp (determined by agarose gel electrophoresis; not shown). In addition, an in-frame Kozak sequence (AAAA) was incorporated immediately upstream of the predicted start codon in the ELF-Fc/-Rb products. This sequence is required for efficient initiation of translation. These sequences were inserted into pCR 4-TOPO and were termed PCR4:ELF-Fb-Rb and PCR4:ELF-Fc-Rb, which encoded the putative ELF with and without the predicted native secretion signal peptide, respectively. The restriction enzymes *EcoRI* and *XbaI* were used to remove the *elf* inserts from PCR4:ELF-Fb-Rb and PCR4:ELF-Fc-Rb and were directionally subcloned into the same sites within the multiple cloning sites of pPicZB and pPicZαA, respectively. The resulting constructs were named PicZ:ELF and PicZα:ELF which could induce expression of the gene of interest under the control of the alcohol oxidase promoter.

The PicZ:ELF and PicZα:ELF vectors were introduced into *E. coli* and one clone with the correct reading frame, which was assessed by sequencing, was selected for each of the two different vector containing strains and grown in 100 mL of Terrific Broth with 25 µg mL^{-1} Zeocin to generate a sufficient amount of each plasmid, which was recovered by the alkaline plasmid extraction (Sambrook and Russell, 2001). For each construct, 25 µg was recovered from

each culture and 12 µg of each construct was linearized separately with *PmeI* or *SacI*, which was assessed by agarose gel electrophoresis. Six micrograms of each linearized vector was used to transform the methylotrophic yeast, *P. pastoris* in duplicate using electroporation and produced 7-248 and 15-47 transformants per µg of PicZ:ELF and PicZα:ELF DNA, respectively. These transformation rates were lower than the expected range of 10^3 to 10^4 transformants per µg of DNA (according to Invitrogen); however, hundreds of CFUs were present, which provided a sufficient pool of clones to analyse. A total of 29 transformants (12 and 17 for each PicZ:ELF and PicZα:ELF, respectively) able to grow on growth medium containing 1000 µg mL^{-1} Zeocin were selected. Growth, as indicated by colony size (measured as the diameter), has been shown to be positively correlated with the expression of the gene of interest, according to the manufacturer.

Colony PCR was used to screen the PicZ:ELF and PicZα:ELF transformants (29 in total) with the primer sets ELF-Fc/-Rb and 5'Aox/3'Aox to confirm they possessed the *elf* insert and that it was within the expression cassette, respectively. Reactions with ELF-Fc/-Rb produced amplicons of ~ 690 bp in all clones tested, while those with the Aox primers produced amplicons of ~ 990 and ~ 1200 bp in PicZ:ELF and PicZα:ELF containing transformants, respectively. These products were of the expected size, due to the knowledge of the annealing locations of the primers and confirmed that the expression cassette was integrated within the genome of the *P. pastoris* and contained the candidate *elf*.

The 29 transformants were also screened on their ability to produce extracellular proteins(s) with approximately the same mass as the ECs produced by *B. bassiana*. This was performed by culturing the transformed *P. pastoris* cell lines in the presence of methanol, using the manufacturer's directions, but was scaled-down to 10 mL. The amount of protein secreted

by the PicZ:ELF and PicZαA:ELF transformants ranged from 5.5 to 33 and 55 to 259 μg mL^{-1}, respectively.

From the above clones, six and eight were selected for further analysis for PicZ:ELF and PicZα:ELF containing *P. pastoris* lines, respectively. These cultures produced the highest extracellular protein contents observed for their respective cell line (see above paragraph). Both the intracellular and extracellular fractions were subjected to SDS-PAGE to analyze their protein banding pattern (Figure 6.12). Only in PicZα:ELF containing *P. pastoris* lines were proteins detected in their extracellular fractions when stained with blue silver dye, which has a detection limit of ~ 1 ng per protein (Candiano *et al.*, 2004). Two bands, corresponding to proteins of ~ 31 and 35 kDa were most prominent, which are ~ 3 and 7 kDa larger than the functional glycoform of ELF (EC1) produced by *B. bassiana*, respectively. Furthermore, both of these proteins were only found to accumulate in the medium when methanol was present, which is indicative of overexpression using this system (αELF2 is shown as a representative for PicZα:ELF containing cell lines in Figure 6.13). In addition, the 31 kDa species was found to accumulate at concentrations that were greater than the 35 kDa species, which indicates that more of it was produced, secreted and/or was more stable in the medium.

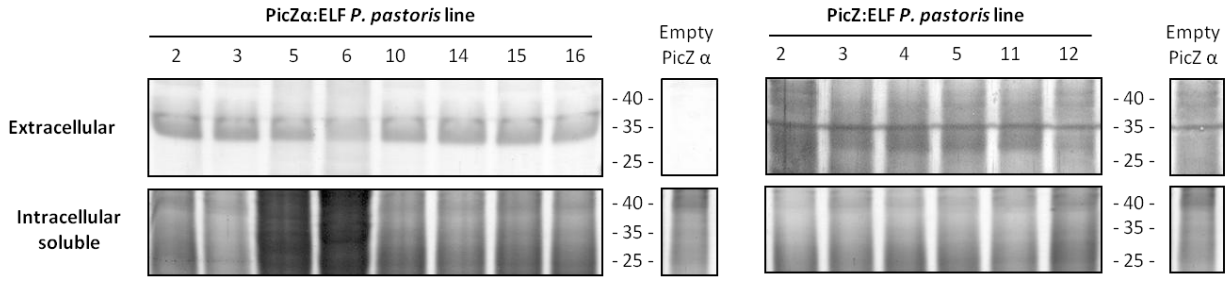

Figure 6.12 The banding patterns following SDS-PAGE of extracellular and soluble intracellular fractions prepared from *P. pastoris* lines containing PicZ:ELF or pPicZα:ELF expression cassettes. The fractions were prepared from cultures grown for 4 d, in the presence of methanol. Lanes with extracellular fractions were loaded with 10 µL of CFF prepared from pPicZα:ELF, PicZ:ELF or PicZα (no insert) cultures and contained 1.7 – 2.6, 0.2 – 0.3 or 0.5 µg of protein, respectively. Intracellular soluble fractions from test and control samples were harvested from cells obtained from 1 mL of the same culture used to prepare their extracellular fractions. Samples were separated through a 12% polyacrylamide (w v^{-1}) gel. All gels were stained with blue silver dye, except the extracellular samples from PicZ:ELF lines and the empty PicZα sample shown to the right of the PicZ:ELF containing extracellular samples, which were stained with silver nitrate to visualize the relatively low amount of protein present. The cell line number for each transformant type is shown above the photographs. The fraction type is indicated to the left and mass (kDa) of molecular ladder to the right of the test samples.

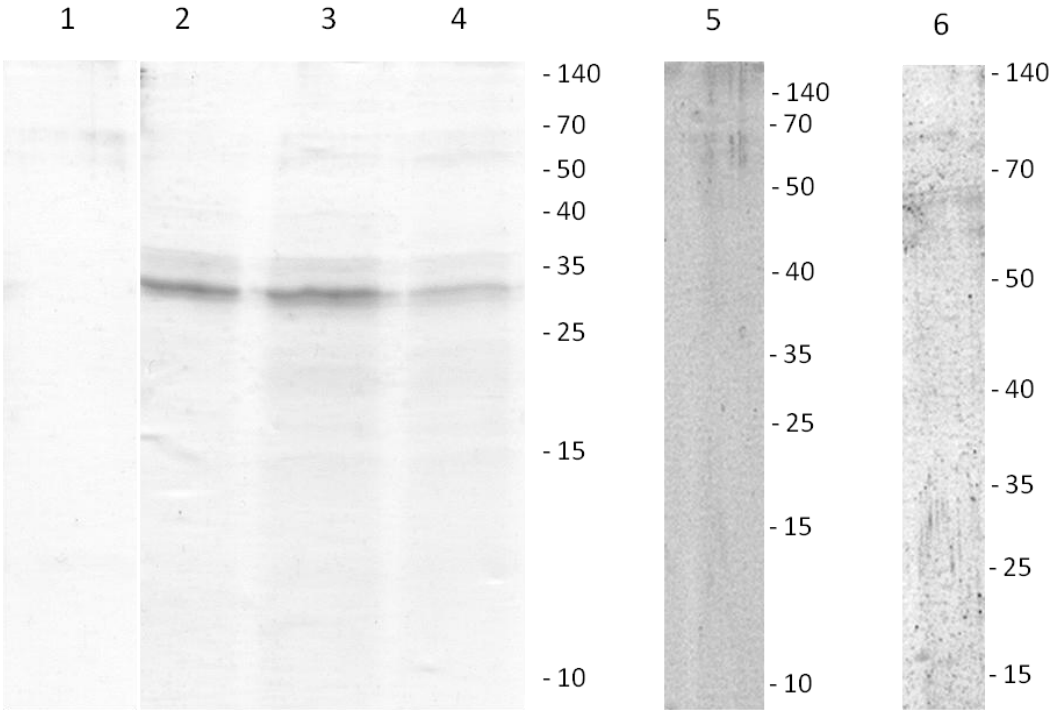

Figure 6.13 Protein banding pattern of CFF prepared from αELF2. Lanes 1-4 were CFF prepared from αELF2 cultures grown in the presence of methanol for 0, 24, 48 or 72 h. Lane 5 was CFF prepared from αELF2 culture grown for 48 h in the absence of methanol. Lane 6 was CFF prepared from *P. pastoris* containing empty pPicZα grown for 48 h in the presence of methanol. Lanes 1-4, 5 and 6 were resolved separately through 15%, 15% and 12% (w v^{-1}) polyacrylamide gels, respectively. All lanes contained 12.5 µL of supernatant from their indicated cell culture. The masses (kDa) of the molecular ladder are indicated to the right of each group that was resolved on the same polyacrylamide gel.

The cell lines containing PicZ:ELF appeared to also secrete a 31 kDa protein species, but required silver staining for its visualization (Figure 6.12). Clearly, secretion of the 31 kDa candidate for TG-ELF by *P. pastoris* was better when under the direction of the signal peptide from *S. cerevisiae`s* α-mating factor, compared to the predicted native signal peptide encoded by the candidate *elf* in *B. bassiana*, which was the case in PicZα:ELF and PicZ:ELF containing lines, respectively. The most prominent band in extracellular fractions prepared from PicZ:ELF lines corresponded to ~ 35 kDa, but also required silver nitrate for its detection. However, this protein band was also found in the extracellular fraction prepared from the negative control cell line that did not contain an insert within pPicZα. Therefore, the 35 kDa protein produced here was not considered to be a candidate for TG-ELF.

A relatively faint band corresponding to ~ 35 kDa was present in intracellular extracts from clones αELF5 and αELF6 (only regions corresponding to the approximate expected size of TG-ELF are shown in Figure 6.12). However, these lanes also contained more protein than the others, which was evident by the increased staining of these lanes. Other than these two possible exceptions, none of the other clones were detected to possess a prominent protein species, 31 kDa or otherwise, within their intracellular soluble fractions, which would have likely indicated intracellular accumulation of an overexpressed protein. However, it was possible that TG-ELF was present intracellularly at low levels that were not detectable by SDS-PAGE analysis. Western blot analysis would provide confirmation of intracellular accumulation, but was not performed since the αELF clones were found to accumulate a putative TG-ELF within their extracellular fractions and could be used to produce this protein.

The size difference between EC1 (28 kDa) produced by *B. bassiana* and candidate TG-ELF (31 kDa) may be attributed to variations in glycosylation, which is a common finding in

transgenic expression experiments using *P. pastoris* (Cregg *et al.*, 2000). For example, N-linked glycosylation in yeasts differs from that of filamentous fungi, which results in yeast proteins possessing more mannose, while in filamentous fungi N-linked glycosylation is more similar to that produced by mammals (Reviewed in Nevalainen *et al.*, 2005). However, the size difference between EC1 and the candidate TG-ELF may be expected to be greater yet if expressed in *S. cerevisiae*, which is known to introduce a greater number of mannose residues per side chain than *P. pastoris* (Tschopp *et al.*, 1987). Nonetheless, the effects of glycosylation on the potential biological function of putative TG-ELF cannot be determined without experimental verification. This was because both N- and O-linked glycosylation have been documented to influence many functional properties in proteins, including binding, thermal stability, secretion and recognition by host immunity (Reviewed in Varki, 1993), all of which may be pertinent in the molecular biology of ELF.

The pPicZ vectors provide researchers the ability to produce their protein of interest with a hexahistidine tail, which allows the use of an anti-hexahistidine antibody for western blot analysis for example. However, the candidate *elf* inserts were designed to contain a stop codon upstream of this to prevent the addition of the hexahistidine tail to ensure that the TG-ELF was as similar to the native ELF as possible. This was done to limit the occurrence of potential experimental artifacts, such as altered protein-protein binding, which are known to occur in recombinant fusion proteins (Wissmueller *et al.*, 2011). In any case, experimental verification of the ability of the candidate TG-ELF to increase heat tolerance in BS (i.e. EIT) is the most definitive test available for its confirmation and is the goal of this study.

Two cells lines that accumulated the greatest amount of 31 kDa and 35 kDa putative TG-ELF in the medium were selected for each construct and used in a scaled-up (100 mL) expres-

sion experiment, performed in spinner flasks. These lines were αELF2 and αELF14 for PicZ:ELF and ELF4 and ELF5 for PicZα:ELF containing cell lines, respectively. Consistent with the screening experiment, both αELF2 and αELF14 produced protein products of ~ 31 kDa and ~ 35 kDa and were at their highest concentration after 48 h (Figure 6.13, αELF2 is shown a representative example for PicZα:ELF lines). This production was dependent on the presence of methanol in the overexpression medium, indicating that its expression was a function of the inducible promoter within the expression cassette. In addition, neither the 31 kDa nor 35 kDa species accumulated to levels detectable by blue silver dye staining in the extracellular fractions prepared from cultures of ELF4, ELF5 or *P. pastoris* that contained pPicZα without an insert (Figure 6.13, ELF4 shown as a representative example for PicZ:ELF lines).

Following incubation, the yeast cells were removed by filtration and the extracellular protein was precipitated with aqueous AS at 80% saturation and solubilized in phosphate buffer. This yielded ~ 50-250 mg of protein per L of culture in three trials with αELF2 or αELF14 (~ 95% of the total protein was recovered), with αELF2 cell lines yielding the most. Conversely, the PicZ:ELF containing strains yielded less; for example, only ~ 10 mg protein per L was recovered from ELF4. Also, the 31 kDa protein was not detected following SDS-PAGE analysis with blue silver dye staining in AS fractions recovered from ELF4, while it was the most predominant protein recovered from αELF2 and was suspected to be TG-ELF based on its size and accumulation (Figure 6.14).

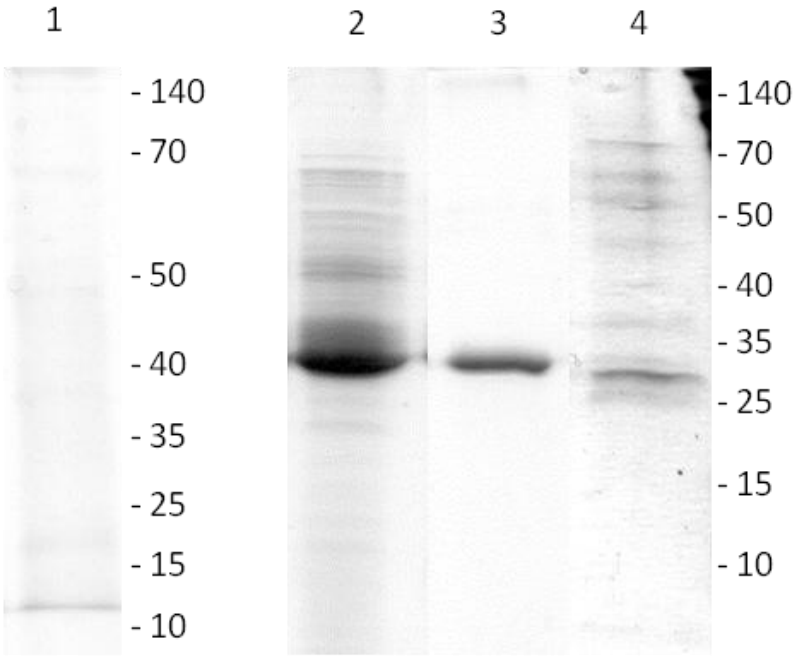

Figure 6.14 Banding pattern of extracellular proteins produced by ELF4 and αELF2 separated by 15% (w v^{-1}) SDS-PAGE. Lanes 1 and 2 show 4 µg and 20 µg of AS precipitated protein prepared from ELF4 and αELF2, respectively, grown for 48 h in the presence of methanol. Lane 3 shows 2 µg of gel purified TG-ELF from αELF2. Lane 4 shows 1 µg of protein in F80 prepared from *B. bassiana* grown for 72 h. The masses of the molecular ladder (kDa) are indicated to the right of gels which contained lanes 1 and 2-4.

The biological activity of TG-ELF was tested using the standard assay to asses EIT to heat in BS (Figure 6.15). The results showed that F80 prepared from CFF recovered from PicZα:ELF containing cell lines (αELF2 and αELF14), significantly increased heat tolerance in BS compared to the other treatments. Blastospores treated with extracellular extracts from PicZ:ELF (ELF4 and ELF5), or empty pPicZα (no insert) containing cell lines or treated with BSA had survival rates that were 3.2- ($p=0.0099$), 6.1- ($p=0.0031$) and 5.5-fold lower ($p=0.0036$) than those treated with extracts from PicZα:ELF containing cell lines, respectively. Furthermore, survival of BS treated with extracts from PicZ:ELF containing lines was comparable to those treated with extracts from cells which contained empty pPicZα or were treated with BSA. This was likely due to the low (undetectable) yields of 31 kDa, putative TG-ELF in the PicZ:ELF cells lines. Since extracts from both PicZα:ELF containing lines produced elevated tolerances to heat in BS, αELF2 was chosen to be used exclusively for the following experiments since it produced the greatest amount of the protein suspected to be TG-ELF.

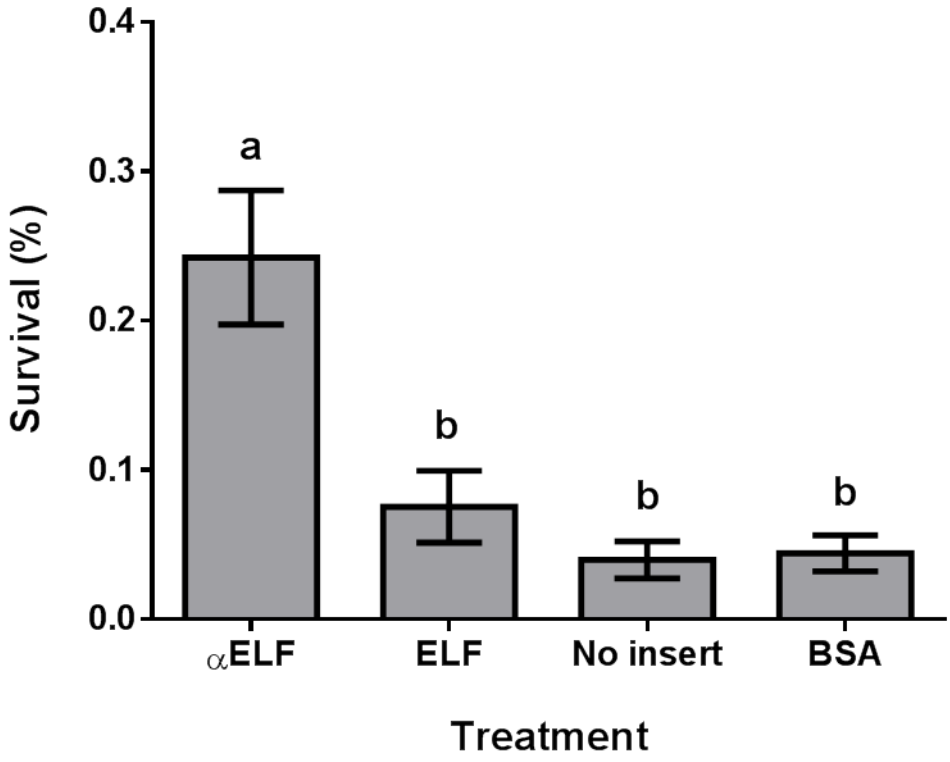

Figure 6.15 Effect of extracellular fractions prepared from *elf* containing *P. pastoris* on BS survival following heat challenge. Heat challenge was performed in PBS supplemented with 30 µg mL^{-1} of the indicated protein treatments. These were AS precipitated protein prepared from the extracellular fractions of *P. pastoris* cultures containing pPicZα:ELF (αELF), pPicZ:ELF (ELF), empty pPicZα (no insert) grown in the presence of methanol or BS supplemented with purified BSA. Bars represent the mean survival, calculated from three trials sampled in quadruplicate. Error bars show SEM and bars containing a same letter in their label were determined to not be significantly different by Tukey's multiple comparison test (α=0.05).

6.4.4 The EIT to heat response is specific to *B. bassiana* BS

The protein suspected to contain ELF activity within the AS extracts from αESC2 was eluted following preparative CN-PAGE and the recovered protein was determined to be pure by SDS-PAGE analysis (Figure 6.14; lane 3). This protein was confirmed to have the ability to increase heat tolerance using the heat challenge bioassay with BS (Figure 6.16). Treatment of BS with purified putative TG-ELF significantly ($p=0.0172$) increased their survival rate following heat challenge compared to those treated with similarly purified BSA. Also, the survival of BS treated with putative TG-ELF was similar to those treated with purified ELF produced by *B. bassiana* (Bb-ELF) and was also significantly greater than those treated with BSA ($p=0.037$). Compared to BSA, BS treated with TG-ELF or Bb-ELF had fold increases in survival of 4.8 and 3.5, respectively. Therefore, TG-ELF, like ELF was able to elevate heat tolerance of BS, which suggested that it too was likely involved in EIT in BS. As a result, this assay provided evidence to support that *elf* encoded ELF.

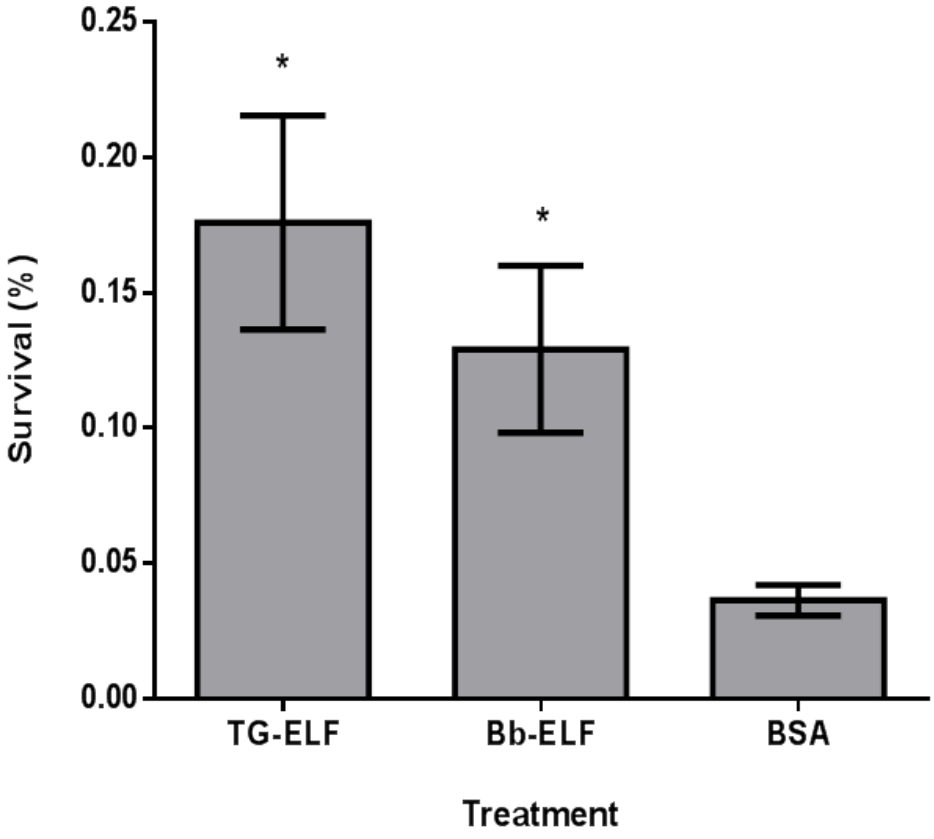

Figure 6.16 The effect of gel purified TG-ELF and ELF on the survival of BS following heat challenge. The heat challenge was performed in 1 mL of PBS that was supplemented with gel purified TG-ELF, *B. bassiana* produced ELF (Bb-ELF) or BSA. Bars show the mean survival of BS treated with TG-ELF, Bb-ELF or BSA and were calculated from 4, 11 and 8 trials, and contained an average of 19, 14 and 13 µg of protein mL^{-1}, respectively. The data analysed from BS treated with TG-ELF or BSA were the same as in Figure 6.17 found at x-values $1.5x10^{-7}$ to $1.5x10^{-6}$ M. Blastospores treated with Bb-ELF contained molar concentrations that were within the same range as the other treatments and three of the datum points were from the EC1 treatment as shown in Figure 5.9. Error bars show SEM and the bars labeled with an asterix symbol were determined to be significantly different compared to BSA by Dunnett's multiple comparisons test (α=0.05).

Furthermore, a dose-response relationship was established, which followed a semi-sigmoidal relationship (Figure 6.17). Sigmoidal dose response curves are typical for responses governed by saturable interactions, which is the case for many agonist-receptor interactions (Lambert, 2004). Also the dose-response relationship suggested that the response of BS to TG-ELF required a threshold concentration. The dose-response relationship and previous data from the pull-down assays provided inferential clues for the binding kinetics of a potential interaction between the ELF agonist and a possible receptor, namely, that the interaction may have had a low binding affinity. This suggestion was supported by the finding that a relatively high amount ($EC_{50} \approx 1.7 \times 10^{-7}$ M or 5.2 µg mL^{-1}) of TG-ELF was required to produce elevated tolerance to heat in BS, since dose response relationships are generally positively correlated with the dissociation constant (i.e. negatively correlated with binding affinity) of the interaction (Lambert, 2004). In other words, more agonist is required to elicit a response in systems governed by low affinity interactions, which is common in signal transduction systems (for example Lemmon, 2009). Nonetheless, the ability of TG-ELF to cause elevated tolerance to heat in BS was established and provided additional confidence that this protein, encoded by the *elf*, likely had ELF activity (i.e. could cause EIT).

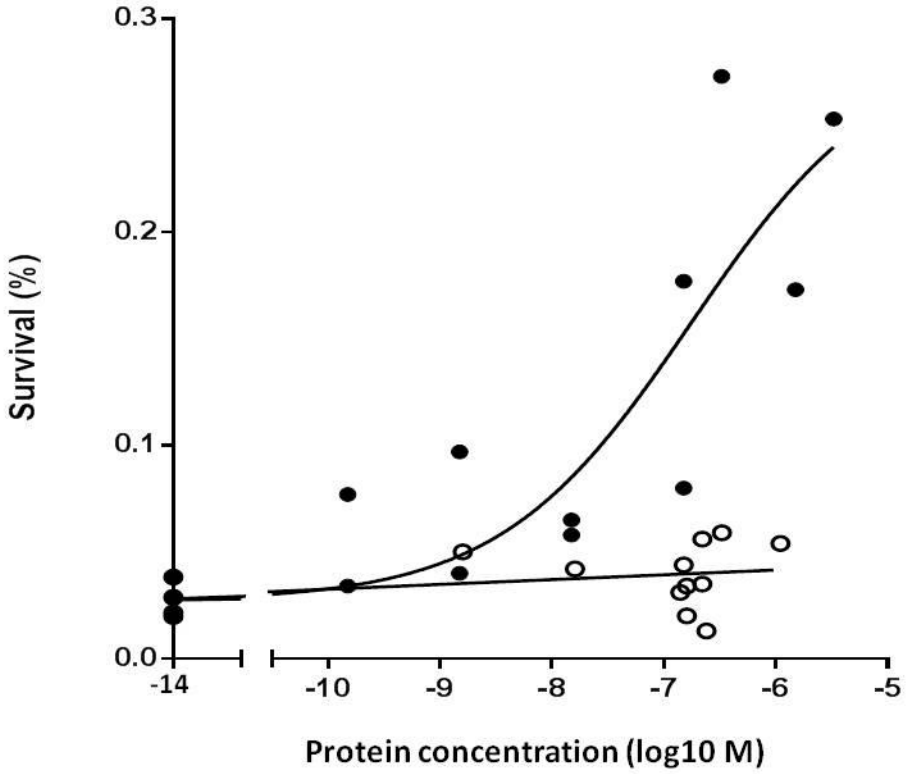

Figure 6.17. Dose effect of gel purified TG-ELF or BSA on the survival of heat challenged BS. The heat challenge was performed in 1 mL of PBS that was supplemented with the indicated concentration of TG-ELF (closed circle) or BSA (open circle), with $1.5x10^{-7}$ M corresponding to ~ 5 µg mL^{-1} or ~ 10 µg mL^{-1} of TG-ELF or BSA, respectively. Fifteen data points were analysed for each treatment and represented the mean survival obtained from a single experiment, sampled in quadruplicate. Regression analysis was performed and provided the corresponding sigmoidal and linear curves for TG-ELF and BSA, which had R^2 values of 0.78 and 0.14, respectively.

It was important to determine if fungal cell types other than BS could respond to TG-ELF. This was performed with the heat challenge bioassay and the various cell types were treated with either purified BSA or TG-ELF (Figure 6.18). Swollen (hydrated) CS, hyphae and BS were harvested from 8, 22 and 72 h cultures, respectively, as per Bidochka *et al*. (1987) with modifications and contained 24%, 47% and ~ 100% of the respective cell type, but not found to contain cell types from more advanced developmental stages. Approximately 100% of the propagules harvested as CS were the desired cell type. Only BS showed a significant increase in survival when treated with TG-ELF, compared to those treated with BSA. Although the survival rates of the other cell types were not significantly different when treated with TG-ELF compared to BSA, they all were observed to have a ~ 1.5-fold increase in survival. Therefore, it may be possible that tolerance to heat was elevated, but occurred to a lesser degree in cell types other than BS. However, it was not possible to establish an EIT-like response, since a relatively high degree of variability in the survival rates was apparent, which may or may not be a characteristic of EIT in non-BS cell types, but has been observed in other distance interactions (Nikolaev, 2000). In any case, the consistency of the magnitude of change in survival between non-BS cell types that were treated with TG-ELF, suggested that their response to TG-ELF differed from that in BS, since the treatment did not provide a significant increase in heat tolerance.

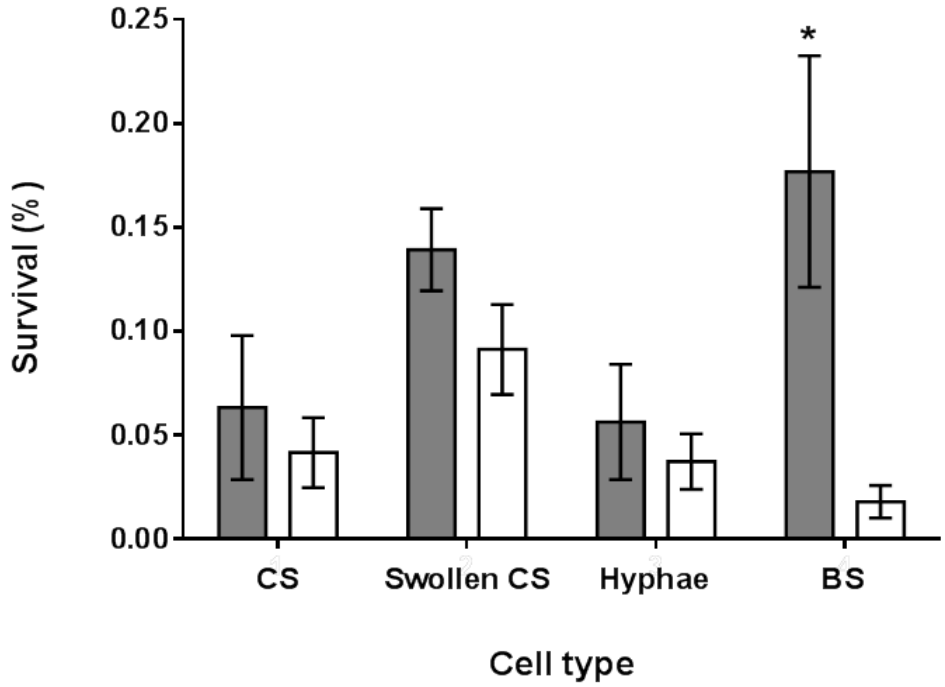

Figure 6.18 The effect of purified TG-ELF on the survival of various heat challenged cell types, produced by *B. bassiana*. The heat challenge was performed in 1 mL of PBS that was supplemented with 10 µg mL^{-1} of gel purified TG-ELF (grey bar) or BSA (white bar). Bars show the mean survival of the indicated cell types calculated from three trials, sampled in quadruplicate. The percentage of the desired cell type present in each was CS, ~ 100%; swollen CS, 24%; hyphae, 47%; and BS, ~ 100%. These values are near the highest obtainable for each under these conditions and were not found to contain cell types from more advanced stages of development (Bidochka *et al.*, 1987). Error bars show SEM and the bar labeled with an asterix symbol was determined to be significantly different compared to BSA by Student's t-test (α=0.05).

The distinct morphological features of hyphae and especially BS are important for the growth of *B. bassiana* within an insect (Reviewed in Khachatourians and Qazi, 2008; Khacha tourians, 2009). For example, BS and hyphae produced by *M. anisopliae* produce a collagenous coat when exposed to hemolymph from various insects and allows BS to evade detection by the host, likely through altering cell surface charge and masking immunogenic cell wall structural components (Wang and St Leger, 2006). Furthermore, an EST containing the 3' end of the candidate *elf* sequence has been found in *B. bassiana* mycelia (which likely also contained BS) during growth in the presence of cuticular extracts from coffee berry borer (Mantilla *et al.*, 2012). Also, this EST was detected in a liquid media, which is consistent with the observation that the accumulation of ECs was correlated with the presence of BS in liquid media. The finding that neither CS nor swollen CS were responsive to TG-ELF appeared to be consistent with the above result.

In nature, swelling of CS is controlled by moisture availability (Khachatourians, 2009). However, they are adapted to being able to hydrate, swell and develop during conditions where free water is limited, such as on the epicuticle (outermost layer of the cuticle) of insects, which is a waxy layer that can prevent the attachment of water droplets. Therefore, the developmental stages starting with conidial attachment to the insect, up to and including penetration by an infection peg, all of which that can occur on the insect's cuticle, may all be unsuitable for ELF functioning during insect infection, since a liquid environment seems to be required. Conidio-spores may also enter an insect through its mouth or other opening; however, EPF are adapted to entering their host through other routes, such as penetration of the insect's cuticle (Reviewed in St Leger and Wang, 2010). Furthermore, a preliminary experiment did not detect an EIT-like

response in CS treated with liquid used to rinse CS as they hydrated, which may indicate that ELFs are not secreted by CS during their hydration (section 4.4.1).

In addition, the polar growth stages of *B. bassiana*'s development, which occurred during hyphal development, also did not respond to TG-ELF. Although both hyphae and BS were present in liquid cultures when a response resembling EIT was detected, > 95% of fungal propagules were BS after 24 h and continued to increase (Bidochka *et al.*, 1987), as did accumulation of proteins correlated with elevated tolerance, with longer incubations periods. The correlation between BS and ELF accumulation is logically required for the ELF-BS interaction and EIT to occur. Both BS and hyphae are produced by *B. bassiana* in the hemocoel of an infected insect. As a result, they could be subjected to supra-optimal temperatures brought on by the behavioral fever of the host, which the insect uses to suppress infections by elevating its internal temperature by 5 to 15 °C above the surrounding air temperature (Carruthers *et al.*, 1992).

The fact that CS do not generally encounter an insect's fever may help explain their apparent lack of an EIT-like response to heat, since it may not provide additional fitness to the fungus. In hyphae, the lack of response is less obvious since they could be exposed to the insect's fever in nature. It is possible that the lack of response is related to hyphal morphology, especially if the ELF-cell interaction was through a receptor that underwent endocytosis. In this case, only near the growing tips of each hypha would be an appropriate location for such a receptor (Shaw *et al.*, 2011). In the above experiment there was generally only one growing tip per propagule, even though multiple segments were present. This effectively created a situation where there were proportionally fewer locations per propagule for a potential interaction to occur with hyphae than with BS, since BS are smaller and each can possesses one or more growing

tips, which could contribute to BS being more responsive to ELF compared to hyphae. However, additional research is needed here, especially regarding the elucidation of potential receptors for ELF, which may shed light on the interaction kinetics and possible downstream physiological effects of the interaction.

To determine the responsiveness of other BS producing EPF to TG-ELF, *I. farinosa* and *T. inflatum* were chosen for assessment. The selection of these two was because they both produced BS in sufficient numbers to assay for EIT to heat (Figure 6.19). However, treatment of either fungus with TG-ELF did not significantly increase their survival rates following a 55 °C heat challenge for 30 or 45 min, compared to BS treated with BSA. This suggested that the TG-ELF inducing elevated tolerance to heat in BS may be species specific.

6.4.5 Sequence structure/function analysis of ELF

It was established in the above sections that the candidate *elf* from *B. bassiana* encoded a protein that was able to increase heat tolerance in BS, when expressed by *P. Pastoris*. The possible involvement of this protein in the establishment of heat tolerance is consistent with EIT, which suggested that *elf* encoded a functional ELF. However, no sequence homologues of ELF with assigned functions were available in the databanks. Therefore, more in-depth analyses were required to establish potential inferences between the primary structure of ELF and its corresponding molecular functions.

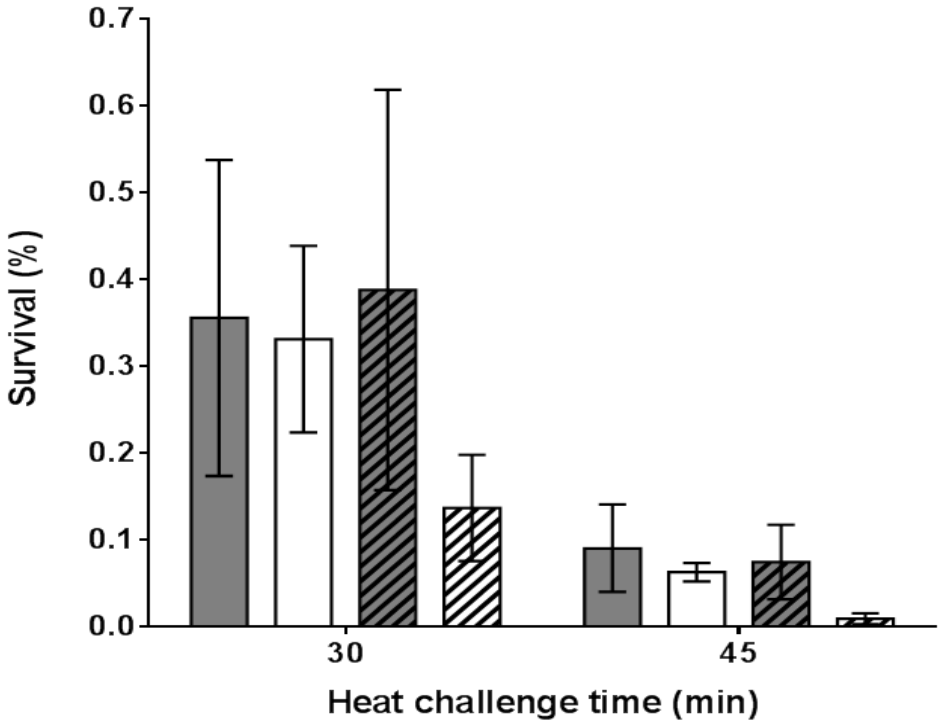

Figure 6.19 The effect of TG-ELF on the survival of heat challenged BS from *I. farinosa* or *T. inflatum*. The BSs were harvested from *I. farinosa* (solid bars) and *T. inflatum* (bars with diagonal lines) cultures grown in YPG. The heat challenge was performed in 1 mL of PBS that was supplemented with 100 µg mL^{-1} of purified TG-ELF (grey bar) or BSA (white bar). Bars show the mean survival calculated from three trials, sampled in quadruplicate. Error bars show SEM and the treatment effect was not determined to be significantly different using Student's t-test (α=0.05), by comparing the results from the same fungus and heat challenge duration.

In this regard, a comparison of ELF's amino acid composition to the average, calculated from 151 extracellular proteins produced by various eukaryotes, yielded some interesting findings (Nakashima and Nishikawa, 1994) (Table 6.3). For example, *elf* encoded a product whose composition per amino acid (compared to the average) differed by $\geq \pm 50\%$, for 7 of the 20 amino acids (Nakashima and Nishikawa, 1994) (Table 6.3). The amino acids tyrosine, histidine, glutamate, tryptophan and cysteine were all present at levels that were $\geq 50\%$ higher, while isoleucine and glutamine were lower by $\geq 50\%$ compared to the average for extracellular eukaryotic proteins. Some of these compositional variations from the average may provide clues into the structure/function of ELF.

For example, histidine was present at 67% higher levels than the average of extracellular eukaryotic proteins. This amino acid possesses an imidazole functional group with a pKa of approximately 6.0. As a result, this amino acid is sensitive to pH changes at values that are physiologically relevant to many organisms (< pH 6.0), where relatively small down-shifts in pH will cause its average charge to become more positive. It has not been established whether the ELF(s) studied here is also involved in the response to acid or alkali stress. However, ESCs have been suggested to be involved in pH sensing of ESC in *E. coli* (Rowbury and Goodson, 1999a). It would be interesting to determine if histidine plays a role in ESC activation, which has been speculated to possibly involve a conformational change (Rowbury and Goodson, 2001). It remains to be determined if ELF(s) produced by *B. bassiana* share similar amino acid compositions with ESC(s) from *E. coli*.

Table 6.3 Deduced amino acid composition of ELF compared to an average calculated from 151 extracellular eukaryotic proteins.

Amino acid	Amino acid composition (%)		Relative difference in composition (%) [b]
	Extracellular eukaryotic proteins [a]	ELF	
Tyr	3.5	7.4	211
His	2.3	3.9	167
Glu	6.6	10.4	158
Trp	1.4	2.2	154
Cys	3.5	5.2	150
Gly	6.9	9.6	139
Asp	5.3	7.0	132
Thr	5.9	7.4	126
Ala	6.6	7.4	112
Lys	5.9	6.5	111
Met	1.8	1.7	92
Pro	5.8	5.2	90
Phe	3.9	3.0	78
Val	5.7	4.3	75
Ser	7.5	4.8	64
Leu	8.0	4.8	60
Arg	5.4	3.0	56
Asn	4.9	2.6	53
Ile	4.4	1.7	39
Gln	4.7	1.7	36

a) These values are the average amino acid composition, based on the sum of amino acids, calculated from 151 extracellular eukaryotic proteins, excluding their signal peptides. These proteins were from a variety of Eukaryotes, which ranged from yeasts to human. This data was adapted from (Nakashima and Nishikawa, 1994).

b) The Relative difference in amino acid composition was calculated by dividing the % composition value for ELF (excluding its predicted signal peptide) by the average value for extracellular eukaryotic proteins for a given amino acid and was multiplied by 100 to convert to an integer. A number greater or lesser than 100% indicated an increase or decrease, respectively, relative to the average of extracellular eukaryotic proteins.

In addition, cysteine composition was found to be higher by 50% in ELF relative to the average of extracellular eukaryotic proteins. Cysteines are known to be more prevalent in extracellular proteins compared to intracellular proteins (Nakashima and Nishikawa, 1994) and are responsible for the formation of stabilizing disulphides in the oxidizing environment outside of the cell (Gilbert, 1990). These disulphide bonds are known to increase stability of proteins to heat and other denaturing conditions as found in IgG1 antibody CH3 domain for example (McAuley *et al.*, 2008). Similarly, the results of a preliminary experiment reported here suggested that ELF may have remained responsive to heat activation following previous heating to 121 °C (see section 4.4.1). Furthermore, an even number of cysteine residues were found in the deduced ELF sequence and implicates their role in disulphide bond formation, which form between two cysteines. Therefore, it is likely that the disulphide bonds may help stabilize ELF, which could be especially important at high temperatures, possibly through the prevention of excessive structural distortion which can lead to denaturation. In turn, this stabilization may help maintain ELF in an active conformation at elevated temperatures, allowing it to promote EIT. Although it remains undetermined if the extracellular factors produced by *E. coli* (Rowbury and Goodson, 1999a), *C. jejuni* (Murphy *et al.*, 2003) and *S. cerevisiae* (Vovou *et al.*, 2004) also possess a high proportion of cysteine, their ability to be activated by heat, and remain stable and responsive to activation by heat following exposure to extreme temperatures (75 °C - 100 °C) may be consistent with this structural characteristic.

Furthermore, a class of proteins termed SSCPs have been described in the literature, primarily in fungi (Brown *et al.*, 2012; Druzhinina *et al.*, 2012) and human (Lavergne *et al.*, 2012). As their name implies, these proteins are small proteins, usually less than 300 aa and have > 4 cysteine (Martin *et al.*, 2008) but often possess up to 5% cysteine, based on the sum of

amino acids (Lavergne *et al.*, 2012). Since the product encoded by *elf* has both of these characteristics it can be classified as a SSCP. Analysis of the genome of *B. bassiana* by Xiao *et al.* (2012) revealed that it encoded 373 SSCPs, which was more than found in the three other available genomes from EPF (average of 307). Although an ELF homologue sequence was present in the strain used by this group, a function was not assigned. However, the function of SSCPs in fungi and mammals commonly possess unknown functions (Brown *et al.*, 2012; Druzhinina *et al.*, 2012; Lavergne *et al.*, 2012). An exception is hydrophobins which are produced by fungi and among the best studied SSCPs. Hydrophobins are characterized by conserved cysteines that occur in doubles, their hydrophobic nature and poor water solubility (Druzhinina *et al.*, 2012). However, ELF does not possess these features as it lacked any consecutive cysteine residues and is water soluble.

Investigation into SSCPs and secreted fungal proteins in general has revealed that many from plant pathogens commonly possessed internal amino acid repeats, which increased phenotypic plasticity and are thought to be involved in escaping detection by the host's immune response (Rudd *et al.*, 2010). Since ELF is also an SSCP and is produced by a pathogen it was important to determine if it too contained internal repeats. This was performed with rapid automatic detection and alignment of repeats (available at http://www.ebi.ac.uk/Tools/pfa/radar/) (Figure 6.20). Three similar repeats of 62-66 aa were identified in the sequence of ELF. These repeats were located at amino acids 45-106, 113-178 and 184-246 and were separated by 6 and 5 aa, respectively. It is difficult to confidently speculate for the reasons for these internal repeats, since they are not well understood in other fungi. Nonetheless, their presence in plant and insect pathogenic fungi may imply that selecting for rapid evolution of secreted fungal proteins through sequence duplication is favorable for the pathogen. However, internal repeats are not limited to pathogenic fungi as they are also found in the model yeast *S. cerevisiae* (Verstrepen *et al.*, 2005).

```
 45  -YGPCMEAVHGDGGREAIEKGCGTEGFCDLLNPVYGPDNLERLSK---KYGYANNTECYAAHDKIP  106
113  DYGACMQAVHSHADREDFEEACGTEGFCDMFNPEYGTESLKRVLETWGQYGFKTHTECYAGHTKKP  178
184  DYGSCHDVAYSVVSREKYEAGCGTETFCDLFNPEYGTDSLERMTK---QYGYATVADCIADHEPQP  246
      **.* :.:.:  .**  * .**** ***::** **.:.*:*: :   :**: . ::* * *   *
```

Figure 6.20 Results of rapid automatic detection of repeats and alignment of identified repeats in ELF. Three similar repeats of 62, 66 and 63 aa were identified and spanned aa 45-106, 113-178 and 184-246. The alignment of these repeats is shown above.

A potential function for ELF could not be confidently predicted through the direct analysis of its primary structure due to a lack of information regarding ELF and similar proteins. Therefore, structural modeling was chosen as a strategy to gain insight into its structure and predict molecular function(s). This was performed with the iTASSER (Roy *et al.*, 2010) and CombFunc (Wass *et al.*, 2012) servers. These servers both use homology modeling which allows proteins with only limited sequence similarity (~ 20%) with known structures to be modeled accurately (Kelley and Sternberg, 2009). In addition, iTASSER can also employ *ab initio* modeling when structural homologues are not available for a protein of interest, but is less accurate than homology modeling.

It was apparent that ELF lacked both sequence and structural homologues within the protein data bank and therefore homology modeling was not possible. As a result, the less accurate *ab initio* method was employed exclusively, which did not yield reliable predictions. The iTASSER reported C-scores [confidence of predicted structure as per [(Roy *et al.*, 2010), (-5 to 2)] of between -3.03 to -4.56 and -3.32 to -4.66 for ELF sequences that did or did not include it predicted signal peptide, respectively (structures with a score of > -1.5 generally are correct). The ELF sequence, with or without its secretion signal peptide was predicted to have highest GO-scores for metal ion binding (GO-score = 0.41) and RNA-binding activities (GO-score = 0.49), respectively. The GO-score can range from 0 to 1, with a higher value indicating better confidence of the prediction. However, more specific enzyme functions could not be assigned because the EC-scores were too low, 0.090-0.148 and 0.097-0.114 for ELF sequences with and without signal peptide, respectively. Like GO-scores, EC-scores can range from 0 to 1. Clearly, the structure/function relationship of ELF cannot be confidently established using homology or *ab initio* modeling to predict these features.

Interestingly, the so-called three component systems require accessory proteins to sense stimuli (usually a chemical) and activate signal transduction pathways (Reviewed in Krell *et al.*, 2010). However, these accessory sensory components have not been found to have a conserved sequence and span several protein families. As a result, currently these sensory components can only been identified experimentally (Reviewed in Krell *et al.*, 2010), which is a similar obstacle that hinders research into ELF, ESCs and other distance interactions. Nonetheless, the lack of sequence and structural homologues suggested that the structure/function of ELF may have potentially novel features and warrants further structural analysis, perhaps through x-ray crystal-lography.

7.0 GENERAL DISCUSSION

Entomopathogenic fungi and their ability to infect insects have been studied since the 1800s. However in the 1940's, with the discovery and widespread use of chemical insecticides, the potential of EPF, and other biological control agents, to be utilized for control of pest insects was overshadowed. A lack of widespread adoption of EPF as alternatives to chemical insecticides was in part, due to the dependence of EPF on a narrow range of environmental conditions (Fargues, 2003). As a result, the use of EPF has been based on an unfair comparison of them to chemical insecticides, rather than in the context of their ecology as a part of an integrated pest management system (Waage, 1998). With the advent of molecular biology in the middle of the 20th century and the development of transgenic technologies, a new set of tools was made available for the study and improvement of EPF and other biological controls. Furthermore, the recent sequencing of the first EPF genomes from *C. militaris* (Zheng *et al.*, 2011), *M. acridum*, *M. anisopliae* (Gao *et al.*, 2011) and *B. bassiana* (Xiao *et al.*, 2012) has provided a plethora of genetic information in this group of fungi. Insights into the 'omics' of EPF, coupled with an improved understanding of their ecology, as well as their developmental and molecular biology may contribute to strategies for improving their usefulness as biological insecticides, such as by improving their ability to tolerate environmental stress conditions. In addition, EPF and other biological agents are becoming more accepted by the public as a potential alternative to synthetic chemical insecticides (Lord, 2005), which has helped to increase the worldwide market for these products (de Guzman, 2009).

Coupled with the determinants of insect disease controlled by the fungus, host and the environment, where they subsist and the environmental stresses they are exposed to is of great

impact (Feng *et al.*, 1994; Khachatourians *et al.*, 2002; Khachatourians and Qazi, 2008). Of particular interest in this thesis were the environmental stressors UVR and lethal heat and how several EPF respond and mitigate their detrimental effects. This is because both stresses can reduce the ability of the fungus to cause pathogenesis and bring about effective insect control (Vestergaard *et al.*, 1995; Inglis *et al.*, 1997). Specifically, *phr-1*, encoding a CPD-PHR in EPF and a novel heat stress response, involving the protein ELF were studied.

Photoreactivation will be discussed first. Although much is known about photoreactivation in fungi, there is a major lack of understanding of the molecular biology that controls this process in EPF (Chelico *et al.*, 2005; Chelico *et al.*, 2006). Central to this is the lack of data regarding the sequence of both *phr-1* and its gene product. The sequences of only four *phr-1* candidates from EPF have been deposited within public data bases. Therefore, it was a goal to establish that a candidate for *phr-1* was present in various EPF and screen the deduced proteins for functional features, which are characteristic for CPD-PHRs and differentiate the products encoded by the candidate *phr-1s* from other closely related PHR/CRY proteins found in fungi.

The photoreactive capabilities were confirmed in UV-C challenged CS from *B. bassiana*, *I. farinosa*, *L. longisporum*, *M.* anisopliae and *T. inflatum*. With the phenomenon established, a conserved region of a putative *phr-1* from each fungus was amplified, cloned and sequenced. *In silico* translation of these sections showed that they encoded a product that appeared to be homologous to class I CPD-PHRs and possessed the most sequence similarity (83% was the maximum) with those from filamentous fungi. Furthermore, functionally important residues in CPD-PHR were found to be conserved in the protein products encoded by the putative *phr-1* sections. Many of these have previously been found to be involved in binding to ligands, such as CPD, FAD and MTFH, or thought to be directly involved in electron transfer from FAD to the

CPD (Reviewed in Sancar, 2003). In contrast, some CPD-PHRs are known to possess an oxidized 8-hydroxy-5-deazaflavin derivative instead of MTHF, but these types are rarer and are dependent on the organism's ability to synthesize this chromophore (Reviewed in Sancar, 2003) and were not found here. Both CPD- and FAD-binding are required for repair of CPDs by this PHR (Sancar *et al.*, 1987a). In contrast, the presence of a light harvesting chromophore (such as MTHF) is not required, but can increase the reaction rate of CPD-PHR by 10 to 100-fold when light is limiting (Payne and Sancar, 1990). In nature, this would presumably allow CPD-PHR to continue DNA repair during times when solar light is low (such as the evening). Clearly, this ability to repair DNA when light is full or limiting would be beneficial to EPF in the field. In addition, neither the presence nor the absence of the light-harvesting chromophores affects the ability of CPD-PHR to interact with CPDs (Hamm-Alvarez *et al.*, 1989; Malhotra *et al.*, 1992). Instead, key structural features are important to the affinity and specificity of the enzyme, including: (i) the positively charged groove that runs across the surface of its α-helical domain, (ii) a 'hole' with correct dimension in the centre of the groove that accommodates a CPD and (iii) the FAD that is at the bottom of the hole (Sancar, 2003). It is the totality of these sites that provide CPD-PHR its interaction specificity.

This CPD-PHR specificity to CPDs is exploited by the cell to improve the functioning of another DNA repair system; NER. The repairosome (Friedberg *et al.*, 2006), which is involved in NER, is known to preferentially bind to sites of damage which cause the greatest amount of structural distortion in the DNA. However, CPDs are known to induce a relatively low level of distortion compared to other types of damage (Sancar *et al.*, 1984). As a result, it is thought the ability of CPD-PHR to bind with CPDs [and to a lesser extent other types of DNA damage (Fox *et al.*, 1994)] and flip the dimer out of the DNA helix, produces additional DNA distortion,

which improves the ability of the repairosome to bind to CPDs and subsequently repair them (Sancar *et al.*, 1984). Refer to Figure 2.2 and section 2.4.2.1 for an overview of the repair pathway of CPD-PHR This function of CPD-PHR is thought to potentially play an important role in the repair of DNA in organisms, such as *E. coli* that may spend a significant amount of its life in the gastro-intestinal system of mammals and would not be exposed to UVR in this environment. Similarly, when presented the opportunity, EPF can also spend a portion of their life in an environment that is shielded from the sun's radiation: inside the insect host.

Photolyases are related to another group of proteins that are termed cryptochromes. Differentiation between PHR/CRY types has been complicated by their many similarities. All CRYs possess a FAD, are generally 50-70 kDa, share 25-40% sequence similarity with PHRs and are very close structural homologues, with their Cα backbones being nearly superimposable with PHR (Reviewed in Sancar, 2003; Müller and Carell, 2009). As a result, the repair ability of CPD-PHRs has required experimental verification (Chelico *et al.*, 2005; Berrocal-Tito *et al.*, 2007). Clearly, experimental verification provides the highest confidence to the assigned functions. However, the extensive characterization of many CPD-PHRs and the availability of many solved structures from PHR/CRYs in the protein data bank provide a threshold of knowledge that enables other forms of analysis to be employed.

In addition to conventional sequence analysis, homology modeling was employed to provide an additional level of understanding to the potential structure/functions of the gene products deduced from sections of putative *phr-1* from the EPF studied here. This method was performed using the iTASSER (Roy *et al.*, 2010) and CombFunc (Wass *et al.*, 2012) servers. Both were able to model the structures encoded by the putative *phr-1* with high confidence, and as a result, the accuracy of the functions predicted for the putative CPD-PHRs (i.e. CPD-PHR

activity) was considered to be very high. Through this analysis it was also possible to differentiate a known CPD-PHR as well as the putative CPD-PHR from EPF from a (6-4)-PHR and DASH-CRY sequence, which are the only other known PHR/CRY types found in fungi. Although the prediction of well-defined functions is possible, unforeseen functions may exist in PHR/CRYs, such as CPD repair in single stranded DNA by DASH-CRY (Selby and Sancar, 2006) and CRY-like function in CPD-PHR (Chaves *et al.*, 2011). Such unforeseen functions do not restrict the ability of homology modeling to accurately predict functions; however experimental verification may be required in certain cases.

The ability of the homology modeling method to aid in the differentiation of very similar protein types provides support to this method having utility in high-throughput functional analysis of proteins; however computational requirements may restrict its use at this time (Roy *et al.*, 2010). Additionally, this method has been employed in structural model creation (Rausch *et al.*, 2012), protein function (Wang *et al.*, 2012a) and ligand discovery (Roche *et al.*, 2012). The availability of experimentally solved structures is paramount for the accuracy of these methods and expansion of the protein data base remains an important objective in the life sciences.

The phenomenon of EIT was also explored in this thesis. In contrast to photoreactivation, very little is known about the molecular component(s) or mechanism(s) that control EIT to any stress. This phenomenon was discovered in *E. coli* (Hussain *et al.*, 1998) and later similar responses were found in *C. jejuni* (Murphy *et al.*, 2003) and *S. cerevisiae* (Vovou *et al.*, 2004). Although this phenomenon is best studied in *E. coli*, a general understanding of the conditions required to produce the ESCs, the environmental stress conditions that can activate them and the tolerances they can induce, largely represents the extent of the knowledge in this field. The findings presented in this thesis may represent a mechanism for the extracellular sensing of

supra-optimal lethal heat in *B. bassiana*. As mentioned, the sensing of extracellular stress conditions, including heat, has been speculated to occur through ESCs in *E. coli*, which appear to be involved in the induction of tolerances to various environmental stress conditions (El-Sharoud and Rowbury, 2006). The resulting tolerance is referred to as EIT in this thesis and currently is the only known effect of ESC and was suspected to also involve ELF in *B. bassiana*. Though the signal transduction pathways involved in the establishment of heat tolerance are fairly well understood, one element has remained elusive to researchers: the true elicitor of the response (Reviewed in Morano *et al.*, 2012). In other words, it is not completely understood how cells sense supra-optimal lethal heat, which is prerequisite for the heat response to be initiated.

The greatest proportion of this thesis was focused on the study of EIT in *B. bassiana* with the goal of identifying an ELF and its encoding gene. Such a discovery would represent an important finding because it would be the first for any such extracellular factor and may be a potentially novel or missing piece in the heat response model. Furthermore, a better understanding of the EIT phenomenon would improve knowledge of the response of *B. bassiana* to environmental stress conditions and may have implications for insect control in the field. This phenomenon was studied through the use of several novel whole cell bioassays using a combination of microbiology and molecular biology based techniques. Here an ELF from *B. bassiana* and its encoding gene, *elf*, was identified and characterized for the first time in any organism.

The initial objective of this study was to establish that a phenomenon resembling EIT to UVR or heat occurs in *B. bassiana*. This was performed with CS and BS and heat was selected as a potential activator of the putative ELF that was predicted to be contained in the extracellular fraction prepared from *B. bassiana* propagated in liquid growth media. These results suggested that a response that resembled EIT to UVR and heat could be triggered in CS and BS, respective-

ly, albeit the cell types appeared to have differing requirements for tolerance to be established. For instance, an increase in UVR tolerance was most pronounced when CS were incubated with preheated CFF prior to heat challenge. While in BS, heat tolerance was apparent when they were challenged in the presence of CFF that was preheated prior to BS being added. The cellular structure and general metabolism of CS and BS may provide clues to the differences in the requirements for this increase in tolerance to UVR and heat to be established in CS and BS, respectively. For example, BS have been described as vegetative, thin-walled, yeast-like propagules which are generated by budding from hyphae (Bidochka *et al.*, 1987). This is in contrast with CS which are non-vegetative cells that possess a relatively thick spore wall. Perhaps the differences in time required for tolerance induced by preheated CFF to occur in BS and CS is a manifestation of the metabolic state of the two cell types. For example, since BS are vegetative it is likely that they would respond to a stimulus (through gene expression for instance) more rapidly than CS, which are not, and may require prerequisite events to occur, such as their hydration (Bidochka *et al.*, 1987). It is also possible that the time required for the establishment of the EIT-like response to heat in BS or UVR in CS is a reflection of the tolerance mechanisms required, in addition to the metabolic state of the cell. However, the temporal requirements of the mechanisms involved remain undetermined.

The locations in or on the insect host where the fungal cell types are generally found would be expected to also influence the type of environmental stress tolerance gained by the cell. For example, BS can be found inside the host, often within the hemolymph during insect infection, while CS are not and generally attach to exterior locations (Wang and St Leger, 2006). As a result, BS may be more likely to be exposed to elevated temperatures due the host insect's behavioral fever response to infection, while CS attached to the exterior could be cooled by

evaporation. When exhibiting behavioral fever, grasshoppers for example, are capable of elevating their internal temperature by 5 to 15 °C above the surrounding air temperature to suppress infections (Carruthers *et al.*, 1992). Although a temperature increase of 5 to 15 °C alone may not be lethal to the EPF, it may be sufficient to prevent fungal growth and mycosis when combined with the responses of the host insect to fungal infection. Clearly the interaction between temperature and the ability of the fungus to cause insect infection is complex and likely involves additional factors controlled by the insect, fungus and environment.

Conversely, BS are shielded from solar UVR within the insect, but may be exposed to UVR in other environments, such as in soil. Furthermore, during the infection cycle, aerial CS are produced outside of the insect cadaver and thus are not shielded from solar UVR, but also are not exposed to the elevated temperatures within the insect that occur as a result of the behavioral fever. The fact that CS do not generally encounter an insect's fever may help explain their apparent lack of responsive which resembles EIT to heat, since it may not provide additional fitness to the fungus. However, preheating of CFF was required for elevated tolerance to UVR in CS and suggested that activation of the suspected ELF may occur in liquid. Therefore, it is difficult to speculate on the functioning of ELF(s) with respect to CS, since this cell type appears to be adapted to non-liquid environments (Jeffs *et al.*, 1999), although CS can also enter the host through ingestion, in chewing insects (Reviewed in St Leger and Wang, 2010). It was not established if the suspected ELFs that may be involved in the induction of tolerance to heat or UVR in BS and CS, respectively, were the same.

As mentioned above, the environmental stress tolerance that was acquired differed depending on the cell type, as preheated CFF that was suspected to contain ELF was able to promote tolerance to UVR or heat in CS and BS, respectively. These findings were consistent

with those using TG-ELF to test for EIT to heat, which showed that BS responded (significant increase in survival compared to BSA) to preheated TG-ELF but CS, swollen CS and hyphae did not, using an assay optimized for BS. This suggested that non-BS cell types respond differently to ELF than BS. Also, the lack of a response that resembled EIT to heat in CS may not solely be a reflection of the requirement of CS for hydration to cue swelling, since swollen CS did not respond either.

Again, the biology of these propagules may provide clues to why the tolerances acquired differed. Generally speaking, BS are produced by budding from hyphae in aqueous environments, such as when grown in liquid media or within the hemocoel of an insect to disseminate throughout the host via the insect's circulatory system (Wang and St Leger, 2006). Conversely, CS are produced from conidiophores which emerge from the growth medium, an insect cadaver or other substrates. A commonality between CS in their non-swollen and swollen (hydrated) states is that in nature they function in primarily non-liquid environments (Jeffs *et al.*, 1999). Although development of CS is initially controlled by moisture availability, they are adapted to being able to swell and develop in conditions where free water is unavailable; for example, on the cuticle of an insect, which is covered by the waxy epicuticle that prevents attachment of water droplets (Khachatourians, 2009). Also, particular limitations may be imposed on ELF functioning due to their location in or on the insect and the corresponding localized environment, which could restrict ELF functioning. Therefore, the infection stages starting with conidial attachment, through breach of the cuticle by a penetration peg, all of which occur on the outer surface of the insect, may not be suitable for EIT to heat to be established. However, it remains to be determined if changes to the epicuticle caused by hydrolytic enzymes secreted by the fungus would influence ELFs ability to function. Nonetheless, degradation of the waxy epicu-

ticle would be expected to disrupt its ability to prevent free water from accumulating and may create a localized aqueous environment (Pedrini *et al.*, 2007; Khachatourians, 2009), which is thought to be required for ELF to interact with cells and promote EIT. Conversely, the insect hemocoel is also an aqueous environment and would be conducive for the movement of ELF throughout and would be aided by diffusion and also advection, through circulation of the hemolymph within the living insect host. This would allow ELFs to come into contact with fungal propagules within the hemocoel, such as BS and hyphae, which are found here during infection.

Interestingly, the hyphal growth stages of *B. bassiana*'s development, which were prepared from liquid growth media, did not acquire EIT to heat, yet BS did. Although both hyphae and BS were present in liquid cultures when ECs were detected, > 95% of fungal propagules were BS after 24 h and continued to accumulate (Bidochka *et al.*, 1987), as did the ECs, with longer incubation periods. A correlation between BS and ELF accumulation is logically required for the suspected ELF-BS interaction and EIT to occur. In nature, all cell types produced by EPF may encounter the supra-optimal temperatures through their environment, but both hyphae and BS are more likely to also be subjected to the insect host's behavioral fever, since they subsist within the insect.

The fact that CS are not as often in a situation to encounter the effects of an insect's fever may help explain their apparent lack of an EIT-like response to heat. Conversely, in hyphae the apparent lack of an EIT to heat response is less obvious, since like BS, hyphae can also be exposed to the behavioural fever response within the insect and would presumably benefit from EIT to heat. However, the reason(s) for the lack of such a response in hyphae is unclear. Furthermore, if an interaction between ELF and cell was to occur through a receptor, hyphae could

be an appropriate cell type for such an interaction. This is because endocytosis following an interaction with ELF was implicated (partially by the results of one of the pull-down assays and also inferred by *in silico* analysis of the product encoded by *elf*) and endocytosis is known to occur near the growing tips of hyphae (Shaw *et al.*, 2011). However, the result of the pull-down experiment was not consistent when performed with purified ELF. Therefore, more studies are needed to better understand the potential interaction between ELF and its receptor.

Hyphae can possess multiple growing tips per propagule, but less than one per segment (cell). In contrast, BS are a single cells and each can possess a growing tip. This may effectively create a situation where there were proportionally fewer locations per propagule for a potential ELF-cell surface interaction to occur with hyphae, than with BS. Also, induction of tolerance would be expected to be delayed in hyphae compared to BS, if the message would need to be relayed to the other non-apical segments for the response to occur in them. Thus, BS may be more responsive to ELF compared to hyphae, in part for this reason. Clearly, more research is needed, especially regarding the elucidation of a receptor for ELF, which would likely shed light on interaction kinetics and downstream physiological effects of the potential interaction between ELF and receptor.

The EIT response may have similarities with another distance interaction: quorum sensing. As mentioned above, the presence of BS and hyphae, with the former representing the vast majority of fungal propagules after 72 h, were correlated with the ability of CFF (containing putative ELF) prepared from the cultures to promote tolerance to UVR in CS. The quorum response, like EIT, was discovered in bacteria and has also been found to also occur in fungi (Reviewed in Albuquerque and Casadevall, 2012). Although both quorum factors and ESC/ELF are secreted, two key differences between these molecules are apparent. Firstly, currently known

examples of true quorum sensing in fungi are generally controlled by aromatic alcohols, while the ELF(s) that controls EIT to UVR and heat are proteins. Secondly, quorum sensing allows microbial communication, but is principally dependent on cell density for the response to occur. While ELF production is correlated with cell density, ELFs alone are not sufficient to produce the elevated tolerance, as these molecules require activation by a stress condition. In *E. coli* activation of ESC has been suspected to occur through a conformational change imposed by the stress conditions (Rowbury and Goodson, 2001). It is the second dissimilarity which appears to differentiate EIT from a true quorum response.

With regards to transcription of *elf* by BS and/or hyphae, an EST containing the 3' end of a candidate *elf*, was present in *B. bassiana* mycelia, which likely contained BS, during growth in the presence of cuticular extracts from coffee berry borer (Mantilla *et al.*, 2012). However, it was undetermined if *elf* expression was specifically effected by the presence of cuticular extracts. Nonetheless, *elf* transcript was present in liquid cultures, which is consistent with the findings of this thesis. Furthermore, a Kozak sequence that is very similar to the consensus was identified in the *elf* from *B. bassiana* GK2016, which is an indicator for efficient translation initiation by ribosomes (Kozak, 1986).

The 26 kDa and 28 kDa ECs accumulated as two of the more abundant proteins detected in the extracellular fractions from liquid cultures. This observation may be consistent with the production and accumulation of ELF in nature, since proteases produced by other organisms may be present and could degrade ELF, as it was sensitive to trypsin for example. The relative abundance of ELF could possibly provide a buffer for its degradation and allow a sufficient number of ELF to remain and be able to elicit a response when required. Clearly, factors such as pH would influence both the accumulation of ELF and enzymatic mediated proteolysis. The

bioassays used to study ELF were conducted at pH 6.5, which is proximate enough to the optimum (pH 7-9) of trypsin to provide approximately 50% of max activity (Sipos and Merkel, 1970) and a suitable condition for protein hydrolysis. Although in nature pH conditions are dependent on the environment and other organisms, *B. bassiana*, like other fungi, possess the ability to adjust their surrounding pH by secreting acids, such as oxalic acid (Bidochka and Khachatourians, 1991). This enables *B. bassiana* to acidify its immediate surroundings; however, the impact of pH change on the accumulation of ELF is unknown, but could influence the activities of proteases that ELF may encounter. Furthermore, ESCs produced by *E. coli* have been found to be responsive to activation by mild acid and alkaline conditions (Rowbury *et al.*, 1998; Rowbury and Goodson, 1999a; Rowbury and Goodson, 2005); however this effect has not been tested in *B. bassiana*. It appears that ELFs may be quite stable, especially to heat stress, other than their sensitivity to trypsin, and remain functional after storage at -30 °C for 4 d.

The accumulation of ELF in *B. bassiana* cultures was consistent with the relatively high concentration required to induce elevated tolerance, as demonstrated in BS with TG-ELF. Here the findings show that the EC_{50} of TG-ELF was $\approx 1.7 \times 10^{-7}$ M or 5.2 µg mL^{-1}. In contrast, Rowbury and Goodson (1999a) found that *E. coli* could respond to ESC concentrations that were not visible on SDS-PAGE even following silver stain which can detect as little as 0.5-5 ng depending on the protein (Winkler *et al.*, 2007). Rowbury and Goodson (1999a) used CFF: growth medium (1:3) which was estimated to contain < 0.0125 to 0.125 µg ESC mL^{-1} to produce EIT to acid. This is $\approx 7 \times 10^{-6}$ to 7×10^{-5} M of ESC, estimating that ESC is 15 kDa, although its actual size was undetermined. Therefore in comparison, *E. coli* may have required > 40 – 400-fold less acid activated ESC to cause EIT to acid than was required to produce EIT to heat in BS with TG-ELF. However, differences are expected since the molecule, activator, stress challenge

and organism all differed, as even similar enzymes that are produced by different organisms may have differing reaction kinetics (Joshi *et al.*, 1997).

The relatively high amount of TG-ELF required to induce the response may be indicative of the kinetics of the potential interaction between ELF and its target(s), since the dose response relationship is often positively correlated with the dissociation constant of the interaction (Lambert, 2004). In addition, signal transduction systems generally utilize agonist-receptor interactions with low affinity (Lemmon, 2009). Furthermore, the dose response of BS to ELF followed a semi-sigmoidal relationship, which is typical for responses governed by a saturable interaction and is the case for many agonist-receptor interactions (Lambert, 2004).

Quantitative binding studies are required to characterize the kinetics of the apparent ELF-BS interaction. However, the dose requirement of ELF for EIT to occur and the results from a pull-down assay with semi-purified ECs provided strong inferential clues for the binding kinetics of a potential interaction between the ELF agonist and the cell surface. Namely, that the interaction may possess low binding affinities and may not follow mass action kinetics. A ligand that is able to bind with a free target then dissociate and retain its ability to bind again can be described as following mass-action kinetics. However, in the case of ELF, it may be possible that active ELF is not free to bind again, following an initial interaction with the cell. The results of a pull-down experiment with semi-purified ECs, suggested that nearly all EC1 was depleted following an interaction with BS. This implicated a possible mechanism for the removal of ELF from the supernatant that did not involve its extracellular degradation, due to the similarity of the banding pattern provided by other proteins that remained in the supernatant following the various treatments. Although others may be conceivable, a possible explanation for the apparent depletion of EC1 is through its endocytosis following an interaction with the cell. Such a phenomenon has

been found to occur in receptor tyrosine kinases, such as ERB-1 in humans (Waterman and Yarden, 2001) and the G-protein coupled receptors, such as the mating a-factor receptor in *S. cerevisiae* (Chen and Davis, 2000). In both examples, upon binding with their proteinaceous ligand, the ligand-receptor complex is activated and is translocated into the cell via endocytosis and the receptor is recycled back to the cell surface where it is free to interact with another ligand and repeat the cycle. In the case of receptor tyrosine kinases, this process required ~ 15 min in human models (Hopkins *et al.,* 1990) and this type of receptor is known to be present at some of the highest numbers ($>10^5$) per cell (Hendriks *et al.*, 2003). Therefore, the ability for direct up-take, speed of receptor recycling and number of receptors may all be consistent with the results of the pull-down assay, but direct evidence is needed to determine if this type of interaction occurs with ELF.

However, some of the components potentially involved in signal transduction pathways that require endocytosis may be present in *B. bassiana*. For instance, a sequence encoding an apparent homologue of PRK-1's substrate is present in the genome of *B. bassiana* (Xiao *et al.*, 2012). A homologue of ERB-1's cytosolic substrate has been found in *S. cerevisiae* and confirmed to be phosphorylated by PRK-1, a tyrosine kinase (Zeng and Cai, 1999). In addition to the conserved pheromone receptors, *B. bassiana* is also known to possess ~ 21 PTH-11-like G-protein coupled receptor homologues (Gao *et al.*, 2011). Furthermore, endocytosis has been established in many filamentous fungi, however the molecular components involved are less understood than in *S. cerevisiae* or higher eukaryotes (Shaw *et al.*, 2011). Nonetheless, many of the involved components have homologues in model filamentous fungi, such as *N. crassa* (Borkovich *et al.*, 2004). Experimental evidence is in support of endocytosis occurring in *B. bassiana*, as demonstrated by uptake of a fluorescent probe by hyphae and BS (Lewis *et al.*,

2009). As a result, a mechanism for extracellular ligand import, such as through receptor endocytosis may be possible in *B. bassiana*. Therefore, endocytosis coupled with the relative abundance of the types of receptors which can exhibit endocytosis could possibly contribute to the depletion of EC1 observed in a whole-cell pull-down assay described in this thesis. Additionally, examples exist which demonstrate that the accumulation of a specific ligand and its target is positively correlated. For example, fibronectin and its target alpha-5 integrin are present in humans at 300 $\mu g\ mL^{-1}$ and $5x10^5$ per cell in blood plasma and the extracellular matrix, respectively (Akiyama and Yamada, 1985). However, additional research is needed to confirm and establish the interaction kinetics of the potential ELF-cell surface receptor interaction.

G protein- and enzyme-coupled receptors were also indirectly implicated by another line of independent evidence. This was revealed once the sequence of the entire ORF encoded by *elf* was obtained, which encoded a SSCP. Many of these proteins in fungi (Brown *et al.*, 2012; Druzhinina *et al.*, 2012; Xiao *et al.*, 2012) and human (Lavergne *et al.*, 2012) have already been identified and like ELF their functions were generally unknown. As a result, Lavergne *et al.* (2012) pursued this group of proteins in humans with the aim of assigning functions to them through the use of a step-wise high throughput algorithm. This showed that many proteins of this type in humans were often ligands for G protein- and enzyme-coupled receptors; two receptor types that have been found to undergo endocytosis following interaction with their ligand. In addition, both types of receptors are involved in signal transduction which can include MAPKs. It is well established that MAPKs, such as HOG-1, are involved in the response to stress in fungi (Reviewed in Morano *et al.*, 2012). Furthermore, the heat response in general is known to involve G protein- and enzyme-coupled receptors (see section 2.7.1). Although these

findings are indirect they are nonetheless consistent with the hypothesis that ELF is involved in the stress response to heat.

Some of the molecular components involved in the signaling pathways required to produce the HSR in other fungi have been characterized in *B. bassiana* (see section 2.7.1). Two MAPKs, HOG-1 (Zhang *et al.*, 2009) and SLT-2 (Luo *et al.*, 2012) as well as a regulator of G protein-signaling (Fang *et al.*, 2008), have all been found to influence thermotolerance in *B. bassiana*. Furthermore, a homologue of the histidine kinase involved in the HOG-1 pathway has been shown to be involved in thermotolerance in *M. robertsii* (Zhou *et al.*, 2012). However, drawing specific inferences between the signaling pathways of filamentous fungi is difficult since their pathways are able to respond to a variety of stresses and are more integrated than in *S. cerevisiae* which function more independently of each other (Bahn *et al.*, 2007). While most bacterial histidine kinases possess extracellular sensor regions, those from fungi generally do not. This implied that many of the signals that fungal histidine kinases respond to may be internal, such as oxidation (Catlett *et al.*, 2003). However, it is also possible that other receptor proteins are involved in signal integration with histidine kinases by receiving the extracellular signals (which could possibly be carried by ELF/ESCs) and relaying them to intracellular histidine kinases. This has been found to occur in *E. coli* and is required for signaling through its chemo-taxis histidine kinase (Reviewed in Levit *et al.*, 1998).

With regards to testing of the EIT system, a difference between the methodologies used in *E. coli* compared to *B. bassiana*, *S. cerevisiae* or *C. jejuni* was apparent. The difference was following activation of ESCs by heat, for example, the CFF was cooled prior to adding *E. coli* cells to promote EIT in them (Rowbury, 2005). Conversely, in the works described here in *B. bassiana* and by others in *S. cerevisiae* (Vovou *et al.*, 2004) or *C. jejuni* (Murphy *et al.*, 2003)

the stress was not removed prior to adding the cells to the medium. Furthermore, in the studies with yeast, CFF was prepared from a heat challenged cell culture, therefore it was not possible to establish that activation occurred independent of cells, since the effect of preheating CFF without cells present was not tested. Although the effect of removing activating stress condition was not tested in *S. cerevisiae* or *C. jejuni*, it was in *B. bassiana*. The results of a single experiment suggested that cooling CFF that was suspected to contain ELFs, removed its ability to induce tolerance to heat in BS, which had survival rates comparable to those treated with fresh growth medium.

In contrast with the above, Rowbury (2005) found that ESCs can also cause EIT once the activating stress is removed, however the duration that ELFs remained active for was not stated. He argues that in *E. coli* this may allow the ESCs to diffuse (or possibly move through other means such as advection) from locations experiencing an insult, remain active and interact with unstressed cells to warn them of the impending stress. This would presumably allow cells to initiate EIT in advance of the challenge so they can better survive it once it is encountered. However, what happens if the 'impending' stress does not reach the cells during the time they have acquired environmental stress tolerance? This would likely lead to a decrease in their fitness, assuming that the tolerance mechanisms involved in EIT are similar to those involved in the HSR or other responses to environmental stress. For example, the HSR is characterized by a large change in cellular metabolism [> 100 genes are responsive to supra-optimal heat in *S. cerevisiae* (Gasch *et al.*, 2000)]. This modulation in genetic expression is needed to survive high temperatures, but it comes at the cost of reducing expression of other genes which encode products that are required for growth.

An overview of the molecular biology of ELF is graphically presented in Figure 7.1. This description is based on sections of the ELF/EIT model that have been observed in this thesis and those that can be integrated from other known systems, such as the general PTM of secreted proteins. The *elf* gene is nuclear and the presence of its transcript is correlated with hyphae and BS, which are all normally present during growth of *B. bassiana* at its optimal temperature. Following translation of the *elf* transcript, as with other nuclear gene transcripts, nascent ELF is likely directed to the rough endoplasmic reticulum by its secretion signal sequence, which is cleaved and removed (Peberdy, 1999). The PTM of ELF is expected to be through glycosylation within the rough endoplasmic reticulum and followed by transportation to the Golgi complex for maturation of the attached oligosaccharide(s). Subsequently, ELF is translocated to the cell membrane within vesicles, for secretion through exocytosis. Once outside of the cell and exposed to heat stress conditions, ELF becomes active through an unknown mechanism that appears to be reversible and may involve a conformational change in its structure, induced by the heat condition or allostery (Rowbury and Goodson, 2001). Active ELF can promote EIT to heat in BS, and similar to ESC in *E. coli* (Rowbury and Goodson, 2001; Rowbury, 2001a; Rowbury, 2001b) it interacts with the cell surface, which may involve an ELF receptor(s). The cellular events that are co- or pre-requisite for the establishment of EIT are hypothetical at this point, but may require transduction of the signal carried by activated ELF (Rowbury, 2001a; Rowbury, 2003a; Rowbury, 2005). In addition, the cellular physiology that characterizes EIT to heat is yet to be established, but may include changes to gene expression. This model is conceptually consistent with other current models of cell-cell communication and signal transduction.

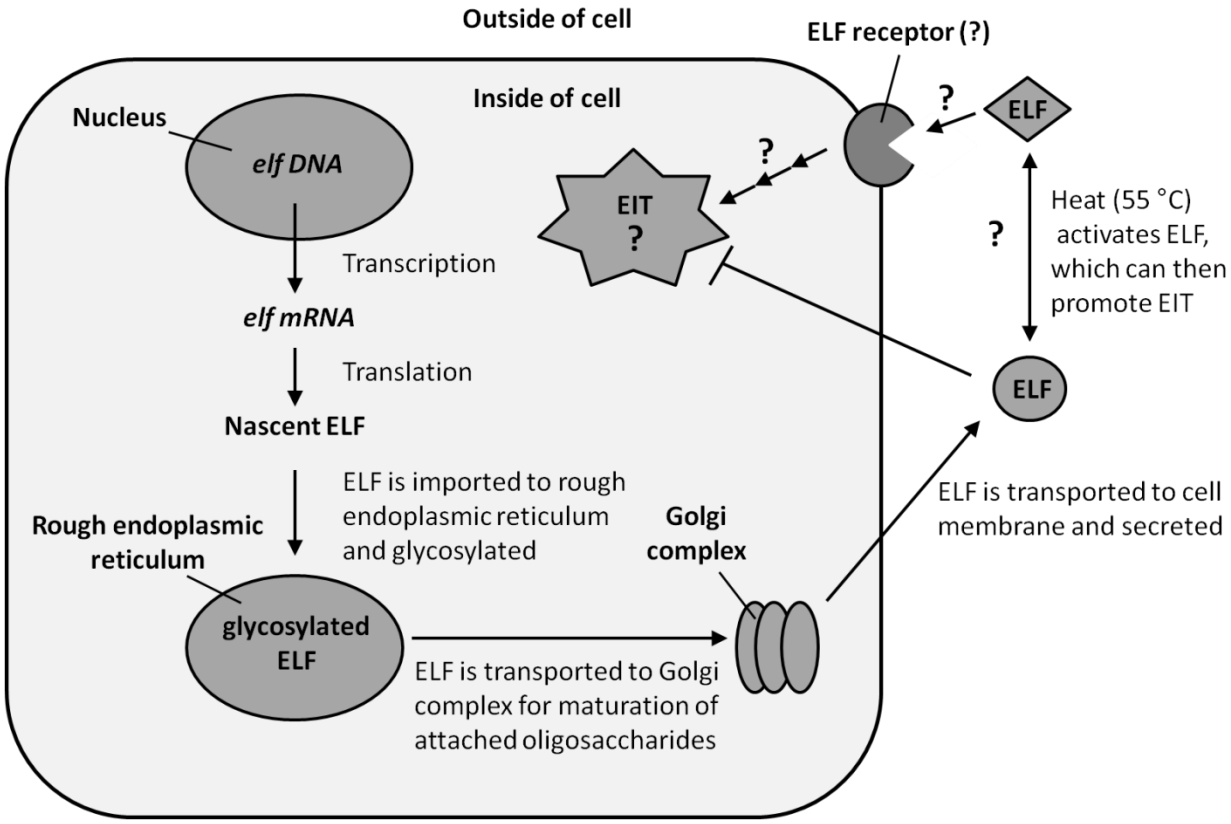

Figure 7.1 Schematic overview of ELF molecular biology and the steps required for the promotion of EIT. The sections of the model without question marks are based on results from this thesis and those that were integrated from other known systems, such as the general PTM of secreted proteins by eukaryotes. Arrows represent putative steps. The flat headed arrow denotes that prior to being exposed to heat, ELF is not in an active state and cannot establish EIT. Question marks indicate sections of the ELF/EIT model that are speculative but required for the establishment of EIT to heat. These include activation of ELF, interaction between ELF and receptor, signal transduction and the cellular physiology which characterizes EIT to heat.

Findings in *B. bassiana* and possibly those in *S. cerevisiae* and *C. jejuni* may be more consistent with the current understanding of the HSR, since the ability of the suspected factors to increase tolerance to UVR in CS may have been reduced following the cooling of CFF to 22 °C. This feature may safeguard cells from undergoing EIT when a stress may not be encountered, allowing it to grow as normal. Of course this would be expected, to some extent, to limit ELFs ability to cause EIT in advance of an environmental stress condition. However, the exact temporal requirements of the exposure of BS to ELF required to promote EIT to heat remains elusive. The discovery of a reporter gene, responsive to ELF would allow this to be studied and provide insight into the requirements for expression needed to produce EIT.

It appears that treatment with preheated ELF can improve survival of heat challenged BS when supplied concurrently or following the stress, as shown by the heat challenge assays or *in situ* ELF assays, respectively. To refresh the reader, the *in situ* assay involved overlaying soft YPGA seeded with heat challenged BS on a polyacrylamide gel strip which contained extracellular F80 proteins that were previously separated by CN-PAGE. The gel strips were also preheated prior to being overlaid with YPGA to promote ELF activation, which is thought to be required to increase the survival of heat challenged BS. Following this, the gels were incubated at 27 °C, enumerated and survival of BS was compared between gel sections. The *in situ* assay demonstrated the ability of the suspected ELF to increase the survival of heat challenged BS immobilized within the agar and was expected to be contingent on its sequential diffusion through polyacrylamide and agar matrices, while remaining in an active state. This suggested that ELF likely can remain active at temperatures less than 55 °C. However, the temperature decrease from 55 °C, experienced by the ECs contained in the gel, would not be as rapid as in CFF cooled to 22 °C (as in the above paragraph), due to the heat insulation provided by the polyacrylamide

gel and agar overlay, which were both preheated to 55 °C and subsequent incubation of the gel at 27 °C would also slow cooling. This less rapid cooling from 55 °C was expected to slow ELFs reversion to an inactivate state that may be incapable of causing EIT. By extension, it is apparent that the reduction in activity of ELF as a function of temperature may not be abrupt, since the polyacrylamide and agar matrices would not remain at 55 °C for the entire duration required for ELF to diffuse and come into contact with BS.

The ability of the suspected ELF to diffuse through these matrices was consistent with the assumption the *in situ* assay was based on. This was namely that putative ELFs could diffuse at a predicted rate that was sufficient for them to encounter some of the immobilized BS before the factors reverted to an inactive state. The estimated rate of diffusion for ELF in polyacrylamide was based on the findings of Lewus and Carta (1999) who, for example, found that a protein of ~ 13 kDa could diffuse a distance of ~ 0.4 mm in a 20% (w v^{-1}) polyacrylamide gel over 1 h. Therefore, it was estimated that a protein of ~ 30 kDa, impregnated in a 10% (w v^{-1}) polyacrylamide gel, could diffuse ≥ 0.4 mm in 1 h. This was because the diffusion rates of the ECs were expected to be increased with a reduction in polyacrylamide concentration more than they would be decreased due to an increase in protein mass, compared to the parameters studied by Lewus and Carta (1999). As a result, it was found that the sections with most surviving BS were correlated with particular protein species and were considered ECs. The increase in survival of BS was dependent on their proximity to the ELF pool, which was the location on the polyacrylamide gel that the protein migrated to during CN-PAGE. As a result, sections containing BS that were further from the source of the diffusing ELFs, yet close enough that the molecules provided a detectable increase in survival, could be distinguished from sections that were further still. This method identified two proteins as ECs. It should be noted that the motive for the creation of

the *in situ* assay was not the development of a high resolution detection assay. Instead it was developed as a means to screen, with relatively high throughput, the many extracellular proteins present in F80 for their ability to provide BS with improved survival following heat challenge and identify ECs.

In conventional models of the stress response, the stressor is indirectly detected inside the cell, such as through the perturbations it causes to cellular physiology, protein denaturation or through sensory integral proteins within the cytoplasmic membrane in bacteria (Reviewed in Neidhardt *et al.*, 1990). In the case of ESCs or ELFs, their function may be as an extracellular sensor and could be able to directly relay a message(s) to the cell. However, the most obvious contrast between the conventional models and responses that may involve ESC/ELFs is that the sensory function appears to occur outside of the cell in the latter. The apparent extracellular sensory function may allow ESCs and ELFs to interact with and cause EIT in cells that did not directly produce them (Rowbury, 2001b). Therefore, it could be possible for a cell that lost its ability to produce ELF, for genetic or other reasons, to still acquire EIT from ELFs that were produced by other nearby cells once activated, as long as the cell retained its ability to receive the signal that is suspected to be carried by active ELF. The ability of ESC molecules produced by *E. coli* to diffuse from one cell and influence the stress responses of others has been considered a pheromonal activity (Rowbury, 2001b). However, the spatial requirements of ESC/ELF producing cells, relative to the ability of ESC/ELFs produced by them to interact with and promote EIT in other cells has yet to be established in any system.

It has been acknowledged that the heat response model is incomplete and the true elicitor of the response remains elusive (Morano *et al.*, 2012). As a result, a secreted sensory component would not be in contention of the current models, especially in filamentous fungi which are

thought to have extensive integration within their signaling pathways that are responsive to environmental stress conditions (Bahn *et al.*, 2007). In addition, a system that is capable of acting extracellularly to sense environmental stress conditions does not likely represent a replacement for the established mechanisms involved in the response to stress. For example, ELFs could instead represent a partially redundant role in stress sensing. Redundancies are not uncommon in biological systems and have been revealed in many fields of study in the life sciences (Nowak *et al.*, 1997). It is logical that important functions have back-up modules which can be employed in the event of failure and have been suspected to be genetically stable (Nowak *et al.*, 1997). Therefore, ELF need not be a substitute for established intracellular sensing mechanisms as direct sensing of heat by other molecules has been established. For example, HSP-70 is known to elevate its ATPase activity in response to high temperatures, which enables it to better perform its function as a chaperone (McCarty and Walker, 1991). Direct responses, such as this allow cells to rapidly alter their physiology in response to a stress, where HSR and possibly EIT would influence global changes to gene expression and have a larger effect on the cell's physiology, but require more time.

Candidate *elf* sequences were also found in two other strains of *B. bassiana*, which may indicates that it is likely a conserved trait in this EPF. Consistent with this, the most similar sequences to ELF not from *B. bassiana* were found in *M. anisopliae*, but did not have assigned functions. It is unclear if putative ELFs exist in other EPF or filamentous fungi. Furthermore, this study was not able to determine a putative function for ELF through various *in silico* methods of sequence analysis. As a result, the determination of the molecular activity of ELF remains a priority in this field of research. However, several of the sequences that were most similar to ELF possessed the highest similarity in their N-terminal regions, which suggested that

this region may contain a conserved structure/function. Conversely, BS from *T. inflatum* and *I. farinosa* were not responsive to TG-ELF, which may indicate that this molecule is specific to *B. bassiana* but does not eliminate the possibility that these fungi are capable of producing their own specific ELF(s). The potential specificity of ELF could restrict its ability to cause EIT in other fungi and only elicit a response in the fungus (species or strain for instance) that produced it and may be controlled by the selective nature of the potential interaction between ELF and its cell surface target.

Production of ELF, by *B. bassiana*, to a threshold concentration needed to produce increased heat tolerance when an activating temperature is reached, are apparent requirements for the phenomenon that resembles EIT in *E. coli* to occur in *B. bassiana*. Therefore, under conditions of environmental stress, restrictions may be imposed on a smaller population of a different fungus from parlaying an established infection or other micro-environment into their own advantage, unless they had produced their own ELF(s) to a sufficient concentration; compared to a situation where they could respond to the already present ELF. This could allow the primary EPF population to sequester more of the resources from the insect or other utilizable organic matter and produce more biomass once the stress conditions has passed. In this regard, the presence of ELFs may be to the detriment of the host insect and could help explain the existence of the internal repeats found in the ELF sequence. In fungal phytopathogens, internal repeats have been thought to be involved in accelerated protein evolution, which is speculated to be involved in them escaping detection by the host's immune system (Rudd *et al.*, 2010).

In addition to behaving as an entomopathogen, *B. bassiana* and other EPF can also exist as saprobes and endophytes (Posada and Vega, 2005), which may convolute the speculated role(s) of ELF. For instance, it has been shown that *M. robertsii* can transfer nitrogen acquired

from infected insects to plants, such as switchgrass (*Panicum virgatum*) through their endophytic relationship (Behie *et al.,* 2012). As a result, it is difficult to confidently speculate as to what role EIT may play when *B. bassiana* engages in its various lifestyles and how ELF influences fungal ecology in each.

This thesis represents the extent of knowledge regarding ELF in EPF and filamentous fungi in general. The results disclosed here have greatly extended the knowledge of EIT and describe for the first time purification of an ELF, its *de novo* sequencing, characterization and discovery of its encoding gene. Still it remains to be determined how these molecules are specifically involved in the stress response. Such a discovery would be aided by the development of reporter genes that are responsive to ELF and the elucidation of potential interaction target(s) for ELF on the cell's surface. Also, the role of ELF in *B. bassiana*'s larger biological context is yet to be determined; however, its ability to increase heat tolerance in BS suggests that it may be involved in surviving the elevated temperatures the fungus may encounter during its various lifestyles.

8.0 GENERAL CONCLUSIONS

1. Regions from a putative *phr-1* were found in six EPF belonging to the genera *Beauveria*, *Isaria*, *Lecanicillium*, *Metarhizium* and *Tolypocladium*.

2. The regions of putative *phr-1* encoded a likely CPD-PHR with conserved, functionally important residues that are known to be involved in CPD-, FAD- and MTHF-binding, in addition to those implicated in electron transfer and are required for CPD repair.

3. The deduced amino acid sequences encoded by the putative *phr-1*s could be differentiated from other related PHR/CRYs through sequence analysis and homology modeling, which predicted that the EPF sequences had CPD-PHR activity.

4. All but one of the six putative CPD-PHR sequences had phylogenetic relationships that were consistent with the established phylogenies of the EPF they were identified in.

5. Proteins that are considered ECs are secreted by *B. bassiana* during growth at its optimal temperature.

6. The ECs in CFF has a requirement for heat stress conditions to be present for it to increase tolerance in CS and BS to UVR and heat, respectively, which resembles the EIT phenomenon in *E. coli*. It was not determined if these responses were controlled by the same extracellular protein(s), but likely have different temporal requirements to promote tolerance.

7. All ECs studied here are proteins and proteolysis removes their ability to increase environmental stress tolerance.

8. The putative ELF that controls EIT to UVR may be heat stable and might exhibit reversible thermal denaturation.

9. It is unlikely that photoreactivation of damaged DNA is involved in increasing UVR survival in CS following treatment with CFF.

10. In BS, the phenomenon that resembles EIT to heat may only be to lethal temperatures and does not affect growth at supra-optimal, sub-lethal temperatures, under the tested conditions.

11. Increased heat tolerance was acquired by BS when F80 containing ECs was supplied during or following heat challenge.

12. The EC1 protein can diffuse through polyacrylamide and agar matrices to increase survival in heat challenged BS, is a glycosylated protein of ~ 28 kDa and may be able to interact with the surface of BS.

13. In addition, a non-glycosylated protein (EC2) is also secreted by *B. bassiana* and shares the same primary structure as its glycosylated form (EC1), but may have a reduced capacity to interact with BS and cause elevated tolerance to heat.

14. Since purified EC1 was able to increase heat tolerance in BS, it was considered to likely be an ELF. This is because the ability to increase tolerance to environmental stress conditions is the only known measureable characteristic of proteins like ESC, which have been shown to be involved in EIT.

15. An intronless gene candidate for *elf* was identified and has an ORF of 741 bp which encoded eight *de novo* peptide sequences identified in both EC1 and EC2, which confirmed that it encoded these ECs.

16. In addition to *B. bassiana* GK2016, *elf* candidates were also found in the strains ARSEF 2860 and ARSEF 3113. The sequences most similar to the *elf* candidates not from *B. bassiana* were found in *M. anisopliae* (*M. robertsii*). The products encoded by several of these sequences had most sequence similarity with ELF in their amino terminal region. However, none of the sequences that were similar to ELF had known functions.

17. Structure/function predictions were not successful in assigning candidate functions to ELF, likely due to a lack of known structural homologues.

18. The structure of ELF may have potentially novel features since no similar structures were identified in the data base.

19. It is likely that ELF is an SSCP and also has three internal sequence repeats.

20. Transgenic expression in *P. pastoris* yielded functional TG-ELF that was able to increase heat tolerance in BS and produced a semi-sigmoidal dose response curve.

21. The CS, swollen CS and hyphae produced by *B. bassiana* were not responsive to TG-ELF as measured by their tolerance to heat challenge, nor were the BS produced by *I. farinosa* or *T. inflatum*.

9.0 REFERENCES

Adams, M.D., Kerlavage, A.R., Fleischmann, R.D., Fuldner, R.A., Bult, C.J., Lee, N.H., Kirkness, E.F., Weinstock, K.G., Gocayne, J.D., White, O., 1995. Initial assessment of human gene diversity and expression patterns based upon 83 million nucleotides of cDNA sequence. Nature 377, 3-174.

Ahmad, M., Cashmore, A.R., 1993. HY4 gene of *A. thaliana* encodes a protein with characteristics of a blue-light photoreceptor. Nature 366, 162-166.

Akiyama, S.K., Yamada, K.M., 1985. The interaction of plasma fibronectin with fibroblastic cells in suspension. J. Biol. Chem. 260, 4492-4500.

Albuquerque, P., Casadevall, A., 2012. Quorum sensing in fungi – a review. Med. Mycol. 50, 337-345.

Alejandre-Durán, E., Roldán-Arjona, T., Ariza, R.R., Ruiz-Rubio, M., 2003. The photolyase gene from the plant pathogen *Fusarium oxysporum* f. sp. *lycopersici* is induced by visible light and α-tomatine from tomato plant. Fungal Genet. Biol. 40, 159-165.

Altschul, S.F., Madden, T.L., Schäffer, A.A., Zhang, J., Zhang, Z., Miller, W., Lipman, D.J., 1997. Gapped BLAST and PSI-BLAST: a new generation of protein database search programs. Nucleic Acids Res. 25, 3389-3402.

Arthurs, S., Thomas, M.B., 2001. Effect of dose, pre-mortem host incubation temperature and thermal behaviour on host mortality, mycosis and sporulation of *Metarhizium anisopliae* var. *acridum* in *Schistocerca gregaria*. Biocontrol Sci. Technol. 11, 411-420.

Attfield, P.V., 1997. Stress tolerance: the key to effective strains of industrial baker's yeast. Nat. Biotechnol. 15, 1351-1357.

Aubert, C., Vos, M.H., Mathis, P., Eker, A.P.M., Brettel, K., 2000. Intraprotein radical transfer during photoactivation of DNA photolyase. Nature 405, 586-590.

Audouin, J.V., 1838. Nouvelles expériences sur la nature de la maladie contagieuse qui attaque les vers à soie et qu'on désigne sous le nom de Muscardine. Ann. Sci. Nat. 8, 257-270.

Bachmann, B., Lüke, W., Hunsmann, G., 1990. Improvement of PCR amplified DNA sequencing with the aid of detergents. Nucleic Acids Res. 18, 1309.

Bahn, Y.S., Xue, C., Idnurm, A., Rutherford, J.C., Heitman, J., Cardenas, M.E., 2007. Sensing the environment: lessons from fungi. Nat. Rev. Microbiol. 5, 57-69.

Baker, D., Sali, A., 2001. Protein structure prediction and structural genomics. Science 294, 93-96.

Barelli, L., Padilla-Guerrero, I.E., Bidochka, M.J., 2011. Differential expression of insect and plant specific adhesin genes, Mad1 and Mad2, in *Metarhizium robertsii*. Fungal Biol. 115, 1174-1185.

Barranco-Florido, E., García-Hernández, L.A., Rodríguez-Navarro, S., Flores-Macías, A., Ramos-López, M.A., 2013. Regulation of gene expression in entomopathogenic fungi in three different environmental conditions: A review. Afr. J. Biotechnol. 12, 989-995.

Barros, B.H., da Silva, S.H., dos ReisMarques Edos, R., Rosa, J.C., Yatsuda, A.P., Roberts, D.W., Braga, G.U., 2010. A proteomic approach to identifying proteins differentially expressed in conidia and mycelium of the entomopathogenic fungus *Metarhizium acridum*. Fungal Biol. 114, 572-579.

Bause, E., 1983. Structural requirements of N-glycosylation of proteins. Studies with proline peptides as conformational probes. Biochem. J. 209, 331-336.

Behie, S.W., Zelisko, P.M., Bidochka, M.J., 2012. Endophytic insect-parasitic fungi translocate nitrogen directly from insects to plants. Science 336, 1576-1577.

Berg, J.M., Tymoczko, J.L., Stryer, L., 2002. Biochemistry. W.H, Freeman, New York, N.Y.

Berrocal-Tito, G.M., Esquivel-Naranjo, E.U., Horwitz, B.A., Herrera-Estrella, A., 2007. *Trichoderma atroviride* PHR1, a fungal photolyase responsible for DNA repair, autoregulates its own photoinduction. Eukaryot. Cell 6, 1682-1692.

Berrocal-Tito, G., Sametz-Baron, L., Eichenberg, K., Horwitz, B.A., Herrera-Estrella, A., 1999. Rapid blue light regulation of a *Trichoderma harzianum* photolyase gene. J. Biol. Chem. 274, 14288-14294.

Bidochka, M.J., Pfeifer, T.A., Khachatourians, G.G., 1987. Development of the entomopathogenic fungus *Beauveria bassiana* in liquid cultures. Mycopathologia 99, 77-83.

Bidochka, M.J., Khachatourians, G.G., 1991. The implication of metabolic acids produced by *Beauveria bassiana* in pathogenesis of the migratory grasshopper, *Melanoplus sanguinipes*. J. Invertebr. Pathol. 58, 106-117.

Billings, F.H., Glenn, P.A., 1911. Results of the artifcial use of the white-fungus disease in Kansas. USDA Bur. Entomol. Bull. 107, 58.

Bluhm, B.H., Dunkle, L.D., 2008. PHL1 of *Cercospora zeae-maydis* encodes a member of the photolyase/cryptochrome family involved in UV protection and fungal development. Fungal Genet. Biol. 45, 1364-1372.

Borkovich, K.A., Alex, L.A., Yarden, O., Freitag, M., Turner, G.E., Read, N.D., Seiler, S., Bell-Pedersen, D., Paietta, J., Plesofsky, N., Plamann, M., Goodrich-Tanrikulu, M., Schulte, U., Mannhaupt, G., Nargang, F.E., Radford, A., Selitrennikoff, C., Galagan, J.E., Dunlap, J.C., Loros, J.J., Catcheside, D., Inoue, H., Aramayo, R., Polymenis, M., Selker, E.U., Sachs, M.S., Marzluf, G.A., Paulsen, I., Davis, R., Ebbole, D.J., Zelter, A., Kalkman, E.R., O'Rourke, R., Bowring, F., Yeadon, J., Ishii, C., Suzuki, K., Sakai, W., Pratt, R., 2004. Lessons from the genome sequence of *Neurospora crassa*: tracing the path from genomic blueprint to multicellular organism. Microbiol. Mol. Biol. Rev. 68, 1-108.

Bradford, M.M., 1976. A rapid and sensitive method for the quantitation of microgram quantities of protein utilizing the principle of protein-dye binding. Anal. Biochem. 72, 248-254.

Braga, G.U., Flint, S.D., Messias, C.L., Anderson, A.J., Roberts, D.W., 2001a. Effects of UVB irradiance on conidia and germinants of the entomopathogenic Hyphomycete *Metarhizium anisopliae*: a study of reciprocity and recovery. Photochem. Photobiol. 73, 140-146.

Braga, G.U., Flint, S.D., Miller, C.D., Anderson, A.J., Roberts, D.W., 2001b. Both solar UVA and UVB radiation impair conidial culturability and delay germination in the entomopathogenic fungus *Metarhizium anisopliae*. Photochem. Photobiol. 74, 734-739.

Braga, G.U., Flint, S.D., Miller, C.D., Anderson, A.J., Roberts, D.W., 2001c. Variability in response to UV-B among species and strains of *Metarhizium* isolated from sites at latitudes from 61 degrees N to 54 degrees S. J. Invertebr. Pathol. 78, 98-108.

Braga, G.U., Rangel, D.E., Flint, S.D., Anderson, A.J., Roberts, D.W., 2006. Conidial pigmentation is important to tolerance against solar-simulated radiation in the entomopathogenic fungus *Metarhizium anisopliae*. Photochem. Photobiol. 82, 418-422.

Braga, G.U.L., Rangel, D.E.N., Flint, S.D., Miller, C.D., Anderson, A.J., Roberts, D.W., 2002. Damage and recovery from UV-B exposure in conidia of the entomopathogens *Verticillium lecanii* and A*phanocladium album*. Mycologia 94, 912-920.

Brenner, S., Williams, S.R., Vermaas, E.H., Storck, T., Moon, K., McCollum, C., Mao, J., Luo, S., Kirchner, J.J., Eletr, S., DuBridge, R.B., Burcham, T., Albrecht, G., 2000. *In vitro* cloning of complex mixtures of DNA on microbeads: physical separation of differentially expressed cDNAs. Proc. Natl. Acad. Sci. U. S. A. 97, 1665-1670.

Brettel, K., Byrdin, M., 2010. Reaction mechanisms of DNA photolyase. Curr. Opin. Struct. Biol. 20, 693-701.

Brewster, J.L., de Valoir, T., Dwyer, N.D., Winter, E., Gustin, M.C., 1993. An osmosensing signal transduction pathway in yeast. Science 259, 1760-1763.

Brown, N.A., Antoniw, J., Hammond-Kosack, K.E., 2012. The predicted secretome of the plant pathogenic fungus *Fusarium graminearum*: a refined comparative analysis. PLoS One 7, e33731.

Brudler, R., Hitomi, K., Daiyasu, H., Toh, H., Kucho, K., Ishiura, M., Kanehisa, M., Roberts, V.A., Todo, T., Tainer, J.A., Getzoff, E.D., 2003. Identification of a new cryptochrome class: structure, function, and evolution. Mol. Cell 11, 59-67.

Candiano, G., Bruschi, M., Musante, L., Santucci, L., Ghiggeri, G.M., Carnemolla, B., Orecchia, P., Zardi, L., Righetti, P.G., 2004. Blue silver: a very sensitive colloidal Coomassie G-250 staining for proteome analysis. Electrophoresis 25, 1327-1333.

Carruthers, R.I., Larkin, T.S., Firstencel, H., Feng, Z., 1992. Influence of thermal ecology on the mycosis of a rangeland grasshopper. Ecology 73, 190-204.

Castellanos-Serra, L.R., Fernandez-Patron, C., Hardy, E., Huerta, V., 1996. A procedure for protein elution from reverse-stained polyarcylamide gels applicable at the low picomole level: An alternative route to the preparation of low abundance proteins for microanalysis. Electrophoresis 17, 1564-1572.

Castresana, J., 2000. Selection of conserved blocks from multiple alignments for their use in phylogenetic analysis. Mol. Biol. Evol. 17, 540-552.

Castrillo, M., Garcia-Martinez, J., Avalos, J., 2013. Light-dependent functions of the *Fusarium fujikuroi* CryD DASH cryptochrome in development and secondary metabolism. Appl. Environ. Microbiol. 79, 2777-2788.

Catlett, N.L., Yoder, O.C., Turgeon, B.G., 2003. Whole-genome analysis of two-component signal transduction genes in fungal pathogens. Eukaryot. Cell 2, 1151-1161.

Chaturvedi, V., Bartiss, A., Wong, B., 1997. Expression of bacterial mtlD in *Saccharomyces cerevisiae* results in mannitol synthesis and protects a glycerol-defective mutant from high-salt and oxidative stress. J. Bacteriol. 179, 157-162.

Chaves, I.N., Romana, M., Biernat, M.A., Bajek, M.I., Brand, K., da Silva, A.C., Saito, S., Yagita, K., Eker, A.P., van, d.H., 2011. The *Potorous* CPD photolyase rescues a cryptochrome-deficient mammalian circadian clock. PLoS ONE 6, 23447.

Cheetham, J., MacCallum, D.M., Doris, K.S., da Silva Dantas, A., Scorfield, S., Odds, F., Smith, D.A., Quinn, J., 2011. MAPKKK-independent regulation of the Hog1 stress-activated protein kinase in *Candida albicans*. J. Biol. Chem. 286, 42002-42016.

Chelico, L., 2004. Nucleotide excision repair of ultraviolet radiation treated *Beauveria bassiana*. Doctor of Philosophy Thesis. University of Saskatchewan, Saskatoon, Saskatchewan, CA .

Chelico, L., Haughian, J.L., Khachatourians, G.G., 2006. Nucleotide excision repair and photoreactivation in the entomopathogenic fungi *Beauveria bassiana, Beauveria brongniartii, Beauveria nivea, Metarhizium anisopliae, Paecilomyces farinosus* and *Verticillium lecanii*. J. Appl. Microbiol. 100, 964-972.

Chelico, L., Haughian, J.L., Woytowich, A.E., Khachatourians, G.G., 2005. Quantification of ultraviolet-C irradiation induced cyclobutane pyrimidine dimers and their removal in *Beauveria bassiana* conidiospore DNA. Mycologia 97, 621-627.

Chelico, L., Khachatourians, G.G., 2008. Isolation and characterization of nucleotide excision repair deficient mutants of the entomopathogenic fungus, *Beauveria bassiana*. J. Invertebr. Pathol. 98, 93-100.

Chen, L., Davis, N.G., 2000. Recycling of the yeast a-factor receptor. J. Cell Biol. 151, 731-738.

Chevenet, F., Brun, C., Banuls, A.L., Jacq, B., Christen, R., 2006. TreeDyn: towards dynamic graphics and annotations for analyses of trees. BMC Bioinformatics 7, 439.

Cortes, C., Vapnik, V., 1995. Support-vector networks. Mach. Learning 20, 273-297.

Costa, H., Robb, K., Wilen, C., 2001. Increased persistence of *Beauveria bassiana* spore viability under high ultraviolet-blocking greenhouse plastic. HortScience 36, 1082-1084.

Craig, E.A., Gross, C.A., 1991. Is hsp70 the cellular thermometer? Trends Biochem. Sci. 16, 135-140.

Cregg, J.M., Cereghino, J.L., Shi, J., Higgins, D.R., 2000. Recombinant protein expression in *Pichia pastoris*. Mol. Biotechnol. 16, 23-52.

Crick, F., 1974. The double helix: a personal view. Nature 248, 766-769.

Crick, F.H., 1970. Central dogma of molecular biology. Nature 227, 561-563.

Crowe, J.H., 2007. Trehalose as a "chemical chaperone": fact and fantasy. Adv. Exp. Med. Biol. 594, 143-158.

de Castro, E., Sigrist, C.J.A., Gattiker, A., Bulliard, V., Langendijk-Genevaux, P.S., Gasteiger, E., Bairoch, A., Hulo, N., 2006. ScanProsite: detection of PROSITE signature matches and ProRule-associated functional and structural residues in proteins. Nucleic Acids Res. 34, W362-W365.

de Crecy, E., Jaronski, S., Lyons, B., Lyons, T.J., Keyhani, N.O., 2009. Directed evolution of a filamentous fungus for thermotolerance. BMC Biotechnol. 9, 74.

de Guzman, D., 2009. Agriculture chemical firms' interest in biopesticides rises. http://www.icis.com/Articles/2009/06/16/9223644/agriculture-chemical-firms-interest-in-biopesticides.html. 2012.

Degols, G., Shiozaki, K., Russell, P., 1996. Activation and regulation of the Spc1 stress-activated protein kinase in *Schizosaccharomyces pombe*. Mol. Cell. Biol. 16, 2870-2877.

Dereeper, A., Audic, S., Claverie, J.M., Blanc, G., 2010. BLAST-EXPLORER helps you building datasets for phylogenetic analysis. BMC Evol. Biol. 10, 8.

Dereeper, A., Guignon, V., Blanc, G., Audic, S., Buffet, S., Chevenet, F., Dufayard, J.F., Guindon, S., Lefort, V., Lescot, M., Claverie, J.M., Gascuel, O., 2008. Phylogeny.fr: robust phylogenetic analysis for the non-specialist. Nucleic Acids Res. 36, W465-W469.

Doberski, J.W., 1981. Comparative laboratory studies on three fungal pathogens of the elm bark beetle *Scolytus scolytus*: effect of temperature and humidity on infection by *Beauveria bassiana, Metarhizium anisopliae*, and *Paecilomyces farinosus*. J. Invertebr. Pathol. 37, 195-200.

Domon, B., Aebersold, R., 2006. Mass spectrometry and protein analysis. Science 312, 212-217.

Don, R.H., Cox, P.T., Wainwright, B.J., Baker, K., Mattick, J.S., 1991. 'Touchdown' PCR to circumvent spurious priming during gene amplification. Nucleic Acids Res. 19, 4008-4008.

Druzhinina, I.S., Shelest, E., Kubicek, C.P., 2012. Novel traits of *Trichoderma* predicted through the analysis of its secretome. FEMS Microbiol. Lett. 337, 1-9.

Duina, A.A., Kalton, H.M., Gaber, R.F., 1998. Requirement for Hsp90 and a CyP-40-type cyclophilin in negative regulation of the heat shock response. J. Biol. Chem. 273, 18974-18978.

Edgar, R.C., 2004. MUSCLE: multiple sequence alignment with high accuracy and high throughput. Nucleic Acids Res. 32, 1792-1797.

Elliot, S.L., Blanford, S., Thomas, M.B., 2002. Host–pathogen interactions in a varying environment: temperature, behavioural fever and fitness. Proc. Biol. Sci. 269, 1599-1607.

El-Sharoud, W.M., Rowbury, R.J., 2006. Recent insights into microbial physiology. Sci. Prog. 89, 141-149.

Fan, Y., Fang, W., Guo, S., Pei, X., Zhang, Y., Xiao, Y., Li, D., Jin, K., Bidochka, M.J., Pei, Y., 2007. Increased insect virulence in *Beauveria bassiana* strains overexpressing an engineered chitinase. Appl. Environ. Microbiol. 73, 295-302.

Fang, W., Pava-ripoll, M., Wang, S., St Leger, R., 2009. Protein kinase A regulates production of virulence determinants by the entomopathogenic fungus, *Metarhizium anisopliae*. Fungal Genet. Biol. 46, 277-285.

Fang, W., Pei, Y., Bidochka, M.J., 2007. A regulator of a G protein signalling (RGS) gene, cag8, from the insect-pathogenic fungus *Metarhizium anisopliae* is involved in conidiation, virulence and hydrophobin synthesis. Microbiology 153, 1017-1025.

Fang, W., Scully, L.R., Zhang, L., Pei, Y., Bidochka, M.J., 2008. Implication of a regulator of G protein signalling (BbRGS1) in conidiation and conidial thermotolerance of the insect pathogenic fungus *Beauveria bassiana*. FEMS Microbiol. Lett. 279, 146-156.

Fang, W., St Leger, R.J., 2012. Enhanced UV resistance and improved killing of malaria mosquitoes by photolyase transgenic entomopathogenic fungi. PLoS One 7, e43069.

Fang, W., Vega-Rodriguez, J., Ghosh, A.K., Jacobs-Lorena, M., Kang, A., St Leger, R.J., 2011. Development of transgenic fungi that kill human malaria parasites in mosquitoes. Science 331, 1074-1077.

Fargues, J., 2003. New challenges for fungal bioinsecticides. Insect pathogens and entomoparasitic nematodes. IOBC/WPRS Bull 26, 9-20.

Fargues, J., Goettel, M.S., Smits, N., Ouedraogo, A., Rougier, M., 1997a. Effect of temperature on vegetative growth of *Beauveria bassiana* isolates from different origins. Mycologia 89, 383-392.

Fargues, J., Rougier, M., Goujet, R., Smits, N., Coustere, C., Itier, B., 1997b. Inactivation of conidia of *Paecilomyces fumosoroseus* by near-ultraviolet (UVB and UVA) and visible radiation. J. Invertebr. Pathol. 69, 70-78.

Feng, M.G., Poprawski, T.J., Khachatourians, G.G., 1994. Production, formulation and application of the entomopathogenic fungus *Beauveria bassiana* for insect control: current status. Biocontrol Sci. Technol. 4, 3-34.

Fernandes, E.K., Keyser, C.A., Chong, J.P., Rangel, D.E., Miller, M.P., Roberts, D.W., 2010. Characterization of *Metarhizium* species and varieties based on molecular analysis, heat tolerance and cold activity. J. Appl. Microbiol. 108, 115-128.

Fernandes, E.K., Rangel, D.E., Moraes, A.M., Bittencourt, V.R., Roberts, D.W., 2008. Cold activity of *Beauveria* and *Metarhizium*, and thermotolerance of *Beauveria*. J. Invertebr. Pathol. 98, 69-78.

Fernandes, E.K., Rangel, D.E., Moraes, A.M., Bittencourt, V.R., Roberts, D.W., 2007. Variability in tolerance to UV-B radiation among *Beauveria* spp. isolates. J. Invertebr. Pathol. 96, 237-243.

Forrester, H.B., Li, J., Hovan, D., Ivashkevich, A.N., Sprung, C.N., 2012. DNA repair genes: alternative transcription and gene expression at the exon level in response to the DNA damaging agent, ionizing radiation. PLoS One 7, e53358.

Fox, M.E., Feldman, B.J., Chu, G., 1994. A novel role for DNA photolyase: binding to DNA damaged by drugs is associated with enhanced cytotoxicity in *Saccharomyces cerevisiae*. Mol. Cell. Biol. 14, 8071-8077.

Franzmann, T.M., Menhorn, P., Walter, S., Buchner, J., 2008. Activation of the chaperone Hsp26 is controlled by the rearrangement of its thermosensor domain. Mol. Cell 29, 207-216.

Friedberg, E.C., Walker, G.C., Siede, W., Wood, R.D., Schultz, R.A., Ellenberger, T. (Eds.), 2006. DNA Repair and Mutagenesis. ASM Press, Washington DC.

Friedberg, E.C., 2003. DNA damage and repair. Nature 421, 436-440.

Frohman, M.A., Dush, M.K., Martin, G.R., 1988. Rapid production of full-length cDNAs from rare transcripts: amplification using a single gene-specific oligonucleotide primer. Proc. Natl. Acad. Sci. U. S. A. 85, 8998-9002.

Fuchs, E., Marchuk, D., 1983. Type I and type II keratins have evolved from lower eukaryotes to form the epidermal intermediate filaments in mammalian skin. Proc. Natl. Acad. Sci. U. S. A. 80, 5857-5861.

Galland, P., Lipson, E.D., 1987. Blue-light reception in *Phycomyces* phototropism: evidence for two photosystems operating in low- and high-intensity ranges. Proc. Natl. Acad. Sci. U. S. A. 84, 104-108.

Gams, W., 1971. *Cephalosporium*-artige Schimmelpilze (Hyphomycetes) Mycologia 65, 253-257.

Gams, W., Zare, R., 2001. A revision of *Verticillium* sect. prostrata. III. generic classification. Nova Hedwigia 72, 329-337.

Gao, Q., Jin, K., Ying, S.H., Zhang, Y., Xiao, G., Shang, Y., Duan, Z., Hu, X., Xie, X.Q., Zhou, G., Peng, G., Luo, Z., Huang, W., Wang, B., Fang, W., Wang, S., Zhong, Y., Ma, L.J., St Leger, R.J., Zhao, G.P., Pei, Y., Feng, M.G., Xia, Y., Wang, C., 2011. Genome sequencing and comparative transcriptomics of the model entomopathogenic fungi *Metarhizium anisopliae* and *M. acridum*. PLoS Genet. 7, e1001264.

Gardner, W.A., Sutton, R.M., Noblet, R., 1977. Persistence of *Beauveria bassiana, Nomuraea rileyi,* and *Nosema necatrix* on soybean foliage. Environ. Entomol. 6, 616-618.

Garreau, H., Hasan, R.N., Renault, G., Estruch, F., Boy-Marcotte, E., Jacquet, M., 2000. Hyperphosphorylation of Msn2p and Msn4p in response to heat shock and the diauxic shift is inhibited by cAMP in *Saccharomyces cerevisiae*. Microbiology 146, 2113-2120.

Gasch, A.P., 2007. Comparative genomics of the environmental stress response in ascomycete fungi. Yeast 24, 961-976.

Gasch, A.P., Spellman, P.T., Kao, C.M., Carmel-Harel, O., Eisen, M.B., Storz, G., Botstein, D., Brown, P.O., 2000. Genomic expression programs in the response of yeast cells to environmental changes. Mol. Biol. Cell 11, 4241-4257.

Giese, A.C., Iverson, R.M., Shepard, D.C., Jacobson, C., Brandt, C.L., 1953. Quantum relations in photoreactivation of *Colpidium*. J. Gen. Physiol. 37, 249-258.

Gilbert, H.F., 1990. Molecular and cellular aspects of thiol-disulfide exchange. Adv. Enzymol. Relat. Areas Mol. Biol. 63, 69-172.

Giles, S.S., Batinic-Haberle, I., Perfect, J.R., Cox, G.M., 2005. *Cryptococcus neoformans* mitochondrial superoxide dismutase: an essential link between antioxidant function and high-temperature growth. Eukaryot. Cell. 4, 46-54.

Glas, A., Maul, M., Cryle, M., Barends, T., Schneider, S., Kaya, E., Schlichting, I., Carell, T., 2009. The archaeal cofactor F0 is a light-harvesting antenna chromophore in eukaryotes. Proc. Natl. Acad. Sci. U. S. A. 106, 11540-11545.

Goldman, G.H., Kafer, E., 2004. *Aspergillus nidulans* as a model system to characterize the DNA damage response in eukaryotes. Fungal Genet. Biol. 41, 428-442.

Goldman, G.H., McGuire, S.L., Harris, S.D., 2002. The DNA damage response in filamentous fungi. Fungal Genet. Biol. 35, 183-195.

Gorner, W., Durchschlag, E., Martinez-Pastor, M.T., Estruch, F., Ammerer, G., Hamilton, B., Ruis, H., Schuller, C., 1998. Nuclear localization of the C2H2 zinc finger protein Msn2p is regulated by stress and protein kinase A activity. Genes Dev. 12, 586-597.

Goto, M., 2007. Protein O-glycosylation in fungi: diverse structures and multiple functions. Biosci. Biotechnol. Biochem. 71, 1415-1427.

Goto, M., Tsukamoto, M., Kwon, I., Ekino, K., Furukawa, K., 1999. Functional analysis of O-linked oligosaccharides in threonine/serine-rich region of *Aspergillus* glucoamylase by expression in mannosyltransferase-disruptants of yeast. Eur. J. Biochem. 260, 596-602.

Grace, M.E., Grabowski, G.A., 1990. Human acid beta-glucosidase: glycosylation is required for catalytic activity. Biochem. Biophys. Res. Commun. 168, 771-777.

Guindon, S., Gascuel, O., 2003. A simple, fast, and accurate algorithm to estimate large phylogenies by maximum likelihood. Syst. Biol. 52, 696-704.

Hajek, A., Delalibera, I., 2010. Fungal pathogens as classical biological control agents against arthropods. Biocontrol 55, 147-158.

Hamm-Alvarez, S., Sancar, A., Rajagopalan, K.V., 1989. Role of enzyme-bound 5,10-methenyltetrahydropteroylpolyglutamate in catalysis by *Escherichia coli* DNA photolyase. J. Biol. Chem. 264, 9649-9656.

Hashikawa, N., Mizukami, Y., Imazu, H., Sakurai, H., 2006. Mutated yeast heat shock transcription factor activates transcription independently of hyperphosphorylation. J. Biol. Chem. 281, 3936-3942.

Hatakeyama, S., Ito, Y., Shimane, A., Ishii, C., Inoue, H., 1998. Cloning and characterization of the yeast RAD1 homolog gene (mus-38) from *Neurospora crassa*: evidence for involvement in nucleotide excision repair. Curr. Genet. 33, 276-283.

Hendriks, B.S., Opresko, L.K., Wiley, H.S., Lauffenburger, D., 2003. Coregulation of epidermal growth factor receptor/human epidermal growth factor receptor 2 (HER2) levels and locations: quantitative analysis of HER2 overexpression effects. Cancer Res. 63, 1130-1137.

Hicks, J.K., Yu, J.H., Keller, N.P., Adams, T.H., 1997. *Aspergillus* sporulation and mycotoxin production both require inactivation of the FadA G alpha protein-dependent signaling pathway. EMBO J. 16, 4916-4923.

Hirouchi, T., Nakajima, S., Najrana, T., Tanaka, M., Matsunaga, T., Hidema, J., Teranishi, M., Fujino, T., Kumagai, T., Yamamoto, K., 2003. A gene for a Class II DNA photolyase from *Oryza sativa*: cloning of the cDNA by dilution-amplification. Mol. Genet. Genomics 269, 508-516.

Hitomi, K., Okamoto, K., Daiyasu, H., Miyashita, H., Iwai, S., Toh, H., Ishiura, M., Todo, T., 2000. Bacterial cryptochrome and photolyase: characterization of two photolyase-like genes of *Synechocystis* sp. PCC6803. Nucleic Acids Res. 28, 2353-2362.

Hollinger, S., Hepler, J.R., 2002. Cellular regulation of RGS proteins: modulators and integrators of G protein signaling. Pharmacol. Rev. 54, 527-559.

Hopkins, C.R., Gibson, A., Shipman, M., Miller, K., 1990. Movement of internalized ligand-receptor complexes along a continuous endosomal reticulum. Nature 346, 335-339.

Hsu, D.S., Zhao, X., Zhao, S., Kazantsev, A., Wang, R., Todo, T., Wei, Y., Sancar, A., 1996. Putative human blue-light photoreceptors hCRY1 and hCRY2 are flavoproteins. Biochemistry 35, 13871-13877.

Hu, W., Hou, R.F., Talekar, N.S., 1996. Pathogenicity of *Beauveria bassiana* to *Riptortus linearis* (Hemiptera: Coreidae), a pest of soybean. Appl. Entomol. Zool. 31, 187-194.

Huang, B.F., Feng, M.G., 2009. Comparative tolerances of various *Beauveria bassiana* isolates to UV-B irradiation with a description of a modeling method to assess lethal dose. Mycopathologia 168, 145-152.

Hube, F., Reverdiau, P., Iochmann, S., Gruel, Y., 2005. Improved PCR method for amplification of GC-rich DNA sequences. Mol. Biotechnol. 31, 81-84.

Hunt, T.R., Moore, D., Higgins, P.M., Prior, C., 1994. Effect of sunscreens, irradiance and resting periods on the germination of *Metarhizium flavoviride* conidia. Biocontrol 39, 313-322.

Hunt, V.L., Charnley, A.K., 2011. The inhibitory effect of the fungal toxin, destruxin A, on behavioural fever in the desert locust. J. Insect Physiol. 57, 1341-1346.

Hussain, N.H., Goodson, M., Rowbury, R.J., 1998. Recent advances in biology: intercellular communication and quorum sensing in micro-organisms. Sci. Prog. 81, 69-80.

Hynes, R.O., 2009. The extracellular matrix: not just pretty fibrils. Science 326, 1216-1219.

Ignoffo, C., Hostetter, D., Sikorowski, P., Sutter, G., Brooks, W., 1977. Inactivation of representative species of entomopathogenic viruses, a bacterium, fungus, and protozoan by an ultraviolet light source. Environ. Entomol. 6, 411-415.

Ignoffo, C.M., Puttler, B., Hostetter, D.L., Dickerson, W.A., 1976. Susceptibility of the cabbage looper, *Trichoplusia ni*, and the velvetbean caterpillar, *Anticarsia gemmatalis*, to several isolates of the entomopathogenic fungus *Nomuraea rileyi*. J. Invertebr. Pathol. 28, 259-262.

Inglis, G.D., Johnson, D.L., Goettel, M.S., 1997. Effects of temperature and sunlight on mycosis (*Beauveria bassiana*) (Hyphomycetes: Sympodulosporae) of grasshoppers under field conditions. Environ. Entomol. 26, 400-409.

Inglis, G.D., Goettel, M.S., Johnson, D.L., 1993. Persistence of the entomopathogenic fungus, *Beauveria bassiana*, on phylloplanes of crested wheatgrass and alfalfa. Biol. Control 3, 258-270.

Inglis, G.D., Johnson, D.L., Goettel, M.S., 1996. Effects of temperature and thermoregulation on mycosis by *Beauveria bassiana* in grasshoppers. Biol Control 7, 131-139.

Inoue, H., 2011. Exploring the processes of DNA repair and homologous integration in *Neurospora*. Mutat. Res. 728, 1-11.

Jeffs, L., Xavier, I., Matai, R., Khachatourians, G., 1999. Relationships between fungal spore morphologies and surface properties for entomopathogenic members of the genera *Beauveria, Metarhizium, Paecilomyces,Tolypocladium*, and *Verticillium*. Can. J. Microbiol. 45, 936-948.

Ji, G., Beavis, R.C., Novick, R.P., 1995. Cell density control of staphylococcal virulence mediated by an octapeptide pheromone. Proc. Natl. Acad. Sci. U. S. A. 92, 12055-12059.

Jorns, M.S., Baldwin, E.T., Sancar, G.B., Sancar, A., 1987. Action mechanism of *Escherichia coli* DNA photolyase. II. Role of the chromophores in catalysis. J. Biol. Chem. 262, 486-491.

Jorns, M.S., 1990. DNA photorepair: chromophore composition and function in two classes of DNA photolyases. Biofactors 2, 207-211.

Joshi, L., St. Leger, R.J., Roberts, D.W., 1997. Isolation of a cDNA encoding a novel subtilisin-like protease (Pr1B) from the entomopathogenic fungus, *Metarhizium anisopliae* using differential display-RT-PCR. Gene 197, 1-8.

Kalsbeek, V., Mullens, B.A., 2001. Field studies of *Entomophthora* (Zygomycetes: Entomophthorales)--induced behavioral fever in *Musca domestica* (Diptera: Muscidae) in Denmark. Biol. Control 21, 264-273.

Kavakli, I.H., Sancar, A., 2004. Analysis of the role of intraprotein electron transfer in photoreactivation by DNA photolyase *in vivo*. Biochemistry 43, 15103-15110.

Kawasaki, L., Sanchez, O., Shiozaki, K., Aguirre, J., 2002. SakA MAP kinase is involved in stress signal transduction, sexual development and spore viability in *Aspergillus nidulans*. Mol. Microbiol. 45, 1153-1163.

Kelley, L.A., Sternberg, M.J.E., 2009. Protein structure prediction on the web: a case study using the Phyre server. Nat. Protoc. 4, 363-371.

Khachatourians, G.G., Qazi, S.S., 2008. Entomopathogenic fungi: biochemistry and molecular biology. In: Brakhage, A.A., Zipfer, P.F. (Eds.), The Mycota, VI, Human and Animal Relationships. Springer, Berlin and Heidelberg, pp. 33-61.

Khachatourians, G., 2009. Insecticides, microbial. In: Schaecter, M. (Ed.), Encyclopedia of Microbiology, Vol. 2. Elsevier, New York and London, pp. 95-109.

Khachatourians, G., Valencia, E., Miranpuri, G., 2002. *Beauveria bassiana* and other entomopathogenic fungi in the management of insect pests. In: Koul, O., Dhaliwal, G. (Eds.), Microbial Biopesticides, Vol. 2. Harwood Academic Publishers, Reading, UK, pp. 239-275.

Kiefer, J., 1971. Target theory and survival curves. J. Theor. Biol. 30, 307-317.

Kihara, J., Moriwaki, A., Matsuo, N., Arase, S., Honda, Y., 2004. Cloning, functional characterization, and near-ultraviolet radiation-enhanced expression of a photolyase gene (PHR1) from the phytopathogenic fungus *Bipolaris oryzae*. Curr. Genet. 46, 37-46.

Kim, S.T., Malhotra, K., Smith, C.A., Taylor, J.S., Sancar, A., 1994. Characterization of (6-4) photoproduct DNA photolyase. J. Biol. Chem. 269, 8535-8540.

Kim, S.T., Sancar, A., Essenmacher, C., Babcock, G.T., 1993. Time-resolved EPR studies with DNA photolyase: excited-state FADH0 abstracts an electron from Trp-306 to generate FADH-, the catalytically active form of the cofactor. Proc. Natl. Acad. Sci. U. S. A. 90, 8023-8027.

Kim, S.T., Malhotra, K., Ryo, H., Sancar, A., Todo, T., 1996a. Purification and characterization of *Drosophila melanogaster* photolyase. Mutat. Res. 363, 97-104.

Kim, S.T., Malhotra, K., Taylor, J.S., Sancar, A., 1996b. Purification and partial characterization of (6-4) photoproduct DNA photolyase from *Xenopus laevis*. Photochem. Photobiol. 63, 292-295.

Kinch, L.N., Shi, S., Cheng, H., Cong, Q., Pei, J., Mariani, V., Schwede, T., Grishin, N.V., 2011. CASP9 target classification. Proteins 79 Suppl. 10, 21-36.

Kinsey, J., 1998. *Neurospora crassa*. Trends in Genetics 14, S.14-S.15.

Kleine, T., Lockhart, P., Batschauer, A., 2003. An *Arabidopsis* protein closely related to *Synechocystis* cryptochrome is targeted to organelles. Plant J. 35, 93-103.

Klinkert, B., Narberhaus, F., 2009. Microbial thermosensors. Cell Mol. Life Sci. 66, 2661-2676.

Knoth, K., Roberds, S., Poteet, C., Tamkun, M., 1988. Highly degenerate, inosine-containing primers specifically amplify rare cDNA using the polymerase chain reaction. Nucleic Acids Res. 16, 10932.

Kouvelis, V.N., Sialakouma, A., Typas, M.A., 2008. Mitochondrial gene sequences alone or combined with ITS region sequences provide firm molecular criteria for the classification of *Lecanicillium* species. Mycol. Res. 112, 829-844.

Kozak, M., 1986. Point mutations define a sequence flanking the AUG initiator codon that modulates translation by eukaryotic ribosomes. Cell 44, 283-292.

Krassilstschik, J., 1888. La production industrielle des parasites ve´ge´taux pour la destruction des insectes nuisibles. Bull. Sci. Fr. Belg. 19, 461-472.

Krell, T., Lacal, J., Busch, A., Silva-Jimenez, H., Guazzaroni, M.E., Ramos, J.L., 2010. Bacterial sensor kinases: diversity in the recognition of environmental signals. Annu. Rev. Microbiol. 64, 539-559.

Kupfer, D.M., Drabenstot, S.D., Buchanan, K.L., Lai, H., Zhu, H., Dyer, D.W., Roe, B.A., Murphy, J.W., 2004. Introns and splicing elements of five diverse fungi. Eukaryot. Cell 3, 1088-1100.

Kushner, S.R., 2004. mRNA decay in prokaryotes and eukaryotes: different approaches to a similar problem. IUBMB Life 56, 585-594.

Lambert, D., 2004. Drugs and receptors. Contin. Educ. Anaesth. Crit. Care. Pain 4, 181-184.

Larkin, M.A., Blackshields, G., Brown, N.P., Chenna, R., McGettigan, P.A., McWilliam, H., Valentin, F., Wallace, I.M., Wilm, A., Lopez, R., Thompson, J.D., Gibson, T.J., Higgins, D.G., 2007. Clustal W and Clustal X version 2.0. Bioinformatics 23, 2947-2948.

Larsen, M.R., Trelle, M.B., Thingholm, T.E., Jensen, O.N., 2006. Analysis of posttranslational modifications of proteins by tandem mass spectrometry. BioTechniques 40, 790-798.

Lavergne, V., Taft, R.J., Alewood, P.F., 2012. Cysteine-rich mini-proteins in human biology. Curr. Top. Med. Chem. 12, 1514-1533.

Lazim, Z., Rowbury, R.J., 2000. An extracellular sensor and an extracellular induction component are required for alkali induction of alkyl hydroperoxide tolerance in *Escherichia coli*. J. Appl. Microbiol. 89, 651-656.

LeClerc, J.E., Borden, A., Lawrence, C.W., 1991. The thymine-thymine pyrimidine-pyrimidone(6-4) ultraviolet light photoproduct is highly mutagenic and specifically induces 3' thymine-to-cytosine transitions in *Escherichia coli*. Proc. Natl. Acad. Sci. U. S. A. 88, 9685-9689.

LeConte, J.L., 1873. Hints for the promotion of economic entomology United States. Am Nat. 7, 710-722.

Lemmon, M.A., 2009. Ligand-induced ErbB receptor dimerization. Exp. Cell Res. 315, 638-648.

Levit, M.N., Liu, Y., Stock, J.B., 1998. Stimulus response coupling in bacterial chemotaxis: receptor dimers in signalling arrays. Mol. Microbiol. 30, 459-466.

Lewis, M.W., Robalino, I.V., Keyhani, N.O., 2009. Uptake of the fluorescent probe FM4-64 by hyphae and haemolymph-derived *in vivo* hyphal bodies of the entomopathogenic fungus *Beauveria bassiana*. Microbiology 155, 3110-3120.

Lewus, R.K., Carta, G., 1999. Protein diffusion in charged polyacrylamide gels: visualization and analysis. J. Chromatogr. A 865, 155-168.

Li, J., Bhat, A., Xiao, W., 2011. Regulation of nucleotide excision repair through ubiquitination. Acta Biochim. Biophys. Sin. 43, 919-929.

Li, Y.F., Kim, S.T., Sancar, A., 1993. Evidence for lack of DNA photoreactivating enzyme in humans. Proc. Natl. Acad. Sci. U. S. A. 90, 4389-4393.

Li, Y.F., Heelis, P.F., Sancar, A., 1991. Active site of DNA photolyase: tryptophan-306 is the intrinsic hydrogen atom donor essential for flavin radical photoreduction and DNA repair *in vitro*. Biochemistry 30, 6322-6329.

Lin, C., Robertson, D.E., Ahmad, M., Raibekas, A.A., Jorns, M.S., Dutton, P.L., Cashmore, A.R., 1995. Association of flavin adenine dinucleotide with the *Arabidopsis* blue light receptor CRY1. Science 269, 968-970.

Liu, Q., Ying, S.H., Feng, M.G., Jiang, X.H., 2009. Physiological implication of intracellular trehalose and mannitol changes in response of entomopathogenic fungus *Beauveria bassiana* to thermal stress. Antonie Van Leeuwenhoek 95, 65-75.

Liu, Z., Guo, X., Tan, C., Li, J., Kao, Y., Wang, L., Sancar, A., Zhong, D., 2012. Electron tunneling pathways and role of adenine in repair of cyclobutane pyrimidine dimer by DNA photolyase. J. Am. Chem. Soc. 134, 8104-8114.

Lord, J.C., 2005. From Metchnikoff to Monsanto and beyond: the path of microbial control. J. Invertebr. Pathol. 89, 19-29.

Luo, X., Keyhani, N.O., Yu, X., He, Z., Luo, Z., Pei, Y., Zhang, Y., 2012. The MAP kinase Bbslt2 controls growth, conidiation, cell wall integrity, and virulence in the insect pathogenic fungus *Beauveria bassiana*. Fungal Genet. Biol. 49, 544-555.

Ma, L., Li, J., Qu, L., Hager, J., Chen, Z., Zhao, H., Deng, X.W., 2001. Light control of *Arabidopsis* development entails coordinated regulation of genome expression and cellular pathways. Plant Cell 13, 2589-2607.

Malhotra, K., Kim, S.T., Walsh, C., Sancar, A., 1992. Roles of FAD and 8-hydroxy-5-deazaflavin chromophores in photoreactivation by *Anacystis nidulans* DNA photolyase. J. Biol. Chem. 267, 15406-15411.

Malhotra, K., Kim, S.T., Batschauer, A., Dawut, L., Sancar, A., 1995. Putative blue-light photoreceptors from *Arabidopsis thaliana* and *Sinapis alba* with a high degree of sequence homology to DNA photolyase contain the two photolyase cofactors but lack DNA repair activity. Biochemistry 34, 6892-6899.

Managbanag, J.R., Torzilli, A.P., 2002. An analysis of trehalose, glycerol, and mannitol accumulation during heat and salt stress in a salt marsh isolate of *Aureobasidium pullulans*. Mycologia 94, 384-391.

Maniatis, T., Tasic, B., 2002. Alternative pre-mRNA splicing and proteome expansion in metazoans. Nature 418, 236-243.

Mantilla, J.G., Galeano, N.F., Gaitan, A.L., Cristancho, M.A., Keyhani, N.O., Góngora, C.E., 2012. Transcriptome analysis of the entomopathogenic fungus *Beauveria bassiana* grown on cuticular extracts of the coffee berry borer (*Hypothenemus hampei*). Microbiology 158, 1826-1842.

Martin, F., Aerts, A., Ahren, D., Brun, A., Danchin, E.G., Duchaussoy, F., Gibon, J., Kohler, A., Lindquist, E., Pereda, V., Salamov, A., Shapiro, H.J., Wuyts, J., Blaudez, D., Buee, M., Brokstein, P., Canback, B., Cohen, D., Courty, P.E., Coutinho, P.M., Delaruelle, C., Detter, J.C., Deveau, A., DiFazio, S., Duplessis, S., Fraissinet-Tachet, L., Lucic, E., Frey-Klett, P., Fourrey, C., Feussner, I., Gay, G., Grimwood, J., Hoegger, P.J., Jain, P., Kilaru, S., Labbe, J., Lin, Y.C.,

Legue, V., Le Tacon, F., Marmeisse, R., Melayah, D., Montanini, B., Muratet, M., Nehls, U., Niculita-Hirzel, H., Oudot-Le Secq, M.P., Peter, M., Quesneville, H., Rajashekar, B., Reich, M., Rouhier, N., Schmutz, J., Yin, T., Chalot, M., Henrissat, B., Kues, U., Lucas, S., Van de Peer, Y., Podila, G.K., Polle, A., Pukkila, P.J., Richardson, P.M., Rouze, P., Sanders, I.R., Stajich, J.E., Tunlid, A., Tuskan, G., Grigoriev, I.V., 2008. The genome of *Laccaria bicolor* provides insights into mycorrhizal symbiosis. Nature 452, 88-92.

Martín, J., Cervero, A., Mir, P., Conejero Martinez, J.A., Pellicer, A., Simón, C., 2013. The impact of next-generation sequencing technology on preimplantation genetic diagnosis and screening. Fertil. Steril. 99, 1054-1061.

Martinez-Pastor, M.T., Marchler, G., Schuller, C., Marchler-Bauer, A., Ruis, H., Estruch, F., 1996. The *Saccharomyces cerevisiae* zinc finger proteins Msn2p and Msn4p are required for transcriptional induction through the stress response element (STRE). EMBO J. 15, 2227-2235.

McAuley, A., Jacob, J., Kolvenbach, C.G., Westland, K., Lee, H.J., Brych, S.R., Rehder, D., Kleemann, G.R., Brems, D.N., Matsumura, M., 2008. Contributions of a disulfide bond to the structure, stability, and dimerization of human IgG1 antibody CH3 domain. Protein Sci. 17, 95-106.

McCarty, J.S., Walker, G.C., 1991. DnaK as a thermometer: threonine-199 is site of autophosphorylation and is critical for ATPase activity. Proc. Natl. Acad. Sci. U. S. A. 88, 9513-9517.

McCready, S.J., Osman, F., Yasui, A., 2000. Repair of UV damage in the fission yeast *Schizosaccharomyces pombe*. Mutat. Res. 451, 197-210.

McKinnon, D.J., Brzezowski, P., Wilson, K.E., Gray, G.R., 2009. Mitochondrial and chloroplastic targeting signals of NADP+-dependent isocitrate dehydrogenase. Biochem. Cell Biol. 87, 963-974.

Miller, M.B., Bassler, B.L., 2001. Quorum sensing in bacteria. Annu. Rev. Microbiol. 55, 165-199.

Mishra, Y., Chaurasia, N., Rai, L.C., 2009. Heat pretreatment alleviates UV-B toxicity in the cyanobacterium *Anabaena doliolum*: A proteomic analysis of cross tolerance. Photochem. Photobiol. 85, 824-833.

Miyamoto, T., Okano, S., Kasai, N., 2009. Irreversible thermoinactivation of ribonuclease-A by soft-hydrothermal processing. Biotechnol. Prog. 25, 1678-1685.

Miyamoto, Y., Sancar, A., 1998. Vitamin B2-based blue-light photoreceptors in the retinohypothalamic tract as the photoactive pigments for setting the circadian clock in mammals. Proc. Natl. Acad. Sci. U. S. A. 95, 6097-6102.

Moore, D., Bridge, P.D., Higgins, P.M., Bateman, R.P., Prior, C., 1993. Ultra-violet radiation damage to *Metarhizium* flavoviride conidia and the protection given by vegetable and mineral oils and chemical sunscreens. Ann. Appl. Bio. 122, 605-616.

Moradas-Ferreira, P., Costa, V., Piper, P., Mager, W., 1996. The molecular defences against reactive oxygen species in yeast. Mol. Microbiol. 19, 651-658.

Morano, K.A., Grant, C.M., Moye-Rowley, W.S., 2012. The response to heat shock and oxidative stress in *Saccharomyces cerevisiae*. Genetics 190, 1157-1195.

Morano, K.A., Liu, P.C., Thiele, D.J., 1998. Protein chaperones and the heat shock response in *Saccharomyces cerevisiae*. Curr. Opin. Microbiol. 1, 197-203.

Morley-Davies, J., Moore, D., Prior, C., 1995. Screening of *Metarhizium* and *Beauveria* spp. conidia with exposure to simulated sunlight and a range of temperatures. Mycol. Res. 100, 31-38.

Morozova, E.V., Baranova, M.V., Kozlov, V.P., Tereshina, V.M., Memorskaia, A.S., Feofilova, E.P., 2001. Characteristics of exogenous dormancy of *Aspergillus niger* conidia. Mikrobiologiia 70, 611-619.

Müller, M., Carell, T., 2009. Structural biology of DNA photolyases and cryptochromes. Curr. Opin. Struct. Biol. 19, 277-285.

Murphy, C., Carroll, C., Jordan, K.N., 2003. Identification of a novel stress resistance mechanism in *Campylobacter jejuni*. J. Appl. Microbiol. 95, 704-708.

Nakajima, S., Sugiyama, M., Iwai, S., Hitomi, K., Otoshi, E., Kim, S., Jiang, C., Todo, T., Britt, A.B., Yamamoto, K., 1998. Cloning and characterization of a gene (UVR3) required for photorepair of 6-4 photoproducts in *Arabidopsis thaliana*. Nucleic Acids Res. 26, 638-644.

Nakashima, H., Nishikawa, K., 1994. Discrimination of intracellular and extracellular proteins using amino acid composition and residue-pair frequencies. J. Mol. Biol. 238, 54-61.

Nascimento, E., da Silva, S.H., Marques Edos, R., Roberts, D.W., Braga, G.U., 2010. Quantification of cyclobutane pyrimidine dimers induced by UVB radiation in conidia of the fungi *Aspergillus fumigatus*, *Aspergillus nidulans*, *Metarhizium acridum* and *Metarhizium robertsii*. Photochem. Photobiol. 86, 1259-1266.

Nathan, D.F., Vos, M.H., Lindquist, S., 1997. *In vivo* functions of the *Saccharomyces cerevisiae* Hsp90 chaperone. Proc. Natl. Acad. Sci. U. S. A. 94, 12949-12956.

Neidhardt, F.C., Ingraham, J., Schaechter, M. (Eds.), 1990. Physiology of the Bacterial Cell: A Molecular Approach. Sinauer Associates, Sunderland, MA.

Nevalainen, K.M.H., Te'o, V.S.J., Bergquist, P.L., 2005. Heterologous protein expression in filamentous fungi. Trends Biotechnol. 23, 468-474.

Ng, W.O., Pakrasi, H.B., 2001. DNA photolyase homologs are the major UV resistance factors in the cyanobacterium *Synechocystis* sp. PCC 6803. Mol. Gen. Genet. 264, 924-930.

Nguyen, A.N., Shiozaki, K., 1999. Heat-shock-induced activation of stress MAP kinase is regulated by threonine- and tyrosine-specific phosphatases. Genes Dev. 13, 1653-1663.

Nikolaev, I., 2000. Distant informational interactions in bacteria. Mikrobiologiia 69, 597-605.

Nikolaev, I., 1997a. Comparative study of properties of two extracellular protectors, isolated from *Escherichia coli* at elevated temperature. Mikrobiologiia 66, 790-795.

Nikolaev, I., 1997b. Participation of exometabolites in adaptation of *Escherichia coli* to stressors. Mikrobiologiia 66, 38-41.

Nikolaev, I., Prosser, J.I., Panikov, N.S., 2000. Extracellular factors of adaptation of *Pneudomonas fluorescens* batch cultures to adverse conditions. Mikrobiologiia 69, 629-635.

Nikolaev, I., Voronina, N.A., 1999. Cross-action of extracellular stress adaptation factors in microorganisms. Mikrobiologiia 68, 45-50.

Nowak, M.A., Boerlijst, M.C., Cooke, J., Smith, J.M., 1997. Evolution of genetic redundancy. Nature 388, 167-171.

Oka, T., Sameshima, Y., Koga, T., Kim, H., Goto, M., Furukawa, K., 2005. Protein O-mannosyltransferase A of *Aspergillus awamori* is involved in O-mannosylation of glucoamylase I. Microbiology 151, 3657-3667.

Ouedraogo, A., Fargues, J., Goettel, M.S., Lomer, C.J., 1997. Effect of temperature on vegetative growth among isolates of *Metarhizium anisopliae* and *M. flavoviride*. Mycopathologia 137, 37-43.

Ouedraogo, R.M., Cusson, M., Goettel, M.S., Brodeur, J., 2003. Inhibition of fungal growth in thermoregulating locusts, *Locusta migratoria*, infected by the fungus *Metarhizium anisopliae* var *acridum*. J. Invertebr. Pathol. 82, 103-109.

Oztürk, N., Kao, Y., Selby, C.P., Kavakli, I.H., Partch, C.L., Zhong, D., Sancar, A., 2008. Purification and characterization of a type III photolyase from *Caulobacter crescentus*. Biochemistry 47, 10255-10261.

Park, H.W., Kim, S.T., Sancar, A., Deisenhofer, J., 1995. Crystal structure of DNA photolyase from *Escherichia coli*. Science 268, 1866-1872.

Parker, C.E., Warren, M.R., Loiselle, D.R., Dicheva, N.N., Scarlett, C.O., Borchers, C.H., 2005. Identification of components of protein complexes. Methods Mol. Biol. 301, 117-151.

Partch, C.L., Sancar, A., 2005. Photochemistry and photobiology of cryptochrome blue-light photopigments: the search for a photocycle. Photochem. Photobiol. 81, 1291-1304.

Pasteur, L., 1874. Observations (au sujet des conclusions de M. Dumas) relatives au phylloxera. Compt. Rend. Hebd. Seances Acad. Sci. 79, 1233-1234.

Payne, G., Sancar, A., 1990. Absolute action spectrum of E-FADH2 and E-FADH2-MTHF forms of *Escherichia coli* DNA photolyase. Biochemistry 29, 7715-7727.

Peberdy, J.F., 1999. Extracellular proteins in fungi: a cytological and molecular perspective. Acta Microbiol. Immunol. Hung. 46, 165-174.

Pedrini, N., Crespo, R., Juarez, M.P., 2007. Biochemistry of insect epicuticle degradation by entomopathogenic fungi. Comp. Biochem. Physiol. C. Toxicol. Pharmacol. 146, 124-137.

Perlinska-Lenart, U., Kurzatkowski, W., Janas, P., Kopinska, A., Palamarczyk, G., Kruszewska, J.S., 2005. Protein production and secretion in an *Aspergillus nidulans* mutant impaired in glycosylation. Acta Biochim. Pol. 52, 195-206.

Petersen, T.N., Brunak, S., von Heijne, G., Nielsen, H., 2011. SignalP 4.0: discriminating signal peptides from transmembrane regions. Nat. Methods 8, 785-786.

Posada, F., Vega, F.E., 2005. Establishment of the fungal entomopathogen *Beauveria bassiana* (Ascomycota: Hypocreales) as an endophyte in cocoa seedlings (*Theobroma cacao*). Mycologia 97, 1195-1200.

Qazi, S.S., Khachatourians, G.G., 2007. Hydrated conidia of *Metarhizium anisopliae* release a family of metalloproteases. J. Invertebr. Pathol. 95, 48-59.

Quan, X., Rassadi, R., Rabie, B., Matusiewicz, N., Stochaj, U., 2004. Regulated nuclear accumulation of the yeast hsp70 Ssa4p in ethanol-stressed cells is mediated by the N-terminal domain, requires the nuclear carrier Nmd5p and protein kinase C. FASEB J. 18, 899-901.

Rahn, R.O., Hosszu, J.L., 1969. Photochemical studies of thymine in ice. Photochem. Photobiol. 10, 131-137.

Ramadan, K., Meerang, M., 2011. Degradation-linked ubiquitin signal and proteasome are integral components of DNA double strand break repair: new perspectives for anti-cancer therapy. FEBS Lett. 585, 2868-2875.

Rangel, D.E., Anderson, A.J., Roberts, D.W., 2008. Evaluating physical and nutritional stress during mycelial growth as inducers of tolerance to heat and UV-B radiation in *Metarhizium anisopliae* conidia. Mycol. Res. 112, 1362-1372.

Rangel, D.E., Braga, G.U., Anderson, A.J., Roberts, D.W., 2005. Influence of growth environment on tolerance to UV-B radiation, germination speed, and morphology of *Metarhizium anisopliae* var. *acridum* conidia. J. Invertebr. Pathol. 90, 55-58.

Rangel, D.E., Butler, M.J., Torabinejad, J., Anderson, A.J., Braga, G.U., Day, A.W., Roberts, D.W., 2006. Mutants and isolates of *Metarhizium anisopliae* are diverse in their relationships between conidial pigmentation and stress tolerance. J. Invertebr. Pathol. 93, 170-182.

Rangel, D.E., Fernandes, E.K., Anderson, A.J., Roberts, D.W., 2012. Culture of *Metarhizium robertsii* on salicylic-acid supplemented medium induces increased conidial thermotolerance. Fungal Biol. 116, 438-442.

Rangel, D.E., Fernandes, E.K., Braga, G.U., Roberts, D.W., 2011. Visible light during mycelial growth and conidiation of *Metarhizium robertsii* produces conidia with increased stress tolerance. FEMS Microbiol. Lett. 315, 81-86.

Rangel, D.E., Fernandes, E.K., Dettenmaier, S.J., Roberts, D.W., 2010. Thermotolerance of germlings and mycelium of the insect-pathogenic fungus *Metarhizium* spp. and mycelial recovery after heat stress. J. Basic Microbiol. 50, 344-350.

Raponi, G., Ghezzi, M.C., Mancini, C., 1997. The release of tumor necrosis factor alpha (TNF-alpha) by interferon gamma (IFN-gamma) induced THP-1 cells stimulated with smooth lipopolysaccharide is inhibited by MAbs against HLA-DR and CD14 receptors on the effector cell. New Microbiol. 20, 1-6.

Rausch, F., Schicht, M., Paulsen, F., Ngueya, I., Brauer, L., Brandt, W., 2012. "SP-G", a putative new surfactant protein--tissue localization and 3D structure. PLoS One 7, e47789.

Ravanat, J., Douki, T., Cadet, J., 2001. Direct and indirect effects of UV radiation on DNA and its components. Photochem. Photobiol. 63, 88-102.

Rice, P., Longden, I., Bleasby, A., 2000. EMBOSS: The european molecular biology open software suite. Trends Genet. 16, 276-277.

Roberts, D.W., Campbell, A.S., 1977. Stability of entomopathogenic fungi. Misc. Publ. Entomol. Soc. 10, 19-76.

Roberts, D.W., St Leger, R.J., 2004. *Metarhizium* spp., cosmopolitan insect-pathogenic fungi: mycological aspects. Adv. Appl. Microbiol. 54, 1-70.

Roche, D.B., Buenavista, M.T., McGuffin, L.J., 2012. FunFOLDQA: a quality assessment tool for protein-ligand binding site residue predictions. PLoS One 7, e38219.

Ronaghi, M., Karamohamed, S., Pettersson, B., Uhlén, M., Nyrén, P., 1996. Real-time DNA sequencing using detection of pyrophosphate release. Anal. Biochem. 242, 84-89.

Rowbury, R.J., 2005. Intracellular and extracellular components as bacterial thermometers, and early warning against thermal stress. Sci. Prog. 88, 71-99.

Rowbury, R.J., 2003a. Extracellular proteins as enterobacterial thermometers. Sci. Prog. 86, 139-155.

Rowbury, R.J., 2003b. UV radiation-induced enterobacterial responses, other processes that influence UV tolerance and likely environmental significance. Sci. Prog. 86, 313-332.

Rowbury, R.J., 2002. Microbial disease: recent studies show that novel extracellular components can enhance microbial resistance to lethal host chemicals and increase virulence. Sci. Prog. 85, 1-11.

Rowbury, R.J., 2001a. Cross-talk involving extracellular sensors and extracellular alarmones gives early warning to unstressed *Escherichia coli* of impending lethal chemical stress and leads to induction of tolerance responses. J. Appl. Microbiol. 90, 677-695.

Rowbury, R.J., 2001b. Extracellular sensing components and extracellular induction component alarmones give early warning against stress in *Escherichia coli*. Adv. Microb. Physiol. 44, 215-257.

Rowbury, R.J., 1999. Extracellular sensors and inducible protective mechanisms. Trends Microbiol. 7, 345-346.

Rowbury, R.J., Goodson, M., 2005. Extracellular sensors and extracellular alarmones, which permit cross-talk between organisms, determine the levels of alkali tolerance and trigger alkali induced acid sensitivity in *Escherichia coli*. Sci. Prog. 88, 133-156.

Rowbury, R.J., Goodson, M., 2001. Extracellular sensing and signalling pheromones switch-on thermotolerance and other stress responses in *Escherichia coli*. Sci. Prog. 84, 205-233.

Rowbury, R.J., Goodson, M., 1999a. An extracellular acid stress-sensing protein needed for acid tolerance induction in *Escherichia coli*. FEMS Microbiol. Lett. 174, 49-55.

Rowbury, R.J., Goodson, M., 1999b. An extracellular stress-sensing protein is activated by heat and u.v. irradiation as well as by mild acidity, the activation producing an acid tolerance-inducing protein. Lett. Appl. Microbiol. 29, 10-14.

Rowbury, R.J., Hussain, N.H., Goodson, M., 1998. Extracellular proteins and other components as obligate intermediates in the induction of a range of acid tolerance and sensitisation responses in *Escherichia coli*. FEMS Microbiol. Lett. 166, 283-288.

Roy, H.E., Steinkraus, D., Eilenberg, J., Hajek, A., Pell, J.K., 2006. Bizarre interactions and endgames: entomopathogenic fungi and their arthropod hosts. Annu. Rev. Entomol. 51, 331-357.

Roy, A., Kucukural, A., Zhang, Y., 2010. I-TASSER: a unified platform for automated protein structure and function prediction. Nat. Protoc. 5, 725-738.

Rudd, J.J., Antoniw, J., Marshall, R., Motteram, J., Fraaije, B., Hammond-Kosack, K., 2010. Identification and characterisation of *Mycosphaerella graminicola* secreted or surface-associated proteins with variable intragenic coding repeats. Fungal Genet. Biol. 47, 19-32.

Rupert, C.S., Goodgal, S.H., Herriott, R.M., 1958. Photoreactivation *in vitro* of ultraviolet-inactivated *Hemophilus influenzae* transforming factor. J. Gen. Physiol. 41, 451-471.

Sambrook, J., Russell, D. (Eds.), 2001. Molecular Cloning: A Laboratory Manual. Cold Spring Harbor, Cold Spring Harbor, N.Y.

Sancar, A., Franklin, K.A., Sancar, G.B., 1984. *Escherichia coli* DNA photolyase stimulates uvrABC excision nuclease *in vitro*. Proc. Natl. Acad. Sci. U. S. A. 81, 7397-7401.

Sancar, A., 2003. Structure and function of DNA photolyase and cryptochrome blue-light photoreceptors. Chem. Rev. 103, 2203-2238.

Sancar, G.B., Jorns, M.S., Payne, G., Fluke, D.J., Rupert, C.S., Sancar, A., 1987a. Action mechanism of *Escherichia coli* DNA photolyase. III. Photolysis of the enzyme-substrate complex and the absolute action spectrum. J. Biol. Chem. 262, 492-498.

Sancar, G.B., Smith, F.W., Reid, R., Payne, G., Levy, M., Sancar, A., 1987b. Action mechanism of *Escherichia coli* DNA photolyase. I. Formation of the enzyme-substrate complex. J. Biol. Chem. 262, 478-485.

Sancar, G.B., 2000. Enzymatic photoreactivation: 50 years and counting. Mutat. Res. 451, 25-37.

Sancar, G.B., Ferris, R., Smith, F.W., Vandeberg, B., 1995. Promoter elements of the PHR1 gene of *Saccharomyces cerevisiae* and their roles in the response to DNA damage. Nucleic Acids Res. 23, 4320-4328.

Schauder, S., Bassler, B.L., 2001. The languages of bacteria. Genes & Development 15, 1468-1480.

Seidler, J., Zinn, N., Boehm, M.E., Lehmann, W.D., 2010. *De novo* sequencing of peptides by MS/MS. Proteomics 10, 634-649.

Selby, C.P., Sancar, A., 2006. A cryptochrome/photolyase class of enzymes with single-stranded DNA-specific photolyase activity. Proc. Natl. Acad. Sci. U. S. A. 103, 17696-17700.

Shah, P.A., Pell, J.K., 2003. Entomopathogenic fungi as biological control agents. Appl. Microbiol. Biotechnol. 61, 413-423.

Shaw, B.D., Chung, D.W., Wang, C.L., Quintanilla, L.A., Upadhyay, S., 2011. A role for endocytic recycling in hyphal growth. Fungal Biol. 115, 541-546.

Shevchenko, A., Sunyaev, S., Loboda, A., Shevchenko, A., Bork, P., Ens, W., Standing, K.G., 2001. Charting the proteomes of organisms with unsequenced genomes by MALDI-quadrupole time-of-flight mass spectrometry and BLAST homology searching. Anal. Chem. 73, 1917-1926.

Shirtliff, M.E., Krom, B.P., Meijering, R.A., Peters, B.M., Zhu, J., Scheper, M.A., Harris, M.L., Jabra-Rizk, M.A., 2009. Farnesol-induced apoptosis in *Candida albicans*. Antimicrob. Agents Chemother. 53, 2392-2401.

Shizhu, Z., Yuxian, X., Keyhani, N.O., 2011. Contribution of the *gas1* gene of the entomopathogenic fungus *Beauveria bassiana*, encoding a putative glycosylphosphatidylinositol-anchored beta-1,3-glucanosyltransferase, to conidial thermotolerance and virulence. Appl. Environ. Microbiol. 77, 2676-2684.

Singer, M.A., Lindquist, S., 1998a. Multiple effects of trehalose on protein folding *in vitro* and *in vivo*. Mol. Cell 1, 639-648.

Singer, M.A., Lindquist, S., 1998b. Thermotolerance in *Saccharomyces cerevisiae*: the Yin and Yang of trehalose. Trends Biotechnol. 16, 460-468.

Sipos, T., Merkel, J.R., 1970. Effect of calcium ions on the activity, heat stability, and structure of trypsin. Biochemistry (N. Y.) 9, 2766-2775.

Smith, K.C., Hanawalt, P.C. (Eds.), 1969. Molecular and Photobiology: Inactivation and Recovery. Academic Press, New York, N.Y.

Smith, D.A., Nicholls, S., Morgan, B.A., Brown, A.J., Quinn, J., 2004. A conserved stress-activated protein kinase regulates a core stress response in the human pathogen *Candida albicans*. Mol. Biol. Cell 15, 4179-4190.

Smits, N., Fargues, J., Rougier, M., Goujet, R., Itier, B., 1996. Effects of temperature and solar radiation interactions on the survival of quiescent conidia of the entomopathogenic hyphomycete *Paecilomyces fumosoroseus* (Wize) Brown and Smith. Mycopathologia 135, 163-170.

Sorger, P.K., Pelham, H.R., 1987. Purification and characterization of a heat-shock element binding protein from yeast. EMBO J. 6, 3035-3041.

Spiro, I., Denman, D., Dewey, W., 1983. Effect of hyperthermia on isolated DNA polymerase-beta. Radiat. Res. 95, 68-77.

St Leger, R., Joshi, L., Bidochka, M.J., Roberts, D.W., 1996. Construction of an improved mycoinsecticide overexpressing a toxic protease. Proc. Natl. Acad. Sci. U. S. A. 93, 6349-6354.

St Leger, R.J., Wang, C., 2010. Genetic engineering of fungal biocontrol agents to achieve greater efficacy against insect pests. Appl. Microbiol. Biotechnol. 85, 901-907.

Subjeck, J.R., Sciandra, J.J., Johnson, R.J., 1982. Heat shock proteins and thermotolerance; a comparison of induction kinetics. Br. J. Radiol. 55, 579-584.

Sung, G.H., Hywel-Jones, N.L., Sung, J.M., Luangsa-Ard, J.J., Shrestha, B., Spatafora, J.W., 2007. Phylogenetic classification of *Cordyceps* and the clavicipitaceous fungi. Stud. Mycol. 57, 5-59.

Suska, A., Filippini, D., Andersson, T.P., Lundstrom, I., 2005. Generation of biochemical response patterns of different substances using a whole cell assay with multiple signaling pathways. Biosens. Bioelectron. 21, 727-734.

Tamada, T., Kitadokoro, K., Higuchi, Y., Inaka, K., Yasui, A., de Ruiter, P.E., Eker, A.P., Miki, K., 1997. Crystal structure of DNA photolyase from *Anacystis nidulans*. Nat. Struct. Biol. 4, 887-891.

Thomas, K.C., Khachatourians, G.G., Ingledew, W.M., 1987. Production and properties of *Beauveria bassiana* conidia cultivated in submerged culture. Can. J. Microbiol. 33, 12-20.

Todo, T., Takemori, H., Ryo, H., Ihara, M., Matsunaga, T., Nikaido, O., Sato, K., Nomura, T., 1993. A new photoreactivating enzyme that specifically repairs ultraviolet light-induced (6-4) photoproducts. Nature 361, 371-374.

Tomar, A.K., Sooch, B.S., Yadav, S., 2011. Computational analysis of concanavalin A binding glycoproteins of human seminal plasma. Bioinformation 7, 69-75.

Trail, F., Xu, H., 2002. Purification and characterization of mannitol dehydrogenase and identification of the corresponding cDNA from the head blight fungus, *Gibberella zeae* (*Fusarium graminearum*). Phytochemistry 61, 791-796.

Trotter, E.W., Kao, C.M., Berenfeld, L., Botstein, D., Petsko, G.A., Gray, J.V., 2002. Misfolded proteins are competent to mediate a subset of the responses to heat shock in *Saccharomyces cerevisiae*. J. Biol. Chem. 277, 44817-44825.

Tschopp, J.F., Sverlow, G., Kosson, R., Craig, W., Grinna, L., 1987. High-level secretion of glycosylated invertase in the methylotrophic yeast, *Pichia pastoris*. Nat. Biotechnol. 5, 1305-1308.

Varki, A., 1993. Biological roles of oligosaccharides: all of the theories are correct. Glycobiology 3, 97-130.

Veluchamy, S., Rollins, J.A., 2008. A CRY-DASH-type photolyase/cryptochrome from *Sclerotinia sclerotiorum* mediates minor UV-A-specific effects on development. Fungal Genet. Biol. 45, 1265-1276.

Verhage, R., Zeeman, A.M., de Groot, N., Gleig, F., Bang, D.D., van de Putte, P., Brouwer, J., 1994. The RAD7 and RAD16 genes, which are essential for pyrimidine dimer removal from the silent mating type loci, are also required for repair of the nontranscribed strand of an active gene in *Saccharomyces cerevisiae*. Mol. Cell. Biol. 14, 6135-6142.

Verstrepen, K.J., Jansen, A., Lewitter, F., Fink, G.R., 2005. Intragenic tandem repeats generate functional variability. Nat. Genet. 37, 986-990.

Vestergaard, S., Gillespie, A., Butt, T., Schreiter, G., Eilenberg, J., 1995. Pathogenicity of the hyphomycete fungi *Verticillium lecanii* and *Metarhizium anisopliae* to the western flower thrips, *Frankliniella occidentalis*. Biocontrol Sci. Technol. 5, 185-192.

Villalonga, M.L., Reyes, G., Fragoso, A., Cao, R., Fernandez, L., Villalonga, R., 2005. Chemical glycosidation of trypsin with O-carboxymethyl-poly-beta-cyclodextrin: catalytic and stability properties. Biotechnol. Appl. Biochem. 41, 217-223.

Vorob'eva, L.I., Khodzhaev, E.I., Ponomareva, G.M., 2003. The extracellular protein of *Luteococcus japonicus* subsp *casei* reactivates cells inactivated by ultraviolet radiation or heating. Mikrobiologiia 72, 482-487.

Vovou, I., Delitheos, A., Tiligada, E., 2004. The heat shock response is dependent on the external environment and on rapid ionic balancing by pharmacological agents in *Saccharomyces cerevisiae*. J. Appl. Microbiol. 96, 1271-1277.

Waage, J., 1998. The future development of IPM. Insect Sci. 5, 257-271.

Walther, T.C., Mann, M., 2010. Mass spectrometry-based proteomics in cell biology. J. Cell Biol. 190, 491-500.

Wang, C., St Leger, R.J., 2007. A scorpion neurotoxin increases the potency of a fungal insecticide. Nat. Biotechnol. 25, 1455-1456.

Wang, J., Zhou, G., Ying, S.H., Feng, M.G., 2013. P-type calcium ATPase functions as a core regulator of *Beauveria bassiana* growth, conidiation and responses to multiple stressful stimuli through crosstalk with signaling networks. Environ. Microbiol. 15, 967-979.

Wang, S.Y. (Ed.), 1976. Photochemistry and Photobiology of Nucleic Acids. Academic Press, New York, N.Y.

Wang, C., St Leger, R.J., 2006. A collagenous protective coat enables *Metarhizium anisopliae* to evade insect immune responses. Proc. Natl. Acad. Sci. U. S. A. 103, 6647-6652.

Wang, S., Wei, W., Zheng, Y., Hou, J., Dou, Y., Zhang, S., Luo, X., Cai, X., 2012a. The role of insulin C-peptide in the coevolution analyses of the insulin signaling pathway: a hint for its functions. PLoS One 7, e52847.

Wang, Z.L., Lu, J.D., Feng, M.G., 2012b. Primary roles of two dehydrogenases in the mannitol metabolism and multi-stress tolerance of entomopathogenic fungus *Beauveria bassiana*. Environ. Microbiol. 14, 2139-2150.

Wang, Z.L., Zhang, L.B., Ying, S.H., Feng, M.G., 2013. Catalases play differentiated roles in the adaptation of a fungal entomopathogen to environmental stresses. Environ. Microbiol. 15, 409-418.

Wass, M.N., Barton, G., Sternberg, M.J.E., 2012. CombFunc: predicting protein function using heterogeneous data sources. Nucleic Acids Res. 40, W466-W470.

Waterman, H., Yarden, Y., 2001. Molecular mechanisms underlying endocytosis and sorting of ErbB receptor tyrosine kinases. FEBS Lett. 490, 142-152.

Wieser, R., Adam, G., Wagner, A., Schüller, C., Marchler, G., Ruis, H., Krawiec, Z., Bilinski, T., 1991. Heat shock factor-independent heat control of transcription of the CTT1 gene encoding the cytosolic catalase T of *Saccharomyces cerevisiae*. J. Biol. Chem. 266, 12406-12411.

Winkler, C., Denker, K., Wortelkamp, S., Sickmann, A., 2007. Silver- and Coomassie-staining protocols: detection limits and compatibility with ESI MS. Electrophoresis 28, 2095-2099.

Wissmueller, S., Font, J., Liew, C.W., Cram, E., Schroeder, T., Turner, J., Crossley, M., Mackay, J.P., Matthews, J.M., 2011. Protein-protein interactions: analysis of a false positive GST pulldown result. Proteins 79, 2365-2371.

Wittig, I., Braun, H.P., Schagger, H., 2006. Blue native PAGE. Nat. Protoc. 1, 418-428.

Worthington, E.N., Kavakli, İ.H., Berrocal-Tito, G., Bondo, B.E., Sancar, A., 2003. Purification and characterization of three members of the photolyase/cryptochrome family blue-light photoreceptors from *Vibrio cholerae*. J. Biol. Chem. 278, 39143-39154.

Xavier, I.J., 1998. Environmental stress response of the hyphomycetous entomopathogenic fungi. Doctor of Philosophy Thesis. University of Saskatchewan, Saskatoon, Saskatchewan, CA .

Xavier, I.J., Khachatourians, G.G., Ovsenek, N., 1999. Constitutive and heat-inducible heat shock element binding activities of heat shock factor in a group of filamentous fungi. Cell Stress Chaperon. 4, 211-222.

Xavier, I.J., Khachatourians, G.G., 1996. Heat-shock response of the entomopathogenic fungus *Beauveria brongniartii*. Can. J. Microbiol. 42, 577-585.

Xiao, G., Ying, S.H., Zheng, P., Wang, Z.L., Zhang, S., Xie, X.Q., Shang, Y., St Leger, R.J., Zhao, G.P., Wang, C., Feng, M.G., 2012. Genomic perspectives on the evolution of fungal entomopathogenicity in *Beauveria bassiana*. Sci. Rep. 2, 483.

Xie, X.Q., Wang, J., Huang, B.F., Ying, S.H., Feng, M.G., 2010. A new manganese superoxide dismutase identified from *Beauveria bassiana* enhances virulence and stress tolerance when overexpressed in the fungal pathogen. Appl. Microbiol. Biotechnol. 86, 1543-1553.

Xu, B., Zhang, Y., Zhao, Z., Yoshida, Y., Magdeldin, S., Fujinaka, H., Ismail, T.A., Yaoita, E., Yamamoto, T., 2011. Usage of electrostatic eliminator reduces human keratin contamination significantly in gel-based proteomics analysis. J. Proteomics 74, 1022-1029.

Yajima, H., Takao, M., Yasuhira, S., Zhao, J.H., Ishii, C., Inoue, H., Yasui, A., 1995. A eukaryotic gene encoding an endonuclease that specifically repairs DNA damaged by ultraviolet light. EMBO J. 14, 2393-2399.

Yang, H., Wu, Y., Tang, R., Liu, D., Liu, Y., Cashmore, A.R., 2000. The C termini of *Arabidopsis* cryptochromes mediate a constitutive light response. Cell 103, 815-827.

Ying, S.H., Feng, M.G., 2011. A conidial protein (CP15) of *Beauveria bassiana* contributes to the conidial tolerance of the entomopathogenic fungus to thermal and oxidative stresses. Appl. Microbiol. Biotechnol. 90, 1711-1720.

Ying, S.H., Feng, M.G., 2006. Medium components and culture conditions affect the thermotolerance of aerial conidia of fungal biocontrol agent *Beauveria bassiana*. Lett. Appl. Microbiol. 43, 331-335.

Ying, S.H., Feng, M.G., 2004. Relationship between thermotolerance and hydrophobin-like proteins in aerial conidia of *Beauveria bassiana* and *Paecilomyces fumosoroseus* as fungal biocontrol agents. J. Appl. Microbiol. 97, 323-331.

Yoon, J., Lee, C., O'Connor, T.R., Yasui, A., Pfeifer, G.P., 2000. The DNA damage spectrum produced by simulated sunlight. J. Mol. Biol. 299, 681-693.

Yu, W., Soprana, E., Cosentino, G., Volta, M., Lichenstein, H.S., Viale, G., Vercelli, D., 1998. Soluble CD14(1-152) confers responsiveness to both lipoarabinomannan and lipopolysaccharide in a novel HL-60 cell bioassay. J. Immunol. 161, 4244-4251.

Zare, R., Gams, W., Culham, A., 2000. A revision of *Verticilium* sect. prostrata. I. phylogenetic studies using ITS sequences. Nova Hedwigia 71, 465-480.

Zeng, G., Cai, M., 1999. Regulation of the actin cytoskeleton organization in yeast by a novel serine/threonine kinase Prk1p. J. Cell Biol. 144, 71-82.

Zhang, C., Xia, Y., 2009. Identification of genes differentially expressed *in vivo* by *Metarhizium anisopliae* in the hemolymph of *Locusta migratoria* using suppression-subtractive hybridization. Curr. Genet. 55, 399-407.

Zhang, Y., Zhao, J., Fang, W., Zhang, J., Luo, Z., Zhang, M., Fan, Y., Pei, Y., 2009. Mitogen-activated protein kinase *hog1* in the entomopathogenic fungus *Beauveria bassiana* regulates environmental stress responses and virulence to insects. Appl. Environ. Microbiol. 75, 3787-3795.

Zhang, Y., Z., Zhang, Y.J., Zhang, J.Q., Jiang, X.D., Wang, G.J., Luo, Z.B., Fan, Y.H., Wu, Z.Q., Pei, Y., 2010. Requirement of a mitogen-activated protein kinase for appressorium formation and penetration of insect cuticle by the entomopathogenic fungus *Beauveria bassiana*. Appl. Environ. Microbiol. 76, 2262-2270.

Zheng, P., Xia, Y., Xiao, G., Xiong, C., Hu, X., Zhang, S., Zheng, H., Huang, Y., Zhou, Y., Wang, S., Zhao, G.P., Liu, X., St Leger, R.J., Wang, C., 2011. Genome sequence of the insect pathogenic fungus *Cordyceps militaris*, a valued traditional Chinese medicine. Genome Biol. 12, R116.

Zhou, G., Wang, J., Qiu, L., Feng, M.G., 2012. A Group III histidine kinase (mhk1) upstream of high-osmolarity glycerol pathway regulates sporulation, multi-stress tolerance and virulence of *Metarhizium robertsii*, a fungal entomopathogen. Environ. Microbiol. 14, 817-829.

Zhou, X., Ma, Y., Sugiura, R., Kobayashi, D., Suzuki, M., Deng, L., Kuno, T., 2010. MAP kinase kinase kinase (MAPKKK)-dependent and -independent activation of Sty1 stress MAPK in fission yeast. J. Biol. Chem. 285, 32818-32823.

Zimmermann, G., 1982. Effect of high temperatures and artificial sunlight on the viability of conidia of *Metarhizium anisopliae*. J. Invertebr. Pathol. 40, 36-40.

APPENDIX I

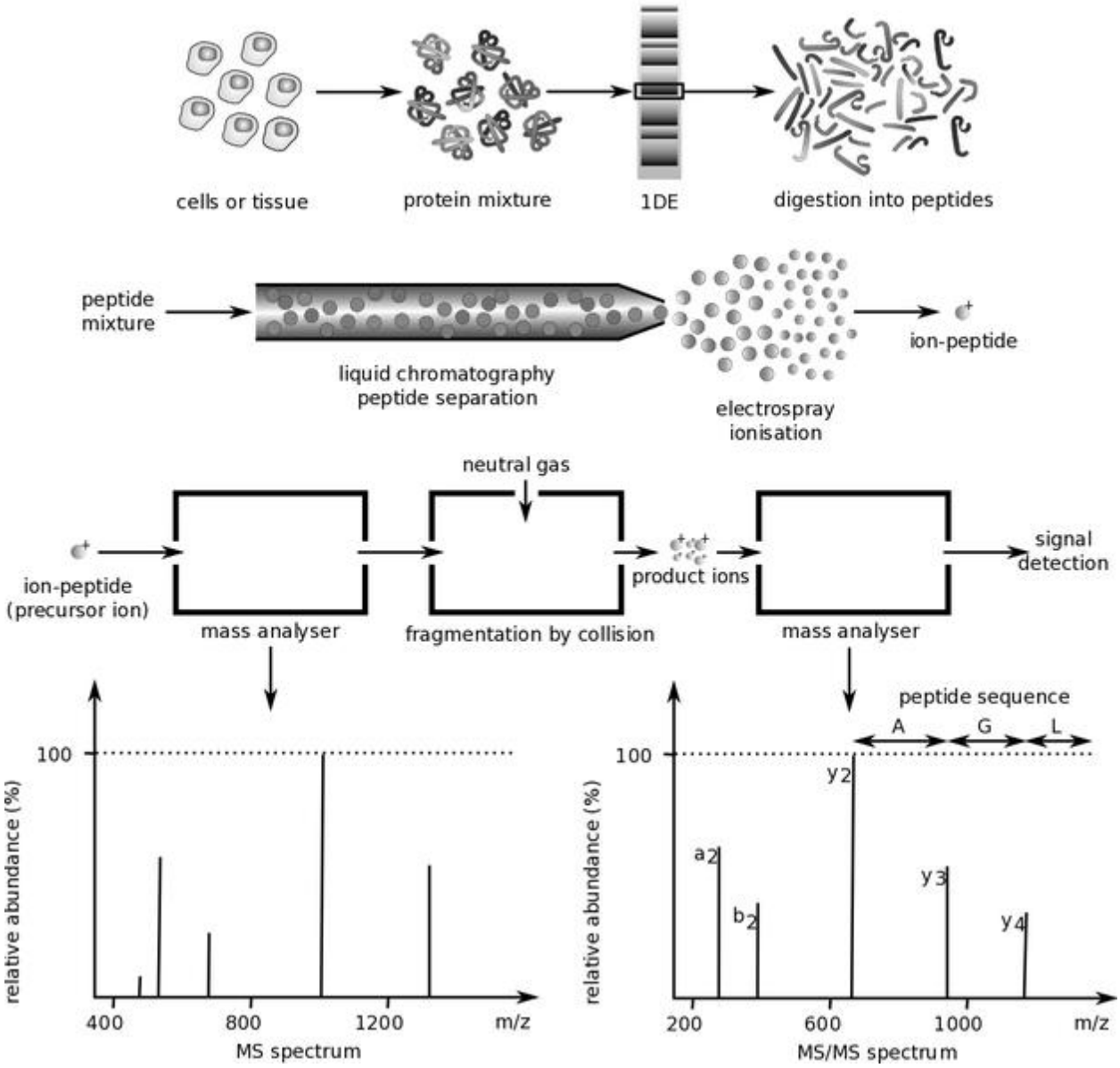

OVERVIEW OF ESI-MS/MS PROTOCOL USED TO OBTAIN *DE NOVO* PEPTIDE SEQUENCES FROM ELF CANDIDATES. This figure was supplied by Wikimedia Commons (available at: http://commons.wikimedia.org/wiki/File:Mass_spectrometry_protocol.png).